Role of endocytic proteins in mechanotransduction and impact on autosomal dominant centronuclear myopathy

Agathe Franck

Université Pierre et Marie Curie

École Doctorale Complexité du Vivant (ED 515)

Institut de Myologie

Équipe Physiopathologie & thérapie de la myopathie centronucléaire autosomique dominante

Rôle des protéines de l'endocytose dans la mécanotransduction et la physiopathologie de la myopathie centronucléaire autosomique dominante

---

Role of endocytic proteins in mechanotransduction and impact on autosomal dominant centronuclear myopathy

Par Agathe Franck

Thèse de doctorat

Devant un jury composé de :

Pr. Onnik Agbulut	Président du jury & examinateur
Dr. Jocelyn Laporte	Rapporteur
Dr. Athanassia Sotiropoulos	Rapporteur
Pr. Frances Brodsky	Examinateur
Dr. Stéphane Vassilopoulos	Directeur de thèse

To Lola

The woods are lovely, dark and deep,

But I have promises to keep,

And miles to go before I sleep,

And miles to go before I sleep.

— Robert Frost, *Stopping by Woods on a Snowy Evening* (1922)

Disclaimer

This thesis is delivered with a pair of red/cyan glasses for viewing of anaglyphs. The following logo means that you can wear the glasses for 3D viewing of the images:

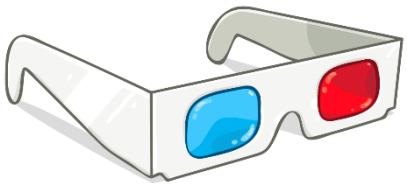

Please be aware that an absence of glasses does not impair reading of this thesis.

Acknowledgements

First of all, I would like to thank Stéphane Vassilopoulos, my thesis supervisor. As I said, I'm not very good at this. Thank you for giving me a chance all these years ago, after reading the letter of a small master 1 student that just "wanted to do microscopy". Thank you for the pep talks, the laughs, the evenings with Jeanne at the electron microscope, open mouthed in front of her beautiful pictures, the late lunches at the Japanese place near Jussieu, the pride I felt when I showed you my pictures, thank you for believing me, for your passion about our work, for maneuvering my boat through these years that have not always been easy… in short, thank you for everything.

I'm also very grateful to Marc Bitoun, our great chief and leader. Thank you for your help, for always being caring and patient. Thank you also for your advices and very (very) pertinent questions.

Jeanne, thank you forever for giving me the beautiful pictures that I included in this thesis manuscript. Thank you for your kindness and always being there when I needed to talk (most of the people I know think you are my shrink). You've helped me stay afloat and I will forever be grateful.

How could I not thank lab 103. This melting pot of characters and personalities. Anaïs Fongy, Éline Lemerle, Corine, Margot, Bernard and Camilla. Sometimes we work there, but we also laugh. A lot. I'd like to thank especially Anaïs, who has helped me believe in myself at a time when no one could achieve it. Éline, I wish you all the best for the future, you can always call me. Anytime. I will also thank the expat members of team 2, Delphine and Gilles, and the one who is even further away, Bruno Cadot. I'm especially grateful to Gilles for the precious help and guidance since his arrival, and I am truly sorry for all the unlucky PCRs my cells have caused.

Valérie Allamand, thank you for your reassuring presence in the lab, during evenings, during the weekends, thank you for your smile and for listening, and also… thank you for the milk!

The YAP/TAZ part of this project could not have been realized without the help and expertise of Catherine Coirault. Thank you for the Flexcell and the various talks about YAP/TAZ shuttling, without you we would have been lost.

This work was completed thanks to the receptiveness of the imaging platforms. A big thank you to the Cytometry and Imaging Platform of Gustave Roussy Institute, particularly to Corinne Laplace-Builhé and Sophie Salomé-Desnoulez. Thank you also to the imaging platforms of the Institut de Biologie Paris-Seine, Michaël Trichet for his enormous help in making metal replicas of our samples possible, and Susanne Bolte, Jean-François Gilles and France Lam for their expertise in fluorescence microscopy. I am also grateful to the Pitié-Salpêtrière cell imaging platform staff who often asked me if I wanted a bed installed next to their microscope.

This work also relied on the biopsies given by patients affected by centronuclear myopathy or desminopathies. We are grateful to Muscle Tissue Culture Collection MTCC at Klinikum der Universität München for providing the p.R350P primary cells, and to Anne and Kamel of the Myology Institute's immortalization platform for the immortalization of these cells and CNM patients' myoblasts. I thank the Morphological Unit, especially Norma Romero, Michel Fardeau, Emmanuelle Lacène, Mai Thao Viou and Guy Brochier, for their precious help regarding the characterization of desmin anomalies in patients affected by AD CNM. Thanks also to Laura Julien of the vectorology platform regarding the production of the AAV used in this study.

Pr. Onnik Agbulut, thank you for your smile, and for the precious help to this study by giving us desmin $^{-/-}$ mice.

I am grateful to the members of thesis committee who have followed me through these years: Stéphanie Miserey-Lenkei, Guillaume Montagnac and Denis Furling. Stéphanie, I will not forget your precious advice.

Marie-Claude Potier, thank you for your support, I carry a bit of the expertise acquired in your lab everywhere I go.

I am grateful to the committee attributing doctoral contracts for believing in my project.

I cannot end without thanking all the people who have carried me to hell and back: my mom, Mallory, Lucile, Emmanuelle, Georges, Clément and Guilhem Salines, Ronan, Aless, Sophie, the Gründ team, my favorite cousin Émilie, Alice, Julie, Gertrude, Florent, Capucine, Romain, Ségolène…

This will seem strange but I'd like to thank my cat. He'll understand.

I owe more than a « thank you » to a person named Lola Salines. Lola, this work is dedicated to you, and I would like to write, as an opening to this thesis manuscript, all my gratitude, and all my love.

Table of contents

Table of figures 10

Table of movies 12

List of tables 12

Abstract 13

French abstract 14

Abbreviations 15

I. Introduction 17

1- The skeletal muscle 17
a. Function 17
b. Development and Myofibers 17
i. A striated pattern of contractile units 18
ii. Excitation-contraction coupling 20
iii. Costameres 21
iv. Intermediate filaments 22
c. Mechanotransduction 26
i. Integrin-mediated mechanotransduction 26
ii. YAP/TAZ pathway 28
iii. MRTF-SRF 31

2- Membranes and vesicular trafficking 32
a. The Cell Theory 32
b. Membrane trafficking 33
c. Clathrin-mediated membrane traffic 35
i. Clathrin 35
ii. Adaptor proteins 38
iii. Dynamin 39
iv. Sequential recruitment of CCV formation actors 42
v. Role of actin filaments 43
d. Diversity of clathrin-coated structures 44
i. A very stable assembly of hexagons 46
ii. Clathrin plaques as… hotspots for endocytosis 48
iii. Clathrin plaques as… adherent structures 49
iv. Clathrin plaques as... signaling hubs 49
v. Clathrin plaques as… actin organisers 50

3- Role of endocytic proteins in muscle: what we know so far 51
a. Clathrin plaques are part of costameres 51
b. Clathrin, AP2 and DNM2 are required for α-actinin scaffold formation 53
c. Clathrin plaques are required for sarcomere maintenance *in vivo* 55

4- Centronuclear myopathies 56
a. X-linked myotubular myopathy (XLMTM) 56
b. Autosomal recessive centronuclear myopathy (AR CNM) 57
c. Autosomal dominant centronuclear myopathy (AD CNM) 58
i. Membrane trafficking hypothesis 59
ii. Focal adhesions hypothesis 59
iii. Cytoskeletal regulation hypothesis 60

iv. T-tubule hypothesis 61
v. A mouse model for AD CNM linked to DNM2 61

2- Unanswered questions – Aims of the study 61
a. Aim one: What are clathrin plaques made of and what are their dynamics? 62
b. Aim two: How are they involved in cytoskeletal scaffolding? 62
c. Aim three: What is their exact role in CNM pathophysiology? 62

II. Methods 63

1- Cell culture 63
a. Primary culture preparation 63
b. Primary cell culture subculturing 64
c. Cell differentiation 64
d. Extended differentiation protocol 64
e. Immortalized cell lines 65
f. siRNA transfection 65
g. Cell stretching 66
i. Flexcell apparatus 66
ii. Quantification of YAP/TAZ location 67
h. Transferrin uptake assay 68

2- Histomorphological and ultrastructural analyses 68
a. Fluorescence microscopy 68
i. Immunofluorescence 68
ii. AAV injection, live microscopy 69
b. Electron microscopy 71
i. Unroofing and preparation of metal replicas 71
ii. Making anaglyphs 74
iii. Thin-section EM 75
c. Histology 75

2- Biochemistry 76
a. Western blotting 76
b. Immunoprecipitation 76

3- RNA extraction and RT-qPCR 77

4- Statistical analysis 77

5- Study approval 77

III. Results 79

1- Ultrastructure and dynamics of clathrin plaques 79
a. Morphology of clathrin plaques 79
i. Regularly spaced structures along the PM 79
ii. AP2 and Dab2 are clathrin plaque adaptors 81
iii. Clathrin plaques act as scaffold for cytoskeletal anchoring 85
iv. Clathrin plaques scaffold intermediate filaments 90
v. Actin surrounding clathrin plaques organizes the cortical IF anchoring 95
b. Stable structures with a dynamic turnover 100
i. Clathrin plaques are stable structures in adherent myotubes 100
ii. In vivo plaque dynamics 101

2- Clathrin platforms are involved in mechanotransduction 104
a. Clathrin plaques respond to cyclic stretching 104

b. Clathrin is required for YAP/TAZ signaling 105
c. Clathrin platforms directly sequestrate YAP/TAZ mechanotransducers 108
d. DNM2 and TAZ biochemical interaction 111
e. DNM2 is required for YAP/TAZ cytoplasmic sequestration and translocation 112
f. Actin and IF remodeling is needed for YAP/TAZ activation 114

3- Costameric disorganization in CNM 117
a. DNM2-linked mutations impair plaque organization 117
b. DNM2 CNM mutation disorganizes the desmin network *in vivo* 119
c. CNM affects desmin distribution in patients 120
d. CNM mutation impairs YAP/TAZ location and expression 122
e. DNM2-linked CNM mutations delay plaque dynamics *in vivo* 124

IV. Discussion and future directions 127

1- Composition and regulation of clathrin plaques 128

2- Plaques, DNM2 and actin 129

3- Impact of clathrin plaques organization on mechanotransduction 131
a. YAP/TAZ 131
b. Intermediate filaments 134

4- Consequences for CNM pathophysiology 135

V. References 139

VI. Appendix 165

1- Movie legends and URLs 165

2- List of siRNA sequences 165

3- List of primers 165

4- Buffers 167
a. Mammalian Ringers ("extracellular" buffer) 167
b. Ca2+ free Ringers 167
c. KHMgE ("intracellular" buffer) 167

5- List of publications and presentations 168
Publications 168
Posters and oral presentations 168

Table of figures

Figure I.1. Structure of the skeletal muscle 17
Figure I.2. Scanning electron micrograph of a muscle fiber 18
Figure I.3. Organization of the sarcomere 19
Figure I.4. Schematic representation of a costamere 22
Figure I.5. Formation and structure of desmin intermediate filaments 23
Figure I.6. Schematic representation of the desmin intermediate filament network 24
Figure I.7. Muscle phenotype of desmin mutation 25
Figure I.8. Progressive recruitment forming focal adhesions 27
Figure I.9. A model of the Hippo pathway 29
Figure I.10. Mechanical stimuli influencing YAP and TAZ subcellular localization and activity 30
Figure I.11. Suber cells 33

Figure I.12. Overview of cellular trafficking pathways 34
Figure I.13. Location of CHC17 and CHC22 in human cells 36
Figure I.14. The clathrin triskelion and the designs of some simple clathrin lattices 37
Figure I.15. Composition and location of AP complexes 39
Figure I.16. Domain organization of dynamin 1 40
Figure I.17. Two models of dynamin-dependent membrane fission 42
Figure I.18. Transition from flat to curved clathrin-coated structures 45
Figure I.19. Design in nature 46
Figure I.20. Chemical structure of [60]Fullerene 47
Figure I.21. Different assemblies of clathrin-coated structures 48
Figure I.22. Budding events occurring at the edge of flat clathrin lattices 48
Figure I.23. CHC patches at the PM of differentiated myotubes 52
Figure I.24. CHC association with α-actinin2 in adult skeletal muscle 52
Figure I.25. α-actinin 2 and actin are localized on large flat clathrin-coated plaques 53
Figure I.26. CHC, AP2, and DNM2 depletion in cultured mouse myotubes perturbs α-actinin distribution 54
Figure I.27. Sarcomeric detachment between sarcolemma and myofibrils upon in vivo CHC depletion 56
Figure I.28. Histological characteristics of DNM2-related CNM 58
Figure I.29. Localization of dynamin-2 mutations linked to CNM. 59
Figure I.30. What we knew about clathrin plaques 62
Figure II.1. Myoblast fusion in cultured muscle cells 64
Figure II.2. Uniflex culture plates for uniaxial cyclic strain of cell monolayers 66
Figure II.3. How to quantify YAP/TAZ nucleocytoplasmic ratio 67
Figure II.4. Muscle intravital microscopy set-up 70
Figure II.5. Principle of FRAP 71
Figure II.6. Metal replicas reveal the ultrastructure of biological membranes 72
Figure II.7. Different types of cytoskeletal filaments in an adherent cell 73
Figure II.8. Protocol for unroofing and metal replica of cells 74
Figure II.9. Realization of anaglyphs for 3D effect 75
Figure III.1. CCS aligning along the plasma membrane 79
Figure III.2. Distribution of clathrin and α-actinin 2 spots in mature myotubes 80
Figure III.3. Myotube membranes studded with flat clathrin-coated structures 81
Figure III.4. Colocalization between AP2 and CHC 82
Figure III.5. Partial colocalization between AP2 and Dab2 by immunofluorescence 83
Figure III.6. AP2 and Dab2 clathrin adaptors are located on clathrin plaques 83
Figure III.7. Abnormal clathrin plaques with depletion of Dab2 84
Figure III.8. Actin attached to AP2 positive structures even after latrunculin B treatment 85
Figure III.9. Arp2/3 interacts with actin surrounding clathrin plaques 86
Figure III.10. Abnormal actin assemblies around clathrin plaques in N-WASP depleted myotubes 87
Figure III.11. Defective Z-band formation in DNM2-depleted myotubes 88
Figure III.12. Interaction between N-WASP and DNM2 89
Figure III.13. DNM2 and N-WASP depletion affect clathrin-coated pits and associated actin 89
Figure III.14. CCS interact with branched actin and intermediate filaments 90
Figure III.15. Clathrin plaques aligning along the PM anchor desmin intermediate filaments 91
Figure III.16. Clathrin-coated structures at the PM are required for IF organization 92
Figure III.17. Desmin aggregates in desminopathy patient immortalized myotubes 93
Figure III.18. CHC- or AP2-depleted myotubes are filled with IF tangles 94
Figure III.19. Clathrin plaques are correctly distributed in myotubes from desmin knock-out mice 95
Figure III.20. N-WASP is required for desmin organization 96
Figure III.21. IF aggregate in N-WASP depleted myotube 96
Figure III.22. DNM2 is indispensable for desmin organization 97
Figure III.23. DNM2-depleted myotubes display desmin bundle aggregates 98
Figure III.24. DNM2 depletion causes intermediate filaments aggregation 99
Figure III.25. αB-crystallin and ArpC2 accumulate in desmin aggregates 100

Figure III.26. AP2-mCherry localizes correctly at the surface of transduced muscle 102
Figure III.27. AP2-mCherry striations are very stable in vivo 102
Figure III.28. CCS in vivo have a very dynamic turnover 103
Figure III.29. Cell stretching increases endocytic rate 104
Figure III.30. Cell stretching increases YAP/TAZ signaling 106
Figure III.31. Clathrin deletion impairs proper YAP/TAZ translocation 107
Figure III.32. Disabling endocytosis affects YAP/TAZ translocation 108
Figure III.33. YAP and TAZ interact with actin surrounding clathrin plaques 109
Figure III.34. TAZ is striated at the surface of mouse skeletal muscle fibers 110
Figure III.35. TAZ colocalize with desmin on costameres at surface of muscle fibers 110
Figure III.36. YAP does not interact with clathrin plaques components 111
Figure III.37. DNM2 interacts with TAZ 111
Figure III.38. DNM2 controls YAP/TAZ translocation in differentiated myotubes 112
Figure III.39. Expression of YAP/TAZ target genes and actin-related genes in DNM2-depleted myotubes 113
Figure III.40. Inhibiting actin polymerization or DNM2 induces a loss of YAP/TAZ signaling 115
Figure III.41. Desmin KO cells show abnormal YAP translocation 116
Figure III.42. DNM2-linked CNM mutations disorganize AP2 striation 117
Figure III.43. Plaque components disorganized in CNM mouse model 118
Figure III.44. CNM mutation impairs desmin distribution at surface of fibers 119
Figure III.45. IF tangles at the surface and around centralized nuclei in CNM animal model 120
Figure III.46. DNM2-linked mutations disorganize desmin IF network in patient muscles 121
Figure III.47. Abnormal translocation of YAP in CNM patient cells 122
Figure III.48. Down-regulation of YAP/TAZ target genes in CNM patient myotubes 123
Figure III.49. CNM mutation impairs costameric TAZ distribution 123
Figure III.50. Increased TAZ content in CNM mouse model 124
Figure III.51. DNM2-linked CNM mutations delay plaque dynamics 125
Figure IV.1. Schematic representation of a clathrin plaque 127
Figure IV.2. Actin around clathrin plaques regulate YAP/TAZ signaling 133
Figure IV.3. Schematic representation of costameric clathrin plaques 134

Table of movies

Movie 1. Stable clathrin-coated structures visualized with AAV-AP2mCherry 165
Movie 2. Clathrin structures on the surface of muscle fibers are long lived 165
Movie 3. Recovery of AP2 fluorescence in WT mouse 165
Movie 4. Recovery of AP2 fluorescence in HTZ KI-Dnm2^{R465W} mouse 165

List of tables

Table 1. Pipetting scheme for transfection of adherent cells with HiPerfect Transfection Reagent 66
Table 2. List of siRNA sequences used in the study 165
Table 3. List of primers used in the study 166
Table 4. List of antibodies 167

Abstract

Clathrin and dynamin 2 (DNM2), two key proteins of the intracellular membrane trafficking machinery, are co-expressed at specialized adhesion and force transmitting sites of muscle fibers called costameres. These assemblies, composed of several large protein complexes, link the plasma membrane to the extracellular matrix and to the contractile units of muscle. Importantly, mutations in costamere components cause several distinct myopathies. At the plasma membrane, clathrin forms large flat lattices interacting with costameric cytoskeleton. Clathrin depletion leads to defective costamere formation and induces an impairment of contractile properties. In addition, it has been shown that DNM2 mutations cause autosomal dominant centronuclear myopathy (CNM). In this project, I set out to investigate the interaction between clathrin plaques and the surrounding cytoskeleton with a particular emphasis on DNM2 contribution. By systematically combining confocal microscopy and high-resolution transmission electron microscopy on siRNA depleted mouse and human patient myotubes or by analyzing DNM2 knock-in mice and human biopsies, my work demonstrates that the compartment centered on clathrin plaques lies at the crossroads of mechanotransduction and cytoskeleton-mediated mechanosensing. I show that actin filaments surrounding mechanically sensitive clathrin plaques anchor a three-dimensional web of muscle-specific intermediate filaments and sequestrate YAP/TAZ, two nucleocytoplasmic shuttling proteins involved in muscle cell proliferation and differentiation. Importantly, my work demonstrates costameric defects *in vivo* in an heterozygous knock-in mouse model harboring the most frequent CNM mutation. By virtue of shaping both clathrin lattices and branched actin filaments, and by forming a complex with TAZ, DNM2 takes center stage as a central regulator of YAP/TAZ-mediated mechanotransduction and intermediate filament organization. This role may be the Achilles' heel of several tissues and its dysfunction may lead to additional neuromuscular disorders or other diseases where abnormal clathrin plaque assembly could perturb the fine coupling between adhesion and force transduction.

Keywords: endocytosis, clathrin, dynamin, actin, desmin, cytoskeleton, centronuclear myopathy, muscle, disease, myopathy

French abstract

La clathrine et la dynamine 2 (DNM2) sont deux protéines clés du trafic intracellulaire, qui sont toutes les deux exprimées aux costamères, des points d'ancrage membranaires spécialisés du muscle essentiels pour l'adhésion et la mécanotransduction des fibres musculaires. Ils sont constitués de complexes protéiques qui relient la matrice extracellulaire à l'appareil contractile du muscle. Des mutations dans divers composants des costamères sont à l'origine de myopathies.

La clathrine forme de grandes plaques plates sur la membrane plasmique, qui interagissent avec le cytosquelette costamérique. La déplétion de la clathrine induit des défauts de formation des costamères et une diminution des propriétés contractiles. De plus, des mutations dans la DNM2 causent la myopathie centronucléaire autosomique dominante.

Avec ce projet, j'ai cherché à examiner l'interaction entre les plaques de clathrine et le cytosquelette qui leur est associé, en mettant l'emphase sur la contribution de la DNM2. En combinant de manière systématique de la microscopie confocale et de la microscopie électronique à transmission de haute résolution sur des myotubes murins traités par ARN interférence et des myotubes humains de patients, ainsi qu'en analysant un modèle de myopathie centronucléaire due à la DNM2 et des biopsies de patients, mon travail démontre que le compartiment centré sur les plaques de clathrine se tient au carrefour de la mécanotransduction et de la mécanosensibilité liée au cytosquelette. Je montre ainsi que les filaments d'actine liée aux plaques de clathrine mécanosensibles servent de point d'ancrage à un réseau tridimensionnel de filaments intermédiaires spécifiques du muscle et séquestrent YAP et TAZ, deux protéines au trafic nucléocytoplasmique impliquées dans la prolifération et la différenciation cellulaires. Mon projet démontre les défauts costamériques présents *in vivo* dans les muscles d'un modèle de souris hétérozygote présentant la mutation dans la DNM2 la plus fréquente. En vertu de ses fonctions régulatrices des plaques de clathrine et du réseau de filaments branchés d'actine, ainsi que par son interaction avec TAZ, la DNM2 prend une place centrale en tant que régulateur de la mécanotransduction médiée par YAP/TAZ et l'organisation des filaments intermédiaires du muscle. Ce rôle pourrait s'avérer être un talon d'Achille de plusieurs tissus et son dysfonctionnement pourrait engendrer des maladies neuromusculaires ou d'autres pathologies où se trouverait perturbé cet équilibre fin entre adhésion et transduction des forces.

Mots-clés: endocytose, clathrine, dynamine, actine, desmin, cytosquelette, myopathie centronucléaire, muscle, myopathie

Abbreviations

-A-

Abp1 — Actin Binding Protein 1

AD-CNM — Autosomal Dominant CentroNuclear Myopathy

ANKRD1 — Ankyrin Repeat Domain 1

AP — Adaptor protein

ARP — Actin-Related Protein

-B-

BIN1 — Bridging Integrator 1

-C-

CCR5 — CC Chemokine Receptor 5

CCS — Clathrin-Coated Structure

CCV — Clathrin-Coated Vesicle

CHC — Clathrin Heavy Chain

CIE — Clathrin-Independent Endocytosis

CLASP — Clathrin-Associated Sorting Protein

CLC — Clathrin Light Chain

CME — Clathrin-Mediated Endocytosis

CMT — Charcot-Marie Tooth

CNM — Centronuclear Myopathy

CTGF — Connective Tissue Growth Factor

CYR61 — CYsteine-Rich angiogenic inducer 61

-D-

DGC — Dystrophin-Glycoprotein Complex

DMEM — Dulbecco's Modified Eagle's Medium

DNM1/2/3 — Dynamin 1/2/3

DRM — Desmin-Related Myopathy

-E-

ECC — Excitation-Contraction Coupling

ECM — Extracellular Matrix

EGF — Epidermal Growth Factor

EM — Electron Microscopy

ER — Endoplasmic Reticulum

-F-

FA — Focal Adhesion

FAK — Focal Adhesion Kinase

FERM — Four point one, Ezrin, Radixin, Moesin

FRAP — Fluorescence Recovery After Photobleaching

-G-

GED — GTPase Enhancing Domain

-H-

Hip1R — Huntingtin-Interacting Protein 1–Related protein

HMDS — HexaMethylDiSilazane

-I-

IF — Intermediate Filament

IP — ImmunoPrecipitation

-M-

MD — Middle Domain

MRTF — Myocardin-Related Transcription Factor

MTM1 — Myotubularin 1

-N-

NADH-TR — Nicotinamide Adenosine Dinucleotide-Tetrazolium Reductase

NPF — Nucleating Promoting Factors

-P-

PBS — Phosphate Buffered Saline

PH — Pleckstrin Homology

PI4,5P2 — Phosphatidylinositol-(4,5)-bisphosphate

PIP3 — Phosphatidylinositol (3,4,5)-trisphosphate

PM — Plasma Membrane

PRD — Proline-Rich Domain

-Q-

QF-DE-RR — Quick-Freeze Deep-Etch Rotary Replication

-R-

RPM — Rotations Per Minute

RYR — Ryanodine Receptor

-S-

SFK — Src Family Kinase

siRNA — Small Interference RiboNucleic acid

SR — Sarcoplasmic Reticulum

SRF — Serum Response Factor

-T-

TA — Tibialis Anterior

TAZ — Transcriptional co-activator with PDZ-binding motif

TEAD — Transcriptional enhancer factor TEF

TEM — Transmission Electron Microscope

TGN — Trans-Golgi Network

-W-

WASP — Wiskott-Aldrich Syndrome Protein

WWTR1 — WW Domain-containing Transcription Regulator 1

-Y-

YAP — Yes-Associated Protein

I. Introduction

1- The skeletal muscle

a. Function

With roughly 600 muscles in the body, muscle mass accounts for 40% of a person's weight. Muscle tissue is classified in one of three major categories: skeletal, cardiac, and smooth muscle. Cardiac muscle is responsible for beating of the heart and pumping blood. Smooth muscles provide majorly involuntary functions such as gut and urinary bladder movements, vessel contraction and childbirth. Striated skeletal muscles are the most common type and produce purposeful movements of the skeleton. They are necessary for voluntary movements, such as walking, but also respiration and more subtle actions like eye movement and facial expressions. They are also responsible for posture and body heat (Frontera and Ochala, 2015).

b. Development and Myofibers

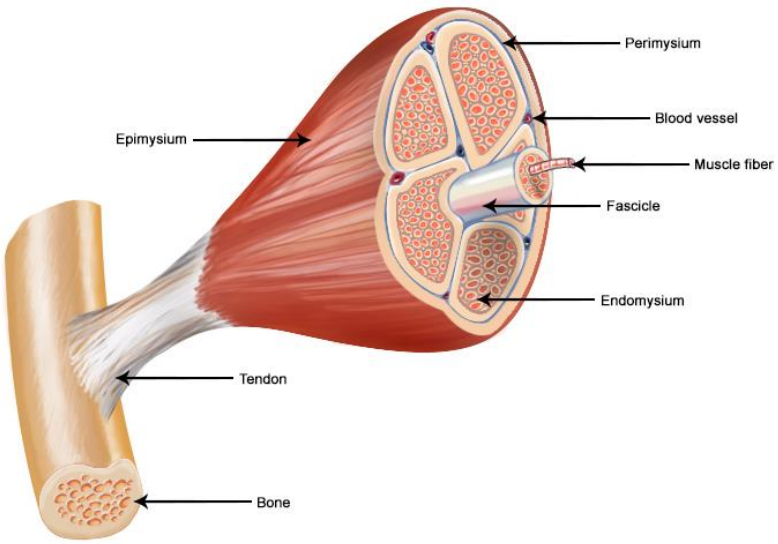

Figure I.1. Structure of the skeletal muscle

The muscle is held together by an ensemble of envelopes of connective tissue. Muscle fibers are delimited the endomysium. Several muscle fibers are wrapped in a fascicle delimited by the perimysium. Hundreds to thousands of muscle fibers are wrapped in an epimysium and connected to the bone via a tendon

SEER Training Modules, Anatomy and Physiology module. U. S. National Institutes of Health, National Cancer Institute. <https://training.seer.cancer.gov/anatomy/muscular/>.

Skeletal muscle is a peculiar tissue for a number of reasons. Myogenesis, the process of muscle formation, is not, in and of itself, typical. It involves a proliferation of committed myoblasts, which

differentiate into post-mitotic myocytes, and those myocytes then fuse into multi-nucleated myotubes. Maturation of the myotubes will give them their main function, with the development of a contractile apparatus. Further maturation and differentiation will induce very specialized and organized, multi-nucleated fibers (nuclei migrating to the periphery of muscle cells) (Bentzinger et al., 2012; Tajbakhsh, 2009). Structurally, the skeletal muscle is resistant and very organized, held together by an ensemble of envelopes of connective tissue. Each skeletal fiber is composed of one muscle cell delimited by the muscle cell plasma membrane – or sarcolemma – and surrounded by the endomysium. Several muscle fibers are wrapped in a fascicle – or fasciculus – delimited by the perimysium. Hundreds to thousands of muscle fibers are thus finally wrapped in an epimysium and connected to the bone via a tendon (**Figure I.1**).

i. A striated pattern of contractile units

In its adult state, skeletal muscle fibers have some abilities but also constraints. A great part of the cytoplasm is occupied by the contractile apparatus, which implies a different organization inside the cell compared to any other cell (**Figure I.2**).

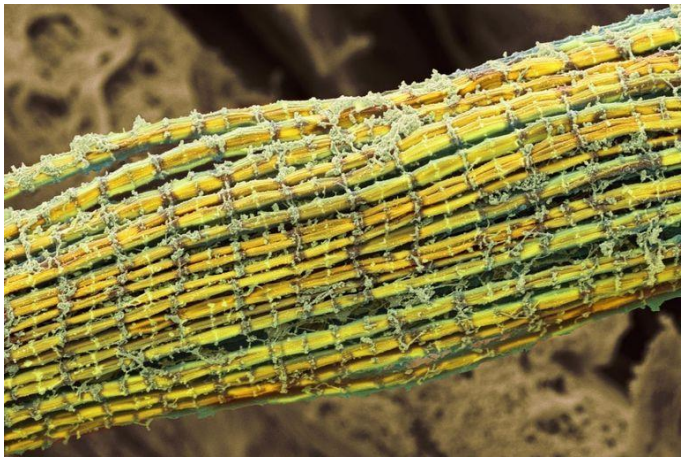

Figure I.2. Scanning electron micrograph of a muscle fiber

Colored scanning electron micrograph of a skeletal, or striated, muscle fiber. It consists of a bundle of smaller fibers called myofibrils, which are crossed by transverse tubules (green) that mark the division of the myofibrils in to contractile units (sarcomeres).

STEVE GSCHMEISSNER/Science Photo Library/Getty Images

Specialized contractile cells exhibit a banded pattern corresponding to the organization of the contractile cytoskeleton, composed of thick filaments of myosin interacting with thin filaments of actin (**Figure I.3**).

Actin microfilaments are polymers of globular actin (or G-actin) assembled to form filamentous actin (or F-actin). There exists six genes coding for different actin isoforms. Two are worth mentioning in this part covering the skeletal muscle. *ACTG1* codes for γ-actin, located to specific parts of the pattern. *ACTA1* gene encodes α-actin, a major component of the skeletal contractile apparatus.

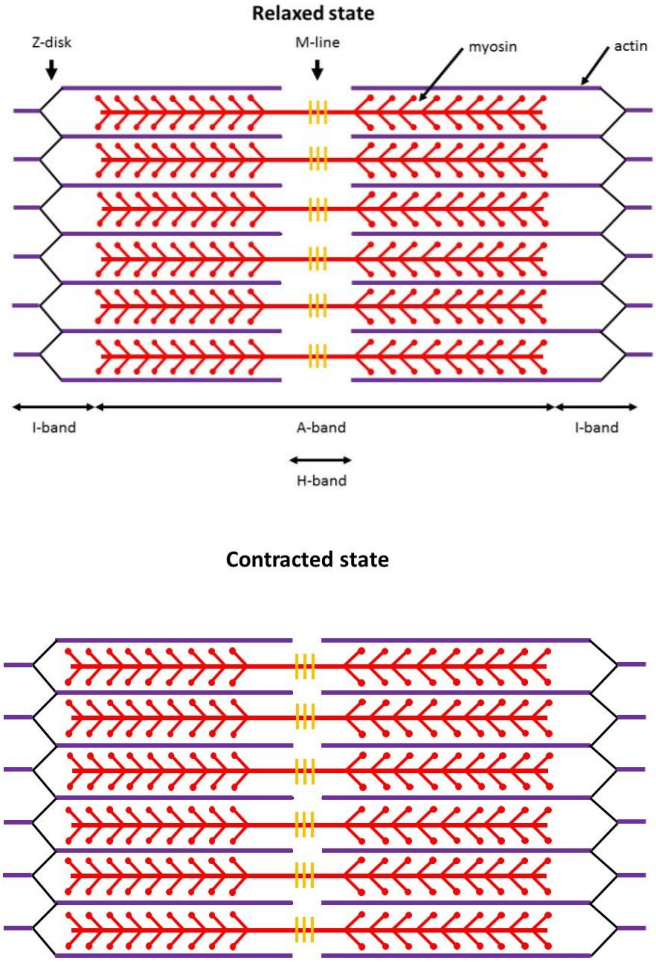

Figure I.3. Organization of the sarcomere

Sarcomeres are composed of filaments of actin and filaments of myosin that slide past each other when a muscle contracts or relaxes. Z-bands anchor actin filaments. Both the I- and H-band shorten when the sarcomeres contract.

Myosins form a family of ATP-dependent motor proteins responsible for actin-based motility. Although they are crucial for muscle contractility, they are not restricted to muscle tissue. Most myosins are composed of a head domain that binds to actin and generates force through ATP hydrolysis, a neck domain acting as a lever, and a tail domain that can bind cargo or other myosins.

Thick filaments of myosin and thin filaments of actin are arranged in repeating units called sarcomeres that form the contractile apparatus of muscle cells and appear as dark and light bands under the microscope. A single muscle cell can contain thousands of sarcomeres that are defined as the segment between two neighboring Z-lines (Z-disks, Z-discs, Z-bands). I-band (for isotropic, a clear band) contains thin filaments that are not superimposed by thick filaments. The A-band (for anisotropic, a dark band) corresponds to the entire length of a thick filaments. The H-band (for "heller" meaning "brighter" in German) is defined by thick filaments that are not superimposed by thin filaments. And finally, in the middle of the sarcomere is the M-line (**Figure I.3**).

Z-lines define the lateral boundaries of sarcomeres. They are electron dense bands of varying size by electron microscopy (EM). Early works attributed the presence of α-actinin to Z-lines (Masaki et al., 1967; Stromer and Goll, 1972; Yamaguchi et al., 1983). This protein belongs to the spectrin gene superfamily and is an actin crosslinking protein. The exact composition of the complex and densely packed Z-lines was later deciphered, notably with the discovery of titin (or connectin) (Maruyama et al., 1977) and nebulin (Horowits et al., 1986; Wang and Wright, 1988). Proteins like titin span a large portion of the sarcomere and many other proteins interact with Z-lines, making it one of the most complex macromolecular structures in biology (Zou et al., 2006). This explains why the integrity of Z-lines is so vital to the function of the muscle and why defects in any of these numerous proteins can induce "discopathies" (Knöll et al., 2011). Z-lines are not only essential to maintain muscle's structure, but it appeared progressively that they could also be involved in mechanotransduction and signaling to the nucleus (Clark et al., 2002; Frank et al., 2006) (*cf* I.1-c Mechanotransduction).

ii. Excitation-contraction coupling

In skeletal muscle, the excitation-contraction coupling (ECC) machinery mediates the communication between electrical events transmitted by the motor neuron and intracellular calcium release by the sarcoplasmic reticulum (SR), inducing muscle contraction. ECC requires a highly specialized membrane structure, the triad, composed of a central plasma membrane (PM) invagination, the T-tubule, surrounded by two sarcoplasmic reticulum terminal cisternae. Propagation of the action potential in the T-tubule leads to the detection of membrane potential changes by dihydropyridine receptors, connected to ryanodine receptors on the SR membrane. The SR releases Ca^{2+} which initiates muscle contraction (Calderón et al., 2014). The process of muscle contraction is explained with the sliding filament theory (Huxley and Niedergerke, 1954; Huxley and Hanson, 1954). With muscle contraction, Z-lines come closer together while the A-bands remain the same size. This is achieved by the sliding of myosin heads over actin thin filaments which are tethered to Z-lines. Myosin performs a "molecular dance" on actin filaments. ADP bound to the globular end of myosin – or S1 segment – form a cross-bridge with actin filaments (Hynes et al., 1987). They undergo a powerstroke: the myosin filament changes its angle, pulling back on the actin and releasing ADP in the process. This causes the sarcomere to shorten. Myosin detaches from actin when a new ATP molecule binds to it. ATPase catalyzes the breakdown of ATP in ADP, returning myosin heads in the resting state (Lorand, 1953).

iii. Costameres

Muscle is a tissue which undergoes an enormous amount of deformation each times it is solicited. Therefore a strong cohesion between the different parts of this complex arrangement is needed to ensure muscular maintenance and proper function.

Scientists observed contracting cells and identified regularly spaced "wrinkles" that appeared at very specific sites. Pardo and colleagues (Pardo et al., 1983a) coined the name "costameres" from Latin *costa*, rib, and Greek *meros*, part. Costameres are specialized muscular focal adhesion-like complexes associated with Z-lines, which gives them this rib-like appearance. Focal adhesions (FAs) represent the major site of cell attachment where a structural and functional link between the extracellular matrix (ECM) and the intracellular actin cytoskeleton occurs. They are composed of macromolecular complexes formed by transmembrane receptors, structural and signaling proteins. At costameres, this complex of numerous proteins which appears dense on EM pictures, ensures structural integrity of muscle fibers and force transmission (Danowski et al., 1992; Pardo et al., 1983b, 1983a; Shear and Bloch, 1985).

In recent years, function and molecular composition of costameres have been further specified. They are composed of several large membrane protein complexes that are linked to the contractile apparatus by intermediate filaments, playing both a mechanical and signaling role during contraction (**Figure I.4**). Two complexes are typically described at the costamere. The dystrophin-glycoprotein complex (DGC) involves dystrophin and a series of proteins such as sarcoglycans and dystroglycans. This complex provides structural support to the sarcolemma by linking contractile elements to the ECM. The vinculin-talin-integrin complex is essential for the linkage of actin to the PM via vinculin and talin, while integrins α and β mediate signaling. γ-actin is localized to Z-discs and costameres of skeletal muscle and is responsible for force transduction and transmission in muscle cells. As such, costameres physically couple force-generating sarcomeres with the sarcolemma, and also form a two-way signaling highway between Z-lines and the extracellular matrix (ECM) (Peter et al., 2011).

Force transmission in the muscle can occur longitudinally (from one sarcomere to the other) or perpendicularly (between costameres until the ECM is reached). Perpendicular – or lateral – force transmission accounts for up to 80% of the force generated by sarcomeres and sustained by costameres (Peter et al., 2011). Early on, costameres were identified as being major sites for force transmission (Craig and Pardo, 1983; Danowski et al., 1992), and it was already thought that small changes or malfunctions in any of their components could have dramatic consequences for muscle integrity (Shear and Bloch, 1985).

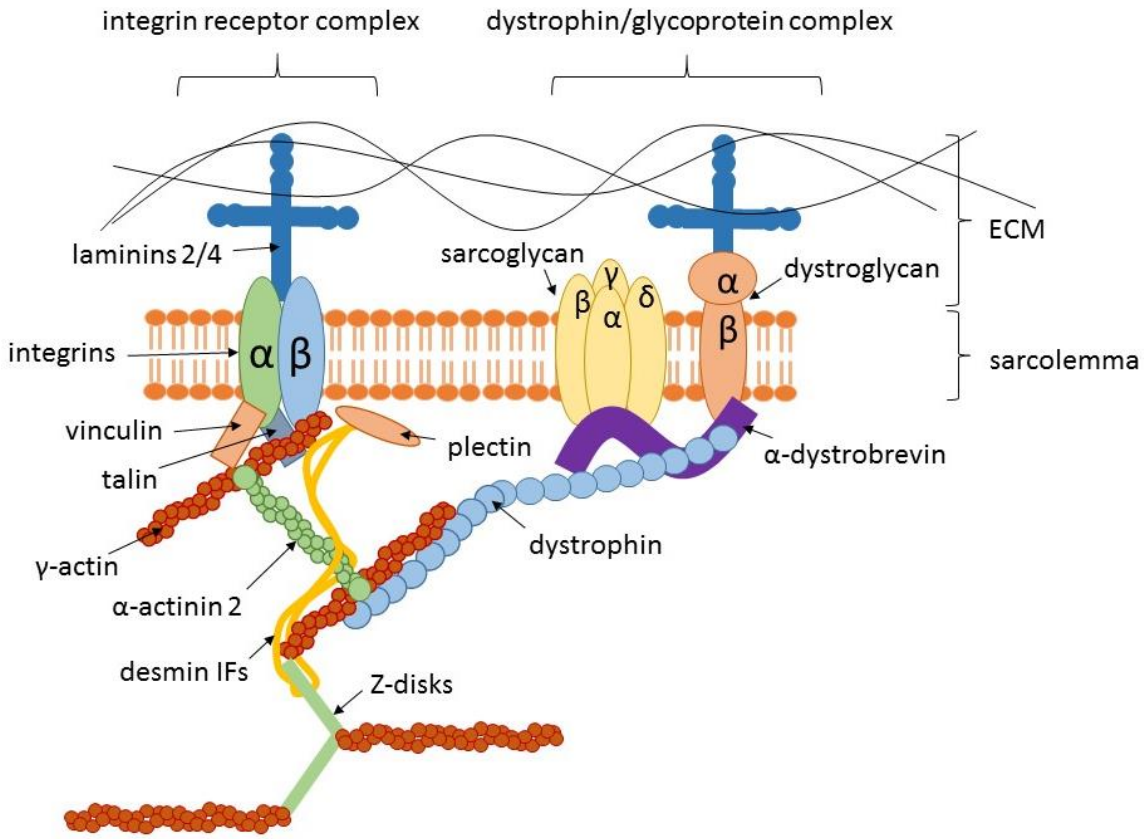

Figure I.4. Schematic representation of a costamere

Two laminin receptors, a dystrophin/glycoprotein complex and an integrin receptor complex are among the sarcolemmal structures that link the contractile apparatus of muscle fibres with the surrounding basal lamina. Components of both receptors co-localize in subsarcolemmal complexes which connect through γ-actin and intermediate filaments to the Z-disc of skeletal muscle fibers.

Since then, many mutations have been identified in key components of costameres and associated with muscle diseases, such as Duchenne muscular dystrophy. Costameres provide structural and functional support to the entire muscle fiber, thus they are of critical importance and have been considered the "Achilles' heel" of muscles (Ervasti, 2003; Peter et al., 2011).

iv. Intermediate filaments

Intermediate filaments (IFs) can vary in composition but are a type of cytoskeletal filaments that share common structural and sequence features. They measure about 10 nm in diameter. Their oligomerization and composition vary depending on the tissue they are situated in, thus harboring different functions depending on the tissue's specific needs. Different types of intermediate filaments are defined by a certain similarity between one another in terms of sequences and

structure. For example, keratins bind to each other to form type I and II intermediate filaments, which help epithelial cells resist mechanical stretch. Neurofilaments are type IV intermediate filaments that are incorporated in the axon of developing neurons and are thought to provide structural support for their growth. Most types of IFs are cytoplasmic but lamins are nuclear, type V IFs, providing structural and transcriptional regulation to the nucleus.

In skeletal muscle, the IF cytoskeleton is mainly composed of the type III IF protein desmin. Desmin is composed of three major domains, an alpha helix rod, a variable non alpha helix head, and a carboxy-terminal tail, and desmin proteins are able to assemble to form homopolymers (Goldfarb et al., 2008). Two parallel monomers form a dimer, which then align with another dimer to form a tetramer. Two sets of antiparallel tetramers will then form a protofilament. A protofilament bundling with seven other protofilaments give the final 10 nm wide IF (**Figure I.5**).

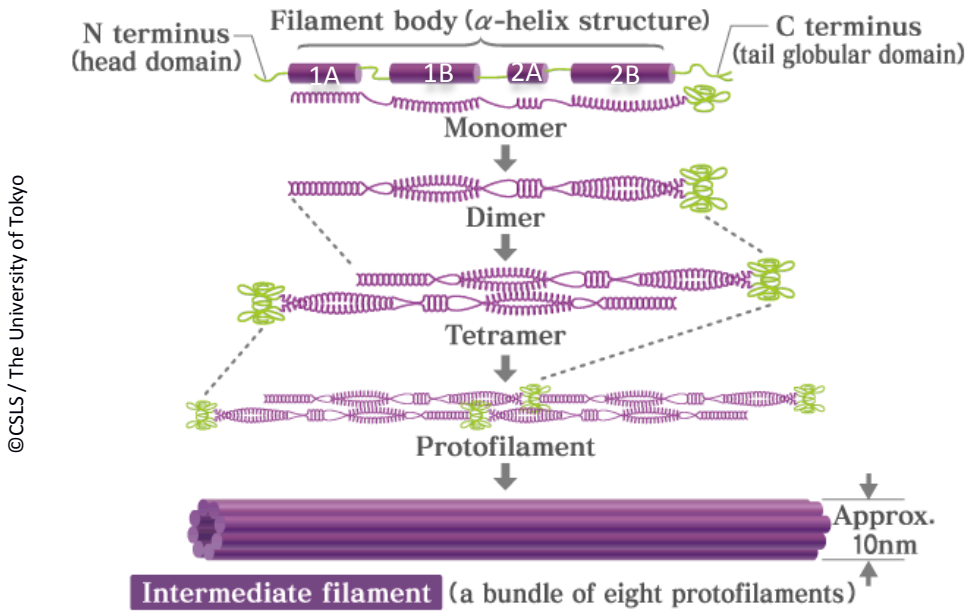

Figure I.5. Formation and structure of desmin intermediate filaments

Sequential assembly of desmin proteins to form type III desmin IFs.

Muscle specific desmin IFs span the entire width of the myofiber, from the sarcolemma to the nucleus (**Figure I.6**) (Capetanaki et al., 2015).

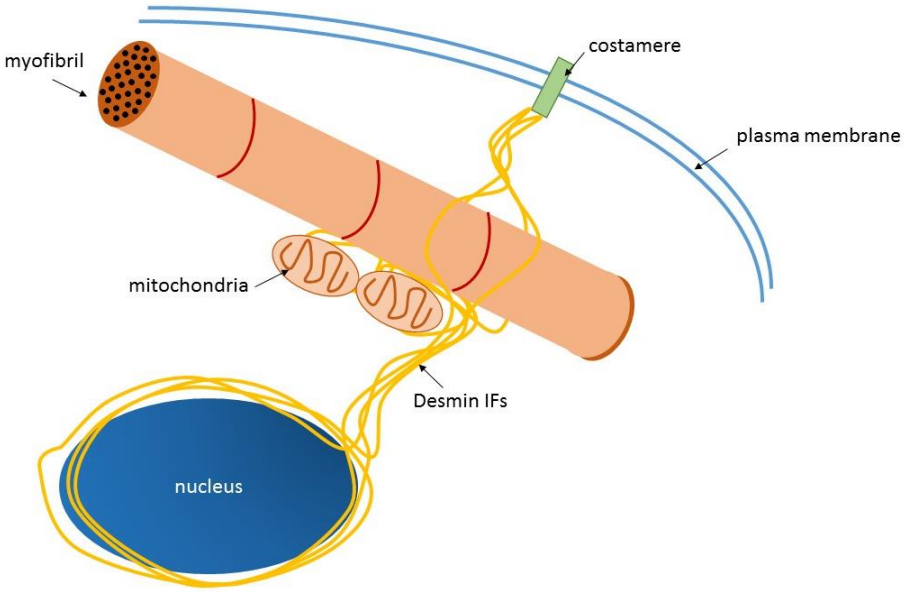

Figure I.6. Schematic representation of the desmin intermediate filament network

The intermediate filament cytoskeleton of skeletal muscle is mainly composed of the type III IF protein desmin. They are connected to the plasmalemma via the costamere and interacting with the entire length of the Z-disk, and enclosing intracellular organelles like mitochondria and the nucleus.

Although they are not necessary for myogenic commitment or differentiation, IFs are essential for cell architecture, force transmission and organelle positioning (Li et al., 1997; Paulin and Li, 2004; Shah et al., 2004), and ablation of desmin by gene targeting induces major defects in the architectural and functional integrity of skeletal muscles (Li et al., 1996). Striated muscle of mice lacking muscle-specific desmin IFs exhibits numerous structural and functional abnormalities (Li et al., 1997; Milner et al., 1996). Most notably, desmin$^{-/-}$ muscle is weak and fatigued more easily (Sam et al., 2000) and lateral force transmission is greatly diminished (Boriek et al., 2001).

Mutations in the desmin (*DES*) gene (Dalakas et al., 2000), or that of its chaperone protein αB-crystallin (*CRYAB*) (Vicart et al., 1998), cause several myopathies belonging to the desmin-related myopathy (DRM) group of IF diseases (Omary et al., 2004). At least 53 mutations in the *DES* gene have been identified, the majority being inherited missense mutations, mostly located in the 2B domain that affect the correct assembly of desmin filaments (Goldfarb et al., 2008; van Spaendonck-Zwarts et al., 2011).

Desminopathies are mostly characterized by weakness in the leg, facial, trunk, and respiratory muscles, but mostly also by cardiac phenotypes, with cardiomyopathy accompanied by cardiac conduction defect (Dalakas et al., 2000; Kostera-Pruszczyk et al., 2008). The pathophysiological implications of *DES* mutations are still being studied. Mostly, its inability to interact with key Z-

disks partners could trigger disease development. Another hypothesis states that some mutations could directly alter the intrinsic biophysical properties of desmin filaments (Bär et al., 2010). However, the most common phenotype at the cellular level is the disruption of the desmin network and accumulation of dense inclusion bodies, granulofilamentous in nature, that stain positive for desmin (**Figure I.7**). Large intracellular aggregates of desmin interfere with a broader spectrum of cellular functions such as organelle positioning and signaling (Clemen et al., 2013).

Mutations in the desmin chaperone protein αB-crystallin gene (*CRYAB*) are also responsible for DRMs, and the first missense mutation identified in *CRYAB* was identified in a muscle biopsy from a DRM patient showing intracellular inclusions positive for desmin but with normal desmin expression. αB-crystallin belongs to the small heat shock protein family and is found in large quantities in the lens but also in a lesser extent in cardiac and skeletal tissue (Dubin et al., 1990). By binding to desmin, it inhibits its assembly, and is paramount for the equilibrium between soluble and filamentous desmin (Nicholl and Quinlan, 1994). Defective in its chaperone function, mutations in αB-crystallin therefore lead to abnormal desmin aggregates accumulating in muscle fibers (Bova et al., 1999).

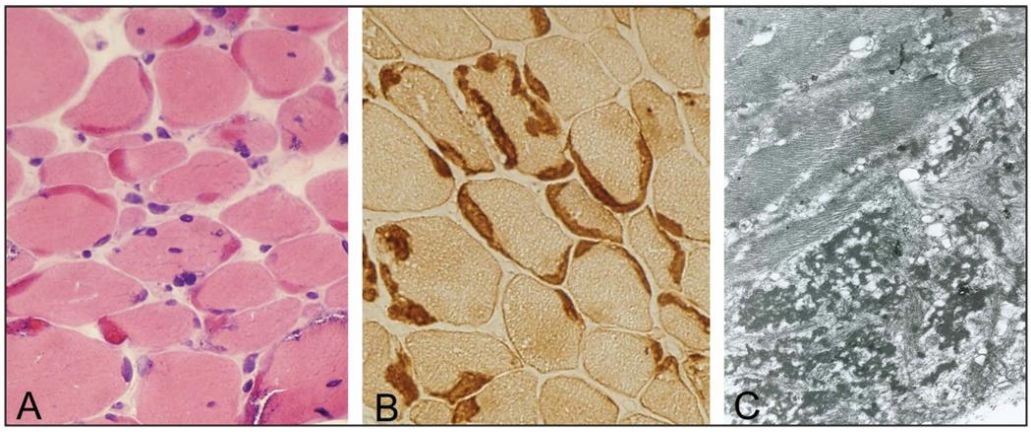

Figure I.7. Muscle phenotype of desmin mutation

Muscle pathology in a patient with homozygosity for the p.Arg173_Glu179del *DES* mutation. Prominent eosinophilic masses located under the sarcolemma and sometimes associated with basophilic granular material (A), displaying strong desmin immunoreactivity (B). By electron microscopy, the masses are composed of a matrix of dense granulofilamentous material (C). Cryostat sections, original magnification in A and B × 200; C × 5000. Figure by Dr. Ana Cabello, from (Goldfarb et al., 2008)

In fact, most of the IFs present in skeletal muscle span the Z-lines. Other IF proteins identified and present in smaller quantities can form copolymers with desmin. We will cite synemin and paranemin (Granger and Lazarides, 1980; Price and Lazarides, 1983). Other IF proteins, nestin and syncoilin, are expressed and especially important at a specialized sites of neuron-muscle

contact sites called the neuromuscular junction (Carlsson et al., 1999; Newey et al., 2001). Adult-muscle IFs also contain members of the cytokeratin family, namely cytokeratins 8 and 19. Present at costameres, they link the contractile apparatus to dystrophin (Ursitti et al., 2004).

Generally, IFs link the contractile apparatus via adaptors such as plectin which allow the interaction with actin, however the exact nature of these interactions remain elusive.

Recently, M. Palmisano and colleagues (San Diego, California) showed that a desmin-null model displayed a decrease in nuclear deformation following cell stretching and lower mechanical function, evidenced by a lower force drop after high-stress contractions (Palmisano et al., 2015). Thus, by linking the nucleus to the PM, desmin IFs are thought to be major players in the transmission of signals from the ECM to the nucleus. This process of transmission of mechanical signals and translation into cellular responses concerns mechanotransduction.

c. Mechanotransduction

Cells constantly integrate information from the physical nature of their environment via different stimuli. These mechanical stimuli need to be converted into signals that can be passed on through the cell all the way to the nucleus which will send an adaptive response. This translation of mechanical into chemical message and cytoskeletal reorganization is the process of mechanotransduction. At the cellular level, mechanical forces influence cytoskeletal organization, gene expression, proliferation and survival. It is of critical importance in skeletal muscle since converting mechanical cues into signals that the cell can interpret is necessary both for development and maintenance of the muscle, an organ that is highly subjected to mechanical stress.

Costameres constitute a major site of force transmission via dystroglycans and integrins. Following mechanical stimulation, several major cellular signaling cascades get activated, through mechanisms that are still largely unknown (Burkholder, 2007).

i. Integrin-mediated mechanotransduction

Integrin-mediated mechanotransduction is a wide field of research, and not confined to skeletal muscle. By linking the ECM to the intracellular cytoskeleton at adhesion sites, integrin-mediated adhesions are intrinsically mechanosensitive and present everywhere in the body.

Integrins are heterodimeric transmembrane receptors composed of an α and a β subunit. There exists at least 18 α subtypes and 8 β subtypes that can generate 24 different binding pairs, allowing a certain adaptation and specialization of cell adhesions depending on the needs (Hynes,

2002). Mechanical-induced conformational changes produce a shift between low- to high-affinity binding for ligands. Upon ligand binding, integrins are able to recruit various proteins that differ depending on the subcellular location of the adhesion structures and the tissue. Via integrins, mechanical stretch on integrins can activate cell proliferation, migration, and direct remodeling of the cytoskeleton.

Major cellular and biophysical studies have focused on α5β1 integrins. The change in conformation subsequent to mechanical stimulation promotes talin binding, bridging the actin cytoskeleton to focal adhesion sites (Martel et al., 2001). The formation of focal adhesion is under the control of small GTPase Rho (Ridley and Hall, 1992). The stabilized actin-integrin-talin complex then allows binding of signaling proteins to integrin tails, such as kinase family members Focal Adhesion Kinase (FAK) (Schaller et al., 1992), paxillin (Mofrad et al., 2004), Src-family kinases (SFK), and zyxin (Beckerle, 1997; Yi et al., 2002) (**Figure I.8**).

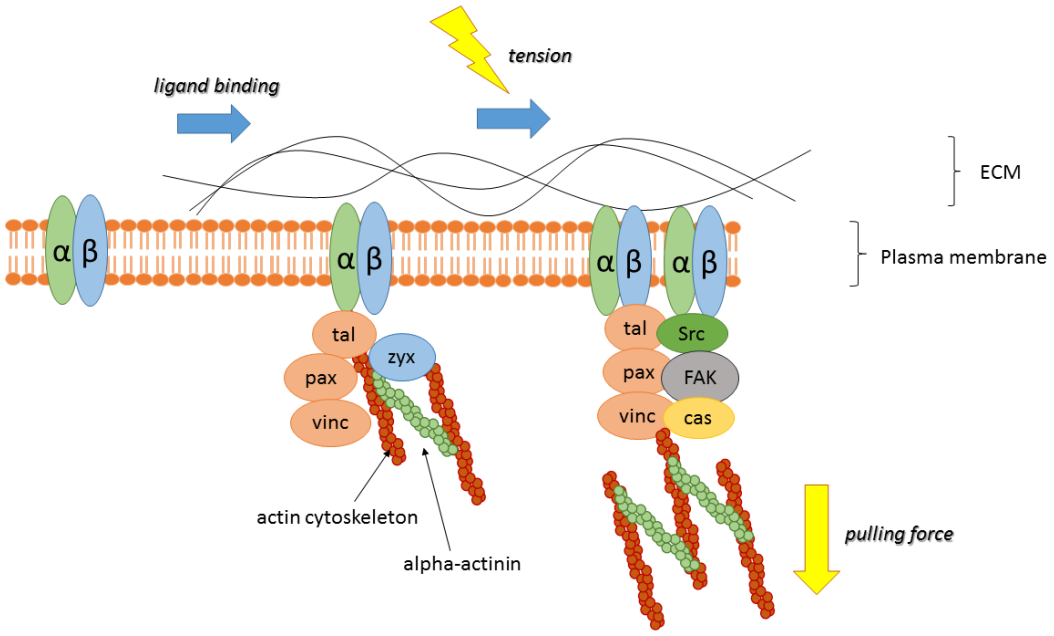

Figure I.8. Progressive recruitment forming focal adhesions

Adhesions initially contain integrins, talin (tal), paxillin (pax) and low levels of vinculin (vinc) and focal adhesion kinase (FAK). The recruitment of vinculin along with talin promotes the clustering of activated integrins, forming a flexible bridge between the receptors and the actin network. Through a tension-dependent process, the maturation of stress fibers induces a redistribution of zyxin (zyx) to thicken them and regulates adhesion reinforcement.

FAK is necessary for inactivation of Rho, a small signaling G protein involved in cytoskeletal regulation, and promotion of focal adhesion turnover (Ren et al., 2000). FAK binding to Src and subsequent phosphorylation cascades also initiate multiple downstream signaling pathways (Zhao and Guan, 2011). SFK induced phosphorylation of p130Cas subsequently serves as a docking hub for downstream signaling molecules (Sawada et al., 2006; Tamada et al., 2004).

Importantly, activation of these mechanosensitive proteins control, activate and modulate the formation of branched actin networks, Rho-Rock-dependent contractile actomyosin bundles (Sun et al., 2016) and vinculin-based protrusion and force generation (Hirata et al., 2014). As we will see in the next parts, remodeling of the actin cytoskeleton can have dramatic effects on cell regulation even at the transcriptional level.

ii. YAP/TAZ pathway

Two recently identified key mechanotransduction players are Yes-associated protein (YAP) (Sudol, 1994) and Transcriptional co-activator with PDZ-binding motif (TAZ) also named WW Domain-containing Transcription Regulator 1 (WWTR1) (Dupont et al., 2011; Kanai et al., 2000). Both are transcriptional cofactors that can shuttle between the cytoplasm and the nucleus in response to mechanical cues from the ECM (Aragona et al., 2013; Halder et al., 2012). They were originally described as parts of the Hippo pathway.

The core of the Hippo pathway consists of a kinase cascade, transcription coactivators, and DNA-binding partners. It mainly regulates cell proliferation, differentiation and migration depending on different cues, such as cellular energy status, and mechanical or hormonal signals (Meng et al., 2016). When the Hippo pathway is inactive, YAP and TAZ are unphosphorylated and localized in the nucleus where they can bind to transcriptional enhancer factor TEF (TEAD) and activate target gene transcription (Zanconato et al., 2015). The Hippo pathway can be activated to phosphorylate MST1/2, which in turn phosphorylates LATS1/2. Phosphorylation of LATS1/2 leads to a phosphorylation of YAP and TAZ on S127 (S89 in TAZ) or S381 (S311 in TAZ), leading to 14-3-3-mediated YAP and TAZ cytoplasmic retention and/or YAP and TAZ degradation (Zhao et al., 2010). A simplified version of the pathway can be found in **Figure I.9**.

Although regulation of YAP/TAZ can be mediated by phosphorylation, it has come to light that inhibition of LATS1/2 only had a marginal effect on YAP/TAZ activation (Dupont et al., 2011), and that their reactivation after contact inhibition is possible by stretching (Pathak et al., 2014), suggesting that YAP/TAZ can be activated via purely mechanical means and independently of the Hippo pathway (**Figure I.10**).

Figure I.9. A model of the Hippo pathway

Hippo signaling is an evolutionarily conserved pathway that controls organ size by regulating cell proliferation, apoptosis, and stem cell self-renewal. When the Hippo pathway is inactive, YAP and TAZ are unphosphorylated and localized in the nucleus to activate gene transcription. The Hippo pathway induces phosphorylation of kinase MST1/2, which in turn phosphorylates LATS1/2. Phosphorylation of LATS1/2 leads to a phosphorylation and subsequent inhibition of YAP and TAZ, by leading to 14-3-3-mediated YAP and TAZ cytoplasmic retention and/or degradation.

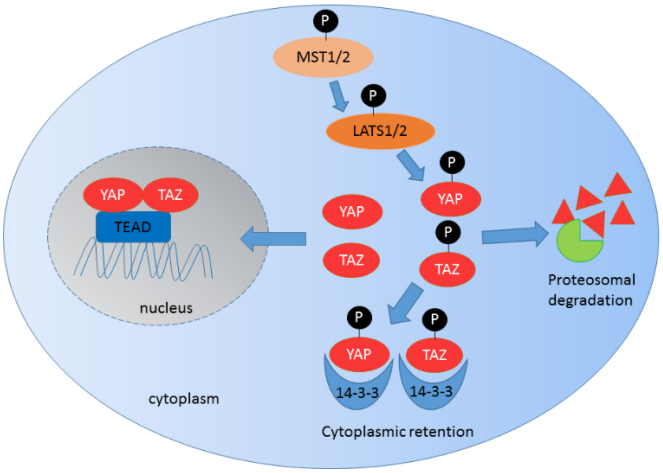

There is still a lot to learn about the mechanical regulation of YAP/TAZ. Although the activity of YAP/TAZ depends on F-actin structures enriched in adherent cells (Aragona et al., 2013; Das et al., 2016), the precise nature of the compartment that YAP and TAZ associate with is currently unknown. It has been described that YAP/TAZ mechanical regulation can be achieved by two means. Indeed, mechanical tension in cell layers can be split in two distinct structures: cell-cell contacts that link adjacent cells and cell-ECM adhesions. YAP and TAZ are generally nuclear in proliferating cells and excluded from the nucleus by cell-cell contact inhibition or by a change in ECM stiffness. Generally, tension through these structures exerts forces on cortical actomyosin fibers. Several teams suggested a role of actomyosin contractility on YAP activation. Using optogenetics, researchers showed that targeting of the small GTPase RhoA to the PM induced increased cellular traction and nuclear translocation of YAP. Reversely, YAP was translocated back to the cytoplasm when RhoA was inhibited (Valon et al., 2017).

Several regulatory pathways are at play. YAP/TAZ are cytoplasmic when cells are plated on a soft substrate (0.7 kPa) but inhibition is lifted when cells are able to spread on a stiffer surface (Dupont et al., 2011). On a soft substrate, YAP/TAZ allows cells to maintain their pluripotency potential by inhibition of the Notch pathway, a highly conserved signaling pathway regulating differentiation (Totaro et al., 2017), and it was shown that YAP/TAZ are inactivated to induce stem cell differentiation (Lian et al., 2010).

Concerning cell adhesion to the substrate, YAP regulation was linked to focal adhesions. Researchers identified the FAK-Src pathway as a negative regulator of YAP activation. Namely cell attachment to fibronectin induced YAP nuclear accumulation that was reduced by FAK or Src inhibition (Kim and Gumbiner, 2015). Regulation of FAK during durotaxis, a form of cell migration that depends on substrate rigidity, was linked to YAP translocation in a very recent study

(Lachowski et al., 2017). Authors showed that in fact, YAP nuclear translocation in response to stiffness required FAK activity.

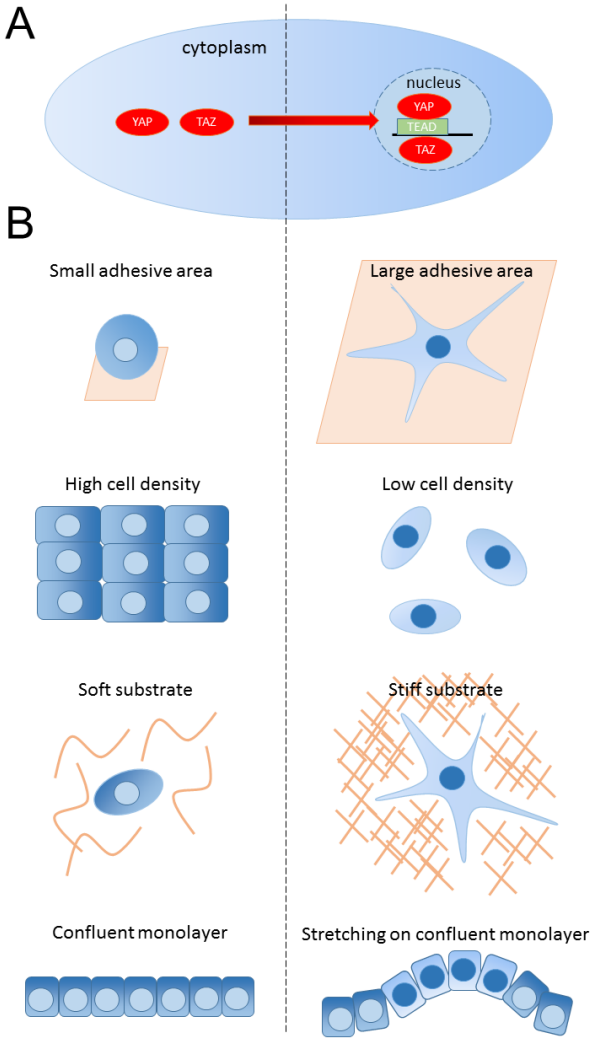

Figure I.10. Mechanical stimuli influencing YAP and TAZ subcellular localization and activity

(A) When YAP and TAZ are mechanically activated, they translocate to the nucleus, where they interact with TEAD factors to regulate gene expression. (B) Schematics illustrating how different matrix, geometry and physical conditions influence YAP and TAZ localization and activity: the left panels show conditions in which YAP and TAZ are inhibited and localized to the cytoplasm, whereas the right panels show conditions that promote YAP and TAZ nuclear localization (indicated by bluer coloring of cell nuclei).

Regulation of YAP/TAZ through cell-cell contacts involves proteins that are part of adherens junctions. Adherens junction proteins such as cadherins and α-catenin form complexes on the PM that help sequestrate YAP/TAZ, thereby inhibiting their activity. H. Hirata and colleagues found a supplementary regulation of YAP in keratinocytes. They showed that tensile forces mediated by RhoA inhibited YAP-driven proliferation in layers of keratinocytes, and found this regulation especially important in multilayered cell systems (Hirata et al., 2017).

Another protein responsible for YAP inhibition at cell-cell contacts is Merlin, also called NF2. It is a FERM (Four point one, Ezrin, Radixin, Moesin)-domain containing protein involved in the establishment of cell polarity. Proteins with a FERM-domain are involved in the regulation of the dialogue between membrane complexes and cortical actin (Fehon et al., 2010). At adherens junctions, Merlin interacts with E-cadherin, β-catenin, α-catenin as well as cortical actin, and is

thought to be a tumor-suppressor and an important regulator of YAP. Inactivation of Merlin induced abnormal cell proliferation that led to hepatocellular carcinoma and bile duct hamartoma, phenotypes that were alleviated by heterozygous deletion of *Yap* (Zhang et al., 2010).

Although the YAP/TAZ field is still in its infancy, there begins to be an important amount of data suggesting a mechanical regulation of YAP/TAZ independent of the Hippo pathway.

Muscle cells being highly sensitive to their environment and subjected to several stresses, one can ponder how are YAP/TAZ particularly regulated in muscle cells? It has been established that in proliferating myoblasts, YAP/TAZ are located in the nucleus where they act as coactivators for several transcription factors including TEAD factors and promote proliferation (Watt et al., 2010). However, during differentiation, both translocate from the nucleus to the cytoplasm thus inhibiting their transcriptional function (Watt et al., 2010), but mechanical cues such as cell stretching can cause YAP/TAZ translocation back into the nucleus (Fischer et al., 2016).

As such, YAP/TAZ mechanotransducers were first thought to be involved in muscle mass regulation. Skeletal muscle mass reflects a dynamic turnover between net protein synthesis and degradation. Fibers can also enlarge with an increased fusion of muscle stem cells called satellite cells. The Hippo-YAP pathway was introduced recently as a regulator of muscle mass through its links with the mTOR pathway (Csibi and Blenis, 2012). Even more recently, YAP was introduced as a direct regulator of muscle mass via its interaction with TEAD. It was shown to be required to maintain muscle size and also induce muscle repair after muscle injury (Watt et al., 2015). Interestingly, while certain studies suggested that expression of YAP could correct defects in hypotrophic muscles (Watt et al., 2015), another study suggested that constitutive expression of YAP in muscle induced hypotrophy and structural defects resembling that of centronuclear myopathies (Judson et al., 2013). Considering the growing evidence of a regulation of YAP/TAZ by mechanical factors and potential effects of their dysregulation on muscle, one can wonder the implications of this pathway regarding the development of myopathies.

iii. MRTF-SRF

Serum response factor (SRF) is a ubiquitous transcription factor, functioning with myocardin-related transcription factors A and B (MRTFs), and is involved in the regulation of most cytoskeletal genes (Esnault et al., 2014; Olson and Nordheim, 2010; Yu-Wai-Man et al., 2017). MRTF-A and MRTF-B are bound to G-actin and thus respond to variations of G-actin concentration induced by Rho GTPase signaling (Vartiainen et al., 2007). F-actin polymerization occurring during mechanical stimulation reduces the amount of G-actin and releases MRTFs to activate SRF–mediated transcription (Miralles et al., 2003). Integrin-mediated force in fibroblasts was shown

to induce RhoA activation and subsequent MRTF nuclear translocation (Zhao et al., 2007). SRF activation by MRTFs activates numerous essential gene responses including actin dynamics, lamellipodial/filopodial formation, integrin-cytoskeletal coupling, myofibrillogenesis, and muscle contraction (Esnault et al., 2014; Miano et al., 2007; Posern and Treisman, 2006). There exists a crosstalk between YAP/TAZ and MRTF/SRF pathways. Interestingly, an in-depth study of MRTF/SRF transcriptional target genes showed an overlap with YAP target genes, including *CTGF* (connective tissue growth factor), *CYR61* (cysteine-rich angiogenic inducer 61), and *ANKRD1* (ankyrin repeat domain 1), and several actin genes that are frequently used as readouts for YAP activation (Esnault et al., 2014). One study found that MRTF/SRF and TAZ were actually downstream effectors of Heregulin β1, protein interacting with mitogen-activated protein kinase (MAPK) and phosphoinositide 3-kinase (PI3K) and promoting proliferation, angiogenesis and invasion of cancer cells (Liu et al., 2016). There was even proof of a direct interaction between MRTF family proteins and YAP (Kim et al., 2017).

While the MRTF/SRF pathway has been extensively studied in the context of cancer, it was also examined in muscle, where it was shown to activate certain regulatory – growth and differentiation – genes in skeletal, smooth, and cardiac muscle (Belaguli et al., 1997). Study of SRF in muscle cells under straining conditions showed that a moderate strain leads to rapid accumulation of MRTF in the nucleus (Montel et al., 2014). It was shown that actin dynamics are essential to activate this pathway in muscle, which in turn regulates vinculin, actin and SRF itself (Sotiropoulos et al., 1999).

2- Membranes and vesicular trafficking

a. The Cell Theory

Magnification technology allowed the crafting of the Cell Theory over centuries, starting in the 1600s. The first official appearance of the word cell occurred in Robert Hooke's *Micrographia* (Hooke, 1667) (**Figure I.11**).

I took a good clear piece of Cork, and with a Pen-knife sharpen'd as keen as a Razor, I cut a piece of it off, and thereby left the surface of it exceeding smooth, then examining it very diligently with a Microscope, me thought I could perceive it to appear a little porous; [...] Next, in that these pores, or cells, were not very deep, but consisted of a great many little Boxes, separated out of one continued long pore. […]

me thinks, it seems very probable, that Nature has in these passages, as well as in those of Animal bodies, very many appropriated Instruments and contrivances, whereby to bring her designs and end to pass, which 'tis not improbable, but that some diligent Observer, if help'd with better Microscopes, may in time detect.

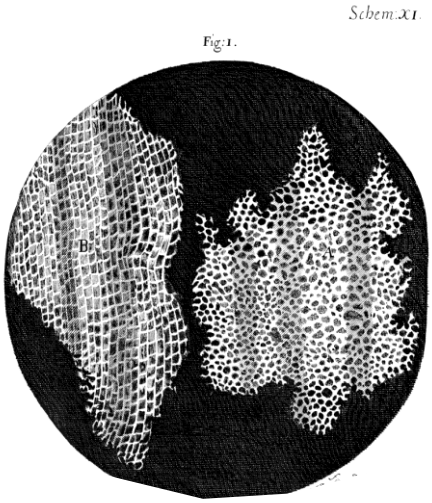

Figure I.11. Suber cells

Drawing of a piece of cork observed by one of the first microscopes (Hooke, 1667).

Although its official author is still debated (Turner, 1890), nowadays biologists agree about the three tenets of the Cell Theory:

1- Living organisms are composed of one or multiple cells.

2- The cell is the basic unit of structure in organisms.

3- Cells arise from pre-existing cells.

All modern day cells present a cell membrane. It is postulated that the first cell appeared after a membrane formed around a self-replicating mixture of RNA and protein in the prebiotic soup. And although cells and their envelopes have been studied as early as the 1600s, it was only much later that the proposed models of PM as a lipid bilayer appeared (Gorter and Grendel, 1925) and as a fluid phase mosaic (Singer and Nicolson, 1972). Its study is now a major field of research in cell biology.

b. Membrane trafficking

Cell specialization allowed the development of larger cells compartmentalized depending on function. This created new problems, mainly the need for communication between different organelles. Vesicles are sent between cellular areas to exchange materials (Palade, 1975). It is a complex trafficking, usually simplified as a bidirectional runway going to and from the PM (**Figure I.12**).

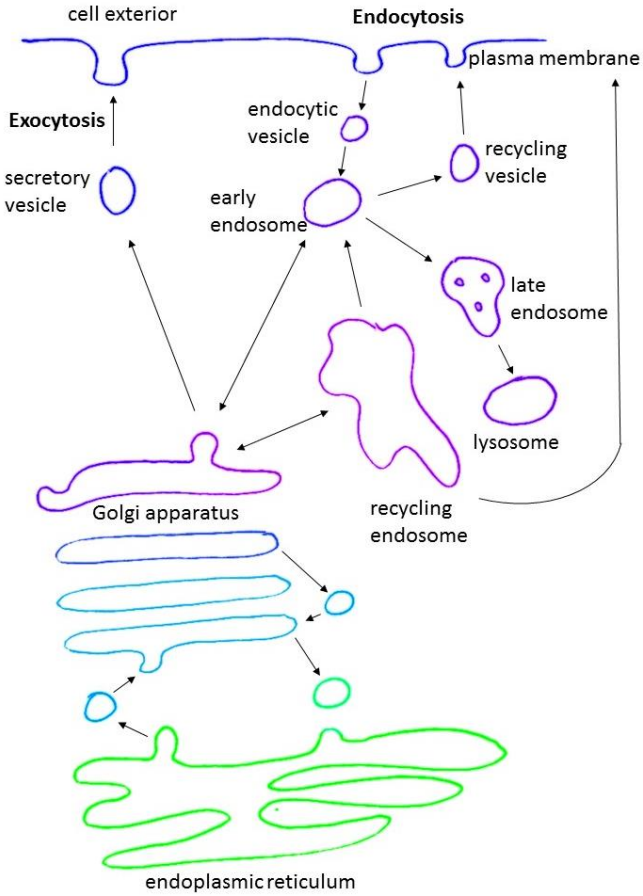

Figure I.12. Overview of cellular trafficking pathways

Vesicles are membrane-bound compartments that shuttle proteins and molecules between different specialized areas of the cell. Molecules and ligands internalized from the PM via the process of endocytosis can follow the pathway to the lysosome where they will be degraded or recycle back to the PM. They can also be transported to the Golgi apparatus. Cells can excrete proteins and molecules by the process of exocytosis.

Intracellular trafficking is based on two principles, the selection of cargo and budding of membrane, mediated by membrane coats. These are composed of cytosolic proteins that can bind to each other as well as to the membrane and that can interact with specific cargoes. Assuming the same role, coat proteins vary greatly in form and size (Faini et al., 2013). They are self-organized well-oiled machines that ensure that cargoes arrive at their targeted destination with great specificity, making cell trafficking a very complex dialogue between its different organelles and compartments (for reviews, see Bonifacino and Lippincott-Schwartz, 2003; Cai et al., 2007; McMahon and Mills, 2004).

The three best-characterized coat proteins are clathrin coats and the two types of coatomer coats. COPI-coated vesicles shuttle proteins within the Golgi and from the Golgi back to the endoplasmic reticulum (ER). COPII-coated vesicles export proteins from the ER. Clathrin-coated vesicles (CCVs) are involved in the late secretory and endocytic pathways (Faini et al., 2013) and are the main route of receptor internalization in mammalian cells.

c. Clathrin-mediated membrane traffic

During evolution, cells became more complex and the apparition of intracellular membranes gave rise to eukaryotic cells, equipped with specialized membrane-bound organelles. To ensure homeostasis, a dialogue connects organelles and the cell environment. Endocytosis is a cellular process describing the internalization of chemical substances that cannot enter via passive means, allowing the entry of proteins, polynucleotides and receptors. It also allows cells to let specific entry across their PM. The process of endocytosis is done via an invagination in the cell membrane. Most endocytic events use a coat protein called clathrin and will be described as clathrin-mediated endocytosis (CME). Processes that do not involve clathrin are termed clathrin-independent endocytosis (CIE). Macropinocytosis (entry of liquids) and phagocytosis (internalization of pathogens) are also means of CIE (Mayor et al., 2014). How these pathways work is still largely unknown but advances in molecular and imaging tools have allowed to discover that small-scale clathrin-independent endocytic processes use caveolae or actin. While CIE is important for cells, CME remains the main way of entry for molecules and proteins, and a major field of study. I will now detail the main actors meeting during the process of CME.

i. Clathrin

Roth and Porter were the first to detect "bristle-coated pits" on plasma membranes of mosquito oocytes, and although the mechanisms and proteins involved were still unknown, they predicted that these pits were involved in the uptake of extracellular material (Roth and Porter, 1964). B. Pearse was the first to isolate, purify and name the protein Clathrin in 1975. She described a protein of 180 kDa that formed basket-like structures when observed by electron microscopy. She suggested that the protein was able to form a coat on cellular membranes and that it allowed the creation of vesicles that would then pinch off (Pearse, 1975). She was correct in her assumptions and the field of clathrin-mediated endocytosis has made enormous progress since that first discovery, and despite remaining grey areas, its structure and functions are now well-described (Maib et al., 2017; Robinson, 2015).

Three identical clathrin heavy chains (CHC) self-assemble into a triskelion. They are bound to three clathrin light chain (CLC) subunits (Ungewickell and Branton, 1981). There exists two isoforms of CHC encoded by two distinct genes. CHC17 is the most common form and is involved in endocytosis but also in many steps of vesicular traffic since it sorts proteins at the PM, at endosomal membranes, and from the trans-Golgi network (TGN). A second clathrin heavy chain gene encoding the CHC22 isoform has been characterized (Sirotkin et al., 1996) but it is is only

present in humans and is restricted to intracellular trafficking steps from the Golgi complex and endosomes (**Figure I.13**).

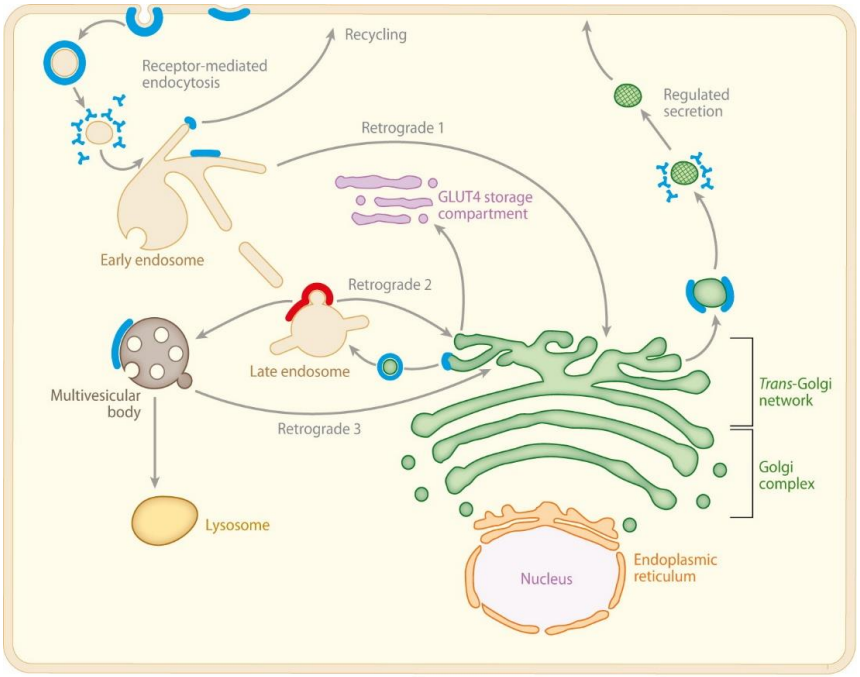

Figure I.13. Location of CHC17 and CHC22 in human cells

CHC17 clathrin (blue) is the most abundant form of clathrin heavy chain and is expressed ubiquitously. It is involved in many cellular transport pathways including receptor-mediated endocytosis and endosomal sorting. The CHC22 clathrin isoform (red), which is 85% identical in protein sequence to CHC17, has distinct biochemical properties and is in charge of the retrograde transport from endosomes to the trans-Golgi network. (Brodsky, 2012)

I will mostly focus on the structure and functions of ubiquitously expressed CHC17 isoform. The structure of the protein was defined at a subnanometer resolution using electron cryo-microscopy (Fotin et al., 2004). Each CHC curls on itself to define a proximal segment, a knee, a distal segment, an ankle, a linker and a terminal domain (**Figure I.14A**). The central portion of the clathrin molecule, known as the hub, is composed of the C-terminal portion of each third, and includes a super-helix of α-helices necessary for trimerization (Ybe et al., 1999) as well as binding sites for clathrin light chain subunits, which regulate clathrin assembly (Brodsky et al., 1991) (**Figure I.14C**). A globular terminal domain and linker form the end of a triskelion leg. It is composed of a seven-blade β propeller, a structure well adapted to interact with multiple partners (ter Haar et al., 1998) (**Figure I.14, B and D**).

Clathrin proteins share these α-solenoid regions and β-propeller domains with other membrane-curving proteins, notably COPI, COPII and components of nuclear pore complexes (Devos et al., 2004; Lee and Goldberg, 2010).

Triskelion legs can spontaneously interact with each other via a close intertwining of clathrin proximal and distal leg segments (Musacchio et al., 1999), further assembling to form a polyhedral basket-like structures made of hexagons and pentagons (**Figure I.14B**). Nucleation occurs with the chance encounter between clathrin, its adaptor protein (AP) and plasma membrane phosphatidylinositol-(4,5)-bisphosphate (PI4,5P2) (Cocucci et al., 2012). Progressive recruitment of other partners and addition of clathrin to the edge of the coat leads to the growth and invagination of the coated pit (Larkin et al., 1986; den Otter and Briels, 2011), before scission by dynamins (DNM) which releases the vesicle in the cytoplasm (Merrifield et al., 2002).

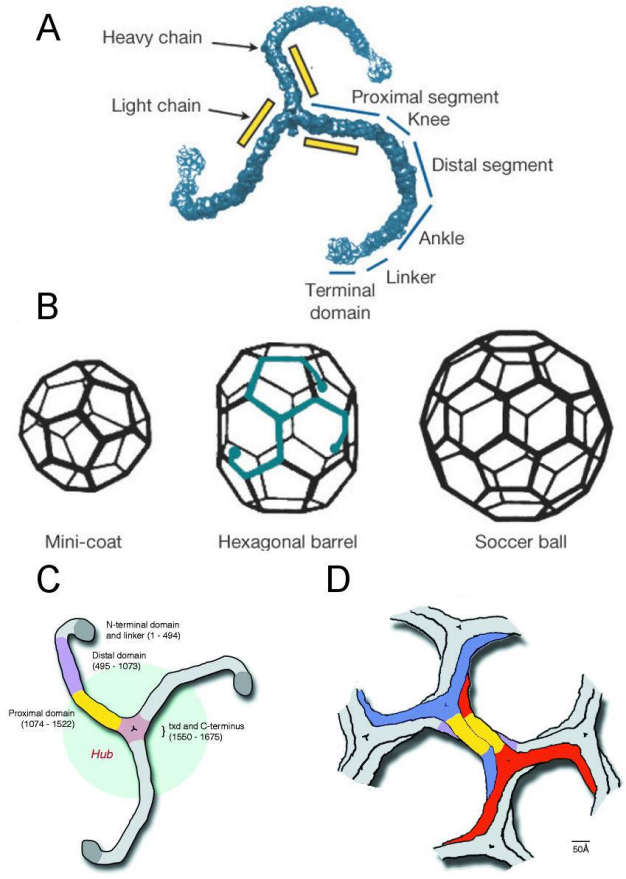

Figure I.14. The clathrin triskelion and the designs of some simple clathrin lattices

(A) Cartoon of the clathrin triskelion, labeled with names for the segments of the heavy chain. The N-terminus of the chain is in the terminal domain, and the C terminus is at the vertex. Positions of the light chains are shown schematically. (B) Three examples of structures that form when clathrin assembles into coats *in vitro*. Schematic representation of one triskelion within the hexagonal barrel is shown in blue. (Fotin et al., 2004) (C) Clathrin triskelion with heavy-chain domains and their approximate sequence boundaries indicated. The light blue circle encompasses the hub region (1,074–1,675). (D) Portion of the clathrin polyhedron lattice, with a triskelion centered at each vertex. Two nearest-neighbor, associating triskelions are colored red and blue. Yellow indicates the portion of the proximal domain determined in the crystal structure. Each lattice edge is comprised of antiparallel-associated proximal domains and antiparallel-associated distal domains (purple) lying underneath. (Ybe et al., 1999)

Although spontaneous polymerization of clathrin units can occur, their bonding constants are weak (Wakeham et al., 2003), and restricted to a pH of 7 (Ybe et al., 1998). Clathrin light chains drop the assembly pH to 6.5 and may have more than one regulatory role since they are able to bind to clathrin but also to calcium and uncoating protein Hsc70 (Brodsky et al., 1991). CLCs are

encoded by two different genes from two different chromosomes. CLCa and CLCb bind to the clathrin molecule in the hub region, each form competing for binding. Although they share only 60% identity, both light chains have similar functions, but are present in different concentrations depending on the tissue (Wakeham et al., 2005).

ii. Adaptor proteins

Assembly of clathrin baskets can be achieved *in vitro* by low pH or calcium, but *in vivo* clathrin needs specific adaptors in order to recognize the right cargoes and assemble at needed sites. Thus different adaptors define different action sites for clathrin. The main adaptors for clathrin are called adaptor proteins (APs). They form heterotetrameric complexes encoded by five different genes in vertebrates, designed from AP1 to AP5 (Hirst et al., 2013; Kirchhausen, 1999; Pearse and Robinson, 1990; Robinson and Bonifacino, 2001). They share similar structures but very distinct cargo recognition patterns and recruitment sites. AP1 is mainly targeted to the traffic pathway between the TGN and endosomes, AP2 is recruited at sites of CME on the PM, AP3 is directed to tubular endosomes, late endosomes, lysosomes and related organelles. Relatively new players AP4 and AP5 mediate specific cargo transport between the trans-Golgi and endosomes respectively, but they seem to work without clathrin (Hirst et al., 2011, 2013) (**Figure I.15C**).

APs are composed of four different types of adaptin chains, two large subunits (γ1 and β1 for AP1, α and β2 for AP2, δ and β3 for AP3, ϵ and β4 for AP4, ζ and β5 for AP5), one medium chain (μ1 to μ5), and one small chain (σ1 to σ5) (**Figure I.15, A-B**).

AP2 is the most abundant adaptor and the one that has been the most studied and described in the literature. Since this project focuses on clathrin recruited on the plasma membrane, I will proceed to explain in detail the way AP2 interacts with cargo and then recruits clathrin at sites of CME.

Quick-freeze deep-etch rotary replication electron microscopy (QFDERR) visualization of bovine brain extract allowed to decipher its structure in great details, a large mass (the "head") flanked by two "Mickey" ears, linked to the head by the hinge (Heuser and Keen, 1988). The ears correspond to the C terminus of the large chains. The large α subunit recognizes the target membrane (Collins et al., 2002; Owen et al., 2004; Robinson, 2004), by specifically binding PIP2 and phosphatidylinositol (3,4,5)-trisphosphate (PIP3) lipids which are particularly enriched in plasma membranes (Ohno, 2006). The other large β subunit of the head is especially important for clathrin binding due to a LϕXϕD/E motif (X indicates any amino acid, ϕ indicates an amino acid with a bulky hydrophobic side chain) named the clathrin box (Robinson and Bonifacino, 2001; Shih et al., 1995). The μ subunit is particularly essential for cargo binding (**Figure I.15A**). It

recognizes a YXXϕ sorting signal present in the cytoplasmic tails of certain transmembrane proteins (Bonifacino and Dell'Angelica, 1999).

A comparison of the crystal structures of AP2, bound or not to cargo, shows that AP2 undergoes a large conformational change from a closed to an open (i.e., active) form upon PIP2 binding, leading to nucleation and stabilization of nascent clathrin-coated pits (Jackson et al., 2010; Kadlecova et al., 2017).

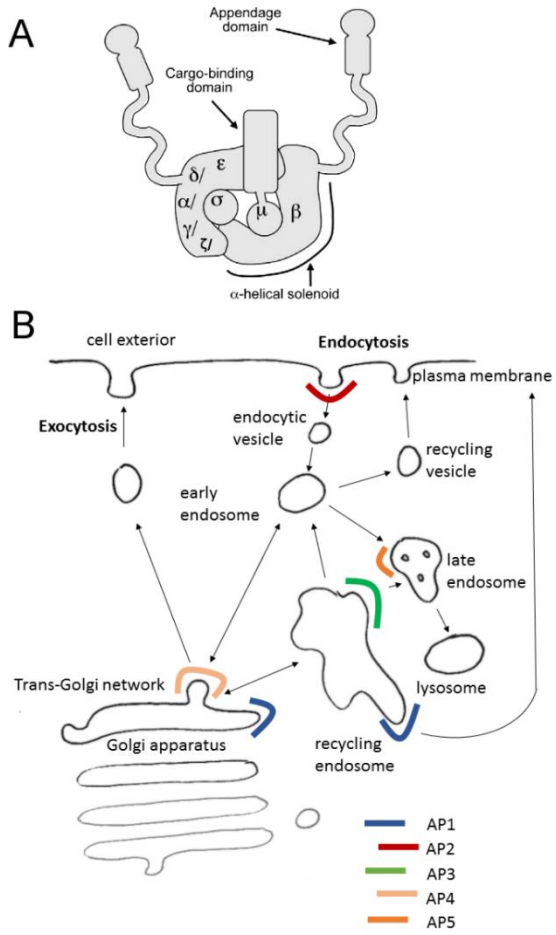

Figure I.15. Composition and location of AP complexes

(A) Structure of an AP complex, showing the positions of the four subunits, and indicating some of the domains on the μ and β subunits. Adapted from (Hirst et al., 2011) (B) Diagram of trafficking pathways and machinery, showing subcellular location of each AP.

The diversity of cargoes explains the discovery along the years of other clathrin associated adaptors called clathrin-associated sorting proteins (CLASPs), such as ARH, Dab2, Numb, CALM, AP180, epsin, and β-arrestin (Traub and Bonifacino, 2013).

iii. Dynamin

The first dynamin was identified as a mechanochemical enzyme associated to microtubules in 1989 (Shpetner and Vallee, 1989). The mechanism of vesicle pinching off from the PM was unknown until the study of a temperature-sensitive *Drosophila melanogaster* mutant, *shibire,*

revealed the inhibitory effect on endocytosis of a mutation in the *Drosophila* homolog of Dynamin (van der Bliek and Meyerowitz, 1991; Poodry et al., 1973).

In mammals, there exist three dynamins encoded by three distinct genes (*Dnm1*, *Dnm2* and *Dnm3*). They belong to a family of large GTPases and are mainly involved in membrane vesicle formation and trafficking, allowing their release by scission. Dynamin 2 (DNM2) is ubiquitously expressed, while dynamin 1 can be found mostly in neurons and dynamin 3 is restricted to specific tissues such as testis, heart, lung and brain. They all share the same domain organization with specific portions critical for oligomerization and protein-protein interactions (**Figure I.16**).

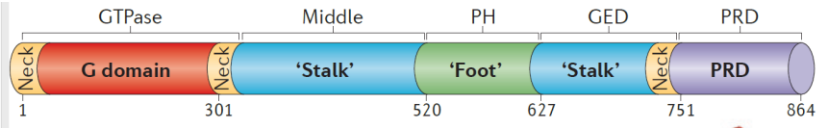

Figure I.16. Domain organization of dynamin 1

Linear representation of the domain organization of dynamin based on its three-dimensional structure, as revealed by crystallographic studies (numbers indicate amino acid position within the primary sequence of the human dynamin 1 xa splice variant). Regions that belong to the same folded module are shown in the same color (created with PyMOL (Schrödinger); Protein Data Bank code 3SNH31). (Ferguson and De Camilli, 2012)

The 98 kDa GTPase DNM2 is composed of five domains, starting from the N-terminus with the G-domain in charge of GTP hydrolysis, connected to the rest of the protein via the neck. The middle domain (MD) is involved in DNM2 self-assembly. The pleckstrin-homology (PH) domain binds phosphoinositides of the PM. The stalk region is composed of the middle domain and the GTPase Enhancing Domain (GED), and it is proposed to mediate oligomerization. Finally, the proline rich domain (PRD) is essential since it binds to the SH3 domains of many proteins, allowing interaction between dynamin and Actin binding protein 1 (Abp1) (Kessels et al., 2001), cortactin (McNiven et al., 2000), Src (Foster-Barber and Bishop, 1998) and amphiphysin (Grabs et al., 1997), to cite only a few.

A plethora of structural and dynamic studies have tried to elucidate dynamin's role (Ferguson and De Camilli, 2012). EM pictures showed that *shibire* mutants typically displayed abnormal pre-synaptic vesicles, arrested in a collared forms, as if coated pits could not complete their scission (Koenig and Ikeda, 1989), suggesting that dynamin is important for scission and release of coated vesicles. Ultrastructural studies further determined how dynamin structure could influence its function. It was established that the protein can form a homodimer and a homotetramer which can further assemble into oligomeric forms like rings and helices (Hinshaw and Schmid, 1995; Muhlberg et al., 1997). Oligomerization increases dynamin GTPase activity (Warnock et al., 1997).

These oligomeric formations can interact with membranes to form tubular structures (Takei et al., 1995) and *in vitro* experiments indicated that purified recombinant dynamin incubated with phosphatidylserine liposomes could bind to lipids in the absence of other proteins and remodel them to form tubular structures (Sweitzer and Hinshaw, 1998). It is noteworthy that DNM2 co-localizes with clathrin before and during the internalization of the coated vesicle suggesting that it also plays a role during maturation of clathrin-coated pits (Aguet et al., 2013; Loerke et al., 2009; Rappoport and Simon, 2003). It is now known that dynamin binding to phosphoinositides occurs through its PH domain and that its presence is critical for dynamin function (Vallis et al., 1999). This binding is therefore independent of dynamin's GTPase activity.

Instinctively, the first models imagined that constriction of dynamin would be sufficient for membrane fission. Early on, it was concluded that dynamin's role in endocytosis is that of a force-generating molecular switch that constricts the neck of clathrin-coated pits to allow their scission. Indeed, cryo-EM observations of dynamin-formed nanotubes also showed that addition of GTP was responsible for constriction until formation of vesicle from the nanotubes (Sweitzer and Hinshaw, 1998). Later on, it was shown that adding GTP resulted in highly ordered and more tightly packed dynamin rings around lipid nanotubes, but was not sufficient for scission (Danino et al., 2004). Since then, mechanisms by which dynamin drives membrane scission has been debated. For example, the "spring model" states that, according to *in vitro* observations (Stowell et al., 1999) and simulations (Kozlov, 1999), dynamin rings show an increase of helical pitch after GDP treatment, which could theoretically tear the forming vesicle from the membrane. Several possible models are described in a detailed review by S. Morlot and A. Roux (Morlot and Roux, 2013).

Two models currently coexist, diverging on how GTP energy is spent (Antonny et al., 2016). The first model is a throwback to the constriction model, where dynamin-mediated constriction allows fission via a difference in membrane elastic energy between dynamin-bound and free membrane (Morlot et al., 2012). The second model proposes that dynamin acts as a motor in cycles of association/powerstroke/dissociation, much like the actin-myosin interaction composing the contractile apparatus that I described previously. In this model, dynamin interacts with another dynamin from the adjacent helix, and GTP hydrolysis induces constriction and twisting of the helix (Antonny et al., 2016; Chappie et al., 2011). The two models are recapitulated in **Figure I.17**.

Although these *in vitro* studies worked with dynamin alone, it is highly probable that other factors are activated (Sever et al., 1999) or recruited for the scission of vesicles in living cells, such as phospholipase D acting as a GTPase activating protein (Lee et al., 2006), BAR-domain containing

proteins (Meinecke et al., 2013) or myosins, actin (Ferguson and De Camilli, 2012; Taylor et al., 2012) and actin-binding proteins (Yarar et al., 2007).

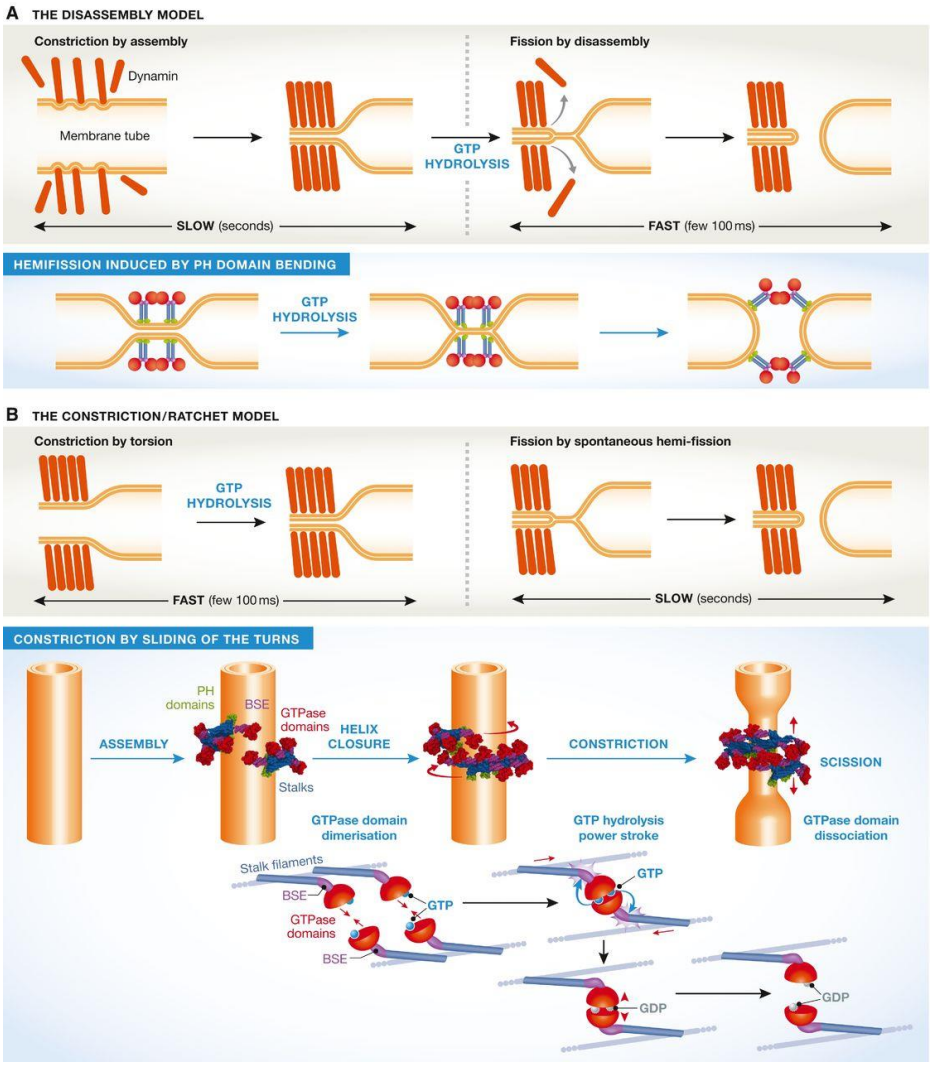

Figure I.17. Two models of dynamin-dependent membrane fission

A) The two-stage model, where constriction is mediated by assembly, and fission by disassembly. (B) The constriction/ratchet model in which constriction is realized by active sliding of the helical turns and fission by spontaneous fusion of the membrane. The one ring state presented here is proposed to be the most common *in vivo*. From (Antonny et al., 2016)

iv. Sequential recruitment of CCV formation actors

Up to 60 proteins will be recruited to the CCV budding site to form a vesicle. Live-cell fluorescence made possible the precise tracking of the different endocytic actors at any point during CCV formation (Kirchhausen, 2009). A detailed analysis of 34 types of endocytic proteins was performed by the Merrifield lab, which showed that this temporal program was very precise and

unvarying depending on the size or the lifetime of the clathrin-coated structure (CCS) (Taylor et al., 2011a).

The recruitment of AP2, Eps15, and F-BAR domain proteins FCHo1 and FCHo2 decreased before scission. This is consistent with previous studies showing that FCHo1/2 were needed to sculpt the initial bud. Although clathrin is able to deform membranes on its own *in vitro*, the presence and activity of membrane-bending proteins are necessary for CCV budding. Proteins presenting a BAR domain form the family of Amphiphysins, essential to early steps of endocytosis (Wigge and McMahon, 1998). Dynamin was seen at low levels associated with CCS as previously described (Macia et al., 2006), but showed a burst 2 to 4 seconds before scission. Interestingly, other actin-binding and actin-remodeling proteins show the same pattern of recruitment, namely Hip1R, confirming that this actin-binding protein is recruited during early stages of endocytosis (Engqvist-Goldstein et al., 2001).

v. Role of actin filaments

In cells, actin filaments can take two forms, mainly bundles or networks, depending on regulatory proteins associated with microfilaments. Structurally, filamentous actin (F-actin) is formed by addition of globular actin (G-actin). Actin filaments are striped when observed by QFDERR and measure about 6 nm in diameter (Hirokawa et al., 1982). This allows bundles of tens, hundreds, or even thousands of microfilaments to perform different functions. Stress fibers enable cell adhesion while the presence of myosin enables contractility. A loosely organized subcortical network of actin forms the cortical actin. Bundles of actin can also form a number of protrusions like podosomes, lamellipodia, filopodia and membrane ruffles (Taylor et al., 2011b). The actors that crosslink actin filaments into bundles – or actin-bundling proteins – usually are small rigid proteins that force the filaments to align closely with one another. Projections of the plasma membrane like filopodia need tight, parallel bundles, organized by an actin-bundling protein like fimbrin. Contractile actin bundles are loosely arranged, allowing myosin proteins to take part in the bundle (Letort et al., 2015). Such an organization can be allowed by cross-linking protein α-actinin (Cooper, 2000). Migration fronts of motile cells are filled with a dense and complex network of branched actin. This network formed of actin filaments at 70 degree angles are organized by ARP2/3 proteins, an assembly of seven subunits, including two actin-related proteins ARP2 and ARP3 (Mullins et al., 1998; Svitkina and Borisy, 1999). ARP2/3 ATP-dependent activity is regulated by nucleating promoting factors (NPFs) when and where it is needed for endocytosis. Thus, actin regulation around endocytic pits and vesicles varies upon several factors (Engqvist-Goldstein and Drubin, 2003; Mooren et al., 2012; Šamaj et al., 2004; Smythe and Ayscough, 2006). Class I NPFs include Wiskott—Aldrich syndrome protein (WASP), N-WASP,

SCAR/WAVE, Myosin-I and CARMIL. Cortactin, Abp1 and Pan1 form the Class II NPFs (Goley and Welch, 2006).

A largely debated aspect in cell biology is the role of actin in endocytosis and conversely, the part the endocytic proteins play in actin regulation. Actin filaments are essential for endocytosis in yeast, as experiments showed that adding the actin-monomer-sequestering drug latrunculin A inhibited endocytosis (Ayscough et al., 1997). The importance of actin in mammalian cell CME was not as clear-cut (Fujimoto et al., 2000; Lamaze et al., 1997; Qualmann and Kessels, 2002). Further studies suggested receptor-mediated endocytosis could be actin dependent, supporting endocytic proteins at all stages of the process, from invagination of the membrane, to forming of the bud, scission and movement of the vesicle away from the membrane (Collins et al., 2011; Kaksonen et al., 2003, 2006; Mooren et al., 2012; Yarar et al., 2005). The current status of knowledge is that actin is highly regulated to dispense actin usage. It is now widely accepted that actin polymerization acts as a mechanical force promoting membrane budding and scission (Merrifield et al., 2005; Saffarian et al., 2009; Taylor et al., 2012). In a very meticulous study, it was shown that clathrin, dynamin and actin are sequentially recruited to forming clathrin pits (Merrifield et al., 2002). Accumulation of actin around forming clathrin-coated pits is likely driven by activators of the ARP2/3 complex. Among these proteins is cortactin, an SH3-containing protein able to bind the PRD domain of DNM2 (McNiven et al., 2000). The precise measuring of protein recruitment at sites of CCV formation distinctly detected several actin-binding proteins, the aforementioned ARP2/3 complex activator N-WASP, which peaked before all the other actin-binding proteins, then the F-actin-binding proteins ARP3, Abp1 and cortactin. Actin polymerization is stopped by the final recruitment of actin-capping protein cofilin and the Arp2/3 suppressor coronin (Taylor et al., 2011a).

d. Diversity of clathrin-coated structures

Early papers about clathrin focused on CME and the ability of the protein to form budding clathrin cages. It can assemble in curved structures as well as flat lattices, as shown by QFDERR (Heuser, 1980) (**Figure I.18**).

Their co-existence led to believe that one form could lead to the other, forming the canonical model of CME (Kirchhausen, 2009; Saffarian et al., 2009) and distinguishing several stages in the formation of a CCV (Cocucci et al., 2012). A debate sparked between those who thought that flat clathrin lattices gave rise to clathrin-coated buds and the tenants of the hypothesis that *de novo* clathrin buds could form on the plasma membrane.

Nucleation of a flat lattice before curving implies a rearrangement of the clathrin hexagons, a hypothesis debated by the defenders of *de novo* canonical coated pit formation (Ehrlich et al., 2004; Kirchhausen, 2009; Kirchhausen et al., 2014). A recent study applying state-of-the-art imaging to a decade-long debate tried to settle the discussion and it would seem that clathrin triskelions arrange in a flat lattice that predetermines the size of the vesicle before subsequent budding (Avinoam et al., 2015).

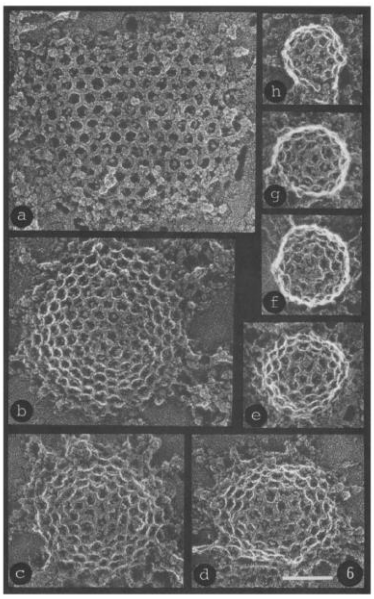

Figure I.18. Transition from flat to curved clathrin-coated structures

Selected examples from the various degrees of curvature found, arranged as a progressive increase in curvature from a to e, to suggest the sequence of invagination that would be expected for coat-mediated endocytosis. Almost fully formed coated vesicles are shown in f to h. Bar, 0.1 μm. From (Heuser, 1980)

Advances in light and electron microscopy exposed a range of clathrin-coated structures, varying from their forms and lifetimes captured by live microscopy. Labeled chimaera endocytic proteins were observed in different cell types and confirmed the canonical model but also showed that these events are not random and that cells can present seeds for endocytic "hot spots" of endocytosis and large clathrin "plaques" that seem stable in time (Gaidarov et al., 1999; Merrifield et al., 2005; Saffarian et al., 2009).

Stable flat clathrin lattices can cover large portions of the PM in several cell types (Batchelder and Yarar, 2010; Grove et al., 2014; Lampe et al., 2016; Saffarian et al., 2009) including HeLa cells (Maupin and Pollard, 1983), fibroblasts (Heuser, 1980) and osteoclasts (Akisaka et al., 2003). Given the structural and chemical stability provided by its structure, what roles could clathrin plaques have in cells?

i. A very stable assembly of hexagons

When working on clathrin, one tends to see clathrin and clathrate designs everywhere. Hexagons have be observed in different conformations, in a wide variety of settings, from volcano rocks formations to soap bubbles to mushrooms. In **Figure I.19**, I have assembled a few examples of hexagonal structures observed in nature. Is it only weird job conditioning or is there a reason that nature seems to be drawn to hexagonal structures?

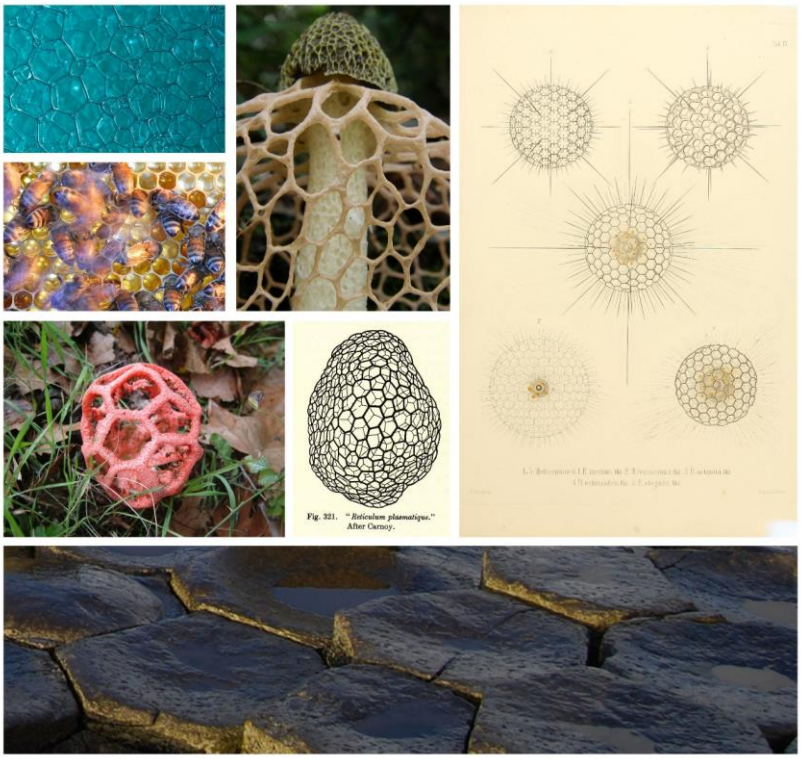

Figure I.19. Design in nature

Macro shot of bubbles (Gemma Stiles). Beehive (Éric Tourneret). Bridal Veil Stinkhorn (Phallus indusiatus) (Ady Kristanto). A mature Clathrus ruber (Red Cage fungi) specimen (Mdakin). "Reticulum plasmatique" after Carnoy (Thompson, 2014). Radiolaria by Ernst Haeckel (Haeckel, 1862). Giant's Causeway, Northern Ireland. Hexagonal basalts. (Chmee2) (Wikimedia Commons)

To tile a plane with cells of equal size and no wasted area, there are only three conformations to choose from: triangles, squares or hexagons. Joseph Plateau stated that angles of 120° are the most mechanically stable, and hexagons minimize the perimeter of tiles in a given area, which is why they tend to be used throughout nature (Ball, 2009). Thus, assembling hexagons with each other is the most efficient way to use a surface.

Graphene is one example of the interesting hallmarks of hexagons. It is made of a single layer of carbon atoms arranged in an hexagonal lattice. It has quite amazing properties, being both one of the most resistant material ever tested, and able to transmit electricity and heat. Currently, graphene is being studied and produced with the objective of revolutionizing solar cells and batteries. So flat surfaces of hexagonal arrangements of carbon are highly resistant, but what about curved assemblies of hexagons?

Man-made architecture took a hint from nature's designs. Geodesic domes are designed to distribute the structural stress throughout the structure, making them able to withstand very heavy loads for their size. Richard Buckminster Fuller was an American engineer and architect who is renowned for his geodesic domes and inspired at the molecular level what are called fullerenes or Buckyballs. It's a hollow molecule of carbon derived from the discovery of C_{60}, a molecule of 60 carbon molecules arranged as 12 pentagons and 20 hexagons (Kroto et al., 1985). It turns out that Euler's law dictates that a system consisting entirely of hexagons cannot close. It also states that closure can occur for any system which includes 12 pentagonal configurations and an unlimited number of hexagonal ones (Hargittai, 2016). From a symmetry point of view, the C_{60} structure is the unique conformation capable of providing geodesic and chemical structural stability.

Figure I.20. Chemical structure of [60]Fullerene

Adapted from (Goodarzi et al., 2017)

Since the early 2000s, the chemical and physical properties of fullerenes have been a hot topic in research and development for new armors but also applications in medicine with the targeting of specific bacteria or cancer cells (Tegos et al., 2005) and whole array of other biomedical applications (Yang et al., 2013). Amongst other potential medicinal uses, fullerenes were considered good candidates for drug and gene delivery (Bakry et al., 2007). Clathrin, by its structure similar to fullerenes and its ability to be recognized by cells trafficking pathways, has been implicated in similar research for drug delivery (Dannhauser et al., 2015).

As we have seen, clathrin is capable of assembling as flat clathrin lattices made mostly of hexagons. We hypothesize that this assembly provides a stability on a fluid plasma membrane in order to

build stable scaffolds needed for cell structural integrity, replicating force transmission properties of graphene (**Figure I.21**). I will try to verify this hypothesis by examining the functions of clathrin plaques described in various cell types.

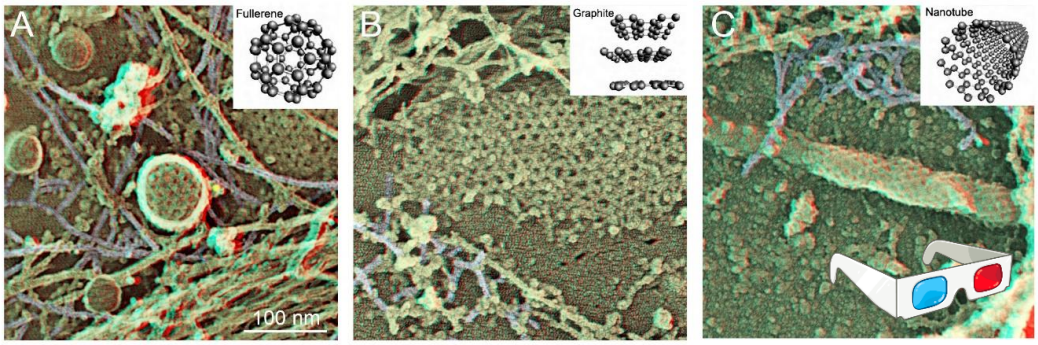

Figure I.21. Different assemblies of clathrin-coated structures

Clathrin-coated vesicles (A), flat lattices (B) or tubes (C) can be related to fullerene cages, graphene sheets or carbon nanotubes respectively. Figure by S. Vassilopoulos.

ii. Clathrin plaques as… hotspots for endocytosis

Although a hypothesis suggested that clathrin-coated plaques moved uniformly inward using an actin scaffold (Saffarian et al., 2009), EM images have been an argument to propose that flat clathrin plaques constitute hotspots for endocytosis and never move inward as one flat plane. Using an elegant alternative pH system, Merrifield and colleagues have been able to detect if a clathrin-coated pit was open or closed depending on pH-sensitive fluorescence probes (Merrifield et al., 2005). Successive puncta were detected at the edge of large persistent clathrin plaques identified by fluorescent CLC (Taylor et al., 2011a). This was consistent with early observations of clathrin plaques in HeLa cells with budding events occurring at the edge of the plaque (**Figure I.22**). These key experiments showed that clathrin plaques may act as hot-spots for budding endocytic vesicles.

Figure I.22. Budding events occurring at the edge of flat clathrin lattices

Micrograph of metal replica from unroofed cell showing budding occurring at the edge of clathrin plaques. Image courtesy of J. Heuser. Adapted from (Humphries and Way, 2013).

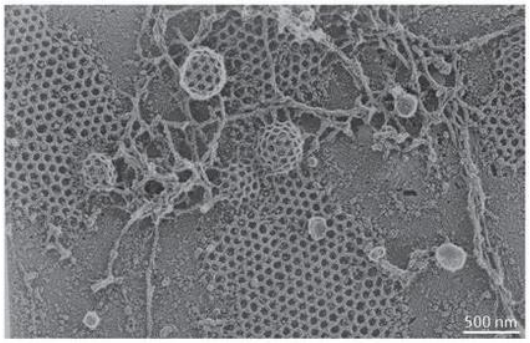

iii. Clathrin plaques as… adherent structures

Clathrin plaques have also long been associated to sites of strong adhesion. Early EM by Maupin and Pollard showed vast clathrin plaques on the adherent face of HeLa cells. Upon seeing the close apposition of the coat to the substrate, they suggested that these could be sites of adhesion. They also observed projections of the membrane that could be due to membrane adherent proteins, much like what was suggested in a previous paper about clathrin-coated phagosomes membranes (Aggeler and Werb, 1982). Live microscopy allowed to differentiate clathrin-coated structures in terms of size but also of dynamics, showing that clathrin plaques are longer-lived (Grove et al., 2014; Saffarian et al., 2009; Taylor et al., 2011a). Playing with the ECM to increase adhesion was shown to promote longer lifetimes of clathrin-coated structures and reduce the rate of endocytosis (Batchelder and Yarar, 2010), suggesting a stabilization of clathrin-coated structures at sites of adhesion. It was thus natural to deduce that clathrin plaques would have a decisive role in cell adhesion, even before studies came out showing their interaction with ECM actors. They were identified at specialized adherent regions, such as the contact zone between osteoclasts and bone (Akisaka et al., 2008), and more recently at the interface between the membrane and collagen fibers (Elkhatib et al., 2017).

Part of their adhesion properties is due to the fact that clathrin plaques are aggregators of integrins. The team of R.J. Bloch described adherent structures in rat myotubes containing αvβ5 integrins included in vitronectin receptors that could associate with clathrin-coated structures. While β1 and β3 integrins can be shown to associate with focal adhesions, it was established early on that β5 integrins form distinct, non-focal contacts with the substrate (Wayner et al., 1991).

iv. Clathrin plaques as... signaling hubs

It has been suggested that clathrin plaques might act as signaling hubs (Lampe et al., 2016), as they are ideally positioned on the plasma membrane at the junction between ECM components and the intracellular cytoskeleton to be intermediates for the transduction of mechanical signals via cytoskeletal rearrangements.

A study was published recently to examine the epidermal growth factor (EGF) pathway relative to clathrin. EGF binds to its receptor EGFR and promotes the activation of several important signaling pathways including the Akt pathway which leads to cell survival. Authors showed that inhibiting clathrin by RNA interference or the clathrin inhibitor pitstop2 affected Akt phosphorylation in ARPE-19 cells, whereas silencing of DNM2 had no effect on this particular pathway (Garay et al., 2015). Another study showed the clustering of CC chemokine receptor 5

(CCR5) into flat clathrin plaques. Using CCR5-transfected cell lines, immunofluorescence and EM, authors showed the targeting of CCR5 to flat clathrin lattices following chemokine CCL5 treatment. This clustering promotes endocytosis of the receptor since CCR5 was seen in vesicles double-stained for clathrin and CCR5 just below the membrane, and depletion of clathrin inhibited CCR5 internalization. A very recent paper showed that clathrin plaques function as dynamic hubs for actin-dependent assembly of CCVs that regulate signaling and endocytosis of the receptor for lipid lysophosphatidic acid, a major serum component that affects various cellular functions. This study also showed that clathrin plaques respond to external cues (in this case, starvation) and that specific receptors such as activated EGFR could be recruited to clathrin plaques (Leyton-Puig et al., 2017). From these experiments, we can gather that flat clathrin plaques may regulate cellular signaling by clustering receptors and either potentially increase their lifetimes on the plasma membrane or remove them by endocytosis.

Flat clathrin lattices have also been described on the cytoplasmic face of the endosomal limiting membranes, and were termed bilayered coats due to their very particular appearance upon thin-section EM examination (Sachse et al., 2002). It was shown that clathrin located on the endosomal membranes delimits microdomains (Raiborg et al., 2002) and interacts with ubiquitin-binding sorting component Hrs in order to target these membranes for degradation (Raiborg et al., 2006).

Overall, this data provides proof that flat clathrin plaques may regulate signaling, although precise mechanisms and pathways involved are still unclear.

v. Clathrin plaques as… actin organisers

Clathrin plaques have been associated to actin formations almost as soon as they were discovered (Aggeler and Werb, 1982), but their role has remained largely unknown. Cortactin, an activator of ARP2/3, was found in large quantities on flat clathrin assemblies in an rat epithelial cell line (Cao et al., 2003). The lab of T. Svitkina (Pennsylvania University) studied metal replicas of detergent-treated B16F1 mouse melanoma cells and found branched actin network around clathrin-coated structures, mainly clathrin-coated pits and some clathrin-coated plaques (Collins et al., 2011).

A recent study confirmed that plaques are hotspot sites of endocytosis and they also found that N-WASP, with its ability to promote ARP2/3-complex-dependent actin polymerization, is a key clathrin plaque regulator (Leyton-Puig et al., 2017).

3- Role of endocytic proteins in muscle: what we know so far

a. Clathrin plaques are part of costameres

Studies of isolated fibers from mice have shown that endocytosis in muscle is specifically located, with the M-line essentially depleted of coated pits while CCS concentrated gradually closer to the Z-lines (Kaisto et al., 1999).

More and more, it is thought that proteins involved in intracellular traffic might play a role in muscle integrity but also in muscle development and repair. Comparable to focal adhesions, clathrin plaques are tissue-specific macromolecular functional units, containing β3 and β5 integrins (De Deyne et al., 1998; Lampe et al., 2016; Vassilopoulos et al., 2014), which connect extracellular matrix, PM and intracellular actin cytoskeleton at costameres. As such, a third costameric domain was actually described, composed of flat clathrin lattices uncovered by quick-freeze deep-etch electron microscopy (Pumplin, 1989).

A year later, Kaufman et al. noticed a peculiar arrangement of clathrin proteins which can be found in repetitive bands during myoblasts differentiation into myotubes (Kaufman et al., 1990). It was thought by Kaufman that clathrin might be directly involved in sarcomere formation by its interaction with actin and α-actinin, the latter being an actin cross-linking protein, member of the spectrin family, along with spectrin and dystrophin. And in fact, it has been more than 30 years that an interaction between clathrin and α-actinin has been known (Schook et al., 1979), but the implications were never sought out. In spite of this fact, we are led to believe that the interaction between clathrin and α-actinin might be important, since this actin crosslinking protein was shown to be present at costameric sites in the striated muscle, amongst proteins besides clathrin, such as vinculin, talin and β1-integrin (Danowski et al., 1992). Other studies have reported direct protein-protein interaction between CHC, α-actinin and vinculin (Burridge et al., 1980; Fausser et al., 1993; Merisko, 1985; Merisko et al., 1988). Since then, several recent studies have proposed a role for clathrin and dynamin in actin organization that is distinct from coated vesicle formation (Bonazzi et al., 2011, 2012; Lampe et al., 2016; Veiga et al., 2007). In particular, it was found that they are especially important in muscle (Vassilopoulos et al., 2014).

In muscle cells in culture, clathrin forms large patches on the PM that exceed the resolution limit of light microscopy. There, it colocalizes with α-actinin 2 before it starts to striate in the cytoplasm (**Figure I.23**).

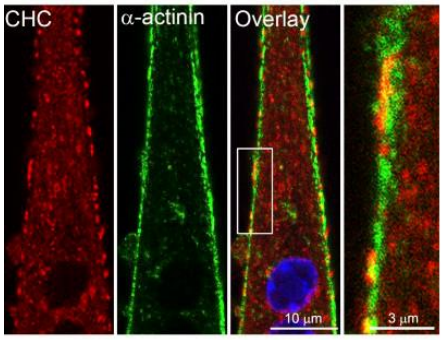

Figure I.23. CHC patches at the PM of differentiated myotubes

Localization of α-actinin (green) and CHC (red) in mouse primary myotubes differentiated for 4 days. Inset in Overlay panel is displayed on the right. (Vassilopoulos et al., 2014)

In adult skeletal muscle, both CHC and DNM2 are organized in a striated pattern overlapping with the costameric protein α-actinin 2 (**Figure I.24A**). At costameres, CHC interacts with α-actinin 2 but not with other focal adhesion proteins such as talin 1 or vinculin, as seen by co-immunoprecipitation (**Figure I.24B**).

Unroofing followed by QFDERR of myotube plasma membranes showed the presence of large flat clathrin plaques, sometimes attaining 1 µm whereas clathrin vesicles have a diameter of about 100 nm (**Figure I.25**).

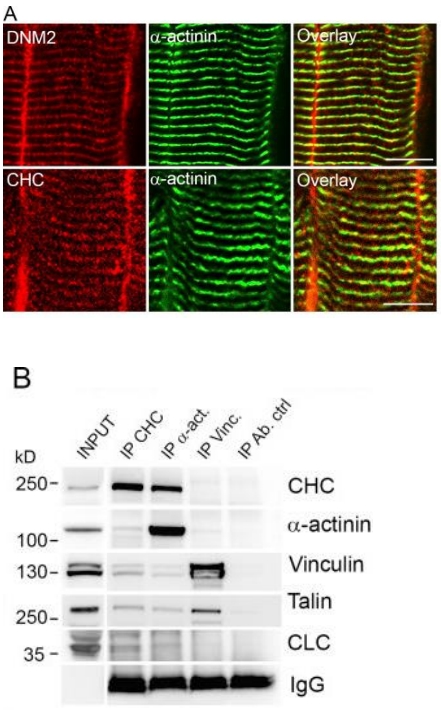

Figure I.24. CHC association with α-actinin2 in adult skeletal muscle

(A) Confocal imaging of sections of mouse skeletal muscle processed for double-immunofluorescent labeling of DNM2 (red) and α-actinin (green) or CHC (red) and α-actinin (green). Bars, 10 µm. (B) Immunoblot of proteins associated with CHC, α-actinin 2, vinculin, or control immunoprecipitates from mouse muscle lysates and 1–5% lysate input. Bands for coimmunoprecipitated CHC, α-actinin 2, vinculin, talin, or CLC are indicated at the right. (Vassilopoulos et al., 2014)

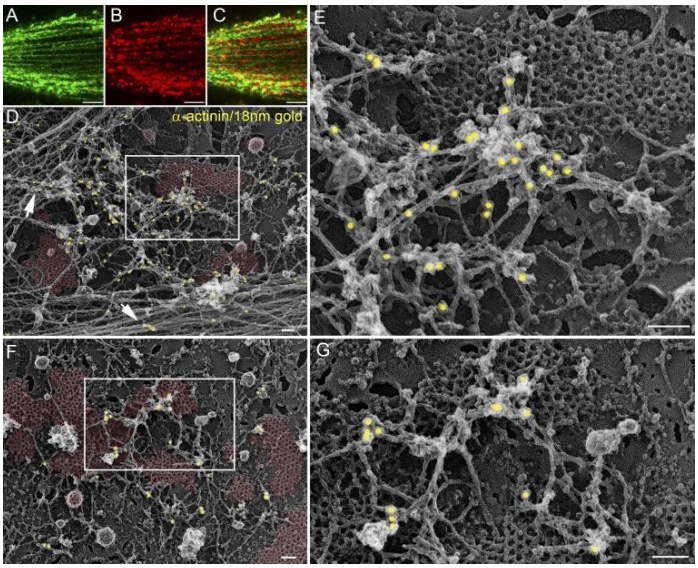

Figure I.25. α-actinin 2 and actin are localized on large flat clathrin-coated plaques

(A–C) Immunofluorescent staining of α-actinin (A), CHC (B), and merged images (C) in untreated primary mouse myotubes visualized using confocal microscopy. Bars, 5 µm. (D–G) Adherent plasmalemmal sheets prepared from control primary myotubes differentiated for 4 days and labeled with α-actinin antibodies followed by secondary antibodies conjugated to 18-nm colloidal gold particles. Gold particles are pseudocolored yellow (D–G) and clathrin lattices are pseudocolored pale red (D and F). The boxed region in D and F is magnified in E and G, respectively. Note that α-actinin is found on both actin cables (D, arrows) and branched filaments lying on top of flat clathrin-coated plaques. Bars, 100 nm. (Vassilopoulos et al., 2014)

These clathrin "plaques" were seen in a complex interaction with a dense typical actin network, crosslinked by the costameric protein α-actinin 2 (**Figure I.25, D-G**), as shown via immunostaining. These flat lattices also contained adhesion markers β5 integrins.

The presence of clathrin clearly distributed on costameres in muscles as well as its particular arrangement into flat clathrin lattices prompted an entire study of the role of clathrin plaques in muscle cells.

b. Clathrin, AP2 and DNM2 are required for α-actinin scaffold formation

From this point on, it was suspected a link between clathrin plaques and the muscle cytoskeleton. Knowing the importance that costameres play in the anchoring of the contractile apparatus, the team wanted to test the effect of clathrin or dynamin depletion on the maintenance of the forming sarcomeres. In order to do this, primary mouse myotubes were depleted of CHC by small-interference RNA (siRNA) before immunostaining of the costameric protein α-actinin 2. After 6 days of differentiation, control C2C12 murine myotubes presented a striated α-actinin distribution. siRNA against CHC provoked the disruption of these α-actinin striations, and clusters of α-actinin 2 were randomly dispersed in the cytoplasm.

During my internship with S. Vassilopoulos, we devised an siRNA strategy to specifically deplete components of the clathrin machinery and study the effect on the actin cytoskeleton. Depletion of AP1 and AP3 would perturb CHC recruitment to intracellular compartments whereas depletion of AP2 would inhibit CHC recruitment only at the plasma membrane. We also wanted to check DNM2 role in muscle organization so we used a siRNA against DNM2 as well (**Figure I.26**).

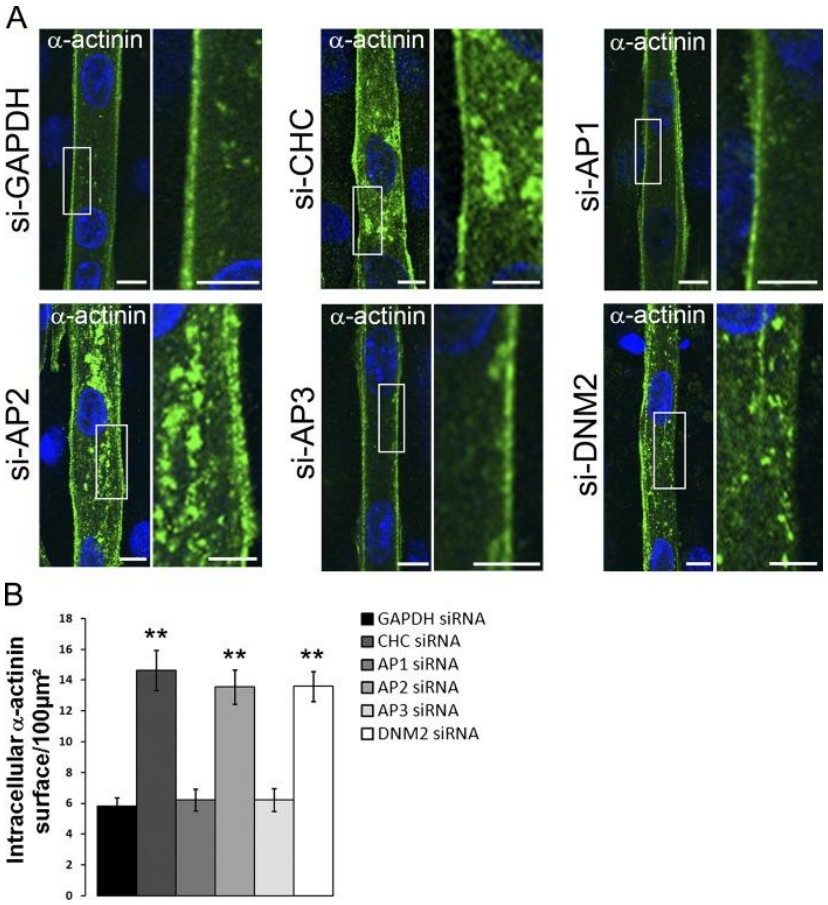

Figure I.26. CHC, AP2, and DNM2 depletion in cultured mouse myotubes perturbs α-actinin distribution

(A) C2C12 myotubes were treated with siRNA targeting proteins (indicated at the left). Immunofluorescent staining of α-actinin in myotubes treated with control siRNA against GAPDH or siRNA targeting either CHC, AP1, AP2, AP3, or DNM2. DNA staining (DAPI blue) identifies differentiated, multinucleated myotubes. The boxed region in the merged images is magnified in the insets. Bars: (main panels) 10 µm; (insets) 5 µm. (B) Quantification of α-actinin fluorescence surface as a function of total myotube surface in 4-day differentiated myotubes treated with siRNA against GAPDH, CHC, AP1, AP2, AP3, or DNM2 (n = 30–50 myotubes, data are presented as mean ± SEM; **, P < 0.01, Student t-test was used). (Vassilopoulos et al., 2014)

I subjected C2C12 myotubes to siRNA treatments before immunofluorescent staining. I performed confocal microscopy and found that α-actinin 2 formed aggregates in the cytoplasm of AP2- and DNM2-depleted cells but not with AP1 nor AP3 depletion (**Figure I.26A**).

I developed a quantification method in order to count and measure these aggregates and came to the conclusion that indeed, AP2 and DNM2 depletion phenocopied CHC depletion, indicating that clathrin recruited to the PM and DNM2 were important for the correct organization of α-actinin 2 striations during muscle differentiation (**Figure I.26B**).

The work was pursued after I left, to study the role of clathrin plaques on actin distribution as well as their importance *in vivo*.

During endocytosis, the protein huntingtin-interacting protein 1–related protein (Hip1R) mediates the interaction between clathrin and actin. It was previously shown to be localized on clathrin pits and flat clathrin lattices (Engqvist-Goldstein et al., 2001, 2004). Hip1R-depleted myotubes exhibited abnormal clathrin and actin distribution, with an accumulation of both proteins on their PM. In parallel, depletion of Hip1R induced massive accumulations of α-actinin 2 on the plasma membrane of myotubes. This showed the importance of the regulation of actin both in clathrin localization and sarcomeric assembly.

c. Clathrin plaques are required for sarcomere maintenance *in vivo*

A depletion of CHC via an shRNA strategy was put in place to study the role of clathrin *in vivo* after differentiation and maturation of the muscle had occurred. Depletion of CHC *in vivo* induced a streaming of the Z-lines and detachment of myofibrils from the PM (**Figure I.27**), which translated by a reduced muscle strength in those animals.

Direct maximal force was severely reduced in muscle depleted of clathrin, before any histological defects or muscle atrophy was observed, an indication that force transmission was affected in the absence of CHC.

All these results published by Vassilopoulos and colleagues proved the critical importance of endocytic proteins in the development and maintenance of muscle cells (Vassilopoulos et al., 2014). It also suggested AP2, CHC and DNM2 as part of a new compartment that would provide a scaffold for actin polymerization.

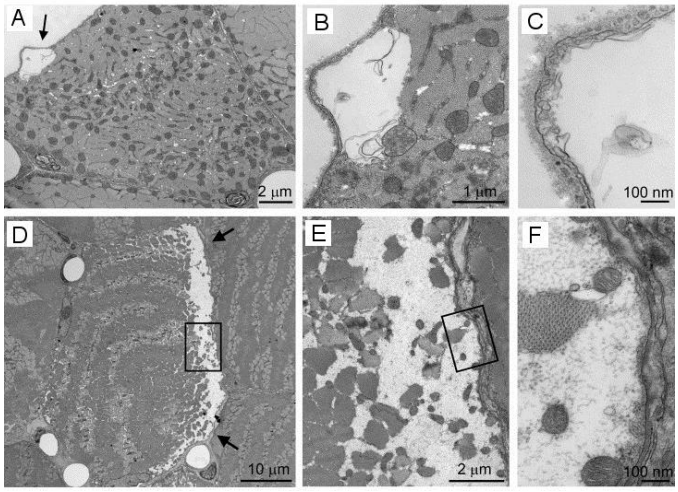

Figure I.27. Sarcomeric detachment between sarcolemma and myofibrils upon *in vivo* CHC depletion

Transmission electron microscopy of transverse muscle sections from mice injected with AAV-shCHC constructs at day 18 (A-C) and day 25 post injection (D–F). In (A-C), small detachments between the sarcolemma and the contractile apparatus are visible at day 18 PI. At day 25 PI, large detachments are seen (D-F). EM by J. Lainé. (Vassilopoulos et al., 2014)

4- Centronuclear myopathies

Centronuclear myopathies (CNM) belong to the group of congenital myopathies which consist in a group of rare genetic diseases that can be autosomal dominant, autosomal recessive or X-linked. They usually have an early onset. They are diagnosed via muscle biopsies followed by histomorphological and ultrastructural studies. Three main forms of CNM are distinguished relative to the mode of inheritance and the mutated genes.

a. X-linked myotubular myopathy (XLMTM)

X-linked myotubular myopathy is due to mutations in the *MTM1* gene located on the X chromosome and therefore affects mostly male individuals with severe symptoms, resulting in hypotonia and respiratory failure (Jungbluth et al., 2008). There is no specific treatment for the condition and most patients die during infancy following respiratory failure. At first, myotubular myopathy was thought to be caused by an arrest of the muscle fiber development (Spiro et al., 1966). It was later found that the culprit was a mutation in the *MTM1* gene which codes for myotubularin, a phosphoinositide phosphatase involved in phosphoinositides metabolism and trafficking (Blondeau et al., 2000). MTM1 dephosphorylates the PI3P and the PI3,5P2 at the position 3 leading to the production of PI and PI5P. In muscle, it was suspected that cellular levels of PI3P might regulate myogenesis and cell differentiation (Taylor et al., 2000), highlighting the

regulatory role of MTM1. In fact, myotubularin has been found to be involved in a whole array of cellular processes that rely on membrane trafficking, including endosomal trafficking (Tsujita et al., 2004), excitation-contraction coupling (Al-Qusairi et al., 2009), neuromuscular junction functions (Dowling et al., 2012), cytoskeletal organization especially desmin intermediate filament architecture (Hnia et al., 2011), which might explain the gravity of the disease caused by its mutation (Lawlor et al., 2016). It was shown that muscles rely heavily on the regulation of integrin turnover and that myotubularin was required for integrin trafficking for adhesion in muscle. Also, depletion of myotubularin leads to an accumulation of integrin with PI3P on endosomal inclusions (Ribeiro et al., 2011). Muscle specific depletion of *MTM1* in mice led to a dramatic phenotype in adult mice, indicating that the protein is necessary even in adult muscles (Joubert et al., 2013).

Myotubular myopathies are often diagnosed by histopathology from muscle biopsies. Are generally observed: myofiber hypotrophy of type 1 fibers, central nuclei in variable numbers, central aggregations of organelles including mitochondria, lysosomes, and sarcoplasmic reticulum, pale peripheral halos seen with staining for oxidative enzymes and perinuclear vacuole-like areas. Ultrastructural studies will reveal a disorganization of triads and sometimes the apparition of dark tubules, probably of sarcoplasmic reticulum origin (Lawlor et al., 2016).

b. Autosomal recessive centronuclear myopathy (AR CNM)

The autosomal recessive form of CNM is due to mutations in *BIN1*, which codes for Myc box-dependent-interacting protein 1 also known as bridging integrator 1 or Amphiphysin 2. It is a ubiquitous protein, but BIN1 is mostly expressed in brain and muscle where it is involved in CME and intracellular endosome trafficking.

Two missense mutations were identified, affecting its membrane tubulation properties in transfected cells, and another mutation abrogated the interaction with DNM2 and its recruitment to the membrane tubules (Nicot et al., 2007). These results suggest that CNM due to mutations in *BIN1* occur by an abnormal remodeling of T tubules and/or endocytic membranes, and that the interaction between BIN1 and DNM2 is important for normal muscle function and nuclei positioning.

Another autosomal recessive form of CNM is due to a mutation in *MTMR14*, a myotubularin related protein involved in phosphoinositide regulation and autophagy (Gibbs et al., 2010; Tosch et al., 2006), highlighting the role of autophagy process in CNM. MTMR14$^{-/-}$ mice displayed muscle weakness and fatigue similar to patients suffering from CNM and further examination showed that

this was due to a Ca^{2+} leakage caused by an accumulation of MTMR14 substrates PI3,5P2 and PI3,4P2 (Shen et al., 2009).

c. Autosomal dominant centronuclear myopathy (AD CNM)

In autosomal dominant centronuclear myopathy (AD-CNM), the severity of the condition varies between individuals, though it is mostly a late-onset form of the disease. It is generally characterized by a slowly progressive muscular weakness and wasting. Histologically, it is recognized by type 1 fiber predominance of small size and a radial arrangement of sarcoplasmic strands around abnormally centralized nuclei on nicotinamide adenosine dinucleotide-tetrazolium reductase staining (NADH-TR) (Jeannet et al., 2004) (**Figure I.28**).

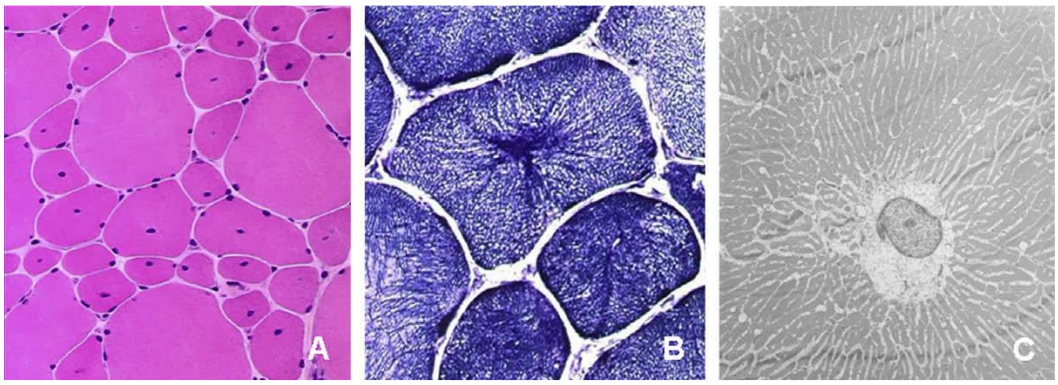

Figure I.28. Histological characteristics of DNM2-related CNM

Transverse muscle sections (A and B) show centralized nuclei especially in small fibers (A; HE). Typical aspect of radiating sarcoplasmic strands is seen on NADH-TR (B). Electron micrograph of transverse section shows the nucleus in the center of the fiber and the radial distribution of sarcoplasmic strands (C). (Romero, 2010)

In 2005, it was shown by Bitoun et al. to be due to *Dnm2* mutations (Bitoun et al., 2005). Later, the spectrum of *Dnm2* mutations was enlarged with a total of 24 heterozygous mutations causing CNM. The mutations mainly affect the middle or PH domain of the protein (**Figure I.29**).

Among them, a group of *Dnm2* mutations were identified in the PH domain. In contrast with the previously reported *Dnm2* mutations located in the C-terminal part of the PH domain were associated with a neonatal onset and a more severe phenotype (Bitoun et al., 2007). Another set of mutations in the middle domain of the protein cause an entirely different disease, the Charcot-Marie Tooth (CMT) neuropathy, which affects both motor and sensory nerves and is characterized by an impaired myelination of neurons (Sidiropoulos et al., 2012).

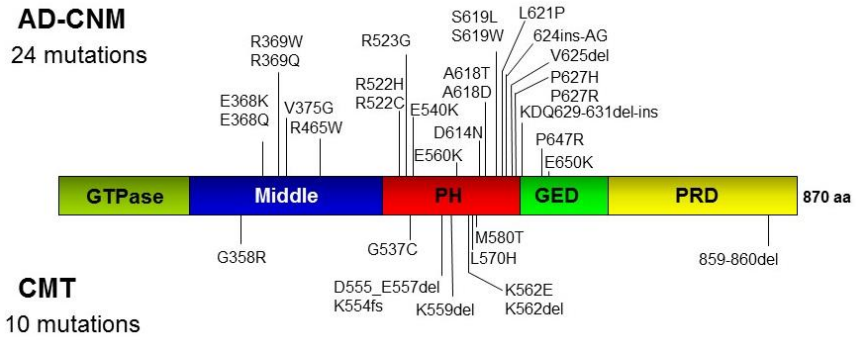

Figure I.29. Localization of dynamin-2 mutations linked to CNM.

Dynamins are multimodular proteins comprising five highly conserved structural domains: a large N-terminal GTPase domain, a middle domain, a PH domain that bind phosphoinositides, a GTPase effector domain (GED), and a C-terminal proline rich domain (PRD) that interacts with SH3-domain containing proteins. The most common disease-related dynamin-2 mutations are represented. Note that almost all dynamin-2 mutations identified in CNM and CMT patients are clustered into the Middle and the PH domains.

Recently, a study was performed by the group of J. Laporte to identify the genetic basis for patients affected by an autosomal dominant form of CNM without mutations in *Dnm2*. They discovered heterozygous *BIN1* mutations in all patients that were studied, identifying *BIN1* as the second gene for dominant CNM (Böhm et al., 2014).

Although the pathophysiological implications of these mutations remain largely unknown, I will now detail their potential impact.

i. Membrane trafficking hypothesis

Both *Dnm2* and *BIN1*, which mutations cause autosomal dominant CNM, play a major role in membrane trafficking. Also, in mature skeletal muscle fibers, DNM2 and CHC colocalize, especially in the peripheral region of the fibers called costameres. Cells expressing *Dnm2* mutants related to either CNM or CMT showed impaired endocytosis (Bitoun et al., 2009; Koutsopoulos et al., 2011), implying an important role of the affected domains in CME regulation in muscle. However, fundamental data are lacking concerning CME in skeletal muscle, thus it is impossible to draw a conclusion at this stage.

ii. Focal adhesions hypothesis

DNM2 and clathrin are located at costameres that are FA-like structure vitally important for muscle maintenance. The team published a review recapitulating the role of DNM2 in FA structure and disassembly. Indeed, DNM2 is involved in endocytosis of FA components, and it is targeted to

FAs where it forms a complex with FAK and Src. This complex promotes endocytosis and recycling of FAs via Src-dependent DNM2 phosphorylation (Briñas et al., 2013). A possible hypothesis states that CNM-related *Dnm2* mutations may alter FA turnover.

iii. Cytoskeletal regulation hypothesis

While dynamin was implicated quite early in actin-driven processes such as lamellipodia at the leading edge of migrating cells (Krueger et al., 2003), it was considered an indirect actor of actin remodeling by endocytosis of actin regulators like Rac, a member of the Rho family of small GTPases (Schlunck et al., 2004). What is starting to emerge today is a direct role of dynamin in actin remodeling. First, experiments performed using dynamin with a mutated GTPase domain inhibited the formation of F-actin comets in *Listeria* (Lee and De Camilli, 2002). When expressed in mammalian cells, this mutations causes a decrease of actin dynamics within the cortical network (Schafer et al., 2002) and an inhibition of actin-based phagocytosis (Gold et al., 1999). In fact, dynamin could remodel actin via two ways, its oligomerization and GTPase properties, and its interaction with actin-related proteins. This fundamental activity of dynamin is particularly important in the context of CNM. *Dnm2* mutations, mostly segregated in the middle domain, cause the autosomal dominant centronuclear myopathy (CNM) and it is highly probable that the CNM phenotype observed in patients with *Dnm2* mutations directly stems from defective cortical actin turnover at several PM sites, including both branched actin foci surrounding clathrin plaques and stress fibers. These defects could directly interfere with sarcomere anchorage at the PM and produce dysfunctional force transmission at costameres which would at least in part explain reduced force generation in muscle from HTZ KI-*Dnm2*^{R465W} mice (Durieux et al., 2010).

Various studies have also looked at the effects of *Dnm2* mutations on microtubule organization. In *Dnm2*-related CNM, the majority of mutations affects the middle domain, which is essential for the centrosomal localization of DNM2 and mediates the interaction with γ-tubulin (Thompson et al., 2004). CMT-related *Dnm2* mutants can disorganize the microtubule cytoskeleton (Züchner et al., 2005) and one particular CMT-mutant was shown to impair microtubule-dependent membrane transport (Tanabe and Takei, 2009).

Concerning the third type of cell filament, a novel pathophysiological mechanism involving intermediate filaments recently emerged in CNM. Indeed, the desmin network was shown to be disorganized in the X-linked form of CNM (Hnia et al., 2011), however consequences of the disorganization of the desmin network still have to be sought out.

iv. T-tubule hypothesis

ECC is vital in muscle and regulates the release of Ca^{2+} by the SR. A recent paper provided cell-/animal-based experiments demonstrating that CNM-dynamin mutants lead to T-tubule disorganization in muscle (Chin et al., 2015). In fact, abnormal T-tubule formation has been linked to several forms of CNM, since *BIN1* (Lee et al., 2002; Toussaint et al., 2011) and *MTM1* (Al-Qusairi et al., 2009) were shown to be involved in biogenesis and maintenance of this plasma membrane invagination. ECC impairment could be a common pathomechanism explaining muscle weakness found in patients and animal models. In accordance to this, an elevated cytosolic Ca^{2+} concentration was also reported in the mouse model of *Dnm2*-linked CNM developed by the lab (Durieux et al., 2010). Afterwards, calcium impairment was linked to a muscle weakness and a defect of ECC was described in the same DNM2-CNM mouse model (Fraysse et al., 2016; Kutchukian et al., 2017).

v. A mouse model for AD CNM linked to DNM2

The team developed a knock-in mouse model expressing heterozygously the most frequent mutations found in patients: HTZ KI-*Dnm2*^{465W} (Durieux et al., 2010).

These mice progressively develop muscle atrophy. The mass of their *tibialis anterior* (TA) muscle is significantly lower (by 20%) at 2 months of age, and by this age the fiber size is decreased by 14%. Although atrophy is only declared after 2 months, contractile properties of muscles start being impaired as early as 3 weeks of age. The morphological abnormalities increase with age (30% at 8 months).

This model mimics most of the human CNM features except for nuclear centralization. This shows that, despite giving the disease its name, nuclear centralization is probably not a major pathogenic element of said disease. This is confirmed by the absence of notable centralization in the youngest and most severely affected *Dnm2*-mutated patients.

2- Unanswered questions – Aims of the study

All this data associating clathrin plaques to different types of cells assuming a role in cell adhesion and muscle maintenance, as well as the undeniable role of DNM2 in regulation of actin cytoskeleton dynamics and focal adhesion turnover, highlight a new putative pathomechanism of clathrin plaques in DNM2-related CNM.

With this project, we aimed at pursuing the characterization of this unconventional role of the trafficking machinery in costamere formation and maintenance. With this objective, my project addressed several aims to answer three major questions.

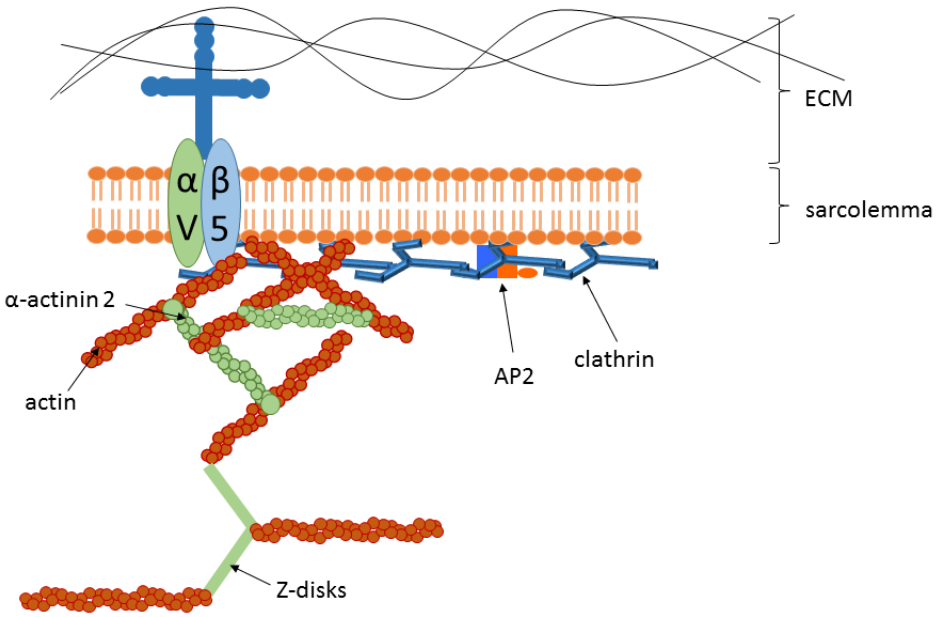

Figure I.30. What we knew about clathrin plaques

Presented here is a simplified view of costamere organization that includes clathrin plaques and what we know about their involvement. Flat clathrin plaques are located on the plasma membrane of muscle cells, in periphery of their Z-disks – thus they are present at costameres. They directly interact with α-actinin 2 and serve for its scaffolding. They also concentrate β5 integrins.

a. Aim one: What are clathrin plaques made of and what are their dynamics?
b. Aim two: How are they involved in cytoskeletal scaffolding?
c. Aim three: What is their exact role in CNM pathophysiology?

To answer these questions, we combined several approaches ranging from, setting-up different myotube cell culture systems, siRNA-based strategies which were used to deplete proteins of interest allied to light and electron microscopy or even molecular biology and biochemistry techniques, that I will now proceed to explain in detail.

II. Methods

1- Cell culture

I used primary mouse satellite cells prepared from mouse pups for ultrastructural analysis and siRNA treatments. These cells present several advantages, mainly being relatively sensitive to siRNA treatments comparing to other cells types and also displaying a high potential of differentiation, which was pivotal to our study of plaque ultrastructure. I also used immortalized myoblasts from healthy control subjects and patients presenting the *Dnm2* p.R369Q and *DES* p.R350P mutations, immortalized by K. Mamchaoui at the Cell Platform of the laboratory.

a. Primary culture preparation

Mouse hind limb muscles of 3 day-old pups sterilized quickly with 70% ethanol were dissected and collected in ice-cold phosphate-buffered saline (PBS). They were then minced using scalpels. The resulting tissue sample was immersed in a digestion mix (0.5 mg/mL collagenase type 2 (#LS004202; Worthington Biochem, USA) and 3.5 mg/mL dispase (#1105-041; Thermo Fisher, France) in Dulbecco's modified Eagle's medium (DMEM) Glutamax (#61965-026; Thermo Fisher, France)) in a water-bath at 37°C, shaking for 10 minutes. Digestion was stopped with dissection medium (DMEM Glutamax, 50 U/ml penicillin, 50 mg/ml streptomycin, 10% Fetal Bovine Serum (#10270-106; Life Technologies, France)) and suspension was centrifuged at 600 rotations per minute (RPM) for 5 minutes.

Supernatant containing cells was centrifuged at 1300 RPM for 5 minutes and then resuspended in 1 mL dissection mix then stored on ice. Pellet was re-digested in digestion mix for 10 minutes at 37°C. This procedure was repeated at least 5 times, until the pellet of digested muscle was greatly reduced and transparent. Cell suspensions were filtered through a 40 µm cell strainer in sequential order (last digestion first to avoid clogging of the filter). Cells were then resuspended in dissection medium and pre-plated on 100 mm Petri dishes. Pre-plating time was 3 hours. This allows fibroblasts to attach to the plastic dish while muscle cells mainly stay in suspension. During pre-plating, 100 mm Petri dishes were coated with 1:100 Matrigel Basement Membrane Matrix (#354234; Corning, France). Supernatant from the pre-plating was collected and centrifuged at 1500 RPM for 10 minutes. The pellet was resuspended in DMEM Glutamax, 50 U/ml penicillin, 50 mg/ml streptomycin, FBS 10%, Chicken Embryo Extract (#CE-650-J; Seralab, UK) 1% and plated on Matrigel-coated 100 mm Petri dishes.

b. Primary cell culture subculturing

Primary muscle cell cultures consist of a mix of proliferating myoblasts and fibroblasts. These cultures will sustain only a few passages before either the myoblasts lose their proliferative ability or fibroblasts take over. Also, one should be careful to keep primary muscle cell cultures at a density below 60%. Above this, myoblasts start to fuse and differentiate spontaneously into myotubes.

c. Cell differentiation

Myoblasts in culture are able to fuse and form differentiated, plurinucleated myotubes. In order to do this, the culture medium was switched to a differentiation medium composed of DMEM Glutamax, Horse Serum 2% (#16050-130; Life Technologies, France), 50 U/mL penicillin, 50 mg/mL streptomycin.

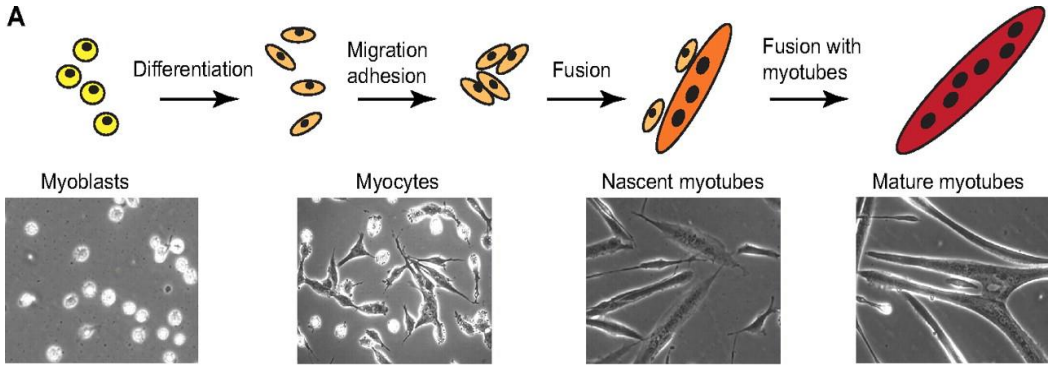

Figure II.1. Myoblast fusion in cultured muscle cells

Adapted from (Abmayr and Pavlath, 2012)

d. Extended differentiation protocol

Mouse primary muscle cells were submitted to extended differentiation, more than 10 days. Normally, after 5-6 days of differentiation, cells attain a level of differentiation that allows them to contract and thus inevitably detach from the substrate. To avoid cell detachment, a layer of 1:3 Growth-Factor Reduced Matrigel Basement Membrane Matrix (#356231; Corning, France) was added on top of differentiated myotubes (Falcone et al., 2014).

e. Immortalized cell lines

C2C12 immortalized mouse myoblast cell line was culture in DMEM Glutamax supplemented with 20% fetal bovine serum and 50 U/mL penicillin, 50 mg/mL streptomycin.

Immortalized control and patient myoblast cells (*DNM2* p.R369Q, *DES* p.R350) were cultured in proliferation medium (1 volume of M199 (#41150020, Invitrogen, France), 4 volumes of DMEM Glutamax, 20% fetal bovine serum, 50 U/mL penicillin, 50 mg/mL streptomycin, 25 µg/mL fetuin (#10344026; Life Technologies, France), 0.5 ng/mL fibroblast growth factor-basic (bFGF; #PHG0026; Life Technologies, France), 5 ng/mL human epidermal growth factor (hEGF; #PHG0311; Life Technologies, France), 0.2 µg/mL dexamethasone (#D4902-100mg; Sigma, France), 5 µg/mL insulin (#91077C-1g; Sigma, France). Differentiation was induced using DMEM Glutamax, 2% Horse Serum, 50 U/mL penicillin, 50 mg/mL streptomycin, supplemented with 5µg/mL insulin (#91077C-1G; Sigma, France).

f. siRNA transfection

There exists several ways to silence the expression of genes. Gene knock-outs can erase a gene from the genome while gene silencing will often affect transcription or translation steps and induce a reduction – sometimes temporary – of gene expression. Reducing the expression of a gene is very often used in research to infer the normal function of a gene. Defaults caused by its absence reflect its function.

I used a strategy of siRNA (small-interfering ribonucleic acid) to cause the short-term silencing of key targeted proteins after differentiation started. Small double-strand siRNAs are designed, a sequence of 19 nucleotides identical to a sequence in the targeted mRNA. They are transfected into cells where the guide strand is loaded into RISC (RNA-induced silencing complex). This activated protein and nucleic acid complex can then induce gene silencing by binding to a complementary mRNA target sequence, thereby targeting it for cleavage and degradation.

All siRNA were purchased from Eurogentec, Belgium. A list of used sequences can be found in **Table 2** of the Appendix. siRNA transfection was performed using HiPerfect Transfection Reagent (#301705, Qiagen, Germany). Mixes were prepared following **Table 1**.

After 10 seconds of vortexing, mixes were incubated for 10 minutes at room temperature to allow formation of transfection complexes. The complexes were added drop-wise onto the cells before completing with differentiation medium. Cells were incubated under their normal growth conditions for the duration of the transfection.

Culture format	Volume of medium on cell (µL)	Final volume of diluted siRNA in µL ([C]i = 20 µM)	Volume of HiPerfect Reagent (µL)	Final siRNA concentration (nM)
6-well plate	2000	20	12	200
12-well plate	1000	10	6	200
24-well plate	500	5	3	200

Table 1. Pipetting scheme for transfection of adherent cells with HiPerfect Transfection Reagent

Cells were transfected once for 48 hours but for the most efficient depletion, and in the case of CHC silencing, two successive siRNA treatments of 48 hours were necessary.

g. Cell stretching

i. Flexcell apparatus

Cells were plated onto flexible-bottom plates (#UF-4001C Uniflex plates; Flexcell International, USA) coated with Matrigel Growth Factor Reduced Basement Membrane Matrix and incubated at 37°C in a CO_2 incubator.

UniFlex culture plates are 35 mm diameter, 6-well plates with 1) flexible silicone elastomer well bottoms and 2) centrally located upper membranes upon which cells are seeded and is the designated uniaxial strain region.

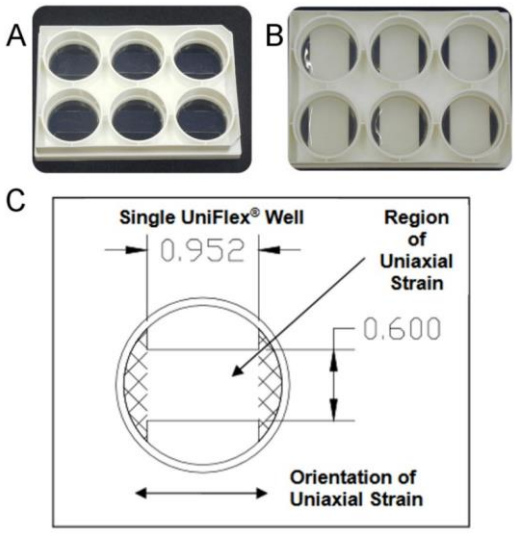

Figure II.2. Uniflex culture plates for uniaxial cyclic strain of cell monolayers

(A) Cells are plated on matrigel-coated flexible elastomer bottomed plates. (B) FlexCell loading stations apply stretching following a vacuum. (C) Uniaxial strain is performed on a limited portion of the wells. Diagram is from the Flexcell International Corporation website. Distances are indicated in centimeters.

The cells were subjected to cyclic stretch at 0.5 Hz during 4 or 6 hours using a computer-controlled vacuum stretch apparatus (FX-4000T Tension Plus System; FlexCell International, Germany) with a vacuum pressure that is sufficient to generate 10% mechanical stretch. 4-hour stretching was used only in the context of transferrin studies since we studied endocytic response of clathrin-

coated structures which would correspond to a fast process. Replicate control samples were maintained under static conditions with no applied cyclic stretch. It should be noted that the only cells that receive uniform strain are those attached to the area of the membrane over the loading post when the membrane is in its fully stretched position. Therefore, it is best to attempt to plate cells only in the uniformly strained area on the upper membrane or to view or test the cells that are only in this uniformly strained area. After stretching, cells were washed with PBS and fixed using 4% PFA for immunofluorescence, NaCl-EDTA 1X buffer for western blotting or TRIzol (#15596018; Life Technologies, France) for RT-PCR.

ii. Quantification of YAP/TAZ location

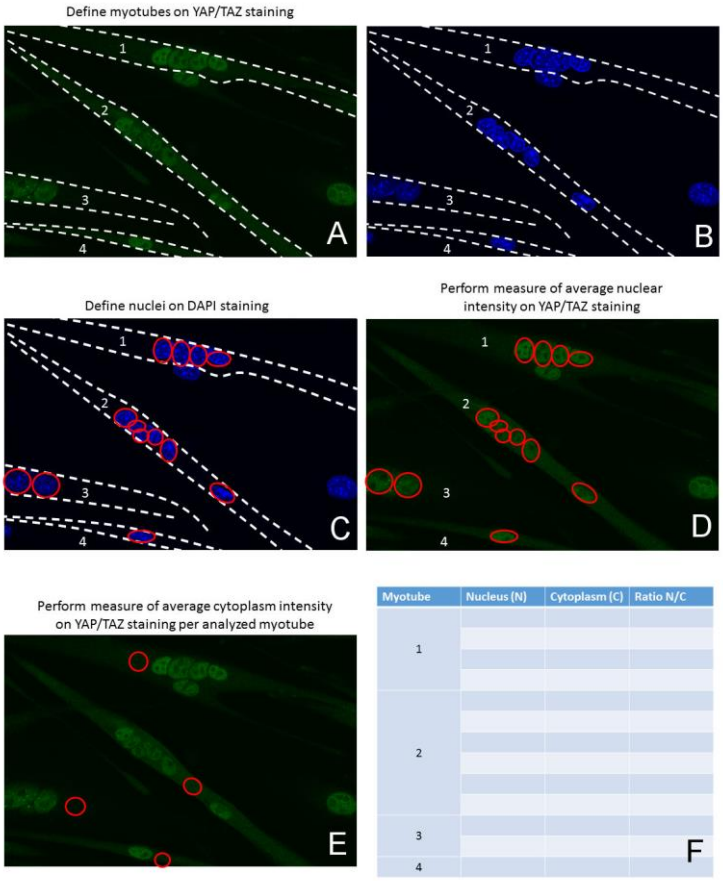

a

Figure II.3. How to quantify YAP/TAZ nucleocytoplasmic ratio

Using ImageJ software, nuclei were detoured on DAPI staining, and average intensity of YAP or TAZ fluorescence was measured in the corresponding ROIs. Average intensity of the same cell's cytoplasm was quantified as well.

I performed a staining of either YAP or TAZ following the protocol that can be found in II.2-Immunofluorescence.

I imaged myotubes at the equatorial level using an upright FV-1000 confocal laser scanning microscope (Olympus, Tokyo) equipped with UPlanS-Apo 60x, 1.35 NA oil immersion objective lenses. Using ImageJ software, nuclei were detoured on DAPI staining, and average intensity of YAP or TAZ fluorescence was measured in the corresponding ROIs. Average intensity of the same cell's cytoplasm was quantified as well.

h. Transferrin uptake assay

Cells were subjected to cyclic stretching for 4 hours with or without 80 µM Dynasore (#D7693; Sigma-Aldrich, France) before incubation 15 min with 40 µg/mL AlexaFluor-488 fluorescently labeled human transferrin (#T13342; Molecular Probes, Life Technologies, France) concomitant to stretching. Endocytosis of this compound was stopped with ice-cold PBS washing and fixed using 4% PFA.

Entire myotubes were imaged using stacks of 500 nm step, with an FV-1200 confocal microscope (Olympus, Tokyo) and 40x oil objective. M. Bitoun measured Transferrin-A488 fluorescence on the sum projection from the confocal stacks by selecting 5 ROIs in myotubes, background noise, and using this formula: Corrected Total Cell Fluorescence (CTCF) = Integrated density – (Area of selected cell X Mean fluorescence of background reading). Experiment was performed twice with similar results.

2- Histomorphological and ultrastructural analyses

a. Fluorescence microscopy

i. Immunofluorescence

Samples (10 µM tissue slices, cells on coverslips) were fixed (15 min, 4% paraformaldehyde in PBS) at room temperature (RT), permeabilized (10 min, 0.5% Triton X-100 in PBS, RT) and blocked (30 min, PBS with 0.1% Triton X-100, 5% bovine serum albumin (BSA)). They were then incubated with a primary antibody diluted in blocking buffer overnight at 4°C. See **Table 4. List of antibodies** for species and dilutions. The next day, samples were washed in PBS with 0.1% Triton X-100. Sections were then incubated with secondary antibodies (60 min, room temperature), washed in PBS with 0.1% Triton X-100, and mounted with Vectashield anti-fading solution containing DAPI (#H-1200; Vector Laboratories, USA). For double or triple labeling, the primary antibodies (from different species) were added simultaneously at the appropriate step. Actin was stained using AlexaFluor-555 Phalloidin (#A34055; Thermo Fisher Scientific, France) for 1 hour at room temperature.

Samples were analyzed by confocal laser scanning microscopy using an upright FV-1000 confocal laser scanning microscope (Olympus, Tokyo) equipped with UPlanS-Apo 60x, 1.35 NA oil immersion objective lenses or a SP5 inversed microscope (Leica, Germany) equipped with a Leica HyD hybrid detector. DAPI, Alexa-488 and Alexa-568 were sequentially excited using lasers with wavelengths of 405 for DAPI, 473 for Alexa-488 and 543 nm for Alexa-568. Imaging was performed at RT using Leica Type F immersion oil. Images (1024 × 1024 pixels) were saved as TIFF files, and levels were adjusted in Adobe Photoshop or Gimp software. Image quantification was performed using National Institutes of Health's FIJI.

I used the "Analyze particles" FIJI plugin (version 1.46) to count intracellular particles on binary confocal images of primary mouse myotubes in a single image from the middle of the cell. Same treatment was performed to measure the length of clathrin plaques of confocal images.

ii. AAV injection, live microscopy

In vivo imagery for biomedical research has made great leaps forward in terms of quality of animal care and quality of resolution both spatial and timewise. Intravital studies mainly makes usage of biphoton, or two-photon, microscopy. This technique allows imaging in living tissue up to hundreds of microns in depth. Two-photon microscopy uses near-infrared light which minimizes scattering in the tissue. It is also well-suited to intravital (*in vivo*) microscopy because of its reduced phototoxicity compared to traditional fluorescence microscopy techniques.

Exposure of skeletal muscle through a simple incision in the skin provides excellent accessibility for *in vivo* imaging by multiphoton microscopy. Several studies have focused on the skeletal muscle in mice to study muscle morphology and mitochondrial function (Rothstein et al., 2005), Ca^{2+} uptake transients during contraction (Rudolf et al., 2004), the shuttling of nuclear factor of activated T cells in skeletal muscle (Tothova et al., 2006) or skeletal muscle microtubules (Oddoux et al., 2013). Several studies used transient transfection of the *tibialis anterior* muscle to introduce fluorescent probes into the muscle for examination of cellular processes by multiphoton microscopy.

AAV9 pseudotyped vectors were prepared by tri-transfection in 293 cells as described in (Rivière et al., 2006). Vectors expressing the µ2 subunit of AP2 tagged with mCherry (AAV9-AP2-mCherry) were prepared by the vectorology platform of the laboratory.

WT and HTZ KI-*Dnm2*^{R465W} mice were injected at 6 months of age. One intramuscular injection (40 µL/TA) of AAV9-AP2-mCherry (1.10^{12} vg/mL) was performed by S. Vassilopoulos in TA muscles using 29G needle.

The following experiment was performed in collaboration with C. Laplace and S. Salomé-Desnoulez (Imaging and Cytometry Platform (PFIC), Gustave Roussy Institute). WT and HTZ KI-*Dnm2*^{R465W} mice (Durieux et al., 2010) injected a month prior with AAV-µ2-mCherry were anesthetized using isofluorane. Skin was removed from the TA before applying the muscle directly on coverslip (with a bit of saline solution to avoid dehydration) and immobilizing with tape. I performed the imaging and FRAP on an inverted Leica SP8 multiphoton microscope optimized for intravital microscopy of small animals, equipped with a complete isofluorane anesthesia unit. The mouse temperature was maintained at 37°C with a heating stage and a heating lamp, and breathing of the animal was monitored visually throughout the experiment.

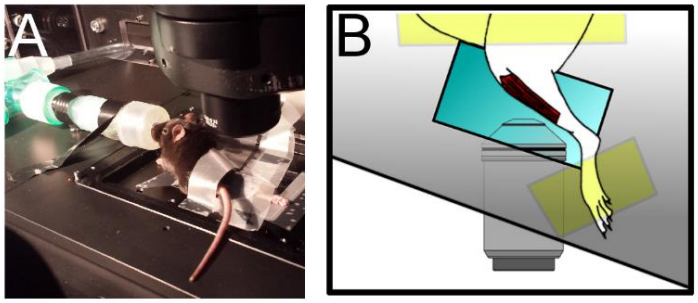

Figure II.4. Muscle intravital microscopy set-up

(A) Representative picture of the intravital setup experiment with live anesthetized mouse. (B) Cartoon of the set-up used to image superficial TA fibers in live mice. Skin above the TA muscle was removed while the mouse was under isofluorane aneasthesia. It was then placed on the coverslip overlooking the objective of a Leica SP8 inversed confocal microscope.

Fluorescence recovery after photobleaching (FRAP) is a method consisting in a powerful laser focused on a small portion of the cell, or in this case, organ. This induces a local and transitory photobleaching since the turn-over of targeted – and thus fluorescent – proteins progressively erases the bleaching. We therefore measure the "recovery after photobleaching" by recording the level of fluorescence in the photobleached area and mapping it on a graph. The plateau represents "recovery" whereas its half-life can be drawn from the slope of the curve (**Figure II.5**).

Quantification of FRAP measurements

FRAP analysis: Drifting was corrected using FIJI plugin JavaSIFT. Intensity of bleached area was compared to overall intensity of the muscle fiber, frame by frame, using FRAP Profiler plugin for FIJI.

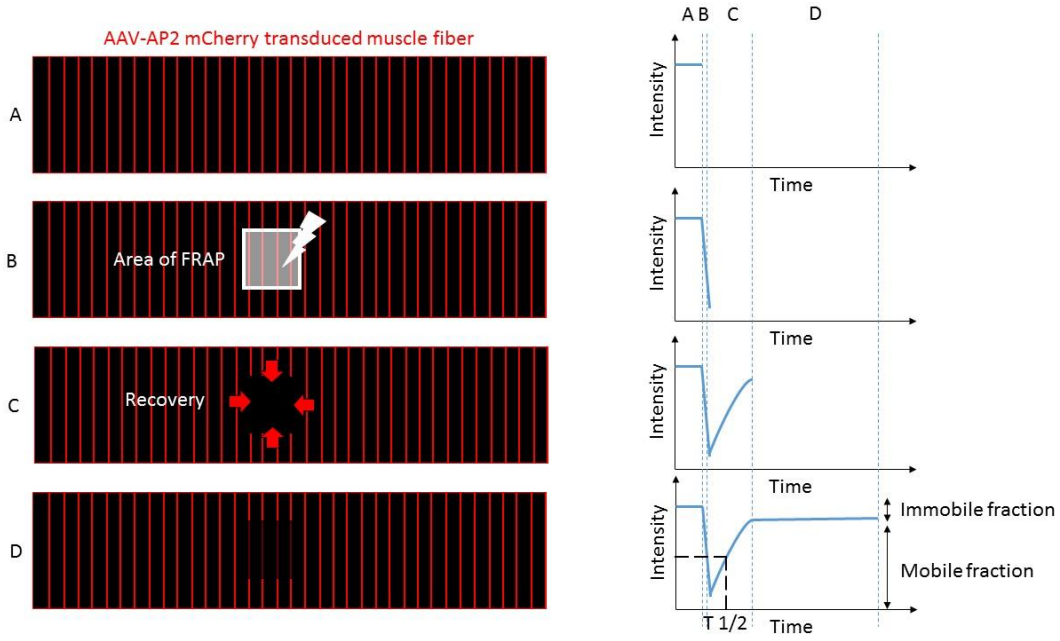

Figure II.5. Principle of FRAP

(A) The sample is labeled with a fluorescent tag. (B) This label is selectively photobleached by a small (~30 micrometre) fast light pulse. (C) The intensity within this bleached area is monitored as the bleached dye diffuses out and new dye diffuses in. (D) Eventually uniform intensity is restored.

b. Electron microscopy

i. Unroofing and preparation of metal replicas

For transmission electron microscopy (TEM), a beam of electrons is transmitted through ultra-thin sections to form an image reflecting the electron density. Preparation of the samples can be very complex, and necessary steps – going from the fixation process to inclusion in resin to staining or contrasting with heavy metals – can all introduce artifacts or structural degradation. Thin sections are inherently limited since they only provide a two-dimensional view of the sectioned structures. In the case of unroofing, the cells bottoms are thin enough for the electrons to go through and provide an excellent contrast while retaining their three-dimensional structure. In the original version of this experiment as described by J. Heuser (Heuser, 1980), cells or tissues are fixed by quick-freezing to avoid the formation of ice crystals in the sample. Biological structures are then split open by a technique called freeze-fracture or directly freeze-dried by deep-etching (water sublimation). Freeze-drying permits to remove the water by sublimation without damaging the underlying structures. Next, an extremely thin metal layer (usually platinum) is deposited on the surface of the sample, followed by a layer of carbon to stabilize the platinum grain. Heuser will later introduce cell unroofing to adapt his technique to visualization

of cytoplasmic faces of biological membranes and membrane proteins (Heuser, 2000a) (examples in this thesis **Figure I.18** p.45, **Figure I.22** p.48, **Figure I.25** p.53).

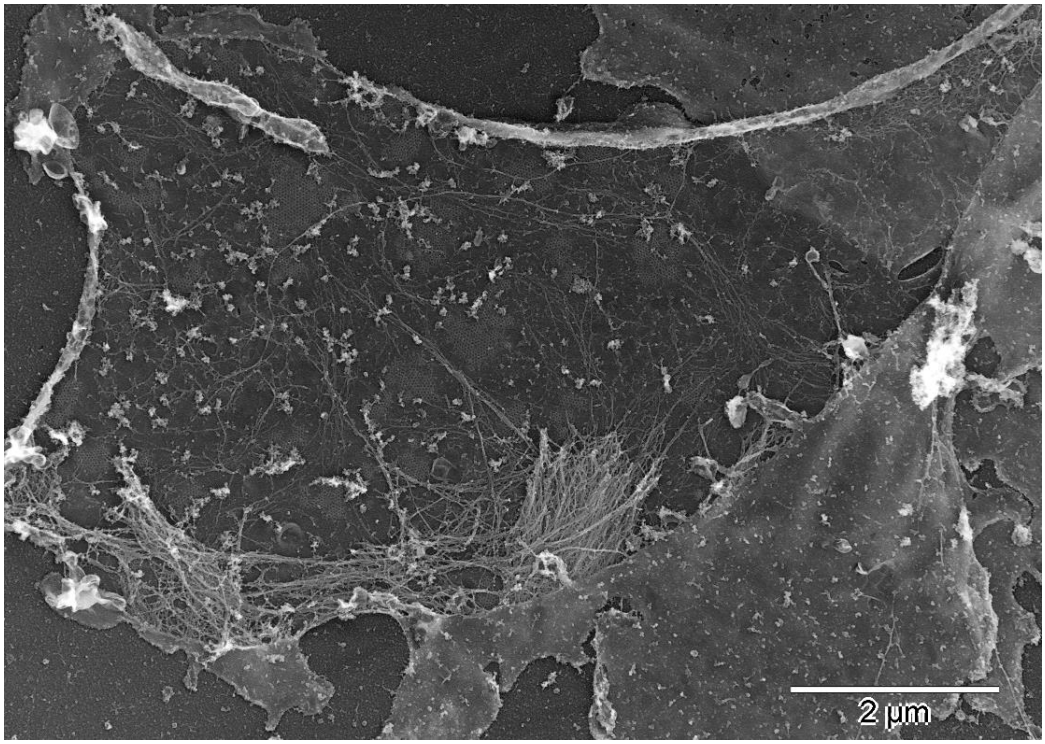

Figure II.6. Metal replicas reveal the ultrastructure of biological membranes

A bird's-eye view of a partially unroofed muscle cell. Membrane that has not been sheared off carries traces of ECM and membrane receptors on its surface. Shearing revealed the cytosolic face of the adherent membrane, studded with dense cytoskeletal networks, flat clathrin lattices and various proteins

This technique revolutionized structural imaging and gave rise to several remarquable discoveries about cell membranes and their associated proteins.

Later on, T. Svitkina developed a technique that involved detergent extraction of cells and chemical fixation, and specialized in visualization of cytoskeleton by TEM and SEM (scanning electron microscopy) (Svitkina, 2009). She was able to break down the complex network of cytoskeletal filaments into categories depending on composition and size. I have color-coded **Figure II.7** in order to show how we were able to recognize cytoskeletal elements on unroofed membranes depending on their morphology and size.

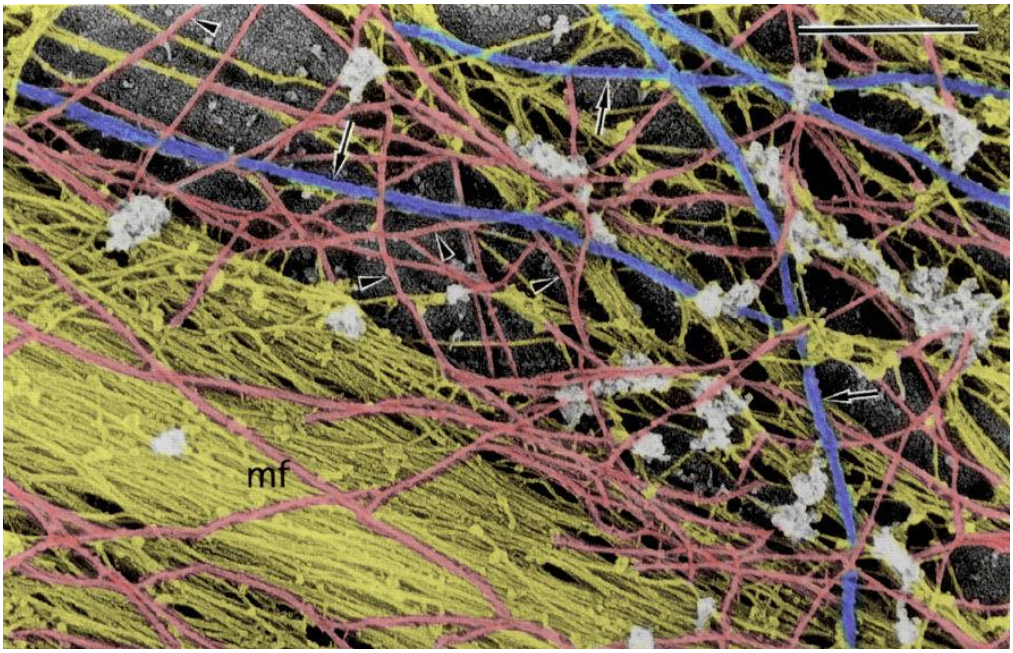

Figure II.7. Different types of cytoskeletal filaments in an adherent cell

Part of a rat embryo fibroblast showing all the cytoskeletal components: microfilament bundle (mf; yellow), microtubules (arrows; blue), intermediate filaments (arrowheads; red). The various diameters of filaments allow to discriminate between microfilaments, IFs and microtubules. Bar, 0.5 µm. Adapted from (Svitkina et al., 1995)

S. Vassilopoulos developed the following protocol with the help of J. Lainé, M. Trichet (Electron Microscopy Facility, UPMC) and myself. Adherent PM from cultured cells grown on glass coverslips were obtained by sonication following a protocol published previously (Heuser, 2000a). Cells were rinsed thoroughly three times with Ringer $+Ca^{2+}$ buffer (see VI.4-a of the Appendix) then briefly subjected to a concentration of 0.5 mg/mL poly-L-lysine (Sigma-Alrich, France) diluted in Ca^{2+} free Ringer buffer. Poly-L-lysine was washed off using Ca^{2+} free Ringer buffer. Coverslips were plunged in a bath of warm KHMgE buffer before unroofing using a VCX 130 Vibra-Cell ultrasonic processor (Sonics, USA) at 20% amplitude. Unroofed membranes were immediately fixed for 20 to 30 minutes with 2% glutaraldehyde/2% paraformaldehyde. Cells were further sequentially treated with 1% OsO_4, 1% tannic acid and 1% uranyl acetate prior to graded ethanol dehydration and Hexamethyldisilazane (HMDS) (#C16700-250; LFG Distribution, France). For immunogold labelling, 4% paraformaldehyde fixed PMs were washed and quenched before incubation with primary antibodies and 15nm gold-coupled secondary antibodies and further fixed with 2% glutaraldehyde. Dried samples were then rotary-shadowed with 2 nm of platinum and 5-8 nm of carbon using an ACE600 metal coater (Leica Microsystems, Germany). The resultant platinum replica was floated off the glass with 5% hydrofluoric acid, washed several times on distilled water, and picked up on 200 mesh formvar/carbon-coated EM grids. The grids

were mounted in a eucentric side-entry goniometer stage of a transmission electron microscope operated at 80 kV (model CM120; Philips) and images were recorded with a Morada digital camera (Olympus, Tokyo). Images were processed in Adobe Photoshop to adjust brightness and contrast and presented in inverted contrast.

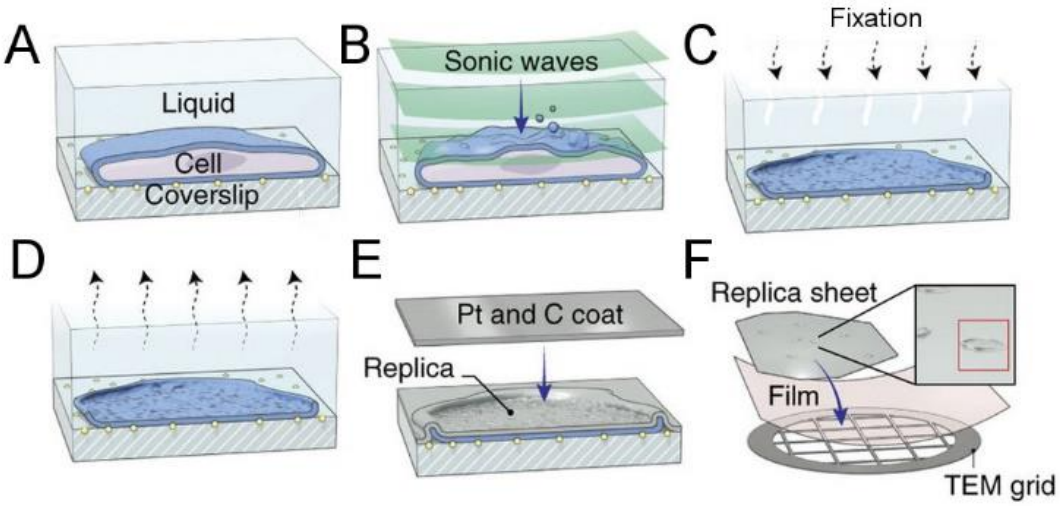

Figure II.8. Protocol for unroofing and metal replica of cells

(A) Cells are grown on a glass coverslip. (B) Cells are sonicated to disrupt the upper cell membrane and expose the inner surface of the plasma membrane (process of "unroofing"). (C) Cells are fixed using 2% paraformaldehyde, 2% glutaraldehyde. (D) The sample is dehydrated and dried using HMDS. (E) The sample is then coated with a thin layer of platinum and carbon to create a replica of the membrane surface. (F) The replica is separated from the coverslip, rinsed and transferred to a TEM grid. Adapted from (Sochacki et al., 2014).

ii. Making anaglyphs

Anaglyph 3D pictures allow to combine two stereoscopic pictures into one to create a 3D effect. In our case, it was particularly useful to examine three-dimensional structures attached to unroofed membranes, especially when complex cytoskeletal structures were involved. One area was imaged by TEM with a tilt angle of -10°, another image was taken with a tilt angle of +10°. Images were then processed in Adobe Photoshop to adjust brightness and contrast and presented in inverted contrast. Anaglyphs were made by converting the -10° tilt image to red and the +10° tilt image to cyan (blue/green), layering them on top of each other using the screen blending mode in Adobe Photoshop, and aligning them to each other (Heuser, 2000b).

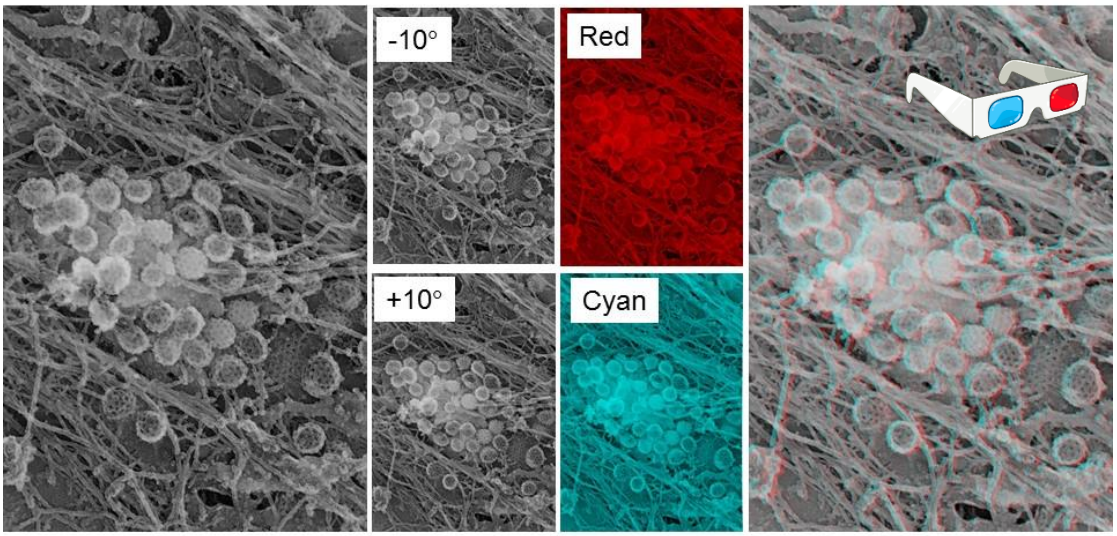

Figure II.9. Realization of anaglyphs for 3D effect

Use view glasses for 3D viewing of anaglyphs (left eye = red).

iii. Thin-section EM

In addition to using metal replicas which only allows visualization of the cell's cortex, we also performed conventional thin-section EM. Preparation and microscopy were performed by J. Lainé. For morphological electron microscopy, J. Lainé fixed muscles by intra-aortic perfusion with 2% paraformaldehyde, 2% glutaraldehyde in 0.1M phosphate buffer (pH 7.4). *Tibialis anterior* samples from WT or KI HTZ-*Dnm2*^{R465W} mice were postfixed with 2% OsO4, in 0.1 M phosphate buffer (pH 7.4) for 1 h, then dehydrated in a graded series of acetone including a 1% uranyl acetate staining step in 70% acetone, and finally embedded in epoxy resin (EMBed-812, Electron Microscopy Sciences, USA).

Myotubes grown on Thermanox coverslips (Nunc, Rochester, USA) were directly fixed for 30 min in the same fixation solution and processed as previously indicated for TA muscles. Ultra-thin (70 nm) sections were stained with uranyl acetate and lead citrate.

Observations were made on a Philips CM120 electron microscope operated at 80kV (Philips, Eindhoven, The Netherlands) and images were recorded with a Morada digital camera (Olympus Soft Imaging Solutions GmbH, Münster, Germany).

c. Histology

Histomorphological study of human biopsies was performed in collaboration with the Morphological Unit of the Institute of Myology, which references and diagnoses biopsies from

patients suffering of neuromuscular diseases. Human open muscle biopsies from two patients carrying the CNM-*Dnm2* mutation p.R465W, one patient carrying the CNM-*Dnm2* mutation p.R369Q, and one healthy control muscle were performed at the Centre de Référence de Pathologie Neuromusculaire Paris-Est, Institut de Myologie, GHU Pitié-Salpêtrière, Assistance Publique-Hôpitaux de Paris, GH Pitié-Salpêtrière, Paris, France, following written informed consent specially dedicated for diagnosis and research. Muscle was frozen in liquid nitrogen-cooled isopentane. For conventional histochemical techniques on human biopsies, 10 µm thick cryostat sections were stained with antibodies against desmin or with reduced nicotinamide adenine dinucleotide dehydrogenase-tetrazolium reductase (NADH-TR) by standard methods. Pictures of each section were obtained with a Zeiss AxioCam HRc linked to a Zeiss Axioplan Bright Field Microscope and processed with the Axio Vision 4.4 software (Zeiss, Germany).

2- Biochemistry

a. Western blotting

Cell samples were collected using Laemli blue 4X directly or a NaCl (150 mM)-EDTA (10 mM) buffer with added 1:100 proteinase inhibitor cocktail (#P8340; Sigma-Aldrich, USA).

Protein samples were separated by electrophoresis in 4-12% 1.5mm 10W bis-acrylamide precast gels (#NP0335BOX; Life Technologies, France) and NUPAGE MOPS SDS running buffer (#NP0001; Life Technologies, France), then electrophoretically transferred to 0.45 µm nitrocellulose membranes (#LC2001; Life Technologies, France) and labelled with primary antibodies that can be found in **Table 4** and secondary antibodies coupled to horseradish peroxidase (Jackson Laboratories, USA). The presence of proteins in samples was detected using Immobilon Western Chemiluminescent HRP Substrate (#WBKLS; Sigma-Alrich, France). Acquisition was performed on a G-Box (Ozyme, France).

b. Immunoprecipitation

Immunoprecipitations (IP) experiments were performed on primary cell cultures or human immortalized myotubes. Myotube pellets were resuspended in 500 µL of lysis buffer (50 mM Tris-HCl, pH 7.5, 0.15 M NaCl, 1 mM EDTA, 1% NP-40) and protein inhibitor cocktail 1:100 (#P8340; Sigma-Aldrich, France). Each sample (500 µg) was precleared twice with 30 µL Protein-G-Sepharose (#11524935; PGS 4 fast flow, Thermo Fisher, France) and incubated with 20 µg of specific antibody overnight (4°C). Washed PGS (40 µL) was first incubated with 2 g/L BSA and further incubated with samples for 2 hours at 4°C. Pelleted PGS was taken up in sample buffer and subjected to electrophoresis and immunoblotting. For all immunoprecipitation experiments,

HRP-conjugated rabbit and mouse IgG TrueBlot secondary antibodies (Rockland Inc., USA) were used.

3- RNA extraction and RT-qPCR

RNA extraction and RT-qPCR were performed by G. Moulay. RNAs were isolated from TA muscles or from myotubes either four days after siRNA transfection, or right after the end of the stretching period, using TRIzol reagent (Life Technologies, France) according to the manufacturer's protocol. Total RNA was then submitted to a DNaseI treatment (New England Biolabs, USA) followed by a phenol-chloroform extraction, and stored at -80°C following Nanodrop ND-1000 spectrophotometer quantification (Nanodrop Technologies, USA). 1 µg of RNA was reverse transcribed using M-MLV first-strand synthesis system according to the manufacturer's instructions (Invitrogen, France) in a total of 20 µL.

To quantify the mRNA expression, real-time PCR was performed using a Lightcycler 480 II (Roche, Switzerland) and 1X SYBR Green (Roche, Switzerland) reactions using 0.2 pmol/µL of forward and reverse primer, and 5 µL of each cDNA diluted to at 1:10 in nuclease-free water. PCR primer sequences for both human and mouse cDNA are listed in **Table 3**. PCR cycles were a 10 min 95°C pre-incubation step followed by 45 cycles with a 95°C denaturation for 10 s, 60°C annealing for 15 s and 72°C extension for 8 s. Each target expression level was normalized using RPLP0 and HPRT1 geometric mean.

4- Statistical analysis

Statistical analysis was performed using Student's t-test except as otherwise stated.

5- Study approval

Animal studies conform to the French laws and regulations concerning the use of animals for research and were approved by an external Ethical committee (approval n°00351.02 delivered by the French Ministry of Higher Education and Scientific Research).

For human studies, all individuals provided informed consent for muscle biopsies according to a protocol approved by the ethics committee of the Centre de Référence de Pathologie Neuromusculaire Paris-Est, Institut de Myologie, GHU Pitié-Salpêtrière, Assistance Publique-Hôpitaux de Paris, GH Pitié-Salpêtrière, Paris, France.

III. Results

1- Ultrastructure and dynamics of clathrin plaques

a. Morphology of clathrin plaques

i. Regularly spaced structures along the PM

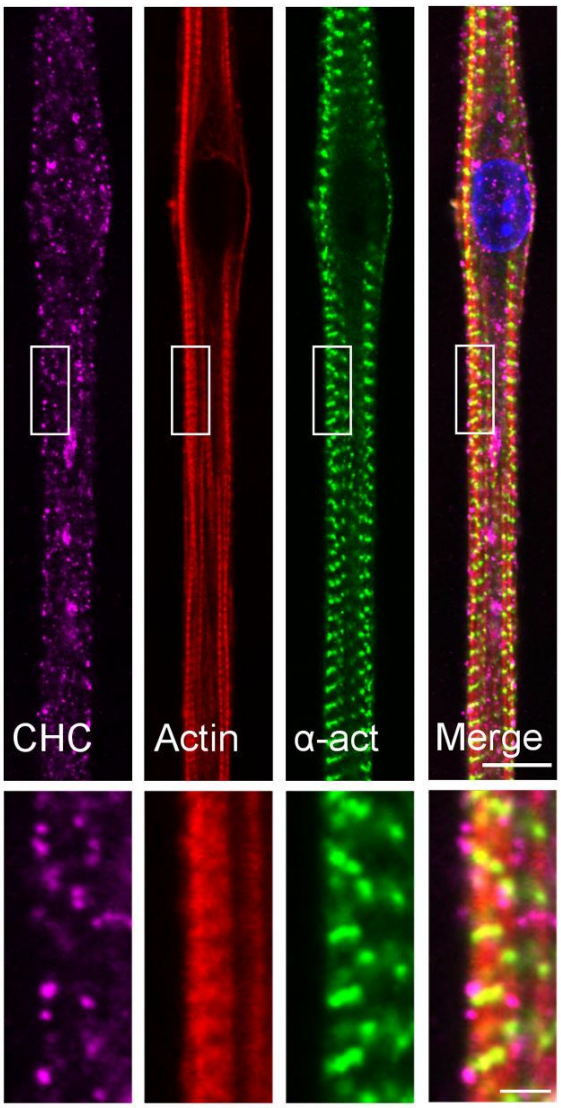

Figure III.1. CCS aligning along the plasma membrane

Immunofluorescent staining of CHC (magenta), actin (red) and α-actinin 2 (green) in mouse primary myotubes differentiated for 10 days. Note the proximity of CHC and α-actinin structures on the insets. Bars are 10 µm and 2 µm for insets.

In order to study the morphology of clathrin plaques, I turned to an *in vitro* model of primary mouse myotubes differentiated for a few days up to two weeks. During cell differentiation, α-actinin 2 reaches a high level of organization with striations regularly spaced on the PM then inside the myotubes. Large clathrin spots cover membranes of myotubes, and these spots tend to get smaller and sparser the longer the differentiation lasts. They also seem to get more organized. At the light microscopy level, after 10 days of differentiation, the actin crosslinking protein α-

actinin 2 and actin itself presented an extremely organized striated distribution approaching that of mature muscle fibers (**Figure III.1**). Reaching this level of differentiation, clathrin-coated structures (CCS) were observed distributed along the PM at roughly periodic intervals of 1 to 3 µm (**Figure III.2**).

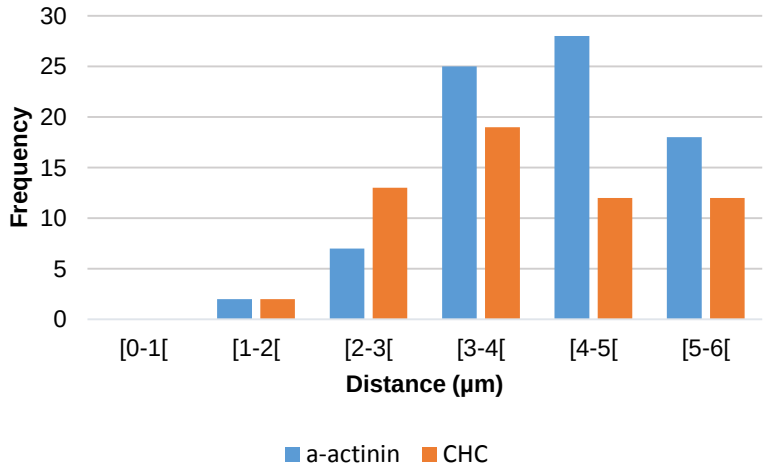

Figure III.2. Distribution of clathrin and α-actinin 2 spots in mature myotubes

Frequency of CHC and α-actinin 2 spots on plasma membrane of a differentiated primary mouse myotube.

Clathrin-positive fluorescent clusters aligned along the α-actinin 2 striations (**Figure II.2**). In order to visualize these structures *en face* at higher resolution, we developed a metal-replica EM approach on highly differentiated unroofed myotubes. We performed the unroofing step exactly with the same procedures as previously described (Heuser, 2000a) but instead of quick-freezing and deep-etching the samples, we combined the simplicity of chemical fixation followed by dehydration and subsequent drying with a solvent whose main property is to have low surface tension. The samples were further metal-coated by platinum sputtering and the replica was backed with a thin layer of carbon. After chemical separation from the glass coverslip, the replicas can be observed using TEM which provides a much higher resolution than scanning EM. This shortcut has turned out to produce extremely good quality replicas but also provides a much higher throughput which enables analysis of more experimental conditions.

Survey views of a myotube's membrane observed with this technique produces very complex images for the unexperienced eye: a difference in contrast allows to define the boundaries of a myotube's membrane. Fixed on it are proteins that resisted shearing: receptors, membranous compartments attached to the membrane, coat proteins and cytoskeletal networks (see II.2-i Unroofing and preparation of metal replicas).

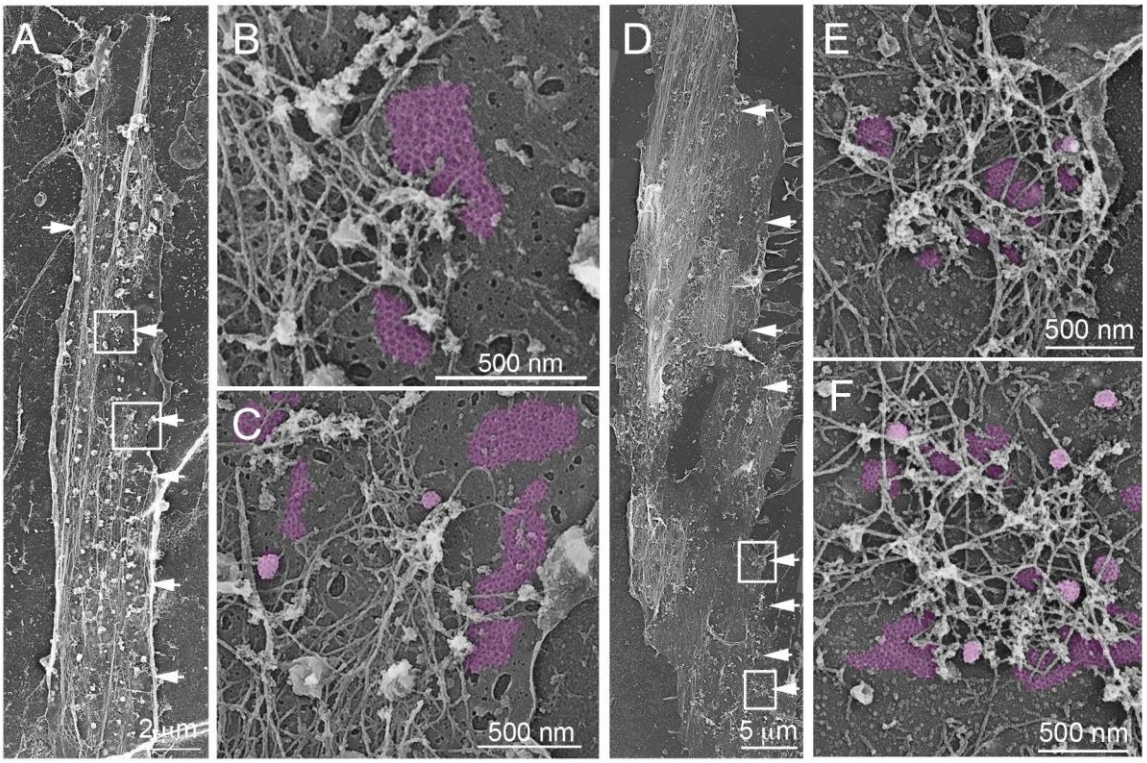

Figure III.3. Myotube membranes studded with flat clathrin-coated structures

(A) Survey view of unroofed primary mouse myotube differentiated for 15 days. (B) (C) Higher magnification views corresponding to the boxed regions in (A). (D) Survey view of the cytoplasmic surface of the PM in an unroofed immortalized human myotube. Arrows denote regularly spaced clathrin plaques. (E) (F) High magnification views of the boxed regions in (D).

Platinum replicas obtained from both primary mouse and human unroofed myotubes presented numerous portions of membrane studded with large clathrin plaques. These were easily recognizable by their honeycombed structure and their degree of curvature discriminated using 3D glases to visualize anaglyphs. They were distributed throughout the plasma membrane, often accumulating in region stress fibers formed by bundled actin cables. Clathrin plaques were surrounded by a branched actin network, recognizable by the thickness of actin filaments and their characteristic 45° angles. They were also interconnected by cytoskeletal elements that formed webs above and between them. Zooming into these structures allowed to observe that these webs looked anchored on clathrin plaques like fingers clutched on the membrane (**Figure III.3**).

ii. AP2 and Dab2 are clathrin plaque adaptors

Studies have characterized the AP2 clathrin adaptor as a *bona fide* component of clathrin plaques in HeLa cells (Grove et al., 2014). Out team demonstrated previously that AP2 colocalized with

CHC on the PM of myotubes and that it participated in α-actinin 2 organization in muscle cells as much as clathrin itself (Vassilopoulos et al., 2014). I performed this staining once again, this time focusing on the adherent part of myotubes, and found a clear colocalization between CHC and its AP2 membrane adaptor (**Figure III.4**).

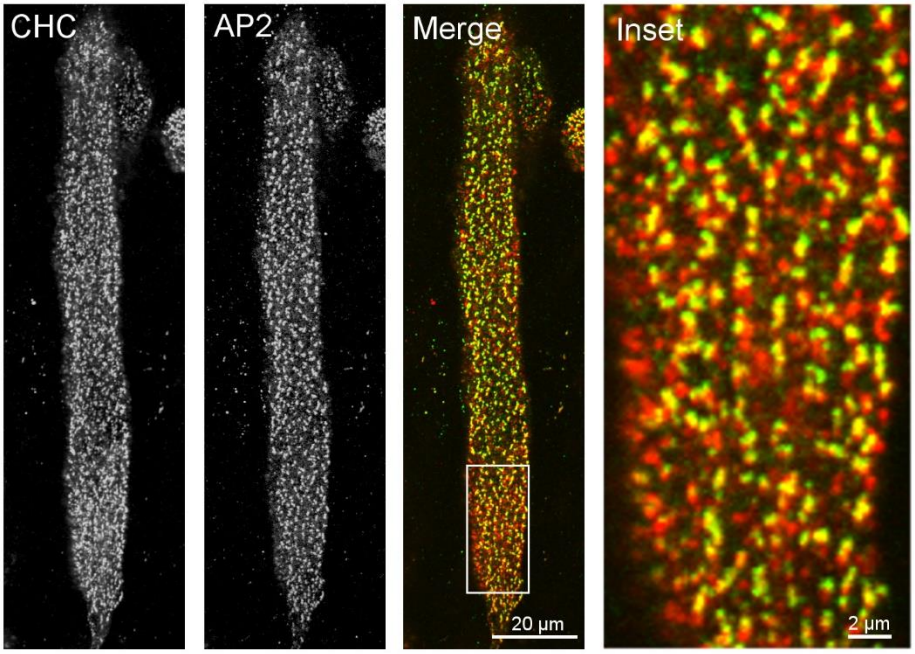

Figure III.4. Colocalization between AP2 and CHC

Immunostaining of CHC and AP2 in primary mouse myotubes. Note the colocalization between AP2 and CHC, particularly at the adherent extremity of the myotube.

Even with the level of colocalization between AP2 and CHC, we wondered if another clathrin adaptor could be located to clathrin plaques. The CLASP Dab2 seemed to be an interesting candidate since a study showed that enhanced levels of Dab2 induced the formation of large clathrin assemblies on the plasma membrane in COS7 cells, and increased adherence and spreading in COS7, HeLa and HBL (human diffuse large B-cell lymphoma) cells (Chetrit et al., 2009). Dab2 is also involved in signaling since it interacts with the Wnt and TGFβ signaling pathways (Hocevar et al., 2001, 2003), as well as with Src and Grb2 (growth-factor-receptor-bound protein 2), which is involved in Ras-mediated signal cascade (Zhou and Hsieh, 2001; Zhou et al., 2003). Importantly, Dab2 is also able to control the location of β1-integrin (Teckchandani et al., 2009).

I performed an immunostaining of Dab2 in mouse myotubes, which indeed showed a recruitment of the protein to the adherent face of cells, but the spots did not completely colocalize with AP2 in primary myotubes (**Figure III.5**).

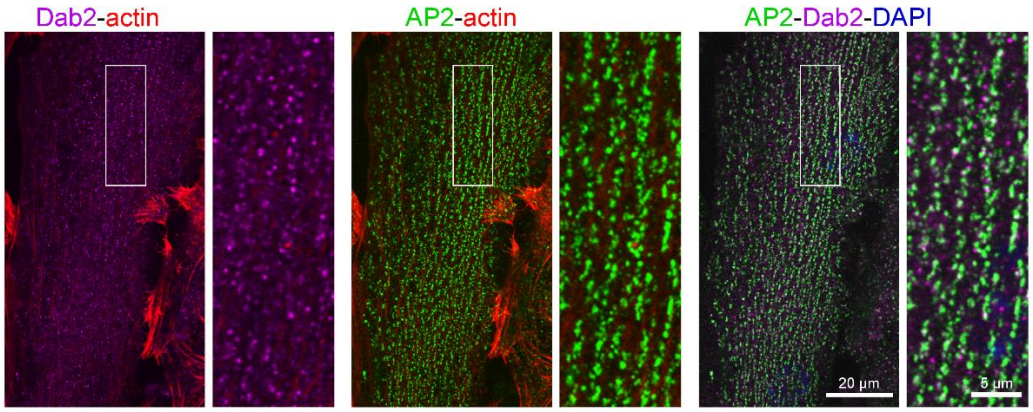

Figure III.5. Partial colocalization between AP2 and Dab2 by immunofluorescence

Immunofluorescent staining of AP2, Dab2 and staining of actin, in C2C12 myotubes. Note that AP2 and Dab2 seem to only partially colocalize.

We also checked the location of Dab2 by immunostaining on unroofed membranes from primary myotubes. We performed the immunogold co-staining of AP2 and Dab2 and were able to precisely locate the proteins on flat clathrin plaques by EM. We found numerous clathrin plaques sharing both antibodies, suggesting that clathrin at plaques is recruited both by AP2 and Dab2 (**Figure III.6**).

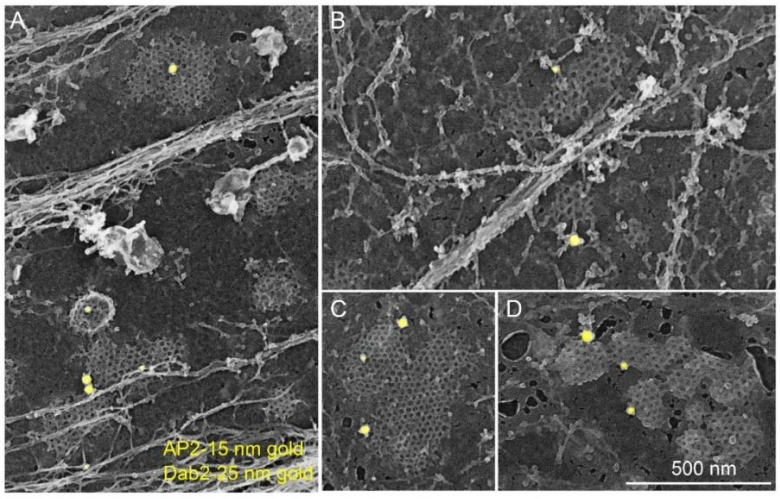

Figure III.6. AP2 and Dab2 clathrin adaptors are located on clathrin plaques

High magnification views of unroofed membranes from control primary mouse myotubes harboring clathrin plaques labelled with AP2 (15 nm gold) and Dab2 (25 nm gold) antibodies. Secondary antibodies conjugated to colloidal gold particles are pseudocolored in yellow. EM performed by S. Vassilopoulos.

We next tested the effect of Dab2 inhibition on primary mouse myotubes by siRNA treatment followed by unroofing and rotary-shadowing. Following Dab2 depletion, we observed oddly shaped clathrin-coated domes on the PM. Although the distortion might arise from the drying process, such large clathrin assemblies are never observed in the control situation, which reminded us of flat clathrin plaques that were somehow unstable or showed a default in attachment to the substrate (**Figure III.7**). In addition, the very few actin processes present at the periphery of such domes in the Dab2-depleted myotubes presented an abnormal appearance.

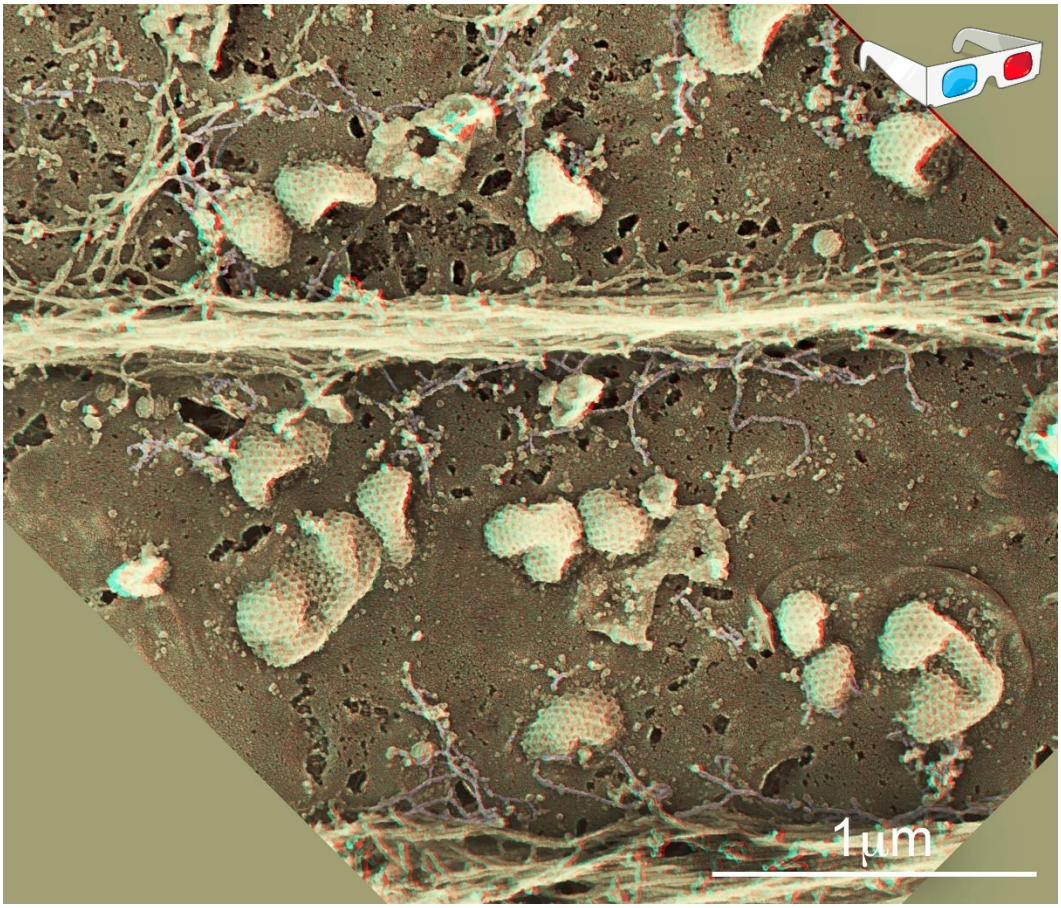

Figure III.7. Abnormal clathrin plaques with depletion of Dab2

Survey view of unroofed membrane from primary mouse myotubes treated with an siRNA targeting N-WASP. Note the abnormal looking clathrin-covered domes associated with membrane deformations. Abnormal looking actin processes are highlighted in purple. Use view glasses for 3D viewing of anaglyphs (left eye = red). EM and 3D performed by S. Vassilopoulos

The membrane on these replicas seemed "loose". This data suggests that Dab2 and AP2 could share domains of clathrin plaques and that removing Dab2 induces defects in clathrin-coated structures. Dab2 could help maintain clathrin plaques and cell adherence by its ability to cluster adhesive β integrins.

iii. Clathrin plaques act as scaffold for cytoskeletal anchoring

Following the characterization of plaque adaptors, we wanted to study the interaction between plaques and the cytoskeleton. Our ultrastructural analysis showed actin formation around clathrin plaques, distinct from actin bundles traveling myotubes from end to end. This suggested the presence of branched actin interacting with flat clathrin plaques (see **Figure III.3** p.81).

I subjected C2C12 myotubes to a 24h treatment of latrunculin B, 100 nM for 24 hours. This compound is used to destabilize the actin cytoskeleton by sequestering G-actin. I found that intracellular actin was disorganized upon drug treatment but that actin anchored on AP2-positive puncta was actually very difficult to destabilize, and bundles remained anchored on the PM at these sites (**Figure III.8**).

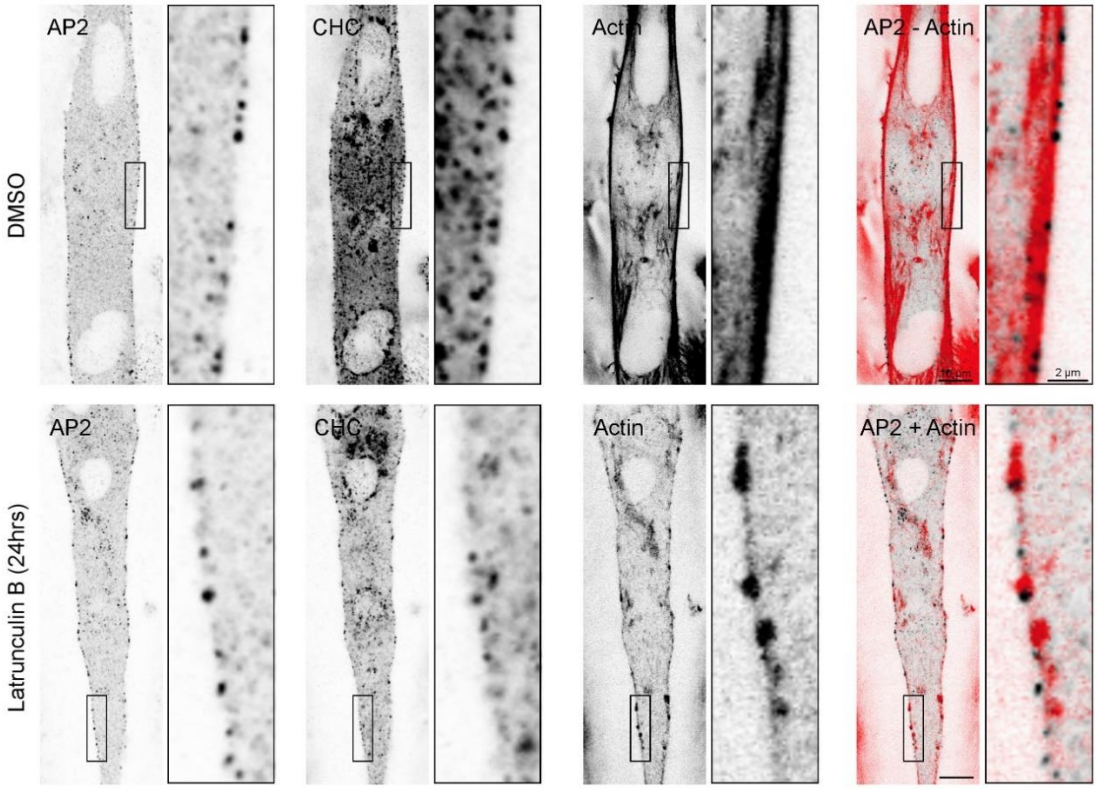

Figure III.8. Actin attached to AP2 positive structures even after latrunculin B treatment

Staining with antibodies against AP2, CHC or staining of actin with Phalloidin-A488, on C2C12 myotubes treated during 24h with a low concentration of latrunculin B (100 nM). Note the remaining bright actin points seemingly anchored on AP2 structures on the merged image, after 24 hours of latrunculin B treatment.

I wanted to know the nature of actin filaments gathered around flat clathrin plaques. Their branched organization reminded us of the typical assembly organized by actin-associated proteins N-WASP and ARP2/3 (Svitkina and Borisy, 1999). I performed an immunogold staining of ARPC2 – a component of the ARP2/3 complex – on unroofed myotube membranes. It was detected on actin filaments surrounding clathrin plaques (**Figure III.9**). This result is in accordance with the role of actin polymerization promoted by ARP2/3 in the regulation of clathrin plaques (Leyton-Puig et al., 2017).

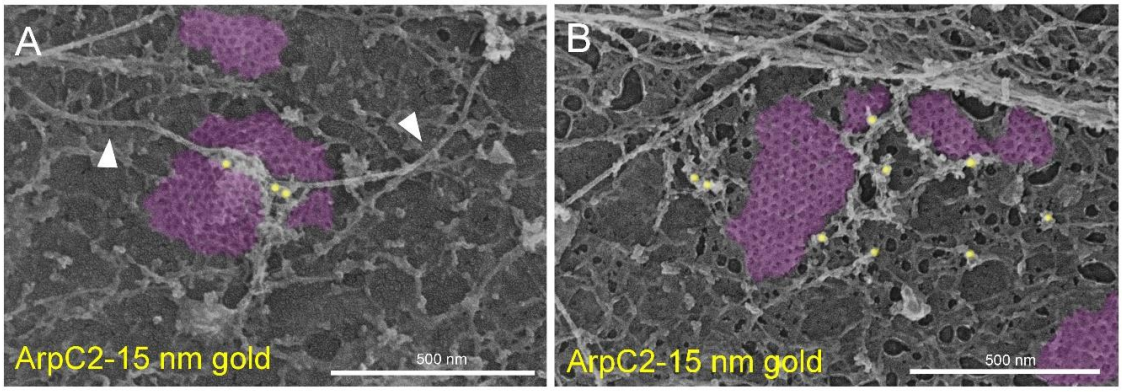

Figure III.9. Arp2/3 interacts with actin surrounding clathrin plaques

(A-B) High magnification views of unroofed membranes from control primary mouse myotubes harboring clathrin plaques surrounded by actin networks labelled with ARPC2 antibodies. Note the IF (arrowhead) caught in an actin clamp labelled with ARPC2 in (A). Clathrin lattices are highlighted in purple. Secondary antibodies conjugated to 15-nm colloidal gold particles are pseudocolored in yellow.

In order to study how branched actin networks formed around clathrin plaques, I turned to the protein Neuronal Wiskott–Aldrich Syndrome protein (N-WASP) which controls the activation of ARP2/3 and that I could readily deplete by siRNA. N-WASP is directly involved in the generation of ARP2/3 branched actin filaments and a known DNM2 indirect partner (Takenawa and Suetsugu, 2007). With G. Moulay (post-doctoral researcher in the team), we designed siRNAs against N-WASP, that I used to specifically deplete the protein in primary mouse myotubes. With S. Vassilopoulos, we performed unroofing on these myotubes followed by metal replicas, and detected abnormal actin formations around clathrin plaques. These abnormal structures consisted of accumulation of poorly branched comet-tail-like actin around some clathrin-coated pits and large masses of unbranched actin around clathrin plaques (**Figure III.10**). These were not unlike the actin structures which have been previously reported in N-WASP knock-out mouse podocytes (Schell et al., 2013). This confirmed the role of N-WASP in regulation of the branched actin network around flat clathrin lattices.

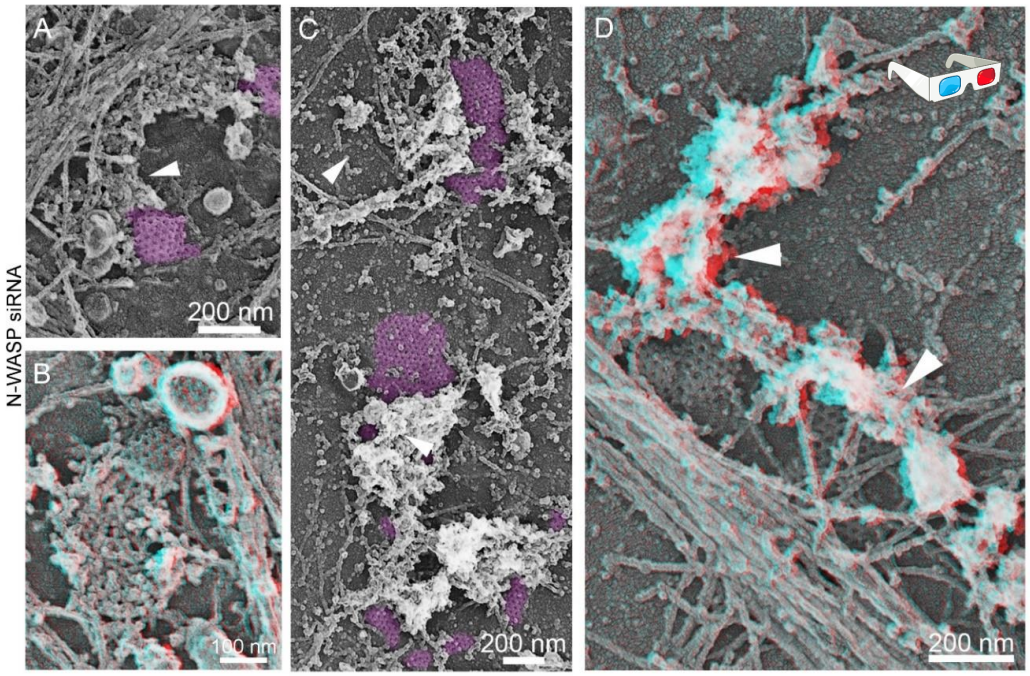

Figure III.10. Abnormal actin assemblies around clathrin plaques in N-WASP depleted myotubes

Representative branched actin (arrowheads) around clathrin-coated structures (purple) in unroofed primary mouse myotubes treated with siRNA against N-WASP. For (B) and (D), use view glasses for 3D viewing of anaglyphs (left eye = red).

Since DNM2 role has been described in a plethora of actin-mediated processes, involved in endocytosis (Mooren et al., 2012; Palmer et al., 2015; Taylor et al., 2012) or distinct from endocytosis (Baldassarre et al., 2003; Cao et al., 1998; Destaing et al., 2013; Gu et al., 2010, 2016; Kurklinsky et al., 2011; McNiven et al., 2000; Ochoa et al., 2000; Yamada et al., 2013), I checked the effect that DNM2 depletion would have on actin in myotubes. First, I let primary mouse myotubes form and differentiate during a few days before fixing them and performing an immunostaining for α-actinin 2. This would allow me to observe immature z-bodies in formation by confocal microscopy. I also performed an siRNA treatment to compare the α-actinin 2 staining between control and DNM2-depleted myotubes. I observed the earlier stages of α-actinin 2 striations in control myotubes, whereas in DNM2-depleted myotubes, I detected clusters of the protein dispersed in the cytoplasm (**Figure III.11A**).

Next, I used an extensive differentiation protocol on primary mouse myotubes in order to achieve the development of mature myofibrils. I depleted DNM2 from these highly differentiated myotubes and wanted to compare the aspect of sarcomeres between control and DNM2-depleted mature myotubes. J. Lainé performed ultra-thin sections followed by EM of mature myotubes

depleted of DNM2. She was able to confirm that clusters of α-actinin 2 that I was seeing by confocal microscopy were in fact dispersed and abnormal Z-bands (**Figure III.11B**).

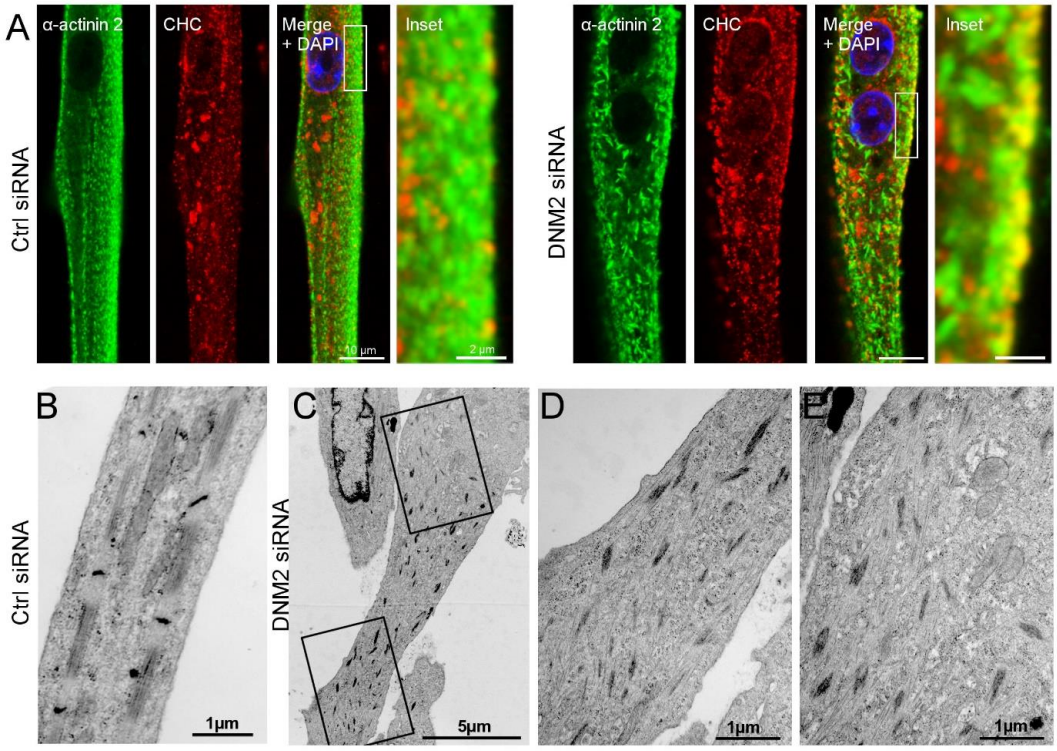

Figure III.11. Defective Z-band formation in DNM2-depleted myotubes

(A) Immunofluorescent staining of α-actinin 2 (green) and CHC (red) in mouse primary myotubes treated with control siRNA or siRNA against DNM2. (B-E) Thin-section EM of primary mouse control (B) or DNM2-depleted (C-E) myotubes (EM by J. Lainé).

More specifically, because of its supposed indirect interaction with N-WASP and direct interaction with cortactin (Cao et al., 2003; Orth et al., 2002), we reasoned that DNM2 could directly participate to organize branched actin filaments surrounding clathrin plaques. Previous studies have shown an interaction between DNM2 and actin-binding proteins via DNM2 PRD domain (Schafer, 2004). I performed co-immunoprecipitation experiments using DNM2 antibodies on mouse myotube lysates. Using antibodies against N-WASP, I was able to co-immunoprecipitate N-WASP with DNM2, suggesting that there was an interaction between DNM2 and N-WASP in differentiated skeletal muscle myotubes (**Figure III.12**).

Since N-WASP depletion had a grave effect on actin organization around clathrin plaques, I wanted to test if DNM2 depletion produced similar abnormal actin accumulations. We decided to directly visualize the effect of DNM2 depletion on the actin structures surrounding clathrin plaques.

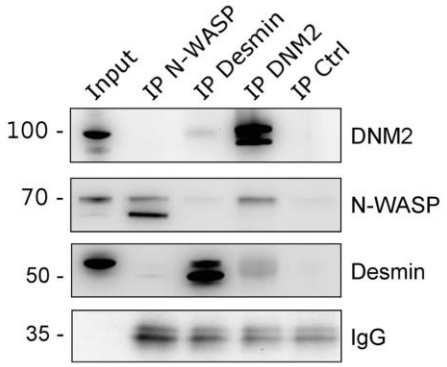

Figure III.12. Interaction between N-WASP and DNM2

Immunoblot of proteins associated with N-WASP, desmin, DNM2, or control immunoprecipitates from control mouse primary myotube lysates and 4% lysate input. Bands for coimmunoprecipitated DNM2, N-WASP or desmin are indicated at the right.

Immature actin-seeds and actin accumulations plagued the plasma membrane of DNM2-depleted myotubes when observed by EM after unroofing and metal replica, much like N-WASP depletion (**Figure III.13**). This confirmed the importance of DNM2 in regulating branched F-actin structures around clathrin plaques.

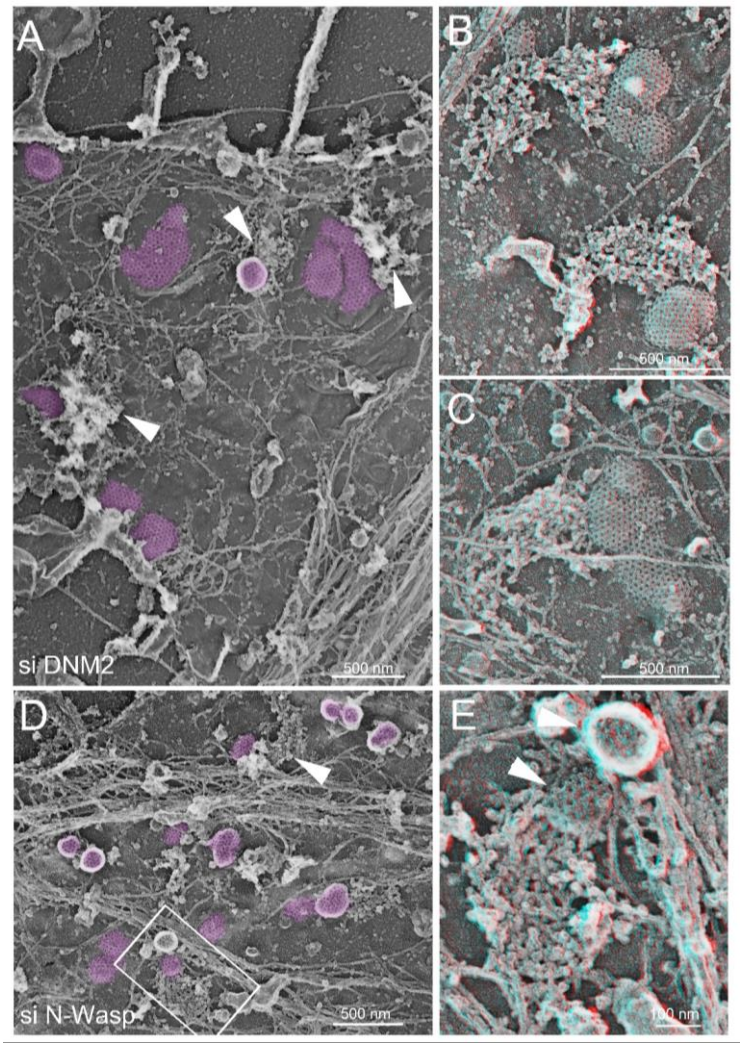

Figure III.13. DNM2 and N-WASP depletion affect clathrin-coated pits and associated actin

(A-C) Cytoplasmic surface of the PM of an unroofed DNM2-depleted primary mouse myotube. Clathrin-coated structures in (A) are highlighted in purple, abnormal actin structures are shown using arrowheads. (D) Survey view of the cytoplasmic surface of the plasma membrane of an unroofed N-WASP-depleted primary mouse myotubes. CCS are highlighted in purple, abnormal actin structures are shown using arrowheads. (E) Higher magnification of boxed region in (D). Arrowheads denote clathrin lattices. For (B, C, E) use view glasses for 3D viewing of anaglyphs (left eye = red).

A very recent study demonstrated that flat clathrin plaques were regulated by N-WASP dependent branched actin in HeLa cells (Leyton-Puig et al., 2017). I performed the experiment several times, and although they were increased in size and sometimes seemed fragmented, we were unable to conclude a direct effect of DNM2 depletion or N-WASP depletion on the morphology of clathrin plaques by EM in myotubes. This argument is in favor on a top-down approach in our system, and that clathrin regulates actin around plaques but not the other way around. The increased plaque size in DNM2-depleted myotubes could be the consequence of decreased endocytosis at these sites.

iv. Clathrin plaques scaffold intermediate filaments

During the imaging of hundreds of clathrin plaques, several components seemed to be present invariably: flat clathrin lattices and branched actin anchored on these flat plaques. We started to notice another type of filaments above these structures, different in appearance from actin filaments. Direct visualization and measurements of filament diameter allowed to observe that these long filaments were thicker – 15 nm in average versus 10 nm for actin filaments – and weaving between actin stress fibers in a distinct pattern. (**Figure III.14**). The more we analyzed those filaments on 3D anaglyphs, the more they reminded us of intermediate filament (IF) structure. IFs are about 15 nm wide, can be very long, and indeed weave through actin networks in this typical configuration (Hirokawa et al., 1982).

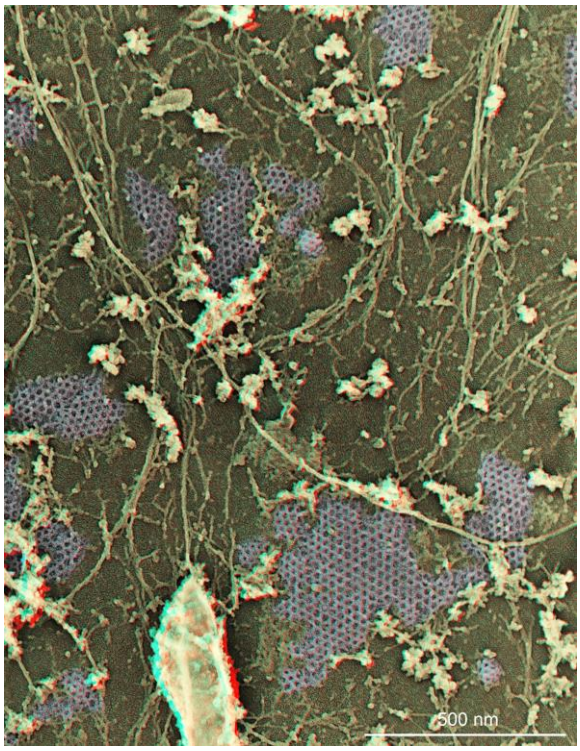

Figure III.14. CCS interact with branched actin and intermediate filaments

View of the cytoplasmic surface of the PM in an unroofed myotube. Clathrin lattices are pseudocolored in purple. Use glasses for 3D viewing of anaglyphs (left eye = red).

To ensure that we were observing a network of muscle-specific intermediate filaments, we used immunogold labelling combined to metal-replica EM to show that this three-dimensional network directly connecting actin stress fibers and branched actin "nests" surrounding flat clathrin plaques is composed of desmin intermediate filaments (**Figure III.15C**). These filaments that weave their way from the plasma membrane, between the sarcolemma, around the organelles and all the way to the nucleus, seemed somewhat pinched by actin networks on the adherent face of the PM.

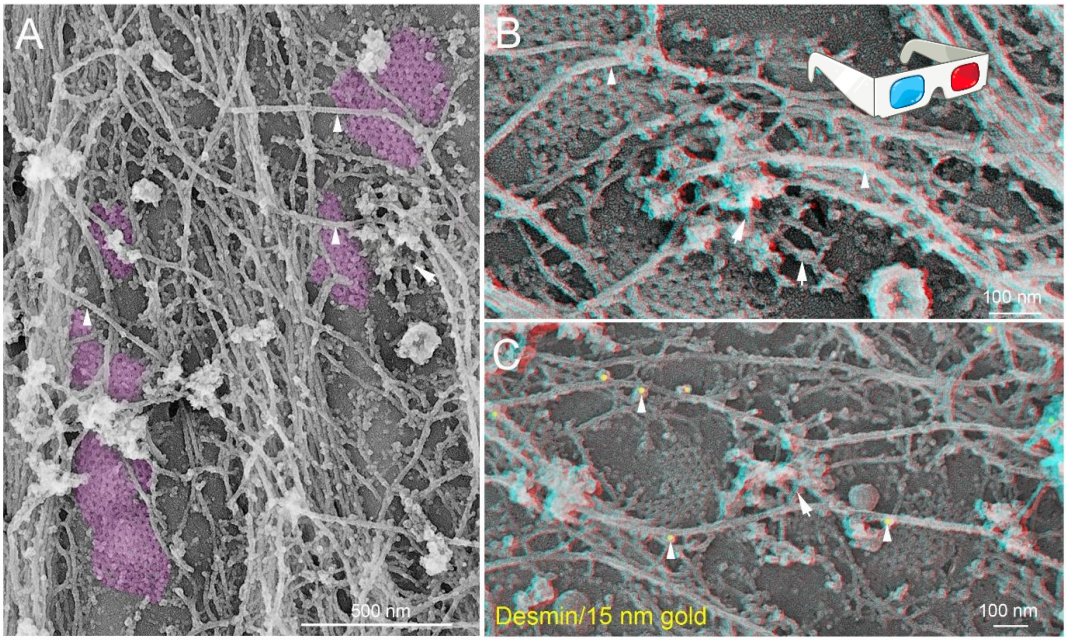

Figure III.15. Clathrin plaques aligning along the PM anchor desmin intermediate filaments

(A) Survey view of the cytoplasmic surface of the plasma membrane of an unroofed primary mouse myotube differentiated for 15 days. Intermediate filaments are denoted with arrowheads and clathrin lattices are highlighted in purple. (B) Higher magnification view of a clathrin plaque from (A) and associated cytoskeleton. IFs are denoted with arrowheads. Arrows indicate the branched actin network. (C) Adherent plasmalemmal sheets prepared from control differentiated primary myotubes labelled with desmin antibodies followed by secondary antibodies conjugated to 15-nm colloidal gold particles (pseudocolored in yellow). For (B-C) use view glasses for 3D viewing of anaglyphs (left eye = red). EM by S. Vassilopoulos.

I wanted to test the possibility that clathrin plaques were directly required for organization of the cortical desmin network. I used an siRNA against CHC (Ezratty et al., 2009; Vassilopoulos et al., 2014) to specifically deplete the protein and observed desmin distribution by confocal microscopy. Desmin striation only appears after an extended differentiation. Following a short differentiation period, myotubes exhibit mainly a plasmalemmal staining of desmin. CHC depletion in myotubes induced a strong aggregation of desmin in the cytoplasm. These aggregates translated by numerous small or large cytoplasmic “balls” of desmin (**Figure III.16A**).

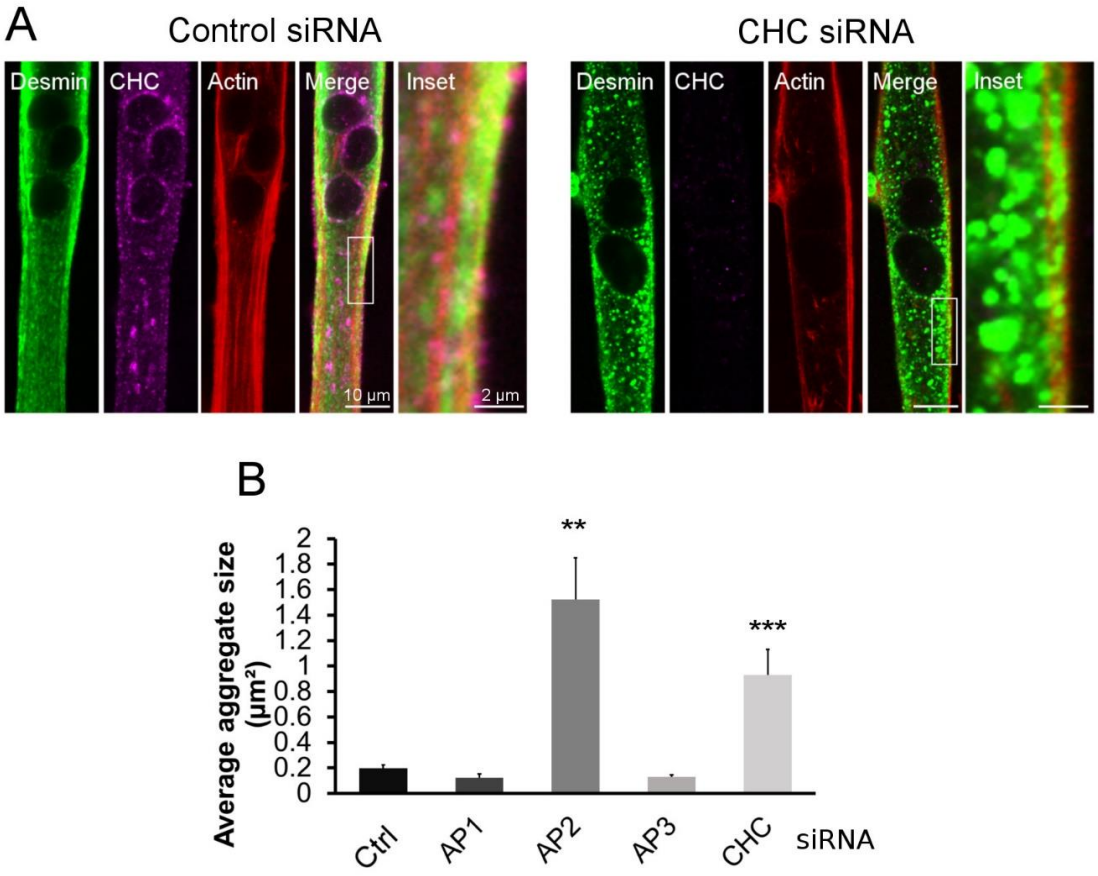

Figure III.16. Clathrin-coated structures at the PM are required for IF organization

(A) Immunofluorescent staining of desmin (green), CHC (magenta) and actin (red) in differentiated mouse primary myotubes from control (left panel) or myotubes treated with siRNA against CHC (right panel). Note that high knock-down efficiency correlates with presence of desmin aggregates inside the cytoplasm. (B) Average desmin aggregate size in myotubes treated with control siRNA or siRNA against CHC (n = 30–40 myotubes, data are presented as mean ± SEM; Student's t-test was performed, **P < 0.01, ***P < 0.001).

I selectively depleted clathrin adaptors to study the effect it would have on the desmin cytoskeleton. I depleted the γ-subunit of AP1 and the δ-subunit of AP3, involved in the recruitment of clathrin to the Golgi apparatus and endosomal systems respectively. The depletion had no effect on desmin distribution. But when I depleted the AP2 adaptor, I observed that it phenocopied CHC depletion and induced the formation of desmin aggregates in the cytoplasm as well (**Figure III.16B**).

We were very surprised because the desmin aggregates were in fact very similar to the abnormal desmin accumulations in myotubes from patients harboring desmin mutations involved in desminopathies (Bär et al., 2005; Clemen et al., 2013). Primary cells from a patient with a *DES* p.R350P mutation were immortalized by K. Mamchaoui at the Cell Platform of the laboratory. I

performed an immunostaining of desmin in myotubes and found very large cytoplasmic aggregates of desmin. These accumulations also systematically excluded actin present as stress fibers in the cytoplasm (**Figure III.17A**). These aggregates of desmin resisted shearing forces induced by unroofing and formed really dense tangles (**Figure III.17D**) associated to clathrin plaques on the cell periphery (**Figure III.17E**).

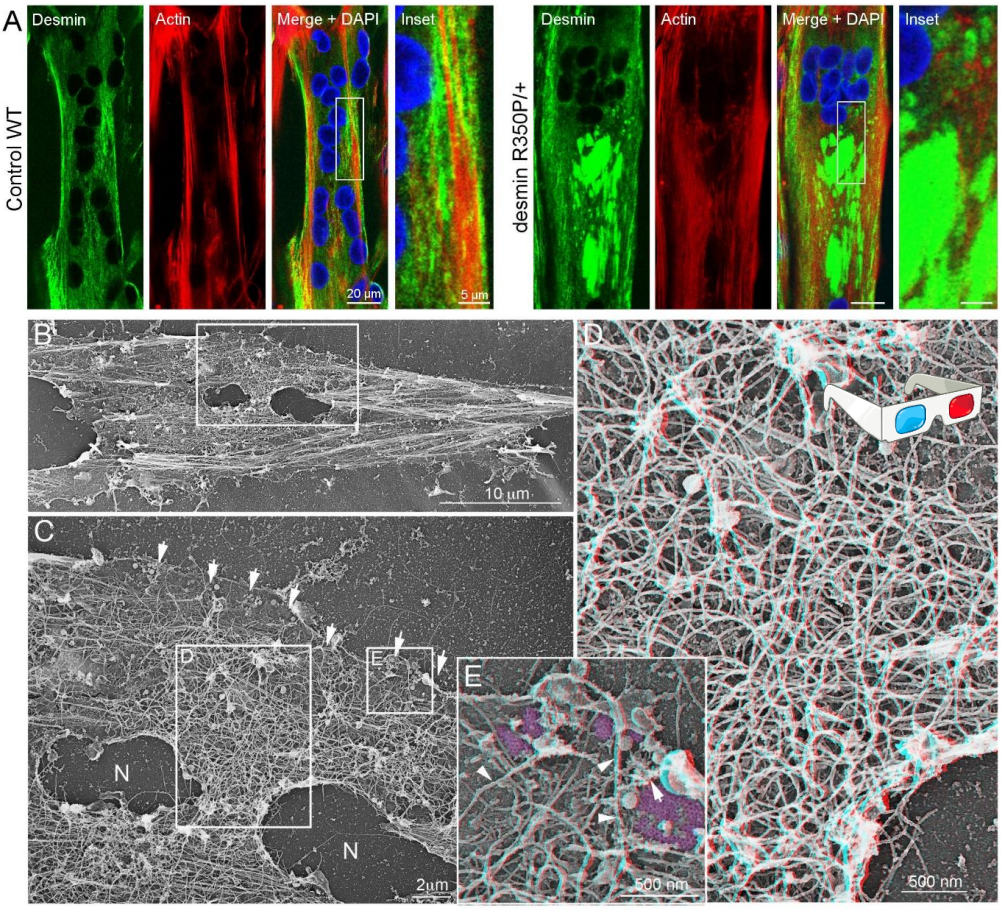

Figure III.17. Desmin aggregates in desminopathy patient immortalized myotubes

(A) Immunofluorescent staining of desmin (green) and actin (red) in immortalized human myotubes from a control subject (left panel) or from a patient with the R350$^{P/+}$ desmin mutation (right panel). (B) Survey view of the cytoplasmic surface of the plasma membrane in unroofed human myotubes from a patient with R350$^{P/+}$ mutation in desmin displaying intermediate filament tangles. (C) Higher magnification view of (B). Clathrin plaques indicated with arrows. (D) Higher magnification view of (C) showing intermediate filament tangles. (E) Higher magnification view of (C) showing clathrin plaques and associated cytoskeleton. Note intermediate filaments (arrowheads), branched actin (arrows) surrounding clathrin lattices (in purple). For (D) and (E) use view glasses for 3D viewing of anaglyphs (left eye = red).

Thin-section EM further demonstrated that the aggregates induced by CHC or AP2 depletion were in fact composed of IF tangles, characterized by their morphology and their size (**Figure III.18**). In CHC- or AP2-depleted myotubes, we observed aggregates of desmin where filaments were very

easily discernible in contrast with the usually very dense desmin aggregates that are often seen by EM in desminopathies.

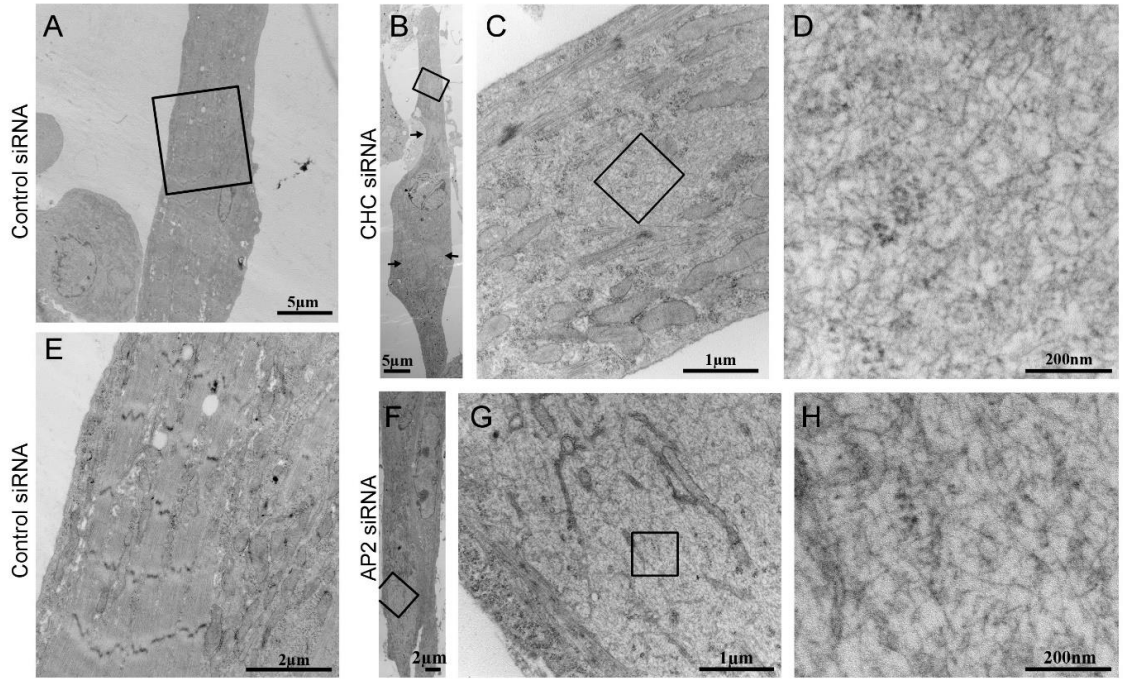

Figure III.18. CHC- or AP2-depleted myotubes are filled with IF tangles

Thin-section EM of primary myotubes treated with control (A) (E), CHC (B-D) or AP2 (F-H) siRNA. EM by J. Lainé.

We concluded from these results that clathrin recruited to the plasma membrane of muscle cells is essential for a correct anchoring of desmin intermediate filaments.

I wanted to test whether the opposite might be true, meaning that desmin is required for clathrin plaque formation. We obtained desmin knock-out mice from O. Agbulut's team (Sorbonne Universités) and isolated satellite cells from homozygote desmin knock-out newborn pups. It is interesting to note that I detected no difference in the distribution of clathrin plaques between WT myotubes and myotubes formed from desmin knock-out mouse myotubes (**Figure III.19**). Therefore, the absence of desmin is compatible with the presence of clathrin plaques. This supports the top-down approach that we envisioned earlier for actin, and the conclusion that clathrin organizes desmin but that the disorganization of the desmin networks does not have a strong impact on clathrin plaque abundance.

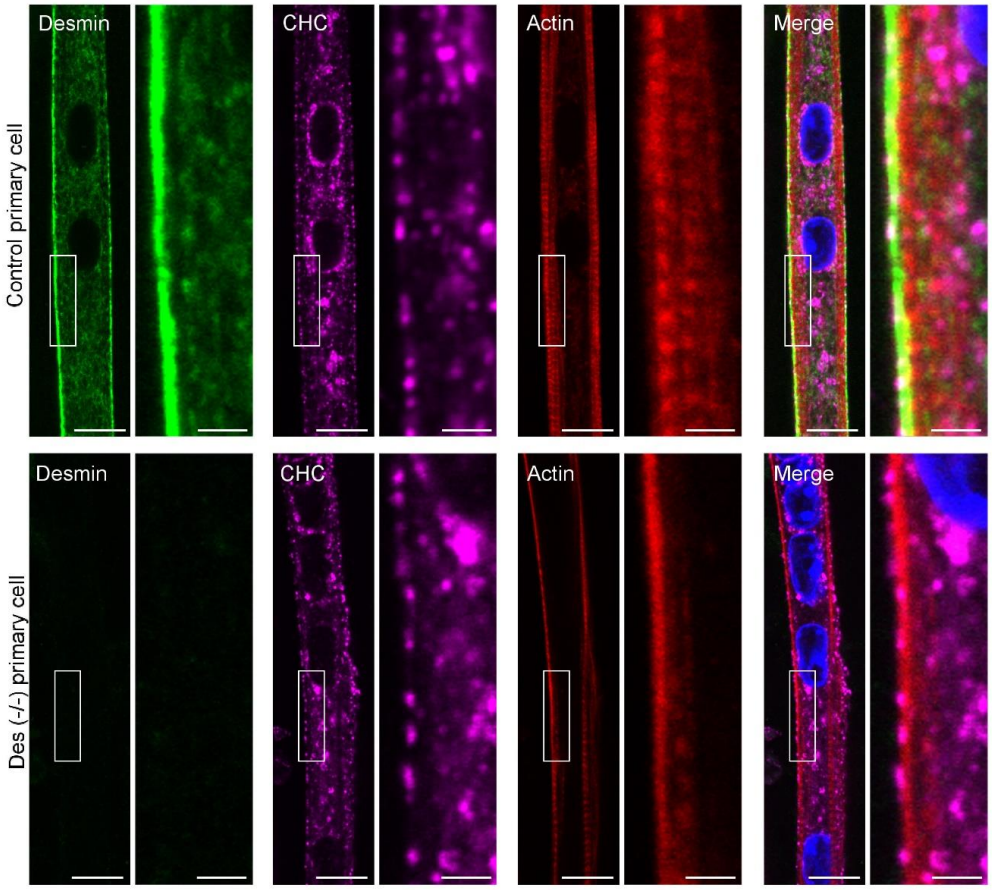

Figure III.19. Clathrin plaques are correctly distributed in myotubes from desmin knock-out mice

Immunofluorescent staining of desmin (green) and CHC (magenta) and actin staining (Phalloïdin-A488, red) in differentiated mouse primary myotubes from WT mice (top panel) or myotubes from desmin knock-out mice ($Des^{-/-}$, bottom panel). Bars 10 µm and 2 µm for insets.

v. Actin surrounding clathrin plaques organizes the cortical IF anchoring

I noticed that the branched actin networks organized by N-WASP and DNM2 seemed to "grab" intermediate filaments by forming a shell around them. Therefore, I wondered if branched actin filaments surrounding clathrin plaques could also anchor cortical desmin IFs.

First, I depleted N-WASP from primary mouse myotubes and performed immunostaining of desmin to observe the effect of the depletion on IF organization. In N-WASP-depleted myotubes, I observed large desmin aggregates similar to those produced by CHC depletion (**Figure III.20**).

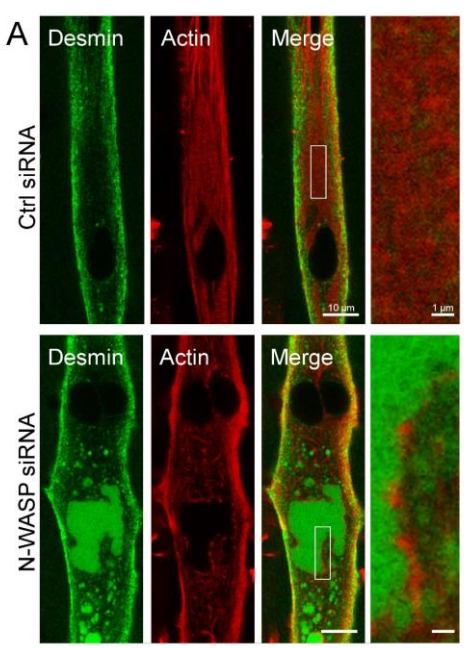

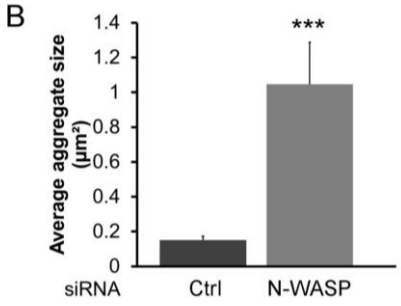

Figure III.20. N-WASP is required for desmin organization

(A) Immunofluorescent staining of desmin (green) and actin (red) in mouse primary myotubes treated with control or N-WASP siRNA. (B) Desmin aggregate fluorescence in myotubes treated with control or N-WASP siRNA (*n* = 20 myotubes; Data are presented as mean ± SEM; ***P < 0.001)

Ultrastructural analysis on unroofed membranes confirmed the presence of these aggregates sometimes still adherent to the PM and resistant to shearing forces induces by unroofing (**Figure III.21**). These looked very similar to unroofed myotubes formed by *DES* p.R350 cells and thin-section EM of CHC-depleted myotubes (compare **Figure III.21C** with **Figure III.17C** and **Figure III.18D**).

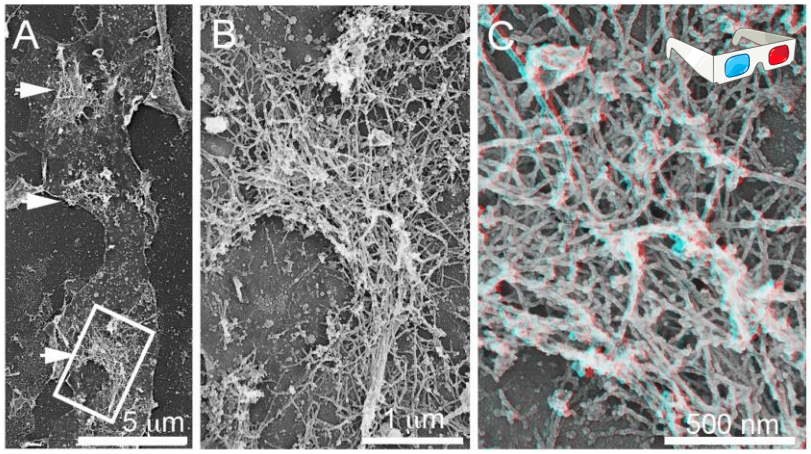

Figure III.21. IF aggregate in N-WASP depleted myotube

(A) Survey view of the cytoplasmic face of the plasma membrane in unroofed primary mouse myotube treated with siRNA against N-WASP. Arrows indicate the presence of intermediate filament tangles still tightly associated with the plasma membrane. (B) (C) Higher magnification views of boxed region in A. For (C), use view glasses for 3D viewing of anaglyphs (left eye = red).

Since I showed that depletion of DNM2 induced abnormal actin structures forming around clathrin plaques, I wondered if these actin structures would still be able to anchor IFs at the plasma membrane. Using an siRNA against DNM2 on primary mouse myotubes, I observed the presence of large desmin aggregates filling large portions of the cytoplasm of myotubes, much like in CHC- or N-WASP-depleted cells (**Figure III.22, A-B**). The phenotype was even more dramatic than that of clathrin depletion, showing that DNM2 is essential for desmin anchoring. I also noticed an increase in clathrin recruitment to the PM (**Figure III.22C**). I propose here that DNM2 has a dual role in the regulation of clathrin plaques, both on the endocytosis of plaque compartments, but also in shaping actin around them, which would explain this very dramatic phenotype.

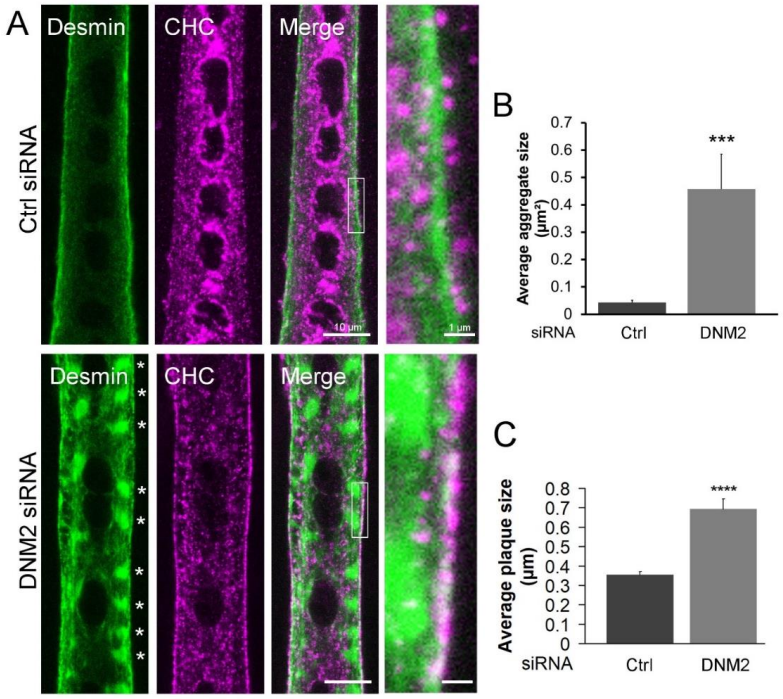

Figure III.22. DNM2 is indispensable for desmin organization

(A) Immunofluorescent staining of desmin (green) and CHC (magenta) in control or DNM2-depleted mouse primary myotubes. Asterisks denote desmin aggregates aligned along the PM. (B) Desmin aggregate fluorescence in mouse primary myotubes treated with control or DNM2 siRNA (n = 20 myotubes). (C) Average CCS size in mouse primary myotubes treated with control or DNM2 siRNA (n = 20 myotubes). (Data are presented as mean ± SEM; ***P < 0.001, ****P < 0.0001)

Ultrastructural analysis by thin-section EM revealed that these aggregates systematically contained IF tangles, very similar to aggregates found in CHC-depleted myotubes (Compare **Figure III.23 to Figure III.18**). We also spotted ER membrane tubes of unknown origin inside the tangles. The abnormal growth of these tubules is still unexplained although it could be due to the membrane remodeling properties of dynamin.

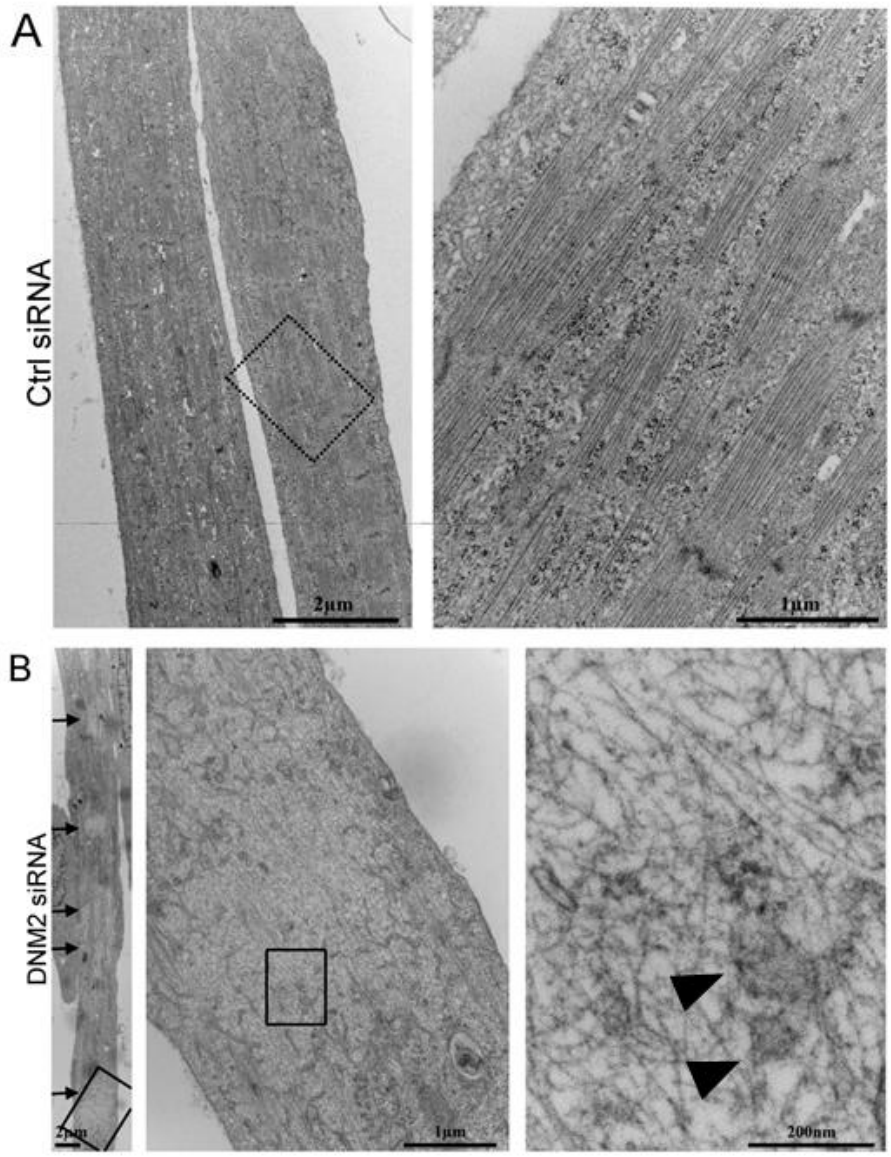

Figure III.23. DNM2-depleted myotubes display desmin bundle aggregates

Thin-section EM of control (A) or DNM2-depleted (B) myotubes. Arrows denote clearer IF bundles. Arrowheads show the presence of ER structures in IF tangles. EM by J. Lainé.

Metal-replica EM on unroofed myotubes confirmed the presence of very complex-looking aggregates that resisted sonication shear forces during unroofing (**Figure III.24**). Surprisingly, pictures also confirmed the presence of intertwining ER membrane tubes inside IF tangles.

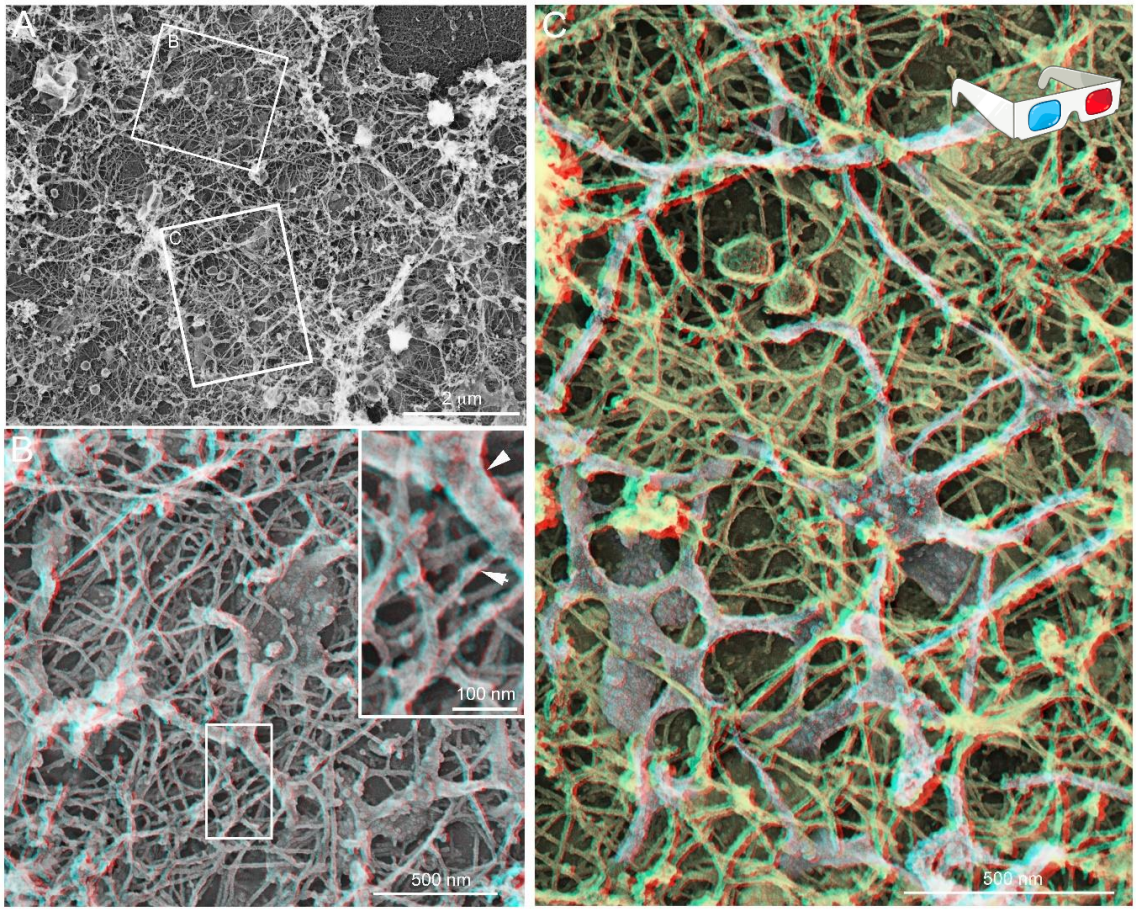

Figure III.24. DNM2 depletion causes intermediate filaments aggregation

Representative picture of sub-sarcolemmal tangles of desmin filaments (arrow) and ER (arrowhead) in unroofed primary mouse myotubes treated with siRNA against DNM2. In (C) ER structures are highlighted in purple. For (B) and (C) use view glasses for 3D viewing of anaglyphs (left eye = red). EM and image manipulation by S. Vassilopoulos.

I detected the presence of large proteins on desmin IFs. By doing a search on usual desmin-interacting proteins, I found the αB-crystallin small heat-shock protein as a common partner of desmin. This protein is a strong regulator of desmin by inhibiting its tendency to aggregate and a mutation in its gene has been involved in the development of DRM (Bova et al., 1999). I performed an immunostaining for αB-crystallin on primary mouse myotubes. While in control cells, αB-crystallin is diffusely spread throughout the cytoplasm, I noticed that this protein formed aggregates in DNM2-depleted myotubes (**Figure III.25**), suggesting that it was recruited to abnormal desmin accumulations but incapable of dismantling them. I performed a co-staining of αB-crystallin with ArpC2 and surprisingly found that accumulations of αB-crystallin in DNM2-depleted myotubes also contained some ARPC2 although they completely excluded actin (**Figure III.25**).

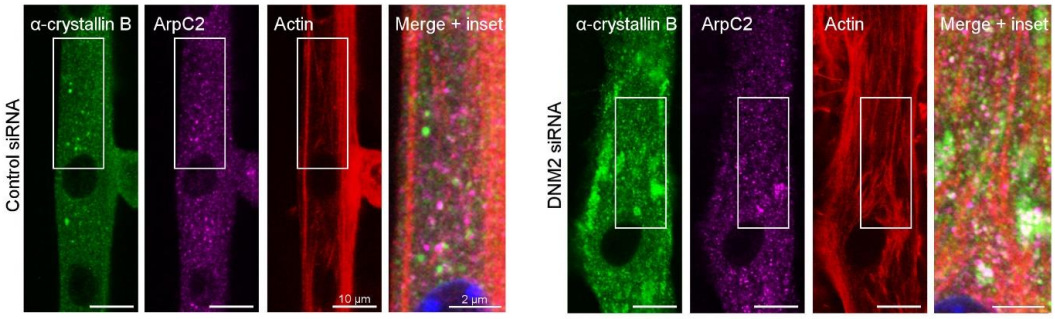

Figure III.25. αB-crystallin and ArpC2 accumulate in desmin aggregates

Immunofluorescent staining of αB-crystallin (green), ArpC2 (magenta) and actin (red) in differentiated mouse primary myotubes from control or myotubes treated with siRNA against DNM2. Note the strong aggregation of αB-crystallin in DNM2-depleted myotubes.

Overall, by combining confocal microscopy to high-resolution observation by TEM of metal replicas, I was able to complete my comprehension of the ultrastructure of this peculiar membrane compartment. I was able to decipher partially the composition of the clathrin plaque. We knew they contained flat clathrin lattices, actin, and the costameric protein α-actinin 2. During this first part of my project, I was able to show that the branched network around clathrin plaques is organized by ARP2/3 and its activator N-WASP, as well as by DNM2. This means that DNM2 take a center stage in clathrin plaques, by regulating their endocytic events but also the complex networks that organize around them.

Secondly, I discovered that these branched actin networks were supporting a web of desmin intermediate filaments, thus explaining why removing clathrin plaques completely destroys sarcomeric integrity.

The first part of my thesis exclusively focused on clathrin plaques and their association with the cytoskeleton *in vitro*. However, in order to understand how these structures participate in muscle physiology and pathophysiology of CNM, it is important to study these processes *in vivo*. The second part of my project consisted in deciphering the dynamics of these newly described structures in adult muscle, and specifically at the costameres.

b. Stable structures with a dynamic turnover

i. Clathrin plaques are stable structures in adherent myotubes

In vitro investigations of clathrin-coated structures have revealed a whole array of forms and dynamics (Lampe et al., 2016) but their *in vivo* dynamics are far less well understood.

In order to analyze the behavior of clathrin exclusively at the surface of cells or fibers, we took advantage of the clathrin adaptor specificity. We reasoned that although CHC is abundantly present in several intracellular compartments, the AP2 adaptor is specifically recruited at the PM and is a *bona-fide* component of clathrin plaques in muscle (Vassilopoulos et al., 2014).

S. Vassilopoulos developed an adeno-associated virus (AAV serotype 9), produced by the vectorology platform of the laboratory, expressing the μ2-subunit of the AP2 clathrin adaptor tagged with mCherry which has previously been shown to be correctly incorporated into coated pits in cultured cells without altering their dynamics (Taylor et al., 2011a). We tested this AAV in mouse myotubes and by live microscopy performed by B. Cadot, we were able to detect large patches of AP2-mCherry that seemed stable through time (**Movie 1**). The persistence of signal observed for AP2 during prolonged times is a characteristic feature of coated plaques as reported in Cos7 and Hela cells (Grove et al., 2014).

ii. In vivo *plaque dynamics*

We next sought to measure dynamics of plaques in muscle from mice using intravital microscopy. We injected the AAV in *tibialis anterior* muscle of WT mice. We first assessed the efficiency of the transduction of the AP2-mCherry protein. 28 days post-injection, we collected the TAs on which I performed 10 μm thick cryo-sections. I observed these sections by confocal microscopy and found that AP2-mCherry was expressed at the surface of muscle fibers, presenting a striated pattern centered on the Z-disk, precisely the location of costameres as it was previously shown for CHC (Vassilopoulos et al., 2014). To test whether AP2-mCherry was indeed recruited at sites of costameres, I performed co-stainings and found that our fluorescent construct colocalized with endogenous AP2, CHC, DNM2 and α-actinin 2, aligning with the Z-bands of muscle fibers (**Figure III.26**).

In order to visualize the dynamics of our fluorescent construct *in vivo*, we performed intravital analysis of AP2 dynamics at the surface of muscle at the Imaging and Cytometry Platform of the Gustave Roussy Institute (Villejuif, France). In order to image superficial fibers of TA muscles, we exposed them by removing the skin from the ventral size of the upper thigh of the injected leg. Anesthetized mice were then directly placed on the stage of a two-photon microscope (**Figure II.4**). Superficial fibers of the exposed TA muscle were imaged for prolonged periods ranging from one to three hours.

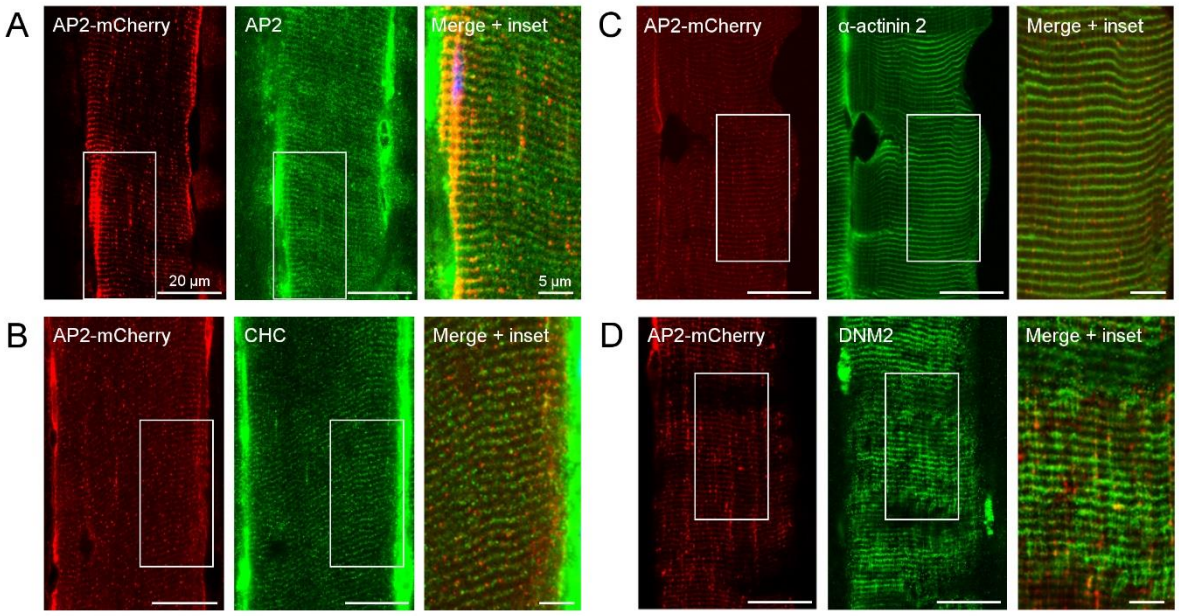

Figure III.26. AP2-mCherry localizes correctly at the surface of transduced muscle

(A-D) AP2 mCherry distribution between WT mice on fixed longitudinal muscle sections labelled with antibodies against endogenous AP2 (A), CHC (B), α-actinin 2 (C) or DNM2 (D) respectively.

AP2-mCherry displayed the expected costameric distribution at the surface of the fiber, forming stripes centered on the Z-band. We next performed time-lapse imaging of the AP2 signal at several regions of the fiber (**Movie 2**). The distribution of AP2, monitored on a kymograph, seemed particularly stable through time, even when imaged at fast acquisition frequencies for several minutes, periods which exceed the average time that it takes to form an endocytic vesicle (**Figure III.27**). Careful analysis of the movies showed blinking inside the stripes, suggesting endocytic activity at these sites.

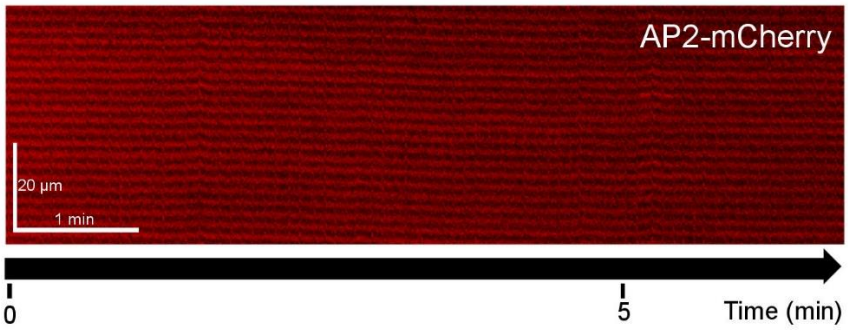

Figure III.27. AP2-mCherry striations are very stable in vivo

Kymograph of AP2 mCherry fluorescence imaged over 6 minute time-lapse.

To check the turnover rate of these structure, we then analyzed AP2 dynamics using intravital fluorescence recovery after photobleaching (FRAP) at the surface of muscle fibers (see II.1-a.ii AAV injection, live microscopy for principle of FRAP). The long lifetimes of clathrin plaques, described in the literature and that we observed by time-lapses, make them particularly well suited for FRAP analysis.

In agreement with experiments performed in HeLa cells (Grove et al., 2014), AP2 recovered quickly (**Movie 3**), and recovery dynamics were comparable to tagged AP2 or clathrin constructs transfected *in vitro* (Wu et al., 2003), reaching 85% plateau in 10 minutes (**Figure III.28**).

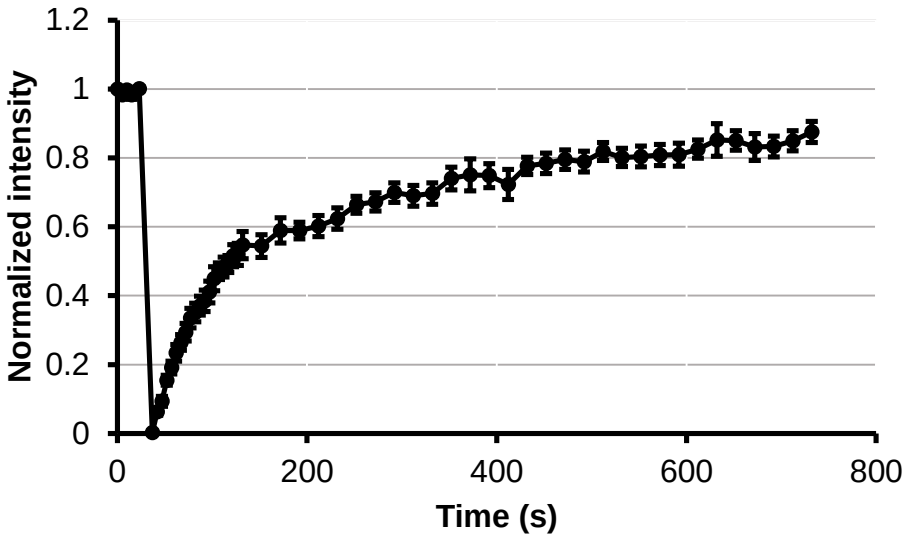

Figure III.28. CCS *in vivo* have a very dynamic turnover

AP2-mCherry fluorescence recovery in WT TA muscle imaging by two-photon intravital microscopy. Data are presented as mean ± SEM.

The dynamic recovery of AP2 in live mouse muscle suggests that although clathrin plaques at the costamere are very stable through time, they constantly exchange their components with cytoplasmic pools.

In conclusion, by performing live-microscopy on AAV-AP2-mCherry transduced muscle cells *in vitro* and *in vivo*, I learned that the complex assemblies described in the first part of this thesis are actually stable structures in the sense that clathrin plaques signal on the adherent face of myotubes in culture or at costameres of mature muscle fibers is persistent. But they are also dynamic structures displaying a high turn-over rate, which is consistent with the hypothesis that clathrin plaques can serve as hot-spots for endocytosis (Lampe et al., 2016).

2- Clathrin platforms are involved in mechanotransduction

a. Clathrin plaques respond to cyclic stretching

Since clathrin plaques localize to costameres which are force transmitting structures, one of the tenants of my PhD project was to analyze clathrin plaques in the context of mechanotransduction. Several hints pointed to a link between clathrin plaques and signaling, whether it be their ability to cluster integrins (Vassilopoulos et al., 2014) or their now proven ability to anchor actin microfilaments and desmin intermediate filaments at costameres. In order to mimic the effect of muscle contractions on the membrane, I subjected differentiated mouse myotubes grown on a flexible substrate to repeated stretching/relaxation cycles using the FlexCell Tension System in collaboration with C. Coirault in our laboratory. After fixation, I performed an immunostaining of both CHC and AP2 to check the status of CCS on the myotubes' membrane. By measuring the size of fluorescently labeled AP2 patches at the surface of myotubes undergoing stretch/relaxation cycles, I observed a decrease in CCS size (**Figure III.29, A-B**). To test if this size reduction was due to increased clathrin-mediated endocytosis rates, I performed together with M. Bitoun a transferrin uptake assay on cyclically stretched/relaxed myotubes. Transferrin internalization was significantly increased in cells subjected to a cyclic mechanical strain, demonstrating higher rates of clathrin-mediated endocytosis (**Figure III.29C**).

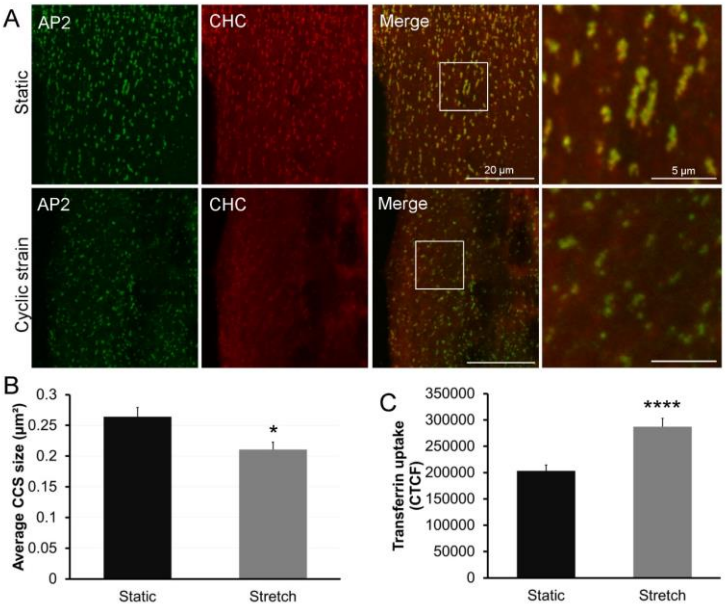

Figure III.29. Cell stretching increases endocytic rate

(A) Immunofluorescent staining of AP2 (green) and CHC (red) in immortalized human myotubes either stretched or left static. (B) Average AP2 patch size in human control myotubes either stretched or left static (n = 35 myotubes). (C) Internalized transferrin in human control myotubes either stretched or left static (n = 90–100 myotubes). (Data are presented as mean ± SEM; *P < 0.05, ****P < 0.0001)

I concluded from this set of experiments the important novel concept that clathrin plaques are stretch-sensitive structures that are dynamically remodeled by endocytosis in response to a mechanical stretch.

b. Clathrin is required for YAP/TAZ signaling

We have seen previously that there are many pathways of mechanoregulation present in muscle. They regulate muscle functions such as stretch-activated hypertrophy and signal transduction. Two new actors in muscle-mechanotransduction have been recently identified that we initially thought could be interesting read-outs for mechanotransduction efficiency (Fischer et al., 2016). YAP and TAZ are mechanosensitive transcriptional cofactors that can shuttle between the cytoplasm and the nucleus in response to mechanical cues from the ECM (Aragona et al., 2013; Halder et al., 2012).

YAP/TAZ have been heavily studied in mononucleated cells, in particular in the study of cancer cells. Although research in the YAP/TAZ pathway is an ever expanding field, except a few studies, analysis of YAP/TAZ behavior in muscle cells has mostly been restricted to mononucleated myoblasts.

In order to test if myotubes could respond to mechanical cues by translocation of YAP/TAZ, I subjected differentiated mouse myotubes grown on a flexible substrate to repeated stretching/relaxation cycles. Then I performed an immunostaining for both YAP and TAZ and observed the distribution of these proteins in primary mouse myotubes using confocal microscopy.

At the basal state, YAP/TAZ were mostly cytoplasmic and nuclear staining of both YAP and TAZ increased significantly upon prolonged cyclic stretching for six hours (**Figure III.30A**). G. Moulay, who is a post-doc in S. Vassilopoulos group, analyzed the expression of common YAP/TAZ target genes in samples with or without cyclic stretching. Because of its importance in muscle, we were also interested in the regulation of actin by the YAP/TAZ pathway at the expression level. Indeed, it has been shown that the Hippo pathway regulates genes with functionally important MCAT elements located in the promoter-enhancer regions of cardiac, smooth, and skeletal muscle-specific genes. These include α-actin, type I myosin heavy chain and several other genes that regulate muscle development or myogenesis (Yoshida, 2008). The RT-PCR analysis revealed that the nuclear translocation of YAP/TAZ after cyclic stretching happened along an increase in expression of *CTGF* and *CYR61,* two YAP/TAZ target genes, without affecting expression levels of YAP or TAZ mRNA (**Figure III.30B**). We also noticed an significant increase in *ACTG1*, coding for γ-actin which has previously been involved in muscle cell force transduction and transmission (Craig and Pardo, 1983).

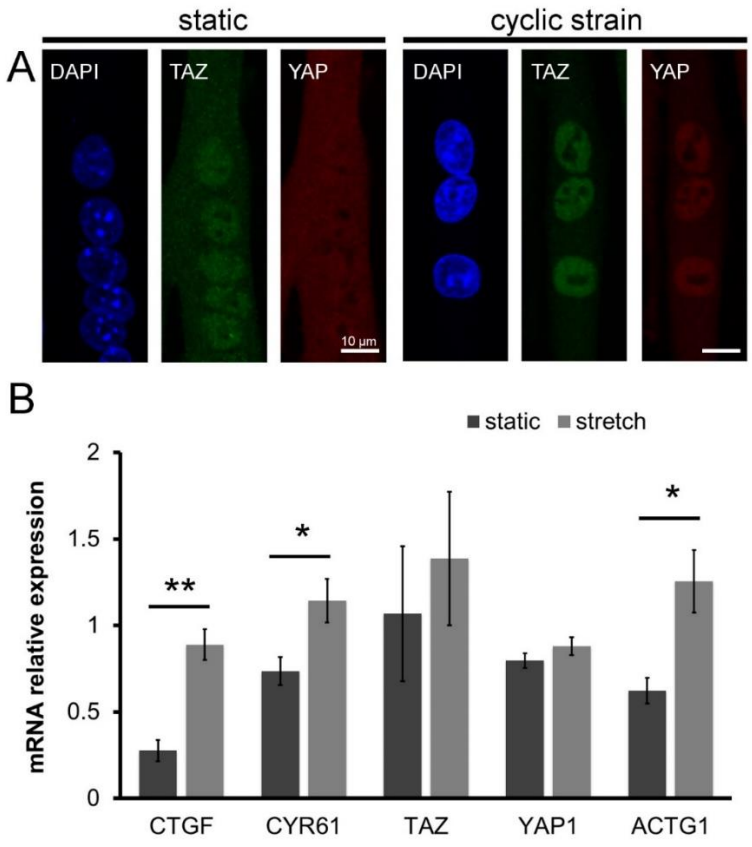

Figure III.30. Cell stretching increases YAP/TAZ signaling

(A) Immunofluorescent staining of YAP (red) or TAZ (green) and nuclei (blue) from mouse primary control myotubes either stretched or left static. (B) Relative expression of YAP/TAZ mRNA target genes (*CTGF*, *CYR61*) or actin gene *ACTG1* in myotubes stretched or left static (n = 3-4 samples) (Data presented as mean ± SEM; *P < 0.05, **P < 0.01). Gene analysis was performed by G. Moulay.

We next wanted to test the contribution of clathrin plaques of YAP/TAZ translocation by depleting CHC. I performed an immunostaining on cells subjected or not to cyclic stretching. I then measured the ratio of nuclear YAP/TAZ compared to their intensity in the cytoplasm. I observed a normal translocation of both YAP and TAZ in the nucleus of control myotubes after cyclic stretching. Concerning CHC-depleted myotubes, at first I noticed a strong nuclear accumulation of YAP/TAZ at the basal state, without cyclic stretching. When I challenged cells with cyclic stretching however, I observed no further nuclear YAP/TAZ increase in these depleted cells, which therefore lost their responsiveness to stretching (**Figure III.31**).

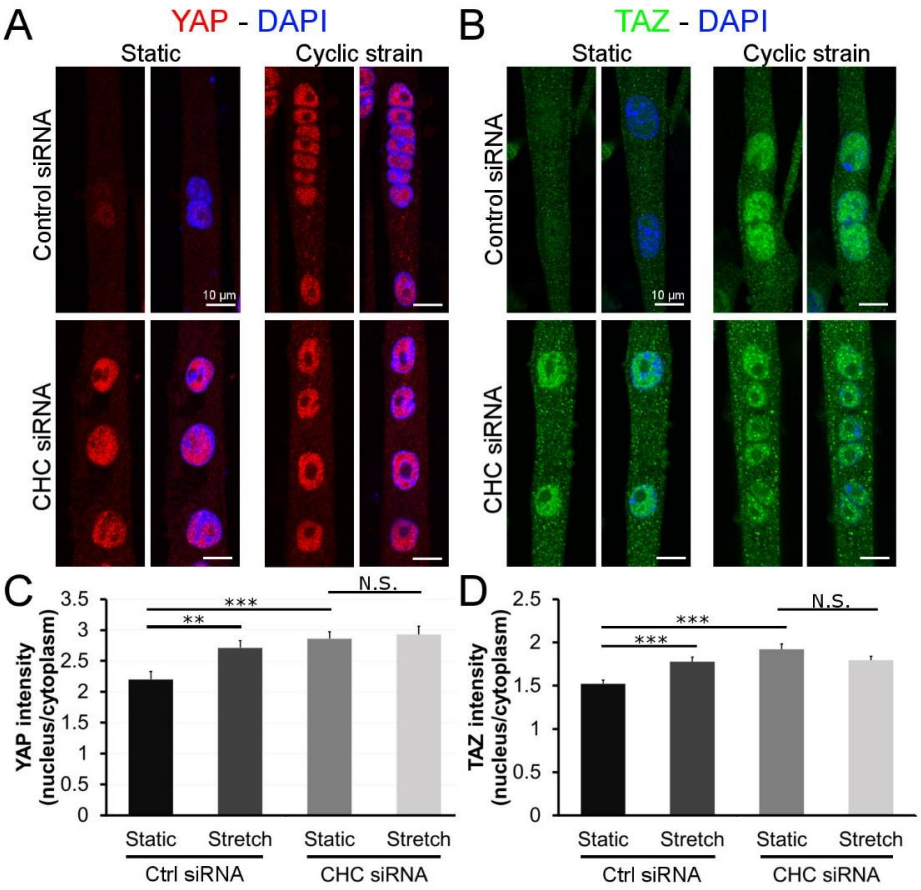

Figure III.31. Clathrin deletion impairs proper YAP/TAZ translocation

(A) (B) Immunofluorescent staining of YAP (red) or TAZ (green) and nuclei (blue) from mouse primary control or CHC-depleted myotubes either stretched or left static. (C) (D) YAP or TAZ fluorescence in control or CHC-depleted myotubes (n = 30-80 myotubes, data presented as mean ± SEM; **P < 0.01, ***P < 0.001).

Altogether, these data suggest that clathrin plaques could sequester YAP/TAZ and release them upon mechanical stimulation via increased endocytosis. Accordingly, acute inhibition of endocytosis using the well-characterized dynamin GTPase activity inhibitor Dynasore also abolished responsiveness to stretch by inhibiting TAZ translocation (**Figure III.32**). However, unlike CHC depletion, Dynasore treatment did not produce a YAP/TAZ accumulation in the nucleus of myotubes, suggesting that removing both clathrin plaques and subsequent endocytosis has a different effect on YAP/TAZ distribution than acutely inhibiting endocytosis in a context where plaques are still present.

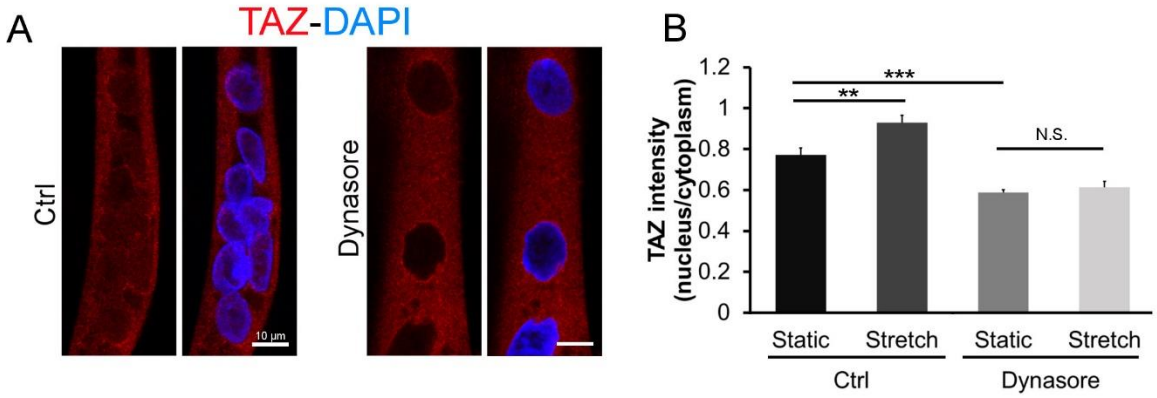

Figure III.32. Disabling endocytosis affects YAP/TAZ translocation

(A) Immunostaining of TAZ in primary mouse myotubes with or without Dynasore 80 µM. (B) TAZ fluorescence in primary myotubes treated or not treated with Dynasore 80 µM (*n* = 35–40 myotubes). (Data presented as mean ± SEM; *P < 0.05, **P < 0.01, ***P < 0.001).

These data all suggest that clathrin plaques are dynamic structures that anchor YAP/TAZ at the cell cortex and are in involved in their shuttling to the nucleus in response to stretching. Inhibiting clathrin or endocytosis strongly affects YAP/TAZ nuclear shuttling and activation of their canonical target genes.

c. Clathrin platforms directly sequestrate YAP/TAZ mechanotransducers

Since clathrin seems important for YAP/TAZ regulation in myotubes and that clathrin plaques are platforms for cytoskeletal anchoring and scaffolding, I reasoned that they could act as a substrate or reservoir for YAP and TAZ associated to the PM. To verify this, we wanted to get access to the exact location of YAP/TAZ on plasma membranes. I performed an immunostaining of both YAP and TAZ on unroofed membranes from primary mouse myotubes. We were able to detect for the first time TAZ and YAP antibodies directly on clathrin plaques and on actin filaments surrounding them. Quantification of YAP and TAZ antibodies on CCS showed a clear enrichment of both YAP and TAZ on CCS compared to aspecific binding on the secondary antibody alone (**Figure III.33E).** TAZ had a higher affinity for clathrin (**Figure III.33, B, D**) whereas YAP was mostly detected on the surrounding actin cytoskeleton (**Figure III.33, A, C**). This proves the basis of our hypothesis that clathrin lattices and their surrounding cytoskeleton could act as a reservoir for these mechanotransducers.

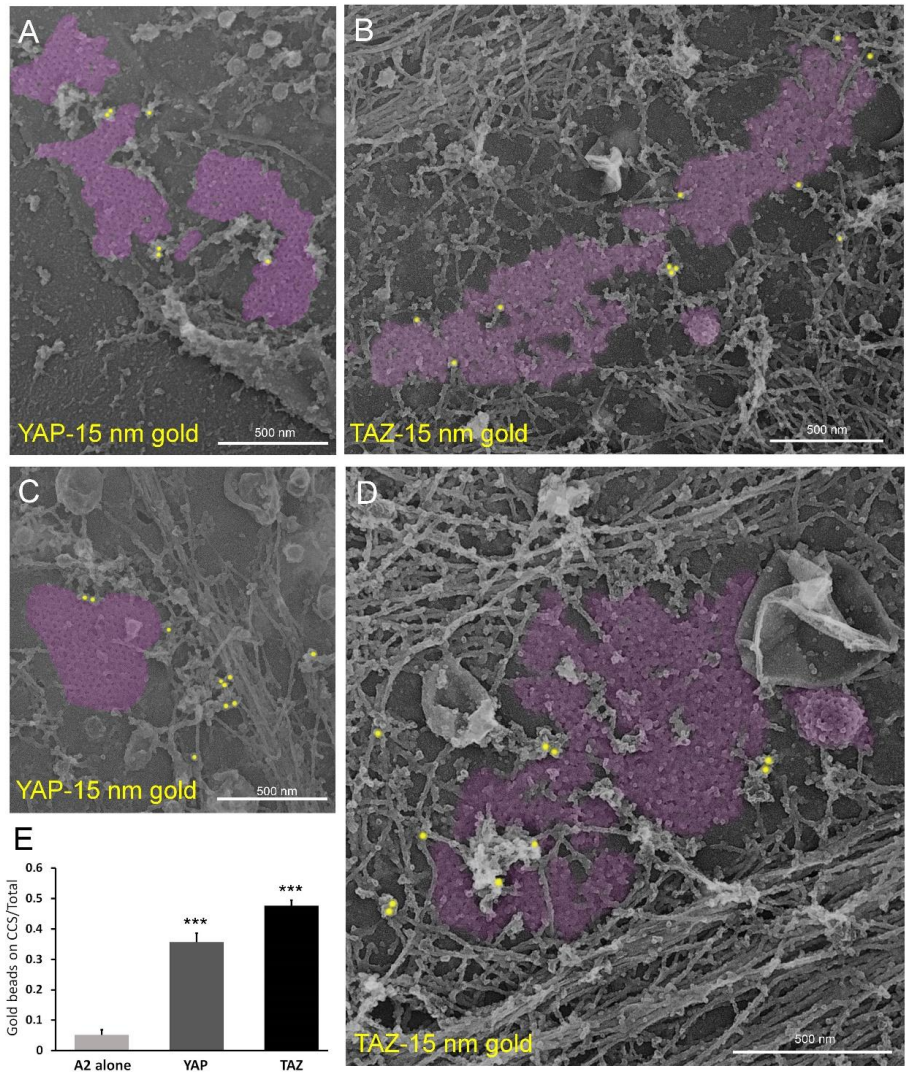

Figure III.33. YAP and TAZ interact with actin surrounding clathrin plaques

(A) (B) High magnification views of clathrin plaques from control human myotubes labelled with YAP (A) or TAZ (B) antibodies. (C) (D) High magnification views of clathrin plaques from control mouse primary myotubes labelled with YAP (C) or TAZ (D) antibodies. (E) Number of gold beads corresponding to YAP and TAZ labelling on clathrin plaques or surrounding actin cytoskeleton (<100 nm or closer from the clathrin lattice) compared to a staining performed using only secondary antibodies conjugated to 15-nm colloidal gold particles (n = 49 to 104 images, data presented as mean ± SEM; ***P < 0.001). For (A-D) clathrin lattices are highlighted in purple. Secondary antibodies conjugated to 15-nm colloidal gold particles are pseudocolored in yellow. EM and quantification were performed by S. Vassilopoulos.

Moving from *in vitro* to *in vivo*, A. Fongy, who is a post-doc in the team, isolated TA muscle fibers from WT mice. I did an immunostaining of TAZ in the fibers and observed the staining by confocal microscopy. I was initially surprised to get such a strong and striated staining of TAZ on the surface of these isolated fibers since its distribution in myotubes is less comprehensive, although this is what one would expect for a costameric distribution (**Figure III.34**). Striation of TAZ,

centered on the Z-discs precisely corresponded to costameres, strengthening our hypothesis of a relation between clathrin plaques and mechanotransducers on costameres.

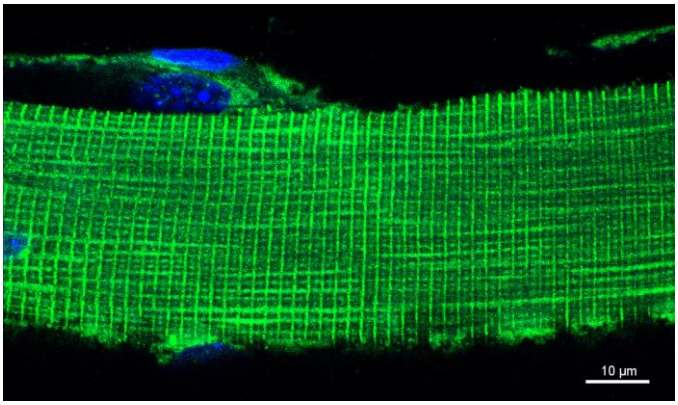

Figure III.34. TAZ is striated at the surface of mouse skeletal muscle fibers

Immunofluorescent staining of TAZ (green) from dissociated TA fibers of WT mouse. DAPI is in blue.

To make sure that TAZ was located on costameres in isolated fibers, I performed a co-staining of TAZ and desmin on isolated fibers from a WT mouse, prepared by A. Fongy. I observed a colocalization between desmin and TAZ at the surface of the fibers, confirming that TAZ was indeed located on costameres (**Figure III.35**).

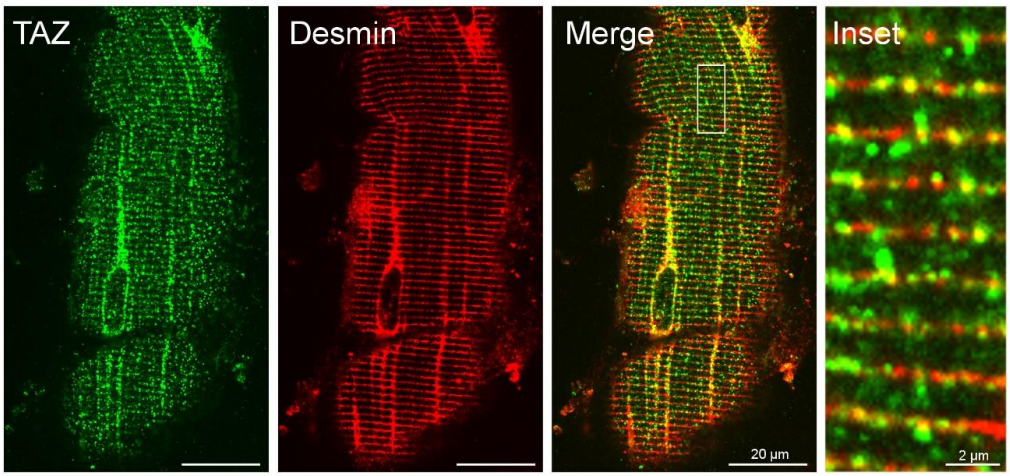

Figure III.35. TAZ colocalize with desmin on costameres at surface of muscle fibers

Immunostaining of TAZ (green) and desmin (red) in mouse TA fibers, imaged by confocal microscopy.

I observed a more punctuated staining of TAZ, reminding me of the CHC staining obtained on isolated muscle fibers. This data shows for the first time a direct association between the mechanotransducing actors YAP/TAZ and costameres.

d. DNM2 and TAZ biochemical interaction

Having shown that both YAP and TAZ required clathrin plaques for efficient sequestration at the cell cortex and nuclear translocation, and that TAZ was located at costameres, I wanted to check how mechanotransducers could be retained at these sites. I performed co-immunoprecipitation experiments in primary mouse myotubes using an antibody against YAP and TAZ. The rationale behind these experiments was that some plaque component could directly interact with either YAP or TAZ and sequestrate them at these sites. I decided to check the interaction between YAP/TAZ and clathrin plaque components such as CHC, DNM2, desmin and N-WASP. I found no interaction between either of these proteins with YAP, which band was expected to show at 70 kDa. The YAP antibody I used is notoriously known to cross-react with TAZ whose protein sequence is highly homologous. I systematically observed a band corresponding to the expected size of TAZ, around 55 kDa, in DNM2 immunoprecipitates (**Figure III.36**).

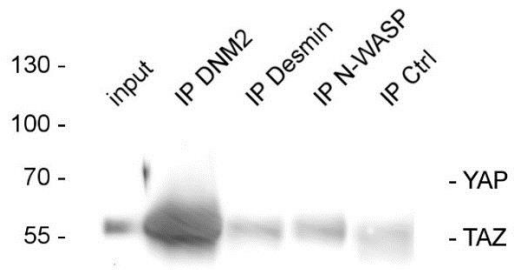

Figure III.36. YAP does not interact with clathrin plaques components

Immunoblot of proteins associated with DNM2, Desmin, N-WASP or control immunoprecipitates from control human myotube lysates and 4% lysate input. Bands for coimmunoprecipitated YAP or TAZ are indicated at the right.

To verify that the band observed with the YAP/TAZ antibody corresponded to TAZ, I probed the CHC, or DNM2 immunoprecipitates using an antibody specific of TAZ which does not recognize YAP. In agreement with a localization of TAZ directly on clathrin plaques and surrounding actin filaments in cells in culture, I observed a strong interaction between DNM2 and TAZ in differentiated myotubes suggesting formation of a DNM2/TAZ complex (**Figure III.37**).

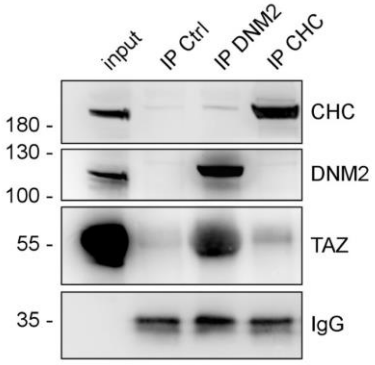

Figure III.37. DNM2 interacts with TAZ

Immunoblot of proteins associated with DNM2, CHC or control immunoprecipitates from control human myotube lysates and 4% lysate input. Bands for coimmunoprecipitated CHC, DNM2 or TAZ are indicated at the right.

This data suggests that flat clathrin plaques are a reservoir for plasmalemmal YAP/TAZ transducers, by their ability to organize a three-dimensional cytoskeletal network around them. The fact that DNM2 and TAZ interact directly seems to point towards DNM2 as a direct sequestering factor for YAP/TAZ on plasma membranes.

e. DNM2 is required for YAP/TAZ cytoplasmic sequestration and translocation

Previous attempts to analyze DNM2 at clathrin plaques revealed dynamin associated with flat clathrin structures by EM (Damke et al., 1994; Sochacki et al., 2017; Warnock et al., 1997) and a punctate distribution as well as persistent recruitment of dynamin by super resolution and live imaging (Grove et al., 2014), indicating direct recruitment at sites within the clathrin plaque. Given its position at the periphery of clathrin plaques, and its role in actin remodeling, we reasoned that DNM2 could have a role in sequestering YAP/TAZ on actin filaments around clathrin plaques. Therefore I used the same strategy as previously and depleted primary mouse myotubes of DNM2. I then subjected these cells to cyclic stretching and checked the location of YAP/TAZ.

DNM2-depletion phenocopied CHC-depletion and increased YAP and TAZ in nuclei at the basal state along with an absence of any further response to cyclic stretching (**Figure III.38**).

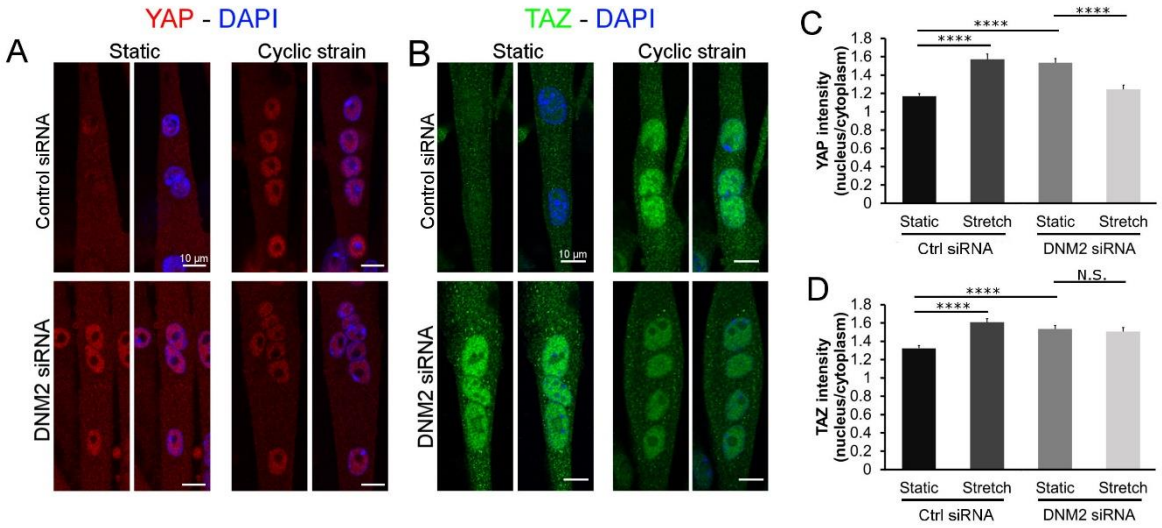

Figure III.38. DNM2 controls YAP/TAZ translocation in differentiated myotubes

(A) (B) Immunofluorescent staining of YAP (red) or TAZ (green) and nuclei (blue) in mouse primary control or DNM2-depleted myotubes either stretched or left static. (C) (D) YAP or TAZ fluorescence in control or DNM2-depleted myotubes (n = 30–45 myotubes). (Data are presented as mean ± SEM; ****P < 0.0001)

We checked the expression levels of YAP/TAZ target genes and actin-related genes in control and DNM2-depleted cells. We concluded that, although YAP/TAZ accumulated in the nuclei, their key target genes, including *CTGF* and *CYR61* which are canonical YAP/TAZ targets and which we previously showed to respond to stretch by translocating into the nucleus, were highly downregulated (**Figure III.39A**). It would also seem that DNM2 depletion directly affected TAZ at both transcriptional (**Figure III.39A**) and protein (**Figure III.39B**) levels. In parallel to YAP/TAZ failure to activate specific genes in DNM2-depleted cells, we saw a decrease of actin-related genes, namely *ACTA2*, *ACTC1* and *ACTG1* (**Figure III.39A**). Contrary to almost every other paper published about YAP/TAZ signaling, here we were observing a strong YAP/TAZ nuclear translocation but this translocation was associated to a strong down-regulation of TAZ itself and its canonical transcriptional targets.

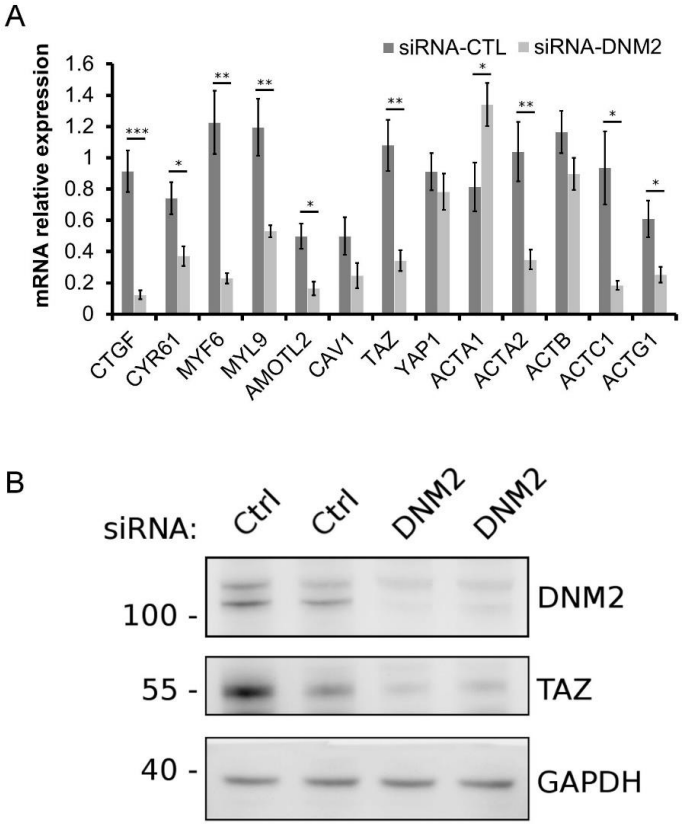

Figure III.39. Expression of YAP/TAZ target genes and actin-related genes in DNM2-depleted myotubes

(A) Relative expression of YAP/TAZ mRNA target genes or of actin-related genes in control or DNM2-depleted myotubes (n = 6-8 samples; Data are presented as mean ± SEM; *P < 0.05, **P < 0.01, ***P < 0.001, ****P < 0.0001). Gene analysis was performed by G. Moulay. (B) Primary mouse myotubes treated with control or DNM2 siRNA and cell lysates immunoblotted for proteins indicated at the right.

Much like the questions raised in a very recent review from the Picollo laboratory (Panciera et al., 2017), our results raise the question whether nuclear localization of YAP/TAZ is sufficient to induce their translational activity. The authors mention a direct mechanical activation of YAP and TAZ mediated, amongst other cues, by the cytoskeleton. Since I have shown throughout this thesis the essential part that clathrin plaques play in terms of organizing the actin and IF cytoskeletons, I wondered if these scaffolds assembled around clathrin plaques could act as the mechanical switches for YAP/TAZ activation, and why this activity was impaired whenever I perturbed this membrane compartment.

f. Actin and IF remodeling is needed for YAP/TAZ activation

Several studies have demonstrated that DNM2 regulates actin cytoskeleton networks through interaction with distinct actin-binding proteins and have proposed functions for clathrin and dynamin in actin organization that are distinct from coated vesicle formation during endocytosis (Bonazzi et al., 2011, 2012; Schafer et al., 2002; Sever et al., 2013; Veiga et al., 2007). We reasoned that DNM2 could function directly at the interface between clathrin plaques and actin polymerization and could shape the substrate required to sequestrate YAP and TAZ in the cytoplasm.

I wanted to test if cytoskeletal regulation directly affected YAP/TAZ translocation in myotubes. Disrupting actin polymerization using latrunculin B (1 μM, 1 hour) strongly blocked YAP/TAZ nuclear translocation (Zhao et al., 2012). Myotubes plated on glass presented a substantial amount of nuclear YAP/TAZ, in agreement with the notion that their adhesion is more efficient on glass or plastic than on the flexible membrane used for cell stretching. Disrupting actin polymerization using latrunculin B in myotubes cultured on glass strongly decreased YAP/TAZ nuclear distribution (**Figure III.40, A-B**). Depleting DNM2 mimicked the effects of latrunculin B (**Figure III.40, C-F**). This translated by a down-regulation of well-described YAP/TAZ key target genes such as *CTGF* and *CYR61*, as well a decrease in the expression of actin-related genes (**Figure III.40, G**).

Therefore, I confirmed in myotubes that YAP/TAZ shuttling can be regulated by the network of F-actin. Thus it is possible that DNM2-mediated actin regulation in myotubes plays a role in YAP/TAZ nuclear translocation and activity.

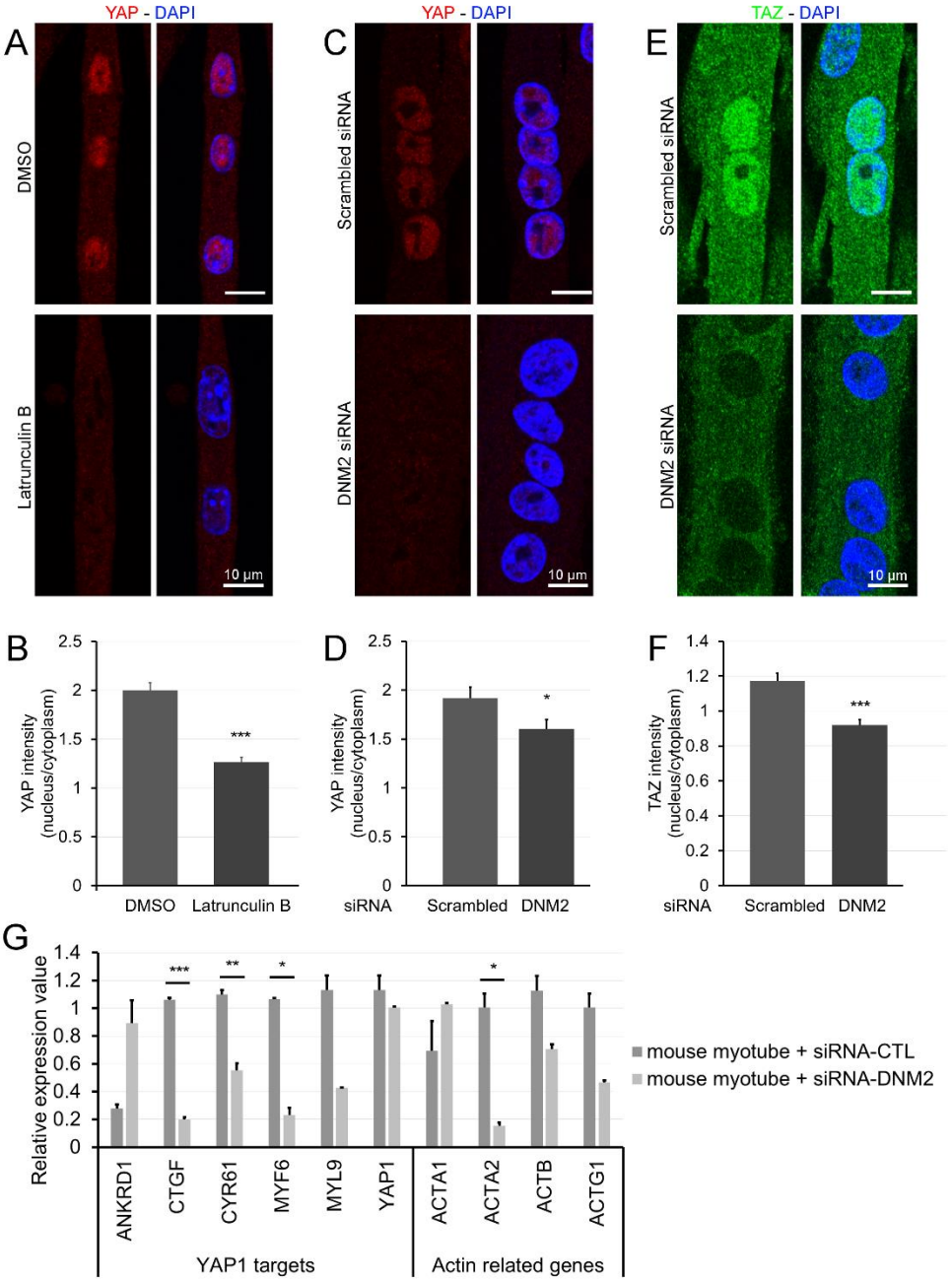

Figure III.40. Inhibiting actin polymerization or DNM2 induces a loss of YAP/TAZ signaling

(A) Immunofluorescent staining of YAP and nuclei in mouse primary myotubes treated or not with latrunculin B (1 µM, 1 hour). (B) YAP fluorescence in mouse primary myotubes treated or not with latrunculin B (1 µM, 1 hour) (n = 40 myotubes). (C) Immunofluorescent staining of YAP and nuclei in control or DNM2-depleted mouse primary myotubes. (D) YAP fluorescence in control or DNM2-depleted mouse primary myotubes (n = 30–40 myotubes). (E) Immunofluorescent staining of TAZ and nuclei in control or DNM2-depleted mouse primary myotubes (F) TAZ fluorescence in control or DNM2-depleted myotubes (n = 2). (Data are presented as mean ± SEM; *P < 0.05, **P<0.01, ***P < 0.001)

We have shown that clathrin plaques are a compartment composed of flat clathrin structures scaffolding branched actin which anchors desmin filaments. More and more, the role of intermediate filaments in muscle evolves, and much like clathrin plaques, it is thought that they serve a dual role of structural and mechanotransducing structures (Palmisano et al., 2015).

As a demonstration of the role of desmin IFs on YAP/TAZ translocation, although they did not present any obvious clathrin defects, primary myotubes from desmin knock-out mice presented a strong accumulation of YAP in myonuclei at the basal state and no further translocation upon stretching (**Figure III.41**). Therefore, desmin KO myotubes phenocopies CHC- and DNM2-depleted myotubes in terms of their basal YAP nuclear accumulation and subsequent failure to correctly shuttle YAP between the nucleus and the cytoplasm in response to cyclic stretching.

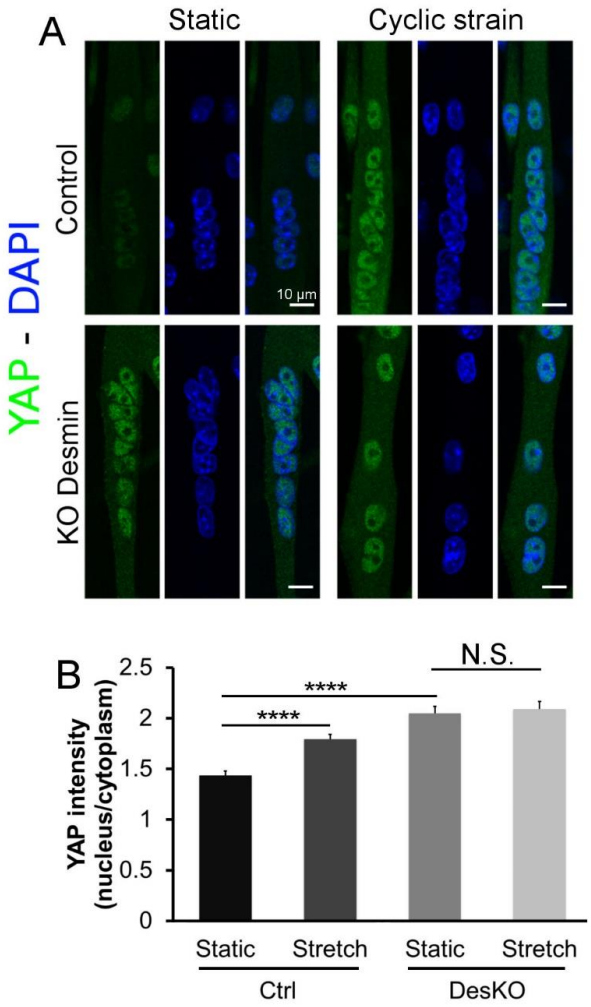

Figure III.41. Desmin KO cells show abnormal YAP translocation

(A) Immunofluorescent staining of YAP (green) and nuclei (blue) in mouse primary myotubes from WT or desmin knock-out ($Des^{-/-}$) littermates either stretched (cyclic strain) or left static. (B) YAP fluorescence in primary myotubes from WT or desmin KO mice (*n* = 35–70 myotubes). (Data presented as mean ± SEM; ****P < 0.0001).

By virtue of organizing branched filaments around clathrin plaques that serve as anchors for muscle-specific intermediate filaments, DNM2 takes the center stage of plaque-related mechanotransduction. We figured that all these data could have grave implications concerning

autosomal dominant centronuclear myopathies due precisely to mutations in *Dnm2*. This congenital myopathy induces abnormal muscle phenotypes with centralized nuclei, muscle atrophy, and deformed T-tubules (Cowling et al., 2011). Although an array of *Dnm2* mutations have been identified, the mechanisms of this disease are still unknown. Thus I wanted to test the possibility that *Dnm2* mutations could affect plaque dynamics, muscle structure and/or YAP/TAZ mechanotransduction pathway.

3- Costameric disorganization in CNM

a. DNM2-linked mutations impair plaque organization

In order to study the distribution of clathrin plaques in muscle, therefore clathrin specifically recruited to the plasma membrane *in vivo*, we made use of our previously developed AAV expressing the µ2-subunit of the AP2 clathrin adaptor tagged with mCherry.

I compared AP2-mCherry distribution in WT mice and in the HTZ KI-*Dnm2*^{R465W} CNM mouse model developed in the laboratory. I observed muscle sections expressing AP2-mCherry by confocal microscopy and noticed a discontinuous distribution AP2 distribution in the animal model compared to the WT. Whereas I saw a regular striation of AP2 on the surface of WT fibers, AP2 patches were completely disorganized in the most severely affected regions of the TA muscle in our animal model (**Figure III.42**).

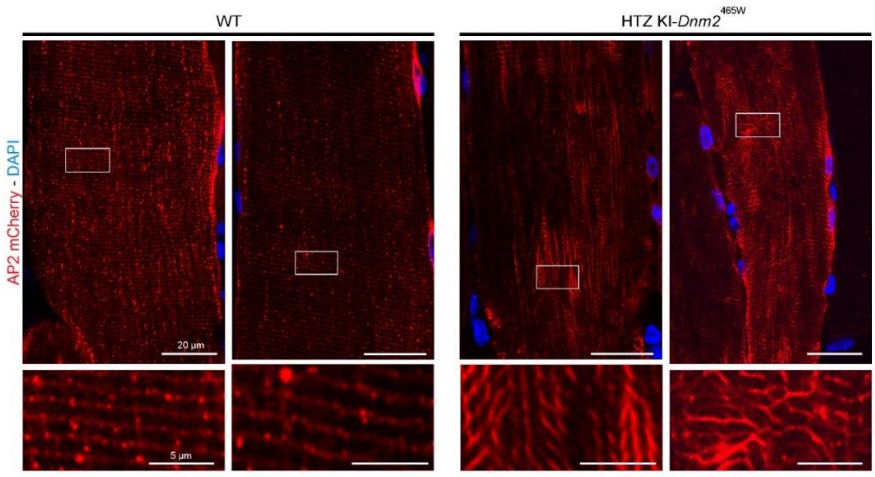

Figure III.42. DNM2-linked CNM mutations disorganize AP2 striation

AP2 mCherry distribution between WT and HTZ KI-Dnm2R465W mice at the surface of myofibers on longitudinal muscle cryosections.

Distribution of endogenous AP2, CHC, α-actinin 2 or DNM2 were affected in those disorganized areas as well (**Figure III.43**). These abnormal striations were reminiscent of abnormal α-actinin 2 distribution on muscle sections of a patient suffering of CNM due to a p.R465W mutation (Cowling et al., 2011).

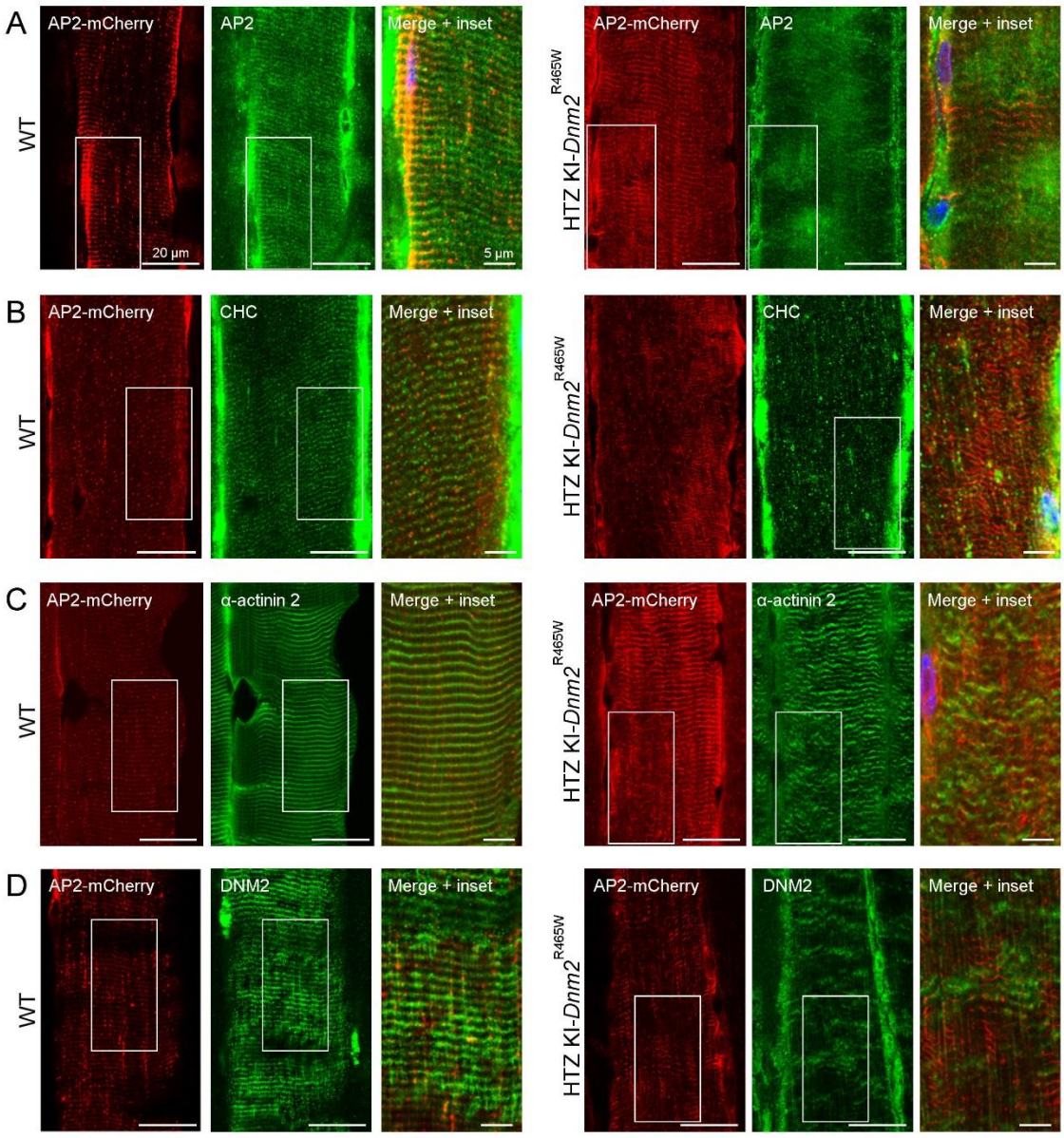

Figure III.43. Plaque components disorganized in CNM mouse model

(A-D) AP2 mCherry distribution between WT (left) and HTZ KI-*Dnm2*^{R465W} (right) mice on fixed longitudinal muscle sections labelled with antibodies against endogenous AP2 (A), CHC (B), α-actinin 2 (C) or DNM2 (D) respectively.

b. DNM2 CNM mutation disorganizes the desmin network *in vivo*

Previously, I showed that DNM2 participates in the desmin cytoskeletal organization *in vitro*, so I reasoned that CNM-causing mutations could induce defects in muscle IF arrangement *in vivo*. I therefore investigated the organization of the desmin network in dissociated fibers from WT and HTZ KI-*Dnm2*^{R465W} mice. Confocal microscopy allowed me to inspect this organization at the surface specifically. I observed a costameric striation of desmin in WT mice, whereas this striation was disorganized in the CNM mouse model (**Figure III.44**).

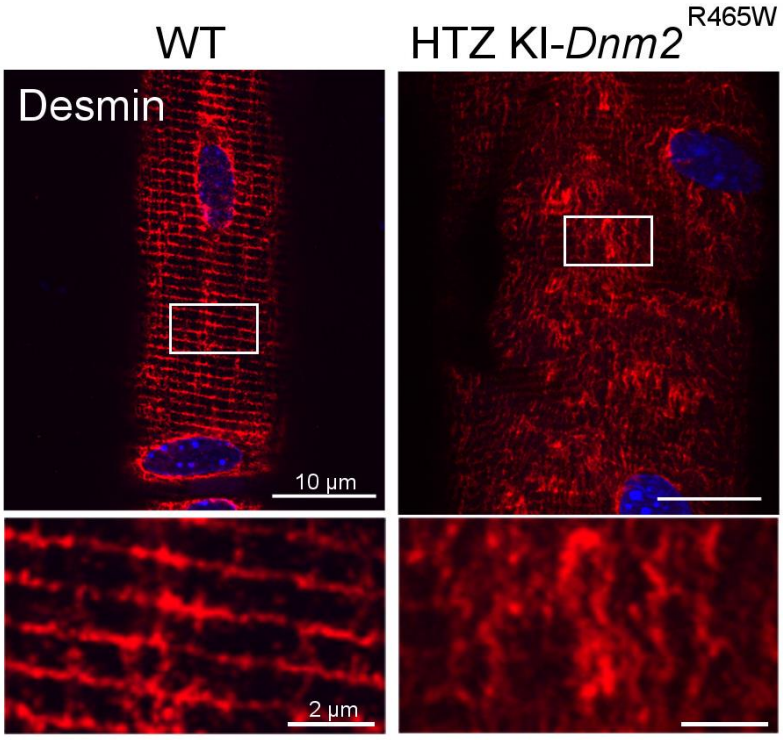

Figure III.44. CNM mutation impairs desmin distribution at surface of fibers

Confocal section from surface of WT or HTZ KI-*Dnm2*^{R465W} mouse dissociated TA fiber immunolabeled with desmin antibodies.

Surprisingly, CNM mutation did not seem to impact intracellular organization of desmin, as observed on confocal sections from top to bottom. This was confirmed by thin-section EM images of TA muscle performed by J. Lainé, showing the presence of large regions of the surface containing IF tangles intertwining with ER tubules (**Figure III.45**), much like what we observed in DNM2-depleted primary mouse myotubes (**Figure III.23** p.98).

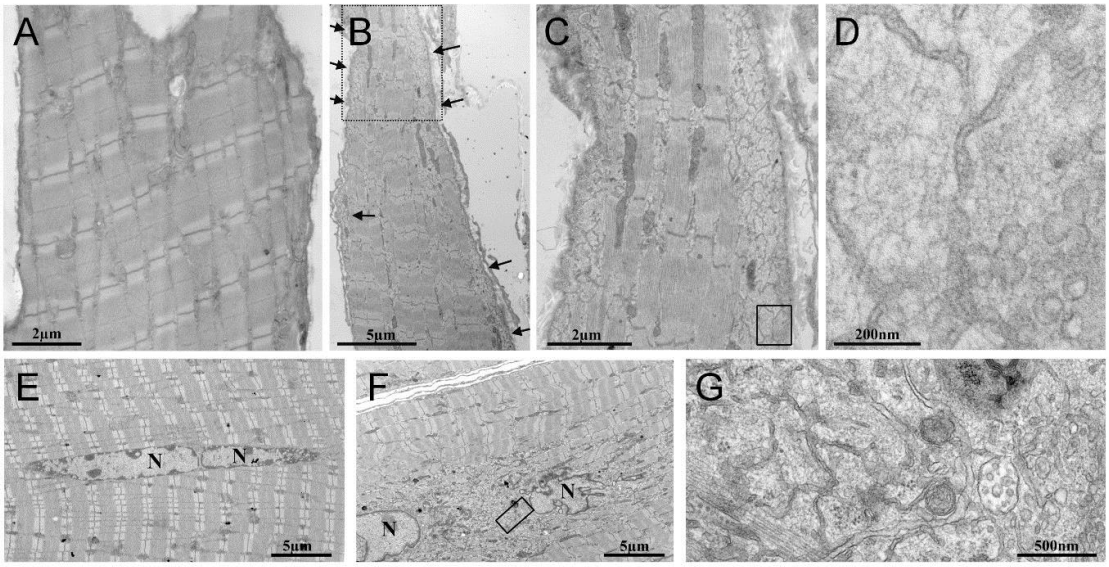

Figure III.45. IF tangles at the surface and around centralized nuclei in CNM animal model

(A-D) Thin-section EM of longitudinal TA skeletal muscle sections from either WT (A) or HTZ KI-*Dnm2*^{R465W} (B-D) mice. (C) is an inset of (B) and (D) is an inset of (C). The presence of intermediate filaments aggregates containing ER membranes at the surface of fibers is clearly visible on the insets. (E-G) Longitudinal skeletal muscle sections from the core of either WT (E) or HTZ KI-*Dnm2*^{R465W} (F-G) mice displaying central nuclei. (G) is an inset of (F) where intermediate filaments aggregates containing ER membranes at the surface of fibers is clearly visible whereas no such aggregate can be found around the central nucleus in WT case (E). EM by J. Lainé.

c. CNM affects desmin distribution in patients

The results from DNM2 knock-in mice prompted us to investigate the organization of desmin IFs in CNM patients with DNM2 mutations. We worked with the Morphological Unit of the Institute of Myology. They provided stained samples for patients carrying *Dnm2* p.R369Q or p.R465W mutations. The team at the morphological unit first performed an NADH-tetrazolium reductase (NADH-TR) reaction, which relies upon the ability of the mitochondrial enzyme NADH-dehydrogenase to transfer electrons to the colorless, soluble tetrazolium salt and convert it into an insoluble formazan compound. This provides an excellent stain of the oxidative compartments (*i.e*. ER and mitochondria) distributed in the space between myofibrils. The analysis of muscle biopsies of DNM2-related CNM patients shows radial arrangement of sarcoplasmic strands with oxidative enzyme reactions conferring a classical spoke-like appearance, nuclear centralization and internalization, and type 1 muscle fiber predominance and hypotrophy (Romero and Bitoun, 2011) (**Figure III.46, E-H**).

In parallel, an histo-immunological staining for desmin was performed on frozen samples from muscle biopsies. We observed a dark staining around centralized nuclei, radiating toward the plasma membrane in a spoke-like manner (**Figure III.46, A-D**), revealing abnormal desmin organization in patients' muscles as well.

At the EM level, central nuclei appeared without morphological abnormality, and the radial distribution of the intermyofibrillar sarcoplasmic strands was easily recognized. These radial strands contained dense protein accumulations, typical of dilated Z-band material containing desmin (**Figure III.46, I**).

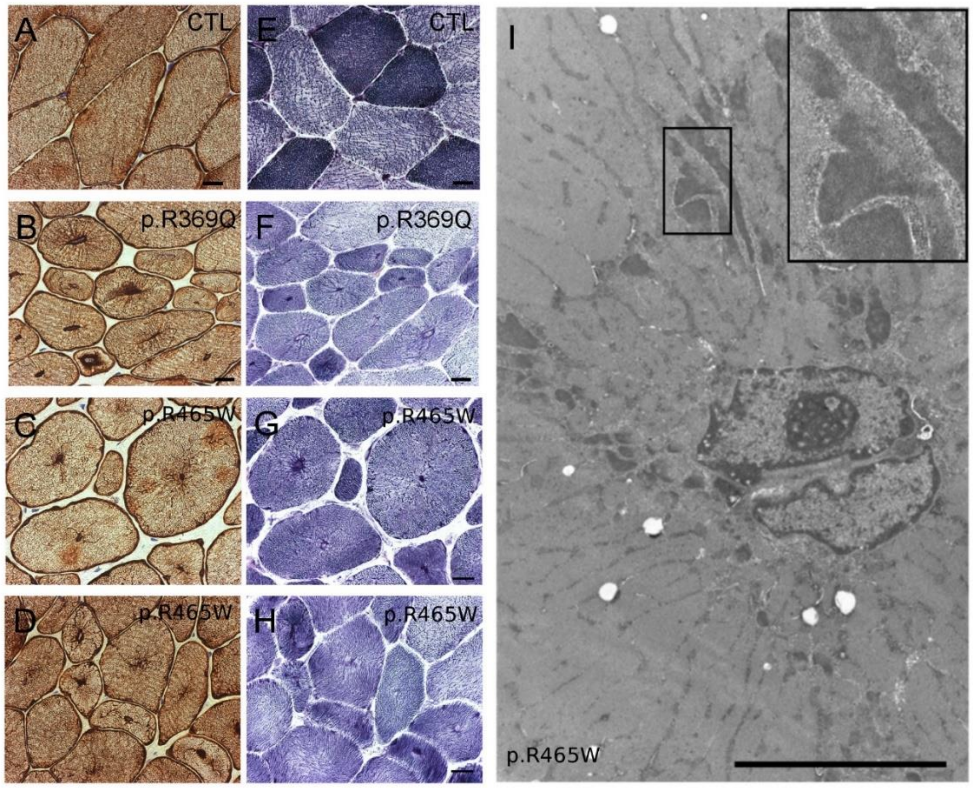

Figure III.46. DNM2-linked mutations disorganize desmin IF network in patient muscles

(A-H) Muscle biopsy sections from a control (A, E) or CNM patient with either a *Dnm2* p.R369Q (B, F) or p.R465W (C, G and D, H) mutation, immunohistochemically labelled against desmin (A-D) or processed for NADH-TR oxidative reaction (E-H). (I) Thin-section EM of CNM patient muscle (p.R465W) displaying characteristic radial strands.

d. CNM mutation impairs YAP/TAZ location and expression

Previously, I found a defect in YAP shuttling in desmin KO mouse myotubes. I wondered if the desmin aggregates induced by CNM mutations could have an impact on YAP translocation. To test the impact of CNM mutations on YAP/TAZ location *in vitro*, I performed YAP immunostaining on control myotubes and myotubes differentiated from immortalized myoblasts of a CNM patient harboring the p.R369Q mutation. This mutation, like the p.R465W mutation, affects the middle domain involved in DNM2 oligomerization and actin remodeling (González-Jamett et al., 2017). I measured the ratio of nuclear YAP versus cytoplasmic YAP to see if there could be an imbalance in mutated cells, and showed that patient-derived myotubes display the exact same YAP/TAZ defects as DNM2-depleted mouse myotubes, with an abnormal accumulation of YAP in nuclei and no response to repeated stretching/relaxation cycles (**Figure III.47**).

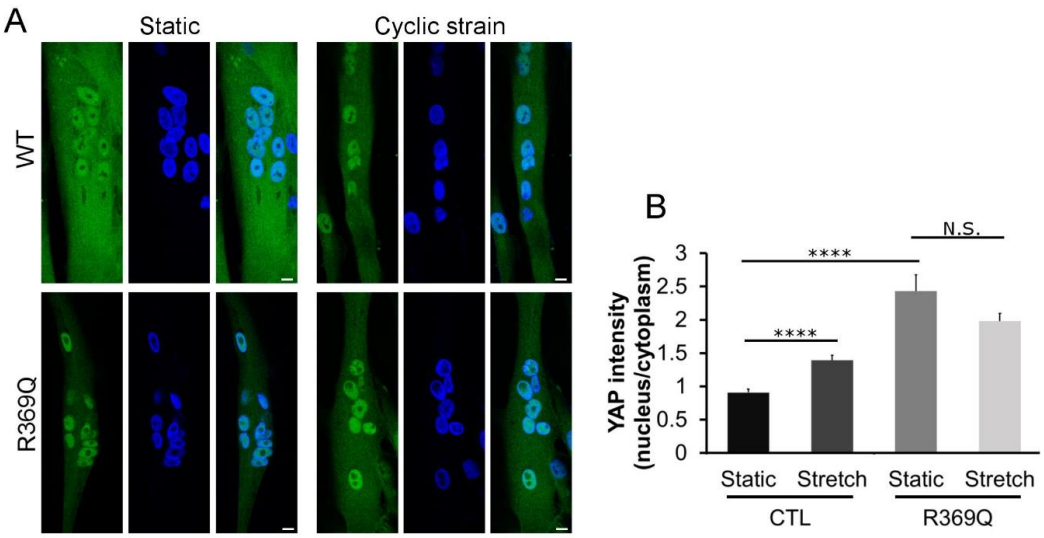

Figure III.47. Abnormal translocation of YAP in CNM patient cells

(A) Immunofluorescent staining of YAP (green) and nuclei (blue) in control and p.R369Q myotubes either stretched (cyclic strain) or left static. (B) YAP fluorescence in control and p.R369Q myotubes either stretched (cyclic strain) or left static. (*n* = 35–60 myotubes). (Data presented as mean ± SEM; ****P < 0.0001).

We next analyzed the expression pattern of YAP/TAZ target genes and actin-related genes in patient cells and found out that their expression also mirrored results obtained from DNM2-depleted cells, meaning a down-regulation of YAP/TAZ canonical target genes *CTGF*, *CYR61* and *ACTG1* genes despite a strong accumulation of YAP in these cells' nuclei. This stresses the importance of DNM2 middle domain in controlling YAP/TAZ signaling and actin transcription.

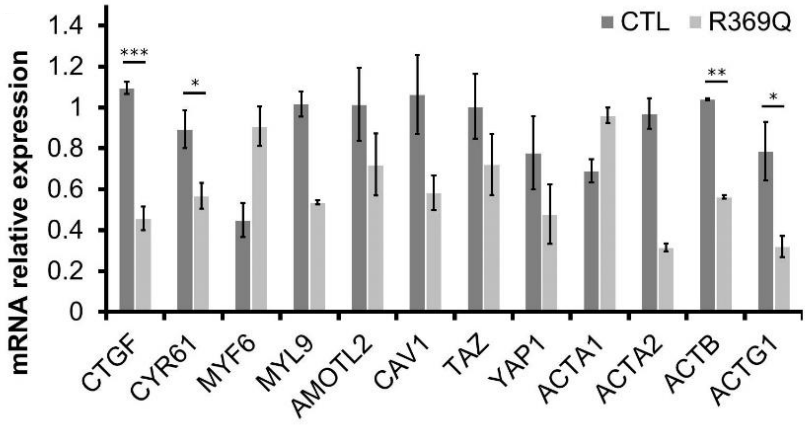

Figure III.48. Down-regulation of YAP/TAZ target genes in CNM patient myotubes

Relative expression of YAP/TAZ mRNA target genes or of actin-related genes in control or p.R369Q myotubes (*n* = 2-4 samples; Data are presented as mean ± SEM; *P < 0.05, **P < 0.01, ***P < 0.001).

Since I found an interaction between TAZ and DNM2 by co-immunoprecipitation experiments, I wanted to test the impact of CNM mutations on TAZ location *in vivo* by analyzing whole muscles lysates and isolated fibers from our CNM model. Immunolabeling of TAZ on isolated fibers revealed a disorganization of TAZ at the surface of these fibers, reminding of the abnormal striations for desmin observed previously (see **Figure III.44** p.119).

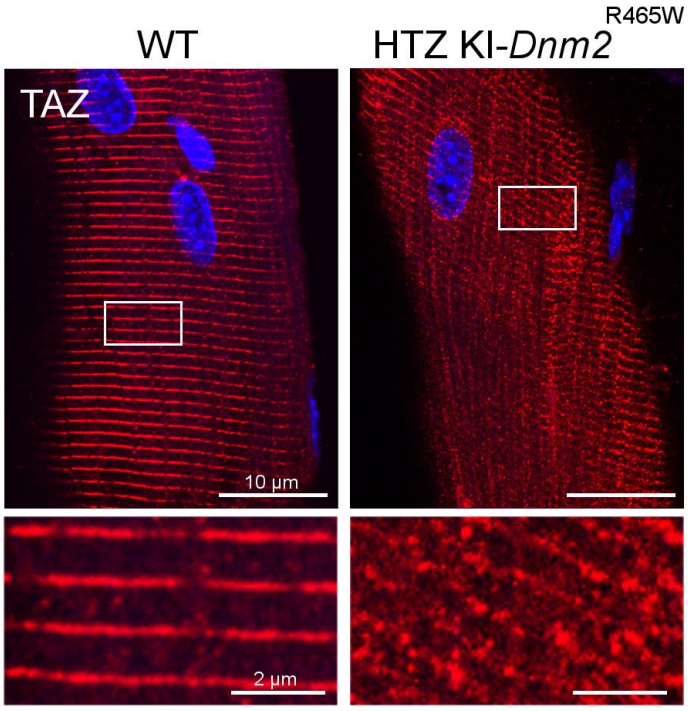

Figure III.49. CNM mutation impairs costameric TAZ distribution

Confocal section from surface of WT or HTZ KI-Dnm2R465W mouse dissociated TA fiber immunolabeled with TAZ antibodies.

I next checked TAZ protein levels in those animals by performing western-blots on skeletal muscle lysates from mouse TA muscle. Although TAZ mRNA levels were unchanged (**Figure III.50C**), the protein levels were significantly increased in HTZ KI-*Dnm2*^{R465W} mice suggesting increased protein stability and/or decreased protein degradation (**Figure III.50, A-B**).

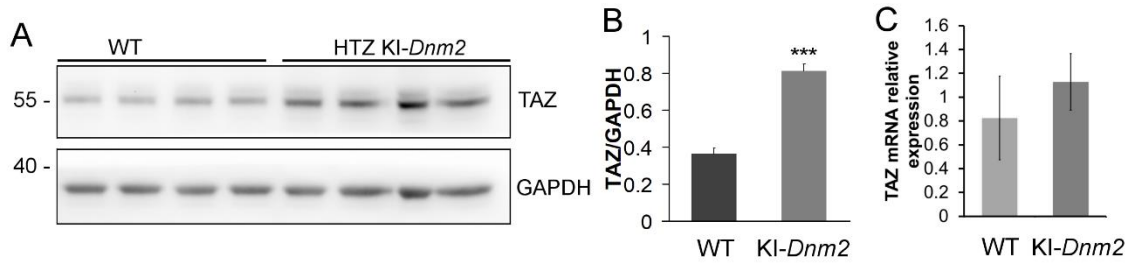

Figure III.50. Increased TAZ content in CNM mouse model

(A) Western blot for TAZ and GAPDH in WT or HTZ KI-*Dnm2*^{R465W}. (B) Expression of TAZ relative to GAPDH in TA muscle from WT or HTZ KI-*Dnm2*^{R465W} mice (KI-*Dnm2*) (n = 3-4 mice per phenotype; Data are presented as mean ± SEM; ***P < 0.001). (C) Relative expression of TAZ mRNA in WT or HTZ KI-*Dnm2*^{R465W} mice (KI-*Dnm2*) (n = 3; Data are presented as mean ± SEM).

Overall, our results on TAZ expression and distribution in HTZ KI-*Dnm2*^{465W} suggest that defective clathrin plaques function at costameres could account for both abnormal distribution and defective TAZ turnover leading to defective signaling.

e. DNM2-linked CNM mutations delay plaque dynamics *in vivo*

In order to test if *Dnm2* mutations could affect protein turnover at clathrin plaques, we tested the dynamics of clathrin plaques in our animal model using the system of AAV2-mCherry followed by FRAP as described before. In HTZ KI-*Dnm2*^{R465W} mice, the speed of fluorescence recovery of AP2 was not significantly delayed, although the plateau only reached 60% of the initial fluorescence intensity (**Movie 4**) (**Figure III.51**).

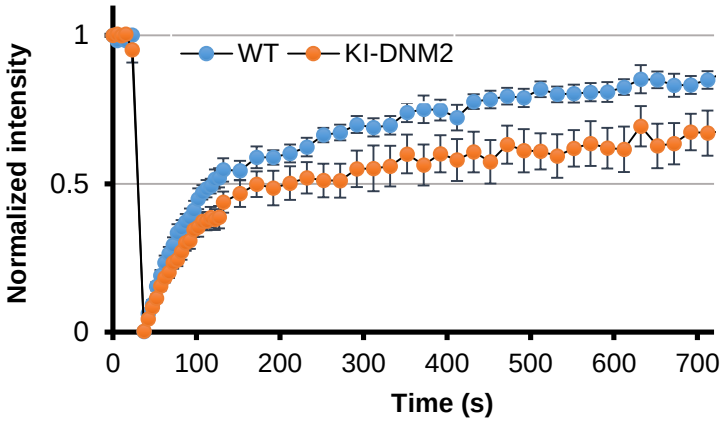

Figure III.51. DNM2-linked CNM mutations delay plaque dynamics

AP2-mCherry fluorescence recovery between WT and HTZ KI-Dnm2R465W mice. Two-Way ANOVA was performed, ****P < 0.0001 (*n* = 17 to 25 fibers from at least 3 mice for each genotype).

This decrease in the mobile fraction of AP2 observed in HTZ KI-*Dnm2*^{R465W} mice suggests defective exchange and turnover of plaque components in our animal model and could explain the increased TAZ stability and subsequent increase in protein levels.

In conclusion to this part, our results show that DNM2 is essential for structural maintenance of muscle, since analysis of muscles affected by *Dnm2* mutations showed costameric defects, abnormal desmin accumulations that translated into defective YAP/TAZ distribution and shuttling. Microscopy performed on live muscle shows that these structural defects are concomitant to a slower turnover of costameric components, which could explain the abnormal YAP/TAZ signaling from these sites.

Overall, these results place clathrin plaques as novel regulators of mechanotransduction in muscle cells. Located at the interface between the ECM and the contractile apparatus, they sequester mechanotransducers YAP and TAZ and are able to release them following mechanical stretching. They also scaffold branched actin and intermediate filaments, organized by DNM2, that form cortical stress-sensitive networks. We can also conclude that CNM-linked mutations affect the turnover of costameric plaques, thereby affecting signaling.

IV. Discussion and future directions

Flat clathrin lattices are not a novel concept. Comparable to focal adhesions, clathrin plaques form macromolecular functional adhesion sites containing integrins, which connect the extracellular matrix and the PM to the intracellular cytoskeleton. They have been studied in a variety of cells and have been associated to more than one function. In particular, they have long been associated to strong adhesion (Batchelder and Yarar, 2010; Ezratty et al., 2009; Maupin and Pollard, 1983; Merrifield et al., 2005; Saffarian et al., 2009; Taylor et al., 2011a). They were associated to specialized adherent regions, such as the contact zone between osteoclasts and bone (Akisaka et al., 2008), at sites of phagocytosis (Aggeler and Werb, 1982), between the membrane and collagen fibers (Elkhatib et al., 2017). Recently, they were associated with the clustering and specific endocytosis of the receptor for lysophosphatidic acid (LPA) which is a phospholipid found in mammalian serum with hormone-like and growth-factor-like activities (Leyton-Puig et al., 2017). Nevertheless, their role beside adhesion has remained hazy at best. What we propose is that clathrin plaques combine all these functions, adhesion, endocytosis, signaling, association to cytoskeleton and integrate them to form molecular platforms.

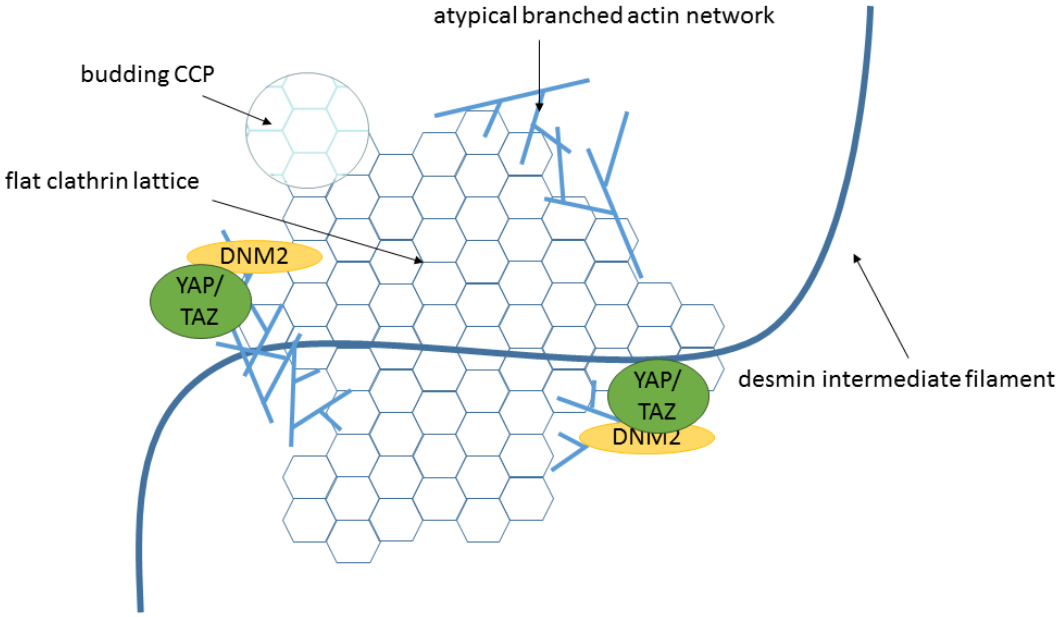

Figure IV.1. Schematic representation of a clathrin plaque

Flat clathrin lattices surrounded by an atypical branched actin network composed of α-actinin and organized by N-WASP, ARP2/3 and DNM2. This network anchors a 3D web of desmin intermediate filaments and sequesters YAP/TAZ mechanotransducers. Clathrin plaques are dynamic structures responsive to cell stretching.

1- Composition and regulation of clathrin plaques

Together with S. Vassilopoulos, we produced metal replicas of unroofed muscles cells, which helped us introduce the concept that flat clathrin lattices were formed by clathrin recruitment at AP2 sites and were surrounded by an atypical branched actin network formed by costameric α-actinin 2 and ARP2/3. In addition to AP2, we showed that clathrin plaques also contained another clathrin adaptor, Dab2. We studied how the depletion of Dab2 would affect clathrin plaques and found that its absence leads to a malformation of plaques, possibly related to abnormal integrin clustering, although we did not test the distribution of integrins in Dab2-depleted myotubes.

Other clathrin-coat constituents have been shown to regulate plaque behavior. FCHO1 and 2 (Fer/CIP4 homology domain only protein 1 or 2) are F-bar proteins belonging to the highly conserved family of proteins called muniscins (Reider et al., 2009). Using a TALEN-based approach, L. Traub's laboratory showed that removing these muniscins induced a reorganization of clathrin in stable and flat lattices in HeLa cells (Umasankar et al., 2014). This highlights the fact that the arrival of AP2, although being the principal cargo-selective adaptor, is paralleled by the recruitment of early-arriving pioneers such as eps15, intersectin, epsin, CALM (Taylor et al., 2011a), NECAP (Ritter et al., 2013) and previously cited muniscins (Umasankar et al., 2014), that are just as important to clathrin coated structures size and dynamics. In an elegant paper by J. Taraska's group (NIH, Bethesda), these proteins (and several others) were in fact identified partitioned on the periphery of clathrin-coated lattices, further defining the topology of this compartment (Sochacki et al., 2017). It would also be interesting on our part to further study the composition of clathrin plaques.

An important part of my thesis also concerns the *in vivo* characterization of clathrin plaques. By intravital imaging, I showed that clathrin plaques are stable structures with a rapid turnover of their constituents. I also showed that cyclic cell stretching could induce a change in CCS size and increase endocytosis. Although my work is one of the first instances where CCS were shown to respond to cell stretching, the concept of CCS reacting to the environment is definitely not novel. Clathrin recruitment was previously shown to be sensitive to membrane tension under cellular osmotic conditions. Low membrane tension promoted budding off *in vitro* giant unilamellar vesicles, whereas budding was inhibited under high tension conditions (Saleem et al., 2015). Therefore the physical properties of the membrane can affect clathrin recruitment and budding.

Clathrin plaque morphology and dynamic turnover could also be regulated by the transmembrane proteins that cluster inside the plaque. Integrin clustering and activation trigger a cascade of phosphorylation events that could either directly or indirectly affect CCP dynamics (Liu et al.,

2009). It was shown that clathrin serves as a hub for the recruitment of proteins that are necessary for the actin rearrangements that occur during maturation of adherens junctions of epithelial cells (Bonazzi et al., 2011, 2012). The authors showed that the initial steps of adherens junction formation trigger phosphorylation of clathrin and its transient localization at forming cell-cell contacts. We can hypothesize that in muscle cells, the process of plaque formation is also regulated by clathrin phosphorylation. FAK, known to be responsible for integrin-mediated mechanotransduction within focal adhesions and costameres, interacts with Src and DNM2 in a complex thought to be responsible for focal adhesion disassembly (Ezratty et al., 2009). The group of F. Brodsky showed that Src-mediated phosphorylation of CHC was pivotal for clathrin redistribution and EGF uptake (Wilde et al., 1999). It is also noteworthy that cell transformation using the v-Src (form of Src expressed by Rous sarcoma virus) overexpression has been shown to induce clathrin phosphorylation and formation of large clathrin positive structures at the cell surface (Martin-Perez et al., 1989). It is therefore tempting to speculate that part of the effect of v-Src is due to an increased clathrin-coated plaque formation resulting from increased clathrin phosphorylation. More recently, it was shown that infection of human foreskin fibroblasts by Kaposi's sarcoma-associated herpes virus induces phosphorylation of myosin IIA, FAK, Src, PI3-K, CHC and AP2 that regulate virus entry (Dutta et al., 2013), suggesting a role of this pathway in the recruitment of clathrin to promote abnormally large clathrin structures. All these clues point towards a possible role of FAK and Src kinases in plaque turnover by phosphorylation of clathrin.

One important corollary is that a precise mechanism involving phosphorylation cascades allows the formation of plaques and that this mechanism is under the control of Src and FAK, two major kinases in adhesion and mechanotransduction. It would be therefore interesting to characterize the functional link between clathrin plaques and focal adhesions, the impact of clathrin phosphorylation on its recruitment in plaques and its functional role in differentiated myotubes and isolated muscle fibers.

2- Plaques, DNM2 and actin

One central question stemming from my work is to understand how the articulation between clathrin plaques, IFs and mechanotransducers occurs. Branched actin filaments, which are at the crossroads of these different complexes, appear as a pivotal actor for this organization. The team already showed that the actin network surrounding clathrin lattices contains α-actinin 2, an actin crosslinking protein (Vassilopoulos et al., 2014). One of the tenants of my PhD project was the study of the interaction between plaques and branched actin, and I showed that it required the ARP2/3 machinery including the actin nucleation-promoting factor N-WASP. It is of interest that hybrid ARP2/3 and α-actinin containing complexes have already been reported (Chorev et al.,

2014; Pizarro-Cerdá et al., 2017) and one could imagine that association of clathrin plaques with these tissue-specific hybrid complexes could be the signature of clathrin's role in adhesion. Actin has been shown to regulate CCS morphology and dynamics (Leyton-Puig et al., 2017), but I propose here the hypothesis that clathrin plaques anchor and regulate actin around them.

Actin remodeling for CME has been linked to the action of clathrin light chains. Depletion of clathrin light chains completely inhibits entry of bacteria and viruses that are too large to be internalized without actin (Bonazzi et al., 2011). Consistent with other studies (Poupon et al., 2008), the group of F. Brodsky proved that CLC depletion in HeLa cells generated short, disorganized actin structures characterized by the presence of cortactin at the tips. (Majeed et al., 2014). These data prove that clathrin light chains are essential for actin processes related or not to CME. Clathrin light chains share a common sequences that allow binding to Hip1 and Hip1R, which mediate actin and CME (Chen and Brodsky, 2005) and was shown to be of pivotal importance in regulating the distribution of actin and clathrin-coated structure on PM of muscle cells (Vassilopoulos et al., 2014). Clathrin light chains seem to be at the heart of clathrin actin-remodeling abilities, therefore it would be interesting to test the impact of CLC depletion on actin organization around flat clathrin plaques.

Additionally, a common element of these processes linking endocytosis to actin is the key recruitment of dynamin. During my PhD, I have established that DNM2 plays an important role in actin remodeling at clathrin plaques. Indeed, depletion of DNM2 induces costameric dysfunction translated by α-actinin 2 disorganization and defects in actin branching around clathrin plaques. Several studies have previously demonstrated that DNM2 regulates actin cytoskeleton networks through interaction with distinct actin-binding proteins via its PRD and have proposed functions for clathrin and dynamin in actin organization that are distinct from coated vesicle formation (Bonazzi et al., 2011, 2012; Saffarian et al., 2009; Schafer et al., 2002; Sever et al., 2013; Tanabe and Takei, 2009; Veiga et al., 2007). We can hypothesize that DNM2 recruits the cellular machinery, including N-WASP together with the ARP2/3 complex, to induce assembly of branched actin filaments to clathrin plaques that would terminate as dynamin oligomers disassembled. In addition, it has been proposed that dynamin can assemble into rings which directly interact with F-actin via the middle domain and participate in actin filament bundling (Gu et al., 2010; Sever et al., 2013). We can therefore propose an additional direct action of DNM2 on actin filament inducing *de novo* assembly at plaques.

3- Impact of clathrin plaques organization on mechanotransduction

a. YAP/TAZ

Mechanical stimuli can be sensed throughout the cell via a combination of signals from cytoskeletal rearrangements and mechanosensors (Mohri et al., 2017). I propose here that clathrin plaques act as novel sensors for YAP/TAZ mechanotransduction by regulation of the actin cytoskeleton surrounding clathrin plaques. Although the precise nature of the compartment that YAP and TAZ associate with in the cytoplasm is unknown, their activity depends on F-actin structures enriched in adhesion sites (Aragona et al., 2013). In some cases, the actin cytoskeletal integrity is essential to YAP nuclear translocation and actin-mediated regulation can even override phosphoregulation of YAP induced by the Hippo pathway (Das et al., 2016). In ciliogenesis, YAP/TAZ have been shown to be modulated by actin-regulating factors (Kim et al., 2015). Very recently also, the group of S. Piccolo showed that the YAP/TAZ pathway could integrate physical signals of matrix changes to affect cell fate. They also proved that F-actin was a key regulator of stemness by sustaining YAP/TAZ in nuclei and opposing differentiation (Totaro et al., 2017). Overall, these studies strongly associate regulation of the actin network to YAP/TAZ signaling.

By cyclically stretching primary mouse myotubes, I showed a defective translocation of YAP/TAZ when CHC or DNM2 were depleted. I observed that although there was an abnormal accumulation of YAP/TAZ in nuclei of DNM2-depleted cells, YAP/TAZ target genes and actin-related genes were downregulated. This was very surprising since most of the previous studies have described an activation of YAP/TAZ signaling when these mechanotransducers are translocated in the nucleus. Concerning these results, we are probably still missing a link between DNM2 and YAP/TAZ transcriptional activity.

This pathway is in fact much more complex than previously thought, due to a number of influencing factors and regulatory loops. A recent review by S. Piccolo's group states that mechanical modulation of YAP/TAZ translocation is primordial regarding their regulation, but also that YAP/TAZ translocation does not equate to YAP/TAZ signaling (Panciera et al., 2017). In this review, Panciera and colleagues cite a paper that examined actin-related regulation of YAP/TAZ and showed that indeed, YAP/TAZ signaling required strain transfer to the nucleus (Driscoll et al., 2015). They suggested that cytoskeletal regulation was important for YAP translocation but also for its activation via a direct mechanical linkage between the PM and the nucleus. Cytoskeletal forces regulate nuclear stress and strain response through connections between the plasma membrane and the nucleus called the linker of nucleoskeleton and

cytoskeleton (LINC) complex. The authors postulated that the LINC complex was essential in YAP/TAZ activation. It has been shown previously that mutations in the LINC complex components or the nuclear lamina affect YAP/TAZ translocation (Bertrand et al., 2014). In isolated nuclei, stretching of the actin binding LINC complex component nesprin 1 induces a rapid change in nuclear stiffness (Guilluy et al., 2014), which directly regulates downstream transcription of mechanically regulated genes. Thus, mechanical signals are able to travel from the PM to the nucleus via the LINC complex, translating cytoskeletal rearrangements into nucleus stiffness that will alter gene transcription. Whether clathrin plaques are involved at all in this function is still unknown, but it is conceivable that the defective YAP/TAZ target gene activation in DNM2-depleted cells could be due to altered nuclear mechanotransduction.

Another explanation for why nuclear YAP/TAZ might not capable of activating their target genes, is if they were unable to interact directly with their transcriptional activators and bind onto DNA. To induce gene transcription, they have to interact with TEAD transcription factors. A recent study found that acylation of TEAD4, which is particularly important in skeletal muscle, significantly increases its stability (Mesrouze et al., 2017). Therefore, although acylation of TEADs does not impact YAP/TAZ binding, authors suggested that it may alter their transcriptional activity, meaning that YAP/TAZ could accumulate in nuclei without any transcriptional impact if TEAD elements are not available. It would therefore be interesting to study TEAD4 regulation in the context of DNM2 depletion and test whether TEAD4 is still capable of interacting with YAP/TAZ.

So how could DNM2 regulate YAP/TAZ nuclear signaling? One can suggest that perhaps elements of the clathrin plaques normally need to accompany YAP/TAZ into the nucleus to perform their function. Kinases such as FAK and Src have been associated to nuclear shuttling to regulate cell function following stress or cell de-adhesion (Bjorge et al., 2000; Lim, 2013). Other FA proteins such as paxillin (Dong et al., 2009; Woods et al., 2002) and zyxin (Nix and Beckerle, 1997) have also been associated to nuclear translocation. In addition, some proteins participating in CME have been associated to nucleocytoplasmic shuttling: monomeric clathrin (Ohmori et al., 2008), EPS15 and epsin (Pilecka et al., 2007), Hip1 (Mills et al., 2005). It would be very interesting to study their nucleocytoplasmic distribution upon stretching and test their interaction with YAP/TAZ in order to decipher if these proteins can directly shuttle mechanotransducers in nuclei in response to mechanical stimulation.

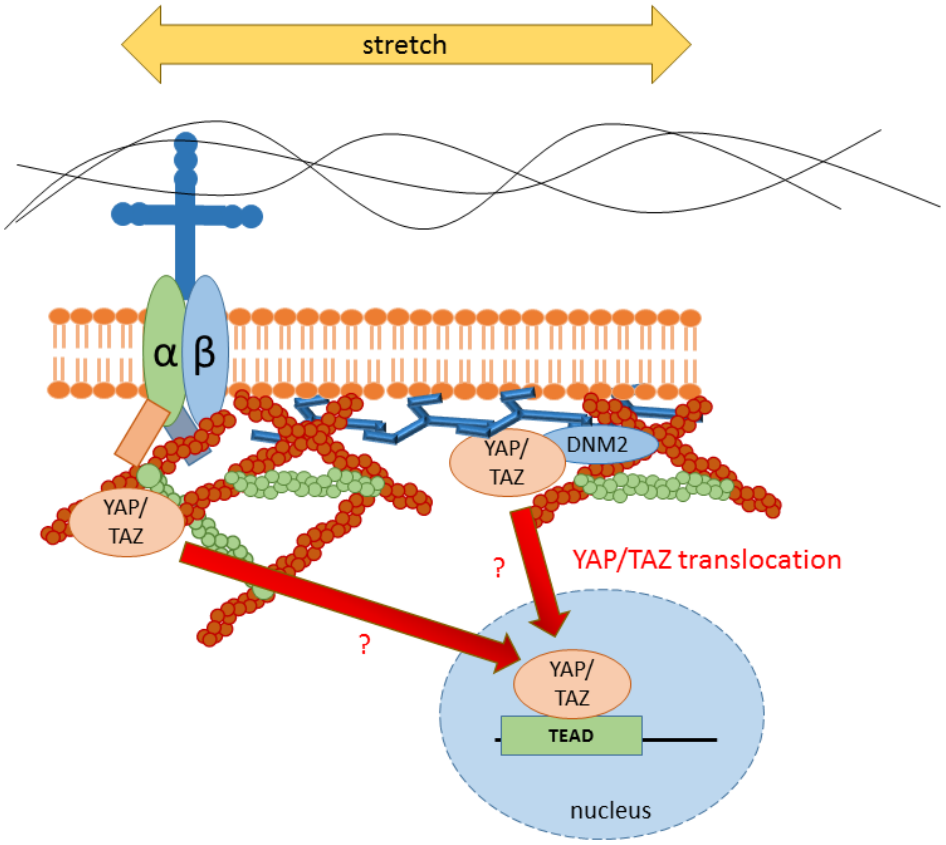

Figure IV.2. Actin around clathrin plaques regulate YAP/TAZ signaling

Possibly one the most interesting candidates to shuttle YAP/TAZ in the nucleus would be Merlin or NF2. Merlin is an F-binding protein associated to adherens junctions. In a proteomic study examining the Hippo interactome, it was found a strong association between components of the Hippo pathway and members of vesicle trafficking. Namely, the authors uncovered an interaction between Merlin and CHC (Kwon et al., 2013). A very recent study provided evidence that Merlin is able to bind to YAP/TAZ. Authors actually postulate that tension sensed through adherens junctions work independently of the regulation occurring at ECM-PM contact sites. Indeed, instead of F-actin promoting YAP/TAZ nuclear translocation, they argue that Merlin is capable of actively shuttling YAP/TAZ out of the nucleus following increase in actin tension caused by high cell density. Regardless, the fact that Merlin can actively target YAP/TAZ to the PM or the nucleus make it a strong candidate for YAP/TAZ regulation outside of adherens junctions. Co-immunoprecipitation experiments could help us determine whether Merlin and CHC interact in muscle cells. It would also be interesting to study the regulation of Merlin in myotubes, whether they follow YAP/TAZ regulation following cell stretching and if this protein is impacted at all by CHC or DNM2 depletion.

b. Intermediate filaments

IFs are prominent in cells subject to mechanical stress. This network was described in a review by E. Fuchs and D.W. Cleveland, as a way for the cell to resist to high external stress (Fuchs and Cleveland, 1998). They are structural elements capable of connecting the exterior of the cell with the interior of the nucleus. They also regulate changes in cytoplasmic mechanics that accompany various physiological activities such as cell contraction, migration, proliferation, and organelle positioning (Guo et al., 2013). If the role of desmin in modulating mechanical functions of muscle is well established, especially for the desmin web at the cell's cortex, mostly responsible for conferring mechanosensitivity to the sarcolemma (Boriek et al., 2001), the biological substratum for the desmin-mediated mechanosensitivity is not fully understood. In this thesis, I postulate that cortical desmin is anchored at costameres by branched actin organized around flat clathrin plaques. Depleting muscle cells of clathrin or DNM2 mimics depletion of actin-remodeling actor N-WASP by inducing a disorganization of desmin.

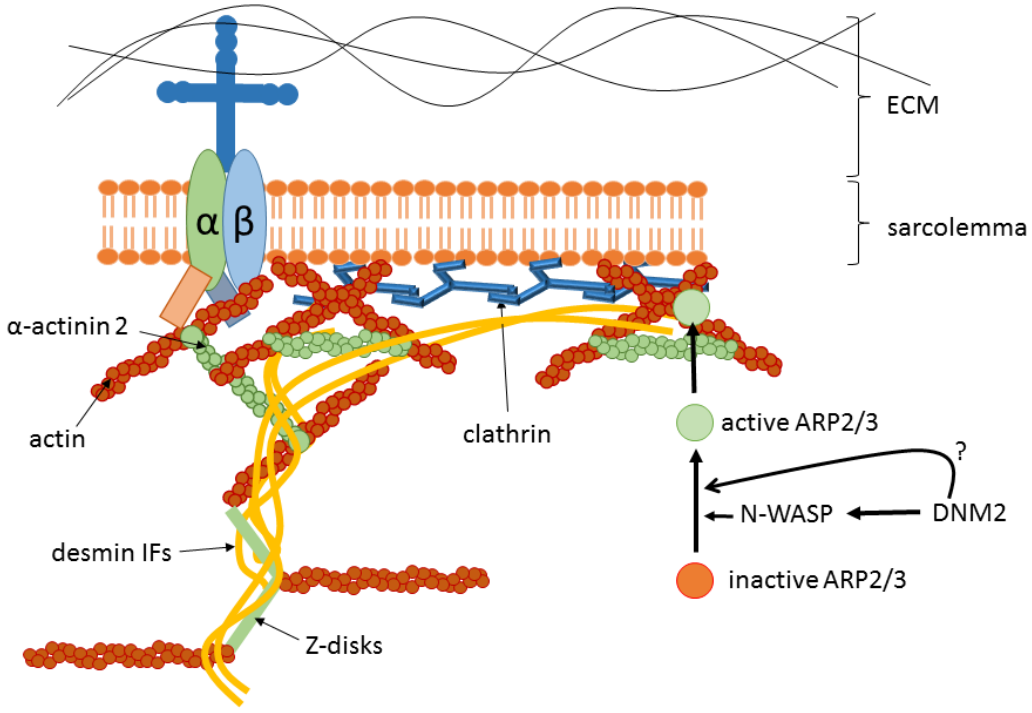

Figure IV.3. Schematic representation of costameric clathrin plaques

In the past, IF-associated proteins have been involved in the cross-linking of intermediate filaments to other cytoskeletal elements. Around the same time, two proteins were identified as important linkers for IFs and microfilaments, namely plectin and BPAC1n (Foisner et al., 1995;

Yang et al., 1996). Diverse studies highlight the implications of IF regulation by microfilaments of actin (Dupin et al., 2011; Hollenbeck et al., 1989; Huber et al., 2015; Jiu et al., 2015) and confirms in our case that actin can be very important to anchor IFs on the plasma membrane. Since it was postulated and tested by protein purification that actin and vimentin could interact directly which each other, i.e. without the need of auxiliary proteins (Esue et al., 2006), it will be pivotal to identify the precise interaction between actin and desmin in muscle cells.

4- Consequences for CNM pathophysiology

The final objective of my PhD project was to put clathrin plaques back in the context of CNM. Gathering from my previous results the importance of clathrin plaques on the anchorage of cytoskeletal filaments (both actin and desmin) and regulation of YAP/TAZ signaling, I wanted to test what would be the effects of *Dnm2* mutations in those processes. By studying immortalized CNM patient cells and our mouse model carrying an heterozygous p.R465W mutation for *Dnm2*, I found that the middle domain affected by those mutations is important to regulate actin, desmin and TAZ distributions.

Faelber and colleagues suggested that CNM mutations may lead to aberrant oligomerization at abnormal cellular sites or prevent helix disassembly after GTP hydrolysis (Faelber et al., 2013). This has implications for clathrin plaques as a whole, since dynamin's ability to oligomerize seems to affect its affinity to certain CCS (James et al., 2014). Structural defects associated to reduced plaque turnover that we observed in the KI HTZ-*Dnm2*^{R465W} animal model might be a consequence of DNM2 abnormal oligomerization.

It has been suggested that the actin-remodeling role of dynamin could have direct consequences on the pathophysiology of CNM. As mentioned before, a very recent study performed in collaboration with our lab showed that CNM-associated mutations in *Dnm2* reduce *de novo* actin filament formation in transfected myoblasts and induced defects in the actin regulation concerning the HTZ KI-*Dnm2*^{R465W} mouse model, pointing out the importance of DNM2-regulated actin assembly (González-Jamett et al., 2017). Interestingly, besides structural defects induced by DNM2 depletion, we showed that depleted or mutated *Dnm2* induced a decrease in γ-actin translation, present at Z-disks and important for muscle maintenance. We can hypothesize that *Dnm2* mutations not only lead to a default of actin structure via recruitment and organization defects but also by lack of necessary actin at costameres. Further studies will be needed to discriminate the consequences of *Dnm2* mutations on actin polymerization versus specific interactions with actin-related proteins, specifically if N-WASP is affected at all by CNM-*Dnm2* mutations.

Moreover, I showed throughout this study that actin defects induced by depletion or *Dnm2* mutations caused abnormal accumulation of intracellular desmin aggregates. The link between desmin IFs with both PM and nuclei in muscle is well established. So can desmin defects explain the central nuclear positioning in CNM? Although abnormal positioning of the nuclei is the histopathological hallmark of all genetically defined forms of CNM, the link between the mutated proteins and abnormal nuclear positioning remains largely unknown. Our results suggest the peculiar organization termed "radial sarcoplasmic strands", found in CNM patient fibers, may be the consequence of the desmin tangles which systematically form at the surface and around nuclei. Interestingly, costamere defects have already been reported for the X-linked form of CNM due to mutation in the myotubularin (MTM1), a phosphoinositide phosphatase which also binds to desmin (Hnia et al., 2011; Ribeiro et al., 2011). Very recently, a study showed that ARP2/3 is involved in the organization of desmin involved in nuclear movement (Roman et al., 2017), which points to the role of actin in desmin organization around nuclei. Our results obtained using the DNM2-related CNM knock-in mouse model corroborate this link and suggest that desmin IF defects are a common component of CNM pathophysiology. Further investigation for a desmin defect in the autosomal recessive form of CNM due to amphiphysin 2 mutations (Nicot et al., 2007) will be required to confirm this common pathophysiological pathway.

Overall, both actin and desmin structural defects induced by CNM *Dnm2* mutations crossed paths in the process of mechanotransduction. This has been suggested recently, as YAP regulation was studied in the context of heart regeneration by cardiomyocyte proliferation. Authors showed that YAP was indeed part of the membrane pool in skeletal muscle cells and sequestered by the dystrophin-glycoprotein complex (Morikawa et al., 2017).

In this thesis, I propose that clathrin plaques act as both anchor points for desmin IFs and sequestering platforms for YAP/TAZ mechanotransducers. The actin cortical cytoskeleton was defined as a regulator of the YAP/TAZ pathway, either to induce its nuclear translocation (Piccolo et al., 2014) or on the contrary, shuttle it back to the nucleus (Furukawa et al., 2017). Concerning the desmin IF cytoskeleton, no particular link was drawn with YAP/TAZ until recently, when it was shown that YAP and TAZ were increased in failing human hearts with a cardiomyopathy and in hearts from mice with a mutated desmin (Hou et al., 2017), linking abnormal YAP/TAZ signaling with myopathies and desmin defects.

Upon witnessing the abnormal translocation of YAP/TAZ in CHC- and DNM2-depleted cells or in *Dnm2* p.R369Q patient cells, I wondered which could be the implications of a defective YAP/TAZ translocation on the pathophysiology of CNM. YAP/TAZ regulation, translocation and signaling have been recently studied in the context of myopathies and neuromuscular diseases.

Interestingly, mice exhibiting a muscle-specific YAP mutation showed neuromuscular junction defects (Zhao et al., 2017). Furthermore, regulation of YAP was implicated in the development (Lima et al., 2016) and regulation of muscle mass in muscle. While certain studies suggested that expression of YAP could correct defects in hypotrophic muscles (Watt et al., 2015) by an upregulation of *MyoD* and *c-Myc* expression (Goodman et al., 2015), another study suggested that constitutive expression of YAP in muscle induced hypotrophy and structural defects resembling that of centronuclear myopathies (Judson et al., 2013). Overall, these upcoming studies show the impact of YAP regulation in the developing muscle.

On the other hand, YAP/TAZ specialists are starting to gather that YAP and TAZ might be differently regulated depending on the cellular context, and it seems to be particularly important in muscle cells. Just last year, a study was published showing that in muscle stem cells, YAP and TAZ share a similar function of cell proliferation. In later stages however, TAZ is able to enhance myoblast differentiation by regulating genes independently of YAP such as *Pax7*, *Myf5*, and *Myod1* that are important for myogenesis (Sun et al., 2017). Although we found that YAP and TAZ was translocated in muscle cells in a similar fashion following cell stretching or siRNA treatments, we also found a specific interaction between TAZ and DNM2 that was not shared by YAP. We can therefore not exclude a TAZ-specific role on clathrin plaques.

CNM affected muscles are characterized by type I fiber atrophy and centralized nuclei, showing a histological phenotype that could be associated to fibers that were incorrectly differentiated (Hohendahl et al., 2016). It would be interesting to find out if YAP/TAZ defects in CNM are a cause or a consequence of the disease, and if symptoms could be alleviated by an upregulation of YAP/TAZ target genes during development.

During my thesis, I defined a completely novel role for clathrin plaques as PM platforms for mechanotransduction in muscle cells. I identified N-WASP and DNM2 as central actors in actin remodeling at clathrin plaques. I showed that DNM2 organizes flat clathrin plaques and surrounding branched actin filaments which sequester YAP/TAZ mechanotransducers at the plasma membrane and are required for efficient nuclear translocation in response to cyclic stretching. Branched actin filaments surrounding clathrin plaques also form anchoring points required for organization of the intermediate filament subcortical web.

Thus, clathrin plaques act as molecular platforms conveying mechanical cues which integrate cell signaling with cytoskeletal regulation. My study on clathrin plaques sheds light on the role of clathrin plaques and highlights their unconventional role which is relevant to muscle physiology and whose dysfunction is associated with the physiopathology of CNM linked to *Dnm2* mutations.

V. References

Abmayr, S.M., and Pavlath, G.K. (2012). Myoblast fusion: lessons from flies and mice. Development *139*, 641–656.

Aggeler, J., and Werb, Z. (1982). Initial events during phagocytosis by macrophages viewed from outside and inside the cell: membrane-particle interactions and clathrin. J. Cell Biol. *94*, 613–623.

Aguet, F., Antonescu, C.N., Mettlen, M., Schmid, S.L., and Danuser, G. (2013). Advances in analysis of low signal-to-noise images link dynamin and AP2 to the functions of an endocytic checkpoint. Dev. Cell *26*, 279–291.

Akisaka, T., Yoshida, H., Suzuki, R., Shimizu, K., and Takama, K. (2003). Clathrin sheets on the protoplasmic surface of ventral membranes of osteoclasts in culture. J. Electron Microsc. (Tokyo) *52*, 535–543.

Akisaka, T., Yoshida, H., Suzuki, R., and Takama, K. (2008). Adhesion structures and their cytoskeleton-membrane interactions at podosomes of osteoclasts in culture. Cell Tissue Res. *331*, 625–641.

Al-Qusairi, L., Weiss, N., Toussaint, A., Berbey, C., Messaddeq, N., Kretz, C., Sanoudou, D., Beggs, A.H., Allard, B., Mandel, J.-L., et al. (2009). T-tubule disorganization and defective excitation-contraction coupling in muscle fibers lacking myotubularin lipid phosphatase. Proc. Natl. Acad. Sci. U. S. A. *106*, 18763–18768.

Antonny, B., Burd, C., Camilli, P.D., Chen, E., Daumke, O., Faelber, K., Ford, M., Frolov, V.A., Frost, A., Hinshaw, J.E., et al. (2016). Membrane fission by dynamin: what we know and what we need to know. EMBO J. e201694613.

Aragona, M., Panciera, T., Manfrin, A., Giulitti, S., Michielin, F., Elvassore, N., Dupont, S., and Piccolo, S. (2013). A mechanical checkpoint controls multicellular growth through YAP/TAZ regulation by actin-processing factors. Cell *154*, 1047–1059.

Avinoam, O., Schorb, M., Beese, C.J., Briggs, J.A.G., and Kaksonen, M. (2015). Endocytic sites mature by continuous bending and remodeling of the clathrin coat. Science *348*, 1369–1372.

Ayscough, K.R., Stryker, J., Pokala, N., Sanders, M., Crews, P., and Drubin, D.G. (1997). High Rates of Actin Filament Turnover in Budding Yeast and Roles for Actin in Establishment and Maintenance of Cell Polarity Revealed Using the Actin Inhibitor Latrunculin-A. J. Cell Biol. *137*, 399–416.

Bakry, R., Vallant, R.M., Najam-ul-Haq, M., Rainer, M., Szabo, Z., Huck, C.W., and Bonn, G.K. (2007). Medicinal applications of fullerenes. Int. J. Nanomedicine *2*, 639–649.

Baldassarre, M., Pompeo, A., Beznoussenko, G., Castaldi, C., Cortellino, S., McNiven, M.A., Luini, A., and Buccione, R. (2003). Dynamin Participates in Focal Extracellular Matrix Degradation by Invasive Cells. Mol. Biol. Cell *14*, 1074–1084.

Ball, P. (2009). Shapes: Nature's patterns: a tapestry in three parts (OUP Oxford).

Bär, H., Fischer, D., Goudeau, B., Kley, R.A., Clemen, C.S., Vicart, P., Herrmann, H., Vorgerd, M., and Schröder, R. (2005). Pathogenic effects of a novel heterozygous R350P desmin mutation on the assembly of desmin intermediate filaments in vivo and in vitro. Hum. Mol. Genet. *14*, 1251–1260.

Bär, H., Schopferer, M., Sharma, S., Hochstein, B., Mücke, N., Herrmann, H., and Willenbacher, N. (2010). Mutations in desmin's carboxy-terminal "tail" domain severely modify filament and network mechanics. J. Mol. Biol. *397*, 1188–1198.

Batchelder, E.M., and Yarar, D. (2010). Differential requirements for clathrin-dependent endocytosis at sites of cell-substrate adhesion. Mol. Biol. Cell *21*, 3070–3079.

Beckerle, M.C. (1997). Zyxin: zinc fingers at sites of cell adhesion. BioEssays News Rev. Mol. Cell. Dev. Biol. *19*, 949–957.

Belaguli, N.S., Schildmeyer, L.A., and Schwartz, R.J. (1997). Organization and Myogenic Restricted Expression of the Murine Serum Response Factor Gene A ROLE FOR AUTOREGULATION. J. Biol. Chem. *272*, 18222–18231.

Bentzinger, C.F., Wang, Y.X., and Rudnicki, M.A. (2012). Building Muscle: Molecular Regulation of Myogenesis. Cold Spring Harb. Perspect. Biol. *4*, a008342.

Bertrand, A.T., Ziaei, S., Ehret, C., Duchemin, H., Mamchaoui, K., Bigot, A., Mayer, M., Quijano-Roy, S., Desguerre, I., Lainé, J., et al. (2014). Cellular microenvironments reveal defective mechanosensing responses and elevated YAP signaling in LMNA-mutated muscle precursors. J. Cell Sci. *127*, 2873–2884.

Bitoun, M., Maugenre, S., Jeannet, P.-Y., Lacène, E., Ferrer, X., Laforêt, P., Martin, J.-J., Laporte, J., Lochmüller, H., Beggs, A.H., et al. (2005). Mutations in dynamin 2 cause dominant centronuclear myopathy. Nat. Genet. *37*, 1207–1209.

Bitoun, M., Bevilacqua, J.A., Prudhon, B., Maugenre, S., Taratuto, A.L., Monges, S., Lubieniecki, F., Cances, C., Uro-Coste, E., Mayer, M., et al. (2007). Dynamin 2 mutations cause sporadic centronuclear myopathy with neonatal onset. Ann. Neurol. *62*, 666–670.

Bitoun, M., Durieux, A.-C., Prudhon, B., Bevilacqua, J.A., Herledan, A., Sakanyan, V., Urtizberea, A., Cartier, L., Romero, N.B., and Guicheney, P. (2009). Dynamin 2 mutations associated with human diseases impair clathrin-mediated receptor endocytosis. Hum. Mutat. *30*, 1419–1427.

Bjorge, J.D., Jakymiw, A., and Fujita, D.J. (2000). Selected glimpses into the activation and function of Src kinase. Oncogene *19*, 5620.

van der Bliek, A.M., and Meyerowitz, E.M. (1991). Dynamin-like protein encoded by the Drosophila shibire gene associated with vesicular traffic. Nature *351*, 411–414.

Blondeau, F., Laporte, J., Bodin, S., Superti-Furga, G., Payrastre, B., and Mandel, J.L. (2000). Myotubularin, a phosphatase deficient in myotubular myopathy, acts on phosphatidylinositol 3-kinase and phosphatidylinositol 3-phosphate pathway. Hum. Mol. Genet. *9*, 2223–2229.

Böhm, J., Biancalana, V., Malfatti, E., Dondaine, N., Koch, C., Vasli, N., Kress, W., Strittmatter, M., Taratuto, A.L., Gonorazky, H., et al. (2014). Adult-onset autosomal dominant centronuclear myopathy due to BIN1 mutations. Brain *137*, 3160–3170.

Bonazzi, M., Vasudevan, L., Mallet, A., Sachse, M., Sartori, A., Prevost, M.-C., Roberts, A., Taner, S.B., Wilbur, J.D., Brodsky, F.M., et al. (2011). Clathrin phosphorylation is required for actin recruitment at sites of bacterial adhesion and internalization. J. Cell Biol. *195*, 525–536.

Bonazzi, M., Kühbacher, A., Toledo-Arana, A., Mallet, A., Vasudevan, L., Pizarro-Cerdá, J., Brodsky, F.M., and Cossart, P. (2012). A common clathrin-mediated machinery co-ordinates cell-cell adhesion and bacterial internalization. Traffic Cph. Den. *13*, 1653–1666.

Bonifacino, J.S., and Dell'Angelica, E.C. (1999). Molecular bases for the recognition of tyrosine-based sorting signals. J. Cell Biol. *145*, 923–926.

Bonifacino, J.S., and Lippincott-Schwartz, J. (2003). Coat proteins: shaping membrane transport. Nat. Rev. Mol. Cell Biol. *4*, nrm1099.

Boriek, A.M., Capetanaki, Y., Hwang, W., Officer, T., Badshah, M., Rodarte, J., and Tidball, J.G. (2001). Desmin integrates the three-dimensional mechanical properties of muscles. Am. J. Physiol. Cell Physiol. *280*, C46-52.

Bova, M.P., Yaron, O., Huang, Q., Ding, L., Haley, D.A., Stewart, P.L., and Horwitz, J. (1999). Mutation R120G in αB-crystallin, which is linked to a desmin-related myopathy, results in an irregular structure and defective chaperone-like function. Proc. Natl. Acad. Sci. U. S. A. *96*, 6137–6142.

Briñas, L., Vassilopoulos, S., Bonne, G., Guicheney, P., and Bitoun, M. (2013). Role of dynamin 2 in the disassembly of focal adhesions. J. Mol. Med. *91*, 803–809.

Brodsky, F.M. (2012). Diversity of clathrin function: new tricks for an old protein. Annu. Rev. Cell Dev. Biol. *28*, 309–336.

Brodsky, F.M., Hill, B.L., Acton, S.L., Näthke, I., Wong, D.H., Ponnambalam, S., and Parham, P. (1991). Clathrin light chains: arrays of protein motifs that regulate coated-vesicle dynamics. Trends Biochem. Sci. *16*, 208–213.

Burkholder, T.J. (2007). Mechanotransduction in skeletal muscle. Front. Biosci. J. Virtual Libr. *12*, 174–191.

Burridge, K., Feramisco, J., and Blose, S. (1980). The association of alpha-actinin and clathrin with the plasma membrane. Prog. Clin. Biol. Res. *41*, 907–924.

Cai, H., Reinisch, K., and Ferro-Novick, S. (2007). Coats, Tethers, Rabs, and SNAREs Work Together to Mediate the Intracellular Destination of a Transport Vesicle. Dev. Cell *12*, 671–682.

Calderón, J.C., Bolaños, P., and Caputo, C. (2014). The excitation–contraction coupling mechanism in skeletal muscle. Biophys. Rev. *6*, 133–160.

Cao, H., Garcia, F., and McNiven, M.A. (1998). Differential distribution of dynamin isoforms in mammalian cells. Mol. Biol. Cell *9*, 2595–2609.

Cao, H., Orth, J.D., Chen, J., Weller, S.G., Heuser, J.E., and McNiven, M.A. (2003). Cortactin Is a Component of Clathrin-Coated Pits and Participates in Receptor-Mediated Endocytosis. Mol. Cell. Biol. *23*, 2162–2170.

Capetanaki, Y., Papathanasiou, S., Diokmetzidou, A., Vatsellas, G., and Tsikitis, M. (2015). Desmin related disease: a matter of cell survival failure. Curr. Opin. Cell Biol. *32*, 113–120.

Carlsson, L., Li, Z., Paulin, D., and Thornell, L.E. (1999). Nestin is expressed during development and in myotendinous and neuromuscular junctions in wild type and desmin knock-out mice. Exp. Cell Res. *251*, 213–223.

Chappie, J.S., Mears, J.A., Fang, S., Leonard, M., Schmid, S.L., Milligan, R.A., Hinshaw, J.E., and Dyda, F. (2011). A pseudoatomic model of the dynamin polymer identifies a hydrolysis-dependent powerstroke. Cell *147*, 209–222.

Chen, C.-Y., and Brodsky, F.M. (2005). Huntingtin-interacting Protein 1 (Hip1) and Hip1-related Protein (Hip1R) Bind the Conserved Sequence of Clathrin Light Chains and Thereby Influence Clathrin Assembly in Vitro and Actin Distribution in Vivo. J. Biol. Chem. *280*, 6109–6117.

Chetrit, D., Ziv, N., and Ehrlich, M. (2009). Dab2 regulates clathrin assembly and cell spreading. Biochem. J. *418*, 701–715.

Chin, Y.-H., Lee, A., Kan, H.-W., Laiman, J., Chuang, M.-C., Hsieh, S.-T., and Liu, Y.-W. (2015). Dynamin-2 mutations associated with centronuclear myopathy are hypermorphic and lead to T-tubule fragmentation. Hum. Mol. Genet. *24*, 5542–5554.

Chorev, D.S., Moscovitz, O., Geiger, B., and Sharon, M. (2014). Regulation of focal adhesion formation by a vinculin-Arp2/3 hybrid complex. Nat. Commun. *5*, 3758.

Clark, K.A., McElhinny, A.S., Beckerle, M.C., and Gregorio, C.C. (2002). Striated muscle cytoarchitecture: an intricate web of form and function. Annu. Rev. Cell Dev. Biol. *18*, 637–706.

Clemen, C.S., Herrmann, H., Strelkov, S.V., and Schröder, R. (2013). Desminopathies: pathology and mechanisms. Acta Neuropathol. (Berl.) *125*, 47–75.

Cocucci, E., Aguet, F., Boulant, S., and Kirchhausen, T. (2012). The First Five Seconds in the Life of a Clathrin-Coated Pit. Cell *150*, 495–507.

Collins, A., Warrington, A., Taylor, K.A., and Svitkina, T. (2011). Structural organization of the actin cytoskeleton at sites of clathrin-mediated endocytosis. Curr. Biol. CB *21*, 1167–1175.

Collins, B.M., McCoy, A.J., Kent, H.M., Evans, P.R., and Owen, D.J. (2002). Molecular Architecture and Functional Model of the Endocytic AP2 Complex. Cell *109*, 523–535.

Cooper, G.M. (2000). Structure and Organization of Actin Filaments.

Cowling, B.S., Toussaint, A., Amoasii, L., Koebel, P., Ferry, A., Davignon, L., Nishino, I., Mandel, J.-L., and Laporte, J. (2011). Increased Expression of Wild-Type or a Centronuclear Myopathy Mutant of Dynamin 2 in Skeletal Muscle of Adult Mice Leads to Structural Defects and Muscle Weakness. Am. J. Pathol. *178*, 2224–2235.

Craig, S.W., and Pardo, J.V. (1983). Gamma actin, spectrin, and intermediate filament proteins colocalize with vinculin at costameres, myofibril-to-sarcolemma attachment sites. Cell Motil. *3*, 449–462.

Csibi, A., and Blenis, J. (2012). Hippo–YAP and mTOR pathways collaborate to regulate organ size. Nat. Cell Biol. *14*, 1244.

Dalakas, M.C., Park, K.Y., Semino-Mora, C., Lee, H.S., Sivakumar, K., and Goldfarb, L.G. (2000). Desmin myopathy, a skeletal myopathy with cardiomyopathy caused by mutations in the desmin gene. N. Engl. J. Med. *342*, 770–780.

Damke, H., Baba, T., Warnock, D.E., and Schmid, S.L. (1994). Induction of mutant dynamin specifically blocks endocytic coated vesicle formation. J. Cell Biol. *127*, 915–934.

Danino, D., Moon, K.-H., and Hinshaw, J.E. (2004). Rapid constriction of lipid bilayers by the mechanochemical enzyme dynamin. J. Struct. Biol. *147*, 259–267.

Dannhauser, P.N., Platen, M., Böning, H., and Schaap, I. a. T. (2015). Durable protein lattices of clathrin that can be functionalized with nanoparticles and active biomolecules. Nat. Nanotechnol. *10*, nnano.2015.206.

Danowski, B.A., Imanaka-Yoshida, K., Sanger, J.M., and Sanger, J.W. (1992). Costameres are sites of force transmission to the substratum in adult rat cardiomyocytes. J. Cell Biol. *118*, 1411–1420.

Das, A., Fischer, R.S., Pan, D., and Waterman, C.M. (2016). YAP Nuclear Localization in the Absence of Cell-Cell Contact Is Mediated by a Filamentous Actin-dependent, Myosin II- and Phospho-YAP-independent Pathway during Extracellular Matrix Mechanosensing. J. Biol. Chem. *291*, 6096–6110.

De Deyne, P.G., O'Neill, A., Resneck, W.G., Dmytrenko, G.M., Pumplin, D.W., and Bloch, R.J. (1998). The vitronectin receptor associates with clathrin-coated membrane domains via the cytoplasmic domain of its beta5 subunit. J. Cell Sci. *111 (Pt 18)*, 2729–2740.

Destaing, O., Ferguson, S.M., Grichine, A., Oddou, C., De Camilli, P., Albiges-Rizo, C., and Baron, R. (2013). Essential function of dynamin in the invasive properties and actin architecture of v-Src induced podosomes/invadosomes. PloS One *8*, e77956.

Devos, D., Dokudovskaya, S., Alber, F., Williams, R., Chait, B.T., Sali, A., and Rout, M.P. (2004). Components of Coated Vesicles and Nuclear Pore Complexes Share a Common Molecular Architecture. PLoS Biol. *2*.

Dong, J.-M., Lau, L.-S., Ng, Y.-W., Lim, L., and Manser, E. (2009). Paxillin nuclear-cytoplasmic localization is regulated by phosphorylation of the LD4 motif: evidence that nuclear paxillin promotes cell proliferation. Biochem. J. *418*, 173–184.

Dowling, J.J., Joubert, R., Low, S.E., Durban, A.N., Messaddeq, N., Li, X., Dulin-Smith, A.N., Snyder, A.D., Marshall, M.L., Marshall, J.T., et al. (2012). Myotubular myopathy and the neuromuscular junction: a novel therapeutic approach from mouse models. Dis. Model. Mech. *5*, 852–859.

Driscoll, T.P., Cosgrove, B.D., Heo, S.-J., Shurden, Z.E., and Mauck, R.L. (2015). Cytoskeletal to Nuclear Strain Transfer Regulates YAP Signaling in Mesenchymal Stem Cells. Biophys. J. *108*, 2783–2793.

Dubin, R.A., Ally, A.H., Chung, S., and Piatigorsky, J. (1990). Human alpha B-crystallin gene and preferential promoter function in lens. Genomics *7*, 594–601.

Dupin, I., Sakamoto, Y., and Etienne-Manneville, S. (2011). Cytoplasmic intermediate filaments mediate actin-driven positioning of the nucleus. J. Cell Sci. *124*, 865–872.

Dupont, S., Morsut, L., Aragona, M., Enzo, E., Giulitti, S., Cordenonsi, M., Zanconato, F., Le Digabel, J., Forcato, M., Bicciato, S., et al. (2011). Role of YAP/TAZ in mechanotransduction. Nature *474*, 179–183.

Durieux, A.-C., Vignaud, A., Prudhon, B., Viou, M.T., Beuvin, M., Vassilopoulos, S., Fraysse, B., Ferry, A., Lainé, J., Romero, N.B., et al. (2010). A centronuclear myopathy-dynamin 2 mutation impairs skeletal muscle structure and function in mice. Hum. Mol. Genet. *19*, 4820–4836.

Dutta, D., Chakraborty, S., Bandyopadhyay, C., Veettil, M.V., Ansari, M.A., Singh, V.V., and Chandran, B. (2013). EphrinA2 Regulates Clathrin Mediated KSHV Endocytosis in Fibroblast Cells by Coordinating Integrin-Associated Signaling and c-Cbl Directed Polyubiquitination. PLOS Pathog. *9*, e1003510.

Ehrlich, M., Boll, W., Oijen, A. van, Hariharan, R., Chandran, K., Nibert, M.L., and Kirchhausen, T. (2004). Endocytosis by Random Initiation and Stabilization of Clathrin-Coated Pits. Cell *118*, 591–605.

Elkhatib, N., Bresteau, E., Baschieri, F., Rioja, A.L., Niel, G. van, Vassilopoulos, S., and Montagnac, G. (2017). Tubular clathrin/AP-2 lattices pinch collagen fibers to support 3D cell migration. Science *356*, eaal4713.

Engqvist-Goldstein, A.E.Y., and Drubin, D.G. (2003). Actin assembly and endocytosis: from yeast to mammals. Annu. Rev. Cell Dev. Biol. *19*, 287–332.

Engqvist-Goldstein, A.E., Warren, R.A., Kessels, M.M., Keen, J.H., Heuser, J., and Drubin, D.G. (2001). The actin-binding protein Hip1R associates with clathrin during early stages of endocytosis and promotes clathrin assembly in vitro. J. Cell Biol. *154*, 1209–1223.

Engqvist-Goldstein, A.E.Y., Zhang, C.X., Carreno, S., Barroso, C., Heuser, J.E., and Drubin, D.G. (2004). RNAi-mediated Hip1R silencing results in stable association between the endocytic machinery and the actin assembly machinery. Mol. Biol. Cell *15*, 1666–1679.

Ervasti, J.M. (2003). Costameres: the Achilles' heel of Herculean muscle. J. Biol. Chem. *278*, 13591–13594.

Esnault, C., Stewart, A., Gualdrini, F., East, P., Horswell, S., Matthews, N., and Treisman, R. (2014). Rho-actin signaling to the MRTF coactivators dominates the immediate transcriptional response to serum in fibroblasts. Genes Dev. *28*, 943–958.

Esue, O., Carson, A.A., Tseng, Y., and Wirtz, D. (2006). A Direct Interaction between Actin and Vimentin Filaments Mediated by the Tail Domain of Vimentin. J. Biol. Chem. *281*, 30393–30399.

Ezratty, E.J., Bertaux, C., Marcantonio, E.E., and Gundersen, G.G. (2009). Clathrin mediates integrin endocytosis for focal adhesion disassembly in migrating cells. J. Cell Biol. *187*, 733–747.

Faelber, K., Posor, Y., Gao, S., Held, M., Roske, Y., Schulze, D., Haucke, V., Noé, F., and Daumke, O. (2011). Crystal structure of nucleotide-free dynamin. Nature *477*, 556–560.

Faelber, K., Gao, S., Held, M., Posor, Y., Haucke, V., Noé, F., and Daumke, O. (2013). Oligomerization of dynamin superfamily proteins in health and disease. Prog. Mol. Biol. Transl. Sci. *117*, 411–443.

Faini, M., Beck, R., Wieland, F.T., and Briggs, J.A.G. (2013). Vesicle coats: structure, function, and general principles of assembly. Trends Cell Biol. *23*, 279–288.

Falcone, S., Roman, W., Hnia, K., Gache, V., Didier, N., Lainé, J., Auradé, F., Marty, I., Nishino, I., Charlet-Berguerand, N., et al. (2014). N-WASP is required for Amphiphysin-2/BIN1-dependent nuclear positioning and triad organization in skeletal muscle and is involved in the pathophysiology of centronuclear myopathy. EMBO Mol. Med. *6*, 1455–1475.

Fausser, J.L., Ungewickell, E., Ruch, J.V., and Lesot, H. (1993). Interaction of vinculin with the clathrin heavy chain. J. Biochem. (Tokyo) *114*, 498–503.

Fehon, R.G., McClatchey, A.I., and Bretscher, A. (2010). Organizing the cell cortex: the role of ERM proteins. Nat. Rev. Mol. Cell Biol. *11*, 276–287.

Ferguson, S.M., and De Camilli, P. (2012). Dynamin, a membrane-remodelling GTPase. Nat. Rev. Mol. Cell Biol. *13*, 75–88.

Fischer, M., Rikeit, P., Knaus, P., and Coirault, C. (2016). YAP-Mediated Mechanotransduction in Skeletal Muscle. Front. Physiol. *7*, 41.

Foisner, R., Bohn, W., Mannweiler, K., and Wiche, G. (1995). Distribution and ultrastructure of plectin arrays in subclones of rat glioma C6 cells differing in intermediate filament protein (vimentin) expression. J. Struct. Biol. *115*, 304–317.

Foster-Barber, A., and Bishop, J.M. (1998). Src interacts with dynamin and synapsin in neuronal cells. Proc. Natl. Acad. Sci. U. S. A. *95*, 4673–4677.

Fotin, A., Cheng, Y., Sliz, P., Grigorieff, N., Harrison, S.C., Kirchhausen, T., and Walz, T. (2004). Molecular model for a complete clathrin lattice from electron cryomicroscopy. Nature *432*, 573–579.

Francis, M.M., Hong, J.H., Schneider, M., and Farrance, I. (2007). Regulation of muscle specific genes by TAZ. FASEB JournalI *21*, A652.

Frank, D., Kuhn, C., Katus, H.A., and Frey, N. (2006). The sarcomeric Z-disc: a nodal point in signalling and disease. J. Mol. Med. Berl. Ger. *84*, 446–468.

Fraysse, B., Guicheney, P., and Bitoun, M. (2016). Calcium homeostasis alterations in a mouse model of the Dynamin 2-related centronuclear myopathy. Biol. Open *5*, 1691–1696.

Frontera, W.R., and Ochala, J. (2015). Skeletal Muscle: A Brief Review of Structure and Function. Calcif. Tissue Int. *96*, 183–195.

Fuchs, E., and Cleveland, D.W. (1998). A structural scaffolding of intermediate filaments in health and disease. Science *279*, 514–519.

Fujimoto, L.M., Roth, R., Heuser, J.E., and Schmid, S.L. (2000). Actin assembly plays a variable, but not obligatory role in receptor-mediated endocytosis in mammalian cells. Traffic Cph. Den. *1*, 161–171.

Furukawa, K.T., Yamashita, K., Sakurai, N., and Ohno, S. (2017). The Epithelial Circumferential Actin Belt Regulates YAP/TAZ through Nucleocytoplasmic Shuttling of Merlin. Cell Rep. *20*, 1435–1447.

Gaidarov, I., Santini, F., Warren, R.A., and Keen, J.H. (1999). Spatial control of coated-pit dynamics in living cells. Nat. Cell Biol. *1*, 1.

Garay, C., Judge, G., Lucarelli, S., Bautista, S., Pandey, R., Singh, T., and Antonescu, C.N. (2015). Epidermal growth factor–stimulated Akt phosphorylation requires clathrin or ErbB2 but not receptor endocytosis. Mol. Biol. Cell *26*, 3504–3519.

Gibbs, E.M., Feldman, E.L., and Dowling, J.J. (2010). The role of MTMR14 in autophagy and in muscle disease. Autophagy *6*, 819–820.

Gold, E.S., Underhill, D.M., Morrissette, N.S., Guo, J., McNiven, M.A., and Aderem, A. (1999). Dynamin 2 Is Required for Phagocytosis in Macrophages. J. Exp. Med. *190*, 1849–1856.

Goldfarb, L.G., Olivé, M., Vicart, P., and Goebel, H.H. (2008). Intermediate Filament Diseases: Desminopathy. Adv. Exp. Med. Biol. *642*, 131–164.

Goley, E.D., and Welch, M.D. (2006). The ARP2/3 complex: an actin nucleator comes of age. Nat. Rev. Mol. Cell Biol. *7*, 713–726.

González-Jamett, A.M., Baez-Matus, X., Olivares, M.J., Hinostroza, F., Guerra-Fernández, M.J., Vasquez-Navarrete, J., Bui, M.T., Guicheney, P., Romero, N.B., Bevilacqua, J.A., et al. (2017). Dynamin-2 mutations linked to Centronuclear Myopathy impair actin-dependent trafficking in muscle cells. Sci. Rep. *7*, 4580.

Goodarzi, S., Da Ros, T., Conde, J., Sefat, F., and Mozafari, M. (2017). Fullerene: biomedical engineers get to revisit an old friend. Mater. Today *20*, 460–480.

Goodman, C.A., Dietz, J.M., Jacobs, B.L., McNally, R.M., You, J.-S., and Hornberger, T.A. (2015). Yes-Associated Protein is up-regulated by mechanical overload and is sufficient to induce skeletal muscle hypertrophy. FEBS Lett. *589*, 1491–1497.

Gorter, E., and Grendel, F. (1925). ON BIMOLECULAR LAYERS OF LIPOIDS ON THE CHROMOCYTES OF THE BLOOD. J. Exp. Med. *41*, 439–443.

Grabs, D., Slepnev, V.I., Songyang, Z., David, C., Lynch, M., Cantley, L.C., and Camilli, P.D. (1997). The SH3 Domain of Amphiphysin Binds the Proline-rich Domain of Dynamin at a Single Site That Defines a New SH3 Binding Consensus Sequence. J. Biol. Chem. *272*, 13419–13425.

Granger, B.L., and Lazarides, E. (1980). Synemin: a new high molecular weight protein associated with desmin and vimentin filaments in muscle. Cell *22*, 727–738.

Grove, J., Metcalf, D.J., Knight, A.E., Wavre-Shapton, S.T., Sun, T., Protonotarios, E.D., Griffin, L.D., Lippincott-Schwartz, J., and Marsh, M. (2014). Flat clathrin lattices: stable features of the plasma membrane. Mol. Biol. Cell *25*, 3581–3594.

Gu, C., Yaddanapudi, S., Weins, A., Osborn, T., Reiser, J., Pollak, M., Hartwig, J., and Sever, S. (2010). Direct dynamin-actin interactions regulate the actin cytoskeleton. EMBO J. *29*, 3593–3606.

Gu, C., Lee, H.W., Garborcauskas, G., Reiser, J., Gupta, V., and Sever, S. (2016). Dynamin Autonomously Regulates Podocyte Focal Adhesion Maturation. J. Am. Soc. Nephrol. ASN.2016010008.

Guilluy, C., Osborne, L.D., Van Landeghem, L., Sharek, L., Superfine, R., Garcia-Mata, R., and Burridge, K. (2014). Isolated nuclei adapt to force and reveal a mechanotransduction pathway in the nucleus. Nat. Cell Biol. *16*, 376–381.

Guo, M., Ehrlicher, A.J., Mahammad, S., Fabich, H., Jensen, M.H., Moore, J.R., Fredberg, J.J., Goldman, R.D., and Weitz, D.A. (2013). The Role of Vimentin Intermediate Filaments in Cortical and Cytoplasmic Mechanics. Biophys. J. *105*, 1562–1568.

ter Haar, E., Musacchio, A., Harrison, S.C., and Kirchhausen, T. (1998). Atomic Structure of Clathrin: A β Propeller Terminal Domain Joins an α Zigzag Linker. Cell *95*, 563–573.

Haeckel, E.H.P.A. (1862). Die Radiolarien (Rhizopoda radiaria) : eine Monographie (Berlin : G. Reimer).

Halder, G., Dupont, S., and Piccolo, S. (2012). Transduction of mechanical and cytoskeletal cues by YAP and TAZ. Nat. Rev. Mol. Cell Biol. *13*, 591–600.

Hargittai, I. (2016). Symmetry 2: Unifying Human Understanding (Elsevier).

Heuser, J. (1980). Three-dimensional visualization of coated vesicle formation in fibroblasts. J. Cell Biol. *84*, 560–583.

Heuser, J. (2000a). The production of “cell cortices” for light and electron microscopy. Traffic Cph. Den. *1*, 545–552.

Heuser, J.E. (2000b). Membrane Traffic in Anaglyph Stereo. Traffic *1*, 35–37.

Heuser, J.E., and Keen, J. (1988). Deep-etch visualization of proteins involved in clathrin assembly. J. Cell Biol. *107*, 877–886.

Hinshaw, J.E., and Schmid, S.L. (1995). Dynamin self-assembles into rings suggesting a mechanism for coated vesicle budding. Nature *374*, 190–192.

Hirata, H., Tatsumi, H., Lim, C.T., and Sokabe, M. (2014). Force-dependent vinculin binding to talin in live cells: a crucial step in anchoring the actin cytoskeleton to focal adhesions. Am. J. Physiol. Cell Physiol. *306*, C607-620.

Hirata, H., Samsonov, M., and Sokabe, M. (2017). Actomyosin contractility provokes contact inhibition in E-cadherin-ligated keratinocytes. Sci. Rep. *7*, 46326.

Hirokawa, N., Tilney, L.G., Fujiwara, K., and Heuser, J.E. (1982). Organization of actin, myosin, and intermediate filaments in the brush border of intestinal epithelial cells. J. Cell Biol. *94*, 425–443.

Hirst, J., Barlow, L.D., Francisco, G.C., Sahlender, D.A., Seaman, M.N.J., Dacks, J.B., and Robinson, M.S. (2011). The fifth adaptor protein complex. PLoS Biol. *9*, e1001170.

Hirst, J., Irving, C., and Borner, G.H.H. (2013). Adaptor protein complexes AP-4 and AP-5: new players in endosomal trafficking and progressive spastic paraplegia. Traffic Cph. Den. *14*, 153–164.

Hnia, K., Tronchère, H., Tomczak, K.K., Amoasii, L., Schultz, P., Beggs, A.H., Payrastre, B., Mandel, J.L., and Laporte, J. (2011). Myotubularin controls desmin intermediate filament architecture and mitochondrial dynamics in human and mouse skeletal muscle. J. Clin. Invest. *121*, 70–85.

Hocevar, B.A., Smine, A., Xu, X.-X., and Howe, P.H. (2001). The adaptor molecule Disabled-2 links the transforming growth factor β receptors to the Smad pathway. EMBO J. *20*, 2789–2801.

Hocevar, B.A., Mou, F., Rennolds, J.L., Morris, S.M., Cooper, J.A., and Howe, P.H. (2003). Regulation of the Wnt signaling pathway by disabled-2 (Dab2). EMBO J. *22*, 3084–3094.

Hohendahl, A., Roux, A., and Galli, V. (2016). Structural insights into the centronuclear myopathy-associated functions of BIN1 and dynamin 2. J. Struct. Biol. *196*, 37.

Hollenbeck, P.J., Bershadsky, A.D., Pletjushkina, O.Y., Tint, I.S., and Vasiliev, J.M. (1989). Intermediate filament collapse is an ATP-dependent and actin-dependent process. J. Cell Sci. *92 (Pt 4)*, 621–631.

Hooke, R. (1667). Micrographia: Or, Some Physiological Descriptions of Minute Bodies Made by Magnifying Glasses. With Observations and Inquiries Thereupon (James Allestry).

Horowits, R., Kempner, E.S., Bisher, M.E., and Podolsky, R.J. (1986). A physiological role for titin and nebulin in skeletal muscle. Nature *323*, 160–164.

Hou, N., Wen, Y., Yuan, X., Xu, H., Wang, X., Li, F., and Ye, B. (2017). Activation of Yap1/Taz signaling in ischemic heart disease and dilated cardiomyopathy. Exp. Mol. Pathol. *103*, 267–275.

Huber, F., Boire, A., López, M.P., and Koenderink, G.H. (2015). Cytoskeletal crosstalk: when three different personalities team up. Curr. Opin. Cell Biol. *32*, 39–47.

Humphries, A.C., and Way, M. (2013). The non-canonical roles of clathrin and actin in pathogen internalization, egress and spread. Nat. Rev. Microbiol. *11*, nrmicro3072.

Huxley, A.F., and Niedergerke, R. (1954). Structural changes in muscle during contraction; interference microscopy of living muscle fibres. Nature *173*, 971–973.

Huxley, H., and Hanson, J. (1954). Changes in the cross-striations of muscle during contraction and stretch and their structural interpretation. Nature *173*, 973–976.

Hynes, R.O. (2002). Integrins: bidirectional, allosteric signaling machines. Cell *110*, 673–687.

Hynes, T.R., Block, S.M., White, B.T., and Spudich, J.A. (1987). Movement of myosin fragments in vitro: domains involved in force production. Cell *48*, 953–963.

Jackson, L.P., Kelly, B.T., McCoy, A.J., Gaffry, T., James, L.C., Collins, B.M., Höning, S., Evans, P.R., and Owen, D.J. (2010). A large-scale conformational change couples membrane recruitment to cargo binding in the AP2 clathrin adaptor complex. Cell *141*, 1220–1229.

James, N.G., Digman, M.A., Ross, J.A., Barylko, B., Wang, L., Li, J., Chen, Y., Mueller, J.D., Gratton, E., Albanesi, J.P., et al. (2014). A mutation associated with centronuclear myopathy enhances the size and stability of dynamin 2 complexes in cells. Biochim. Biophys. Acta *1840*.

Jeannet, P.-Y., Bassez, G., Eymard, B., Laforêt, P., Urtizberea, J.A., Rouche, A., Guicheney, P., Fardeau, M., and Romero, N.B. (2004). Clinical and histologic findings in autosomal centronuclear myopathy. Neurology *62*, 1484–1490.

Jiu, Y., Lehtimäki, J., Tojkander, S., Cheng, F., Jäälinoja, H., Liu, X., Varjosalo, M., Eriksson, J.E., and Lappalainen, P. (2015). Bidirectional Interplay between Vimentin Intermediate Filaments and Contractile Actin Stress Fibers. Cell Rep. *11*, 1511–1518.

Joubert, R., Vignaud, A., Le, M., Moal, C., Messaddeq, N., and Buj-Bello, A. (2013). Site-specific Mtm1 mutagenesis by an AAV-Cre vector reveals that myotubularin is essential in adult muscle. Hum. Mol. Genet. *22*, 1856–1866.

Judson, R.N., Gray, S.R., Walker, C., Carroll, A.M., Itzstein, C., Lionikas, A., Zammit, P.S., Bari, C.D., and Wackerhage, H. (2013). Constitutive Expression of Yes-Associated Protein (Yap) in Adult Skeletal Muscle Fibres Induces Muscle Atrophy and Myopathy. PLOS ONE *8*, e59622.

Jungbluth, H., Wallgren-Pettersson, C., and Laporte, J. (2008). Centronuclear (myotubular) myopathy. Orphanet J. Rare Dis. *3*, 26.

Kadlecova, Z., Spielman, S.J., Loerke, D., Mohanakrishnan, A., Reed, D.K., and Schmid, S.L. (2017). Regulation of clathrin-mediated endocytosis by hierarchical allosteric activation of AP2. J. Cell Biol. *216*, 167–179.

Kaisto, T., Rahkila, P., Marjomäki, V., Parton, R.G., and Metsikkö, K. (1999). Endocytosis in Skeletal Muscle Fibers. Exp. Cell Res. *253*, 551–560.

Kaksonen, M., Sun, Y., and Drubin, D.G. (2003). A pathway for association of receptors, adaptors, and actin during endocytic internalization. Cell *115*, 475–487.

Kaksonen, M., Toret, C.P., and Drubin, D.G. (2006). Harnessing actin dynamics for clathrin-mediated endocytosis. Nat. Rev. Mol. Cell Biol. *7*, 404–414.

Kanai, F., Marignani, P.A., Sarbassova, D., Yagi, R., Hall, R.A., Donowitz, M., Hisaminato, A., Fujiwara, T., Ito, Y., Cantley, L.C., et al. (2000). TAZ: a novel transcriptional co-activator regulated by interactions with 14-3-3 and PDZ domain proteins. EMBO J. *19*, 6778–6791.

Kaufman, S.J., Bielser, D., and Foster, R.F. (1990). Localization of anti-clathrin antibody in the sarcomere and sensitivity of myofibril structure to chloroquine suggest a role for clathrin in myofibril assembly. Exp. Cell Res. *191*, 227–238.

Kessels, M.M., Engqvist-Goldstein, A.E., Drubin, D.G., and Qualmann, B. (2001). Mammalian Abp1, a signal-responsive F-actin-binding protein, links the actin cytoskeleton to endocytosis via the GTPase dynamin. J. Cell Biol. *153*, 351–366.

Kim, N.-G., and Gumbiner, B.M. (2015). Adhesion to fibronectin regulates Hippo signaling via the FAK–Src–PI3K pathway. J Cell Biol *210*, 503–515.

Kim, J., Jo, H., Hong, H., Kim, M.H., Kim, J.M., Lee, J.-K., Heo, W.D., and Kim, J. (2015). Actin remodelling factors control ciliogenesis by regulating YAP/TAZ activity and vesicle trafficking. Nat. Commun. *6*, 6781.

Kim, T., Hwang, D., Lee, D., Kim, J.-H., Kim, S.-Y., and Lim, D.-S. (2017). MRTF potentiates TEAD-YAP transcriptional activity causing metastasis. EMBO J. *36*, 520–535.

Kirchhausen, T. (1999). Adaptors for clathrin-mediated traffic. Annu. Rev. Cell Dev. Biol. *15*, 705–732.

Kirchhausen, T. (2009). Imaging endocytic clathrin structures in living cells. Trends Cell Biol. *19*, 596–605.

Kirchhausen, T., Owen, D., and Harrison, S.C. (2014). Molecular structure, function, and dynamics of clathrin-mediated membrane traffic. Cold Spring Harb. Perspect. Biol. *6*, a016725.

Knöll, R., Buyandelger, B., and Lab, M. (2011). The Sarcomeric Z-Disc and Z-Discopathies. J. Biomed. Biotechnol. *2011*.

Koenig, J.H., and Ikeda, K. (1989). Disappearance and reformation of synaptic vesicle membrane upon transmitter release observed under reversible blockage of membrane retrieval. J. Neurosci. Off. J. Soc. Neurosci. *9*, 3844–3860.

Kostera-Pruszczyk, A., Pruszczyk, P., Kamińska, A., Lee, H.-S., and Goldfarb, L.G. (2008). Diversity of cardiomyopathy phenotypes caused by mutations in desmin. Int. J. Cardiol. *131*, 146–147.

Koutsopoulos, O.S., Koch, C., Tosch, V., Böhm, J., North, K.N., and Laporte, J. (2011). Mild functional differences of dynamin 2 mutations associated to centronuclear myopathy and Charcot-Marie Tooth peripheral neuropathy. PloS One *6*, e27498.

Kozlov, M.M. (1999). Dynamin: possible mechanism of "Pinchase" action. Biophys. J. *77*, 604–616.

Kroto, H.W., Heath, J.R., O'Brien, S.C., Curl, R.F., and Smalley, R.E. (1985). C60: Buckminsterfullerene. Nature *318*, 318162a0.

Krueger, E.W., Orth, J.D., Cao, H., and McNiven, M.A. (2003). A Dynamin–Cortactin–Arp2/3 Complex Mediates Actin Reorganization in Growth Factor-stimulated Cells. Mol. Biol. Cell *14*, 1085–1096.

Kurklinsky, S., Chen, J., and McNiven, M.A. (2011). Growth cone morphology and spreading are regulated by a dynamin-cortactin complex at point contacts in hippocampal neurons. J. Neurochem. *117*, 48–60.

Kutchukian, C., Szentesi, P., Allard, B., Trochet, D., Beuvin, M., Berthier, C., Tourneur, Y., Guicheney, P., Csernoch, L., Bitoun, M., et al. (2017). Impaired excitation-contraction coupling in muscle fibres from the dynamin2R465W mouse model of centronuclear myopathy. J. Physiol. *595*, 7369–7382.

Kwon, Y., Vinayagam, A., Sun, X., Dephoure, N., Gygi, S.P., Hong, P., and Perrimon, N. (2013). The Hippo Signaling Pathway Interactome. Science *342*, 737–740.

Lachowski, D., Cortes, E., Robinson, B., Rice, A., Rombouts, K., and Hernández, A.E.D.R. (2017). FAK controls the mechanical activation of YAP, a transcriptional regulator required for durotaxis. FASEB J. fj.201700721R.

Lamaze, C., Fujimoto, L.M., Yin, H.L., and Schmid, S.L. (1997). The Actin Cytoskeleton Is Required for Receptor-mediated Endocytosis in Mammalian Cells. J. Biol. Chem. *272*, 20332–20335.

Lampe, M., Vassilopoulos, S., and Merrifield, C. (2016). Clathrin coated pits, plaques and adhesion. J. Struct. Biol. *196*, 48–56.

Larkin, J.M., Donzell, W.C., and Anderson, R.G. (1986). Potassium-dependent assembly of coated pits: new coated pits form as planar clathrin lattices. J. Cell Biol. *103*, 2619–2627.

Lawlor, M.W., Beggs, A.H., Buj-Bello, A., Childers, M.K., Dowling, J.J., James, E.S., Meng, H., Moore, S.A., Prasad, S., Schoser, B., et al. (2016). Skeletal Muscle Pathology in X-Linked Myotubular Myopathy: Review With Cross-Species Comparisons. J. Neuropathol. Exp. Neurol. *75*, 102–110.

Lee, C., and Goldberg, J. (2010). Structure of Coatomer Cage Proteins and the Relationship among COPI, COPII and Clathrin Vesicle Coats. Cell *142*, 123–132.

Lee, E., and De Camilli, P. (2002). Dynamin at actin tails. Proc. Natl. Acad. Sci. U. S. A. *99*, 161–166.

Lee, C.S., Kim, I.S., Park, J.B., Lee, M.N., Lee, H.Y., Suh, P.-G., and Ryu, S.H. (2006). The phox homology domain of phospholipase D activates dynamin GTPase activity and accelerates EGFR endocytosis. Nat. Cell Biol. *8*, 477–484.

Lee, E., Marcucci, M., Daniell, L., Pypaert, M., Weisz, O.A., Ochoa, G.-C., Farsad, K., Wenk, M.R., and De Camilli, P. (2002). Amphiphysin 2 (Bin1) and T-tubule biogenesis in muscle. Science *297*, 1193–1196.

Letort, G., Ennomani, H., Gressin, L., Théry, M., and Blanchoin, L. (2015). Dynamic reorganization of the actin cytoskeleton. F1000Research *4*.

Leyton-Puig, D., Isogai, T., Argenzio, E., van den Broek, B., Klarenbeek, J., Janssen, H., Jalink, K., and Innocenti, M. (2017). Flat clathrin lattices are dynamic actin-controlled hubs for clathrin-mediated endocytosis and signalling of specific receptors. Nat. Commun. *8*, 16068.

Li, Z., Colucci-Guyon, E., Pinçon-Raymond, M., Mericskay, M., Pournin, S., Paulin, D., and Babinet, C. (1996). Cardiovascular lesions and skeletal myopathy in mice lacking desmin. Dev. Biol. *175*, 362–366.

Li, Z., Mericskay, M., Agbulut, O., Butler-Browne, G., Carlsson, L., Thornell, L.-E., Babinet, C., and Paulin, D. (1997). Desmin Is Essential for the Tensile Strength and Integrity of Myofibrils but Not for Myogenic Commitment, Differentiation, and Fusion of Skeletal Muscle. J. Cell Biol. *139*, 129–144.

Lian, I., Kim, J., Okazawa, H., Zhao, J., Zhao, B., Yu, J., Chinnaiyan, A., Israel, M.A., Goldstein, L.S.B., Abujarour, R., et al. (2010). The role of YAP transcription coactivator in regulating stem cell self-renewal and differentiation. Genes Dev. *24*, 1106–1118.

Lim, S.-T.S. (2013). Nuclear FAK: a New Mode of Gene Regulation from Cellular Adhesions. Mol. Cells *36*, 1–6.

Lima, J.E. de, Bonnin, M.-A., Birchmeier, C., and Duprez, D. (2016). Muscle contraction is required to maintain the pool of muscle progenitors via YAP and NOTCH during fetal myogenesis. ELife *5*, e15593.

Liu, A.P., Loerke, D., Schmid, S.L., and Danuser, G. (2009). Global and Local Regulation of Clathrin-Coated Pit Dynamics Detected on Patterned Substrates. Biophys. J. *97*, 1038–1047.

Liu, C.-Y., Chan, S.W., Guo, F., Toloczko, A., Cui, L., and Hong, W. (2016). MRTF/SRF dependent transcriptional regulation of TAZ in breast cancer cells. Oncotarget *7*, 13706–13716.

Loerke, D., Mettlen, M., Yarar, D., Jaqaman, K., Jaqaman, H., Danuser, G., and Schmid, S.L. (2009). Cargo and Dynamin Regulate Clathrin-Coated Pit Maturation. PLOS Biol. *7*, e1000057.

Lorand, L. (1953). 'Adenosine Triphosphate–Creatine Transphosphorylase' as Relaxing Factor of Muscle. Nature *172*, 1181–1183.

Macia, E., Ehrlich, M., Massol, R., Boucrot, E., Brunner, C., and Kirchhausen, T. (2006). Dynasore, a cell-permeable inhibitor of dynamin. Dev. Cell *10*, 839–850.

Maib, H., Smythe, E., and Ayscough, K. (2017). Forty years on: clathrin-coated pits continue to fascinate. Mol. Biol. Cell *28*, 843–847.

Majeed, S.R., Vasudevan, L., Chen, C.-Y., Luo, Y., Torres, J.A., Evans, T.M., Sharkey, A., Foraker, A.B., Wong, N.M.L., Esk, C., et al. (2014). Clathrin light chains are required for the gyrating-clathrin recycling pathway and thereby promote cell migration. Nat. Commun. *5*, 3891.

Martel, V., Racaud-Sultan, C., Dupe, S., Marie, C., Paulhe, F., Galmiche, A., Block, M.R., and Albiges-Rizo, C. (2001). Conformation, localization, and integrin binding of talin depend on its interaction with phosphoinositides. J. Biol. Chem. *276*, 21217–21227.

Martin-Perez, J., Bar-Zvi, D., Branton, D., and Erikson, R.L. (1989). Transformation by Rous sarcoma virus induces clathrin heavy chain phosphorylation. J. Cell Biol. *109*, 577–584.

Maruyama, K., Matsubara, S., Natori, R., Nonomura, Y., Kimura, S., Ohashi, K., Murakami, F., Handa, S., and Eguchi, G. (1977). Connectin, an Elastic Protein of Muscle. J. Biochem. (Tokyo) *82*, 317–337.

Masaki, T., Endo, M., and Ebashi, S. (1967). Localization of 6S Component of α-Actinin at Z-band. J. Biochem. (Tokyo) *62*, 630–632.

Maupin, P., and Pollard, T.D. (1983). Improved preservation and staining of HeLa cell actin filaments, clathrin-coated membranes, and other cytoplasmic structures by tannic acid-glutaraldehyde-saponin fixation. J. Cell Biol. *96*, 51–62.

Mayor, S., Parton, R.G., and Donaldson, J.G. (2014). Clathrin-Independent Pathways of Endocytosis. Cold Spring Harb. Perspect. Biol. *6*.

McMahon, H.T., and Mills, I.G. (2004). COP and clathrin-coated vesicle budding: different pathways, common approaches. Curr. Opin. Cell Biol. *16*, 379–391.

McNiven, M.A., Kim, L., Krueger, E.W., Orth, J.D., Cao, H., and Wong, T.W. (2000). Regulated Interactions between Dynamin and the Actin-Binding Protein Cortactin Modulate Cell Shape. J Cell Biol *151*, 187–198.

Meinecke, M., Boucrot, E., Camdere, G., Hon, W.-C., Mittal, R., and McMahon, H.T. (2013). Cooperative Recruitment of Dynamin and BIN/Amphiphysin/Rvs (BAR) Domain-containing Proteins Leads to GTP-dependent Membrane Scission♦. J. Biol. Chem. *288*, 6651–6661.

Meng, Z., Moroishi, T., and Guan, K.-L. (2016). Mechanisms of Hippo pathway regulation. Genes Dev. *30*, 1–17.

Merisko, E.M. (1985). Evidence for the interaction of alpha-actinin and calmodulin with the clathrin heavy chain. Eur. J. Cell Biol. *39*, 167–172.

Merisko, E.M., Welch, J.K., Chen, T.Y., and Chen, M. (1988). Alpha-actinin and calmodulin interact with distinct sites on the arms of the clathrin trimer. J. Biol. Chem. *263*, 15705–15712.

Merrifield, C.J., Feldman, M.E., Wan, L., and Almers, W. (2002). Imaging actin and dynamin recruitment during invagination of single clathrin-coated pits. Nat. Cell Biol. *4*, ncb837.

Merrifield, C.J., Perrais, D., and Zenisek, D. (2005). Coupling between clathrin-coated-pit invagination, cortactin recruitment, and membrane scission observed in live cells. Cell *121*, 593–606.

Mesrouze, Y., Meyerhofer, M., Bokhovchuk, F., Fontana, P., Zimmermann, C., Martin, T., Delaunay, C., Izaac, A., Kallen, J., Schmelzle, T., et al. (2017). Effect of the acylation of TEAD4 on its interaction with co-activators YAP and TAZ. Protein Sci. Publ. Protein Soc. *26*, 2399–2409.

Miano, J.M., Long, X., and Fujiwara, K. (2007). Serum response factor: master regulator of the actin cytoskeleton and contractile apparatus. Am. J. Physiol. Cell Physiol. *292*, C70-81.

Mills, I.G., Gaughan, L., Robson, C., Ross, T., McCracken, S., Kelly, J., and Neal, D.E. (2005). Huntingtin interacting protein 1 modulates the transcriptional activity of nuclear hormone receptors. J. Cell Biol. *170*, 191–200.

Milner, D.J., Weitzer, G., Tran, D., Bradley, A., and Capetanaki, Y. (1996). Disruption of muscle architecture and myocardial degeneration in mice lacking desmin. J. Cell Biol. *134*, 1255–1270.

Miralles, F., Posern, G., Zaromytidou, A.-I., and Treisman, R. (2003). Actin dynamics control SRF activity by regulation of its coactivator MAL. Cell *113*, 329–342.

Mofrad, M.R.K., Golji, J., Abdul Rahim, N.A., and Kamm, R.D. (2004). Force-induced unfolding of the focal adhesion targeting domain and the influence of paxillin binding. Mech. Chem. Biosyst. MCB *1*, 253–265.

Mohri, Z., Del Rio Hernandez, A., and Krams, R. (2017). The emerging role of YAP/TAZ in mechanotransduction. J. Thorac. Dis. *9*, E507–E509.

Montel, L., Sotiropoulos, A., and Hénon, S. (2014). Role of Serum Response Factor as in the Mechanotransduction of the Muscle Cell. Biophys. J. *106*, 163a.

Mooren, O.L., Galletta, B.J., and Cooper, J.A. (2012). Roles for actin assembly in endocytosis. Annu. Rev. Biochem. *81*, 661–686.

Morikawa, Y., Heallen, T., Leach, J., Xiao, Y., and Martin, J.F. (2017). Dystrophin-glycoprotein complex sequesters Yap to inhibit cardiomyocyte proliferation. Nature *547*, 227–231.

Morlot, S., and Roux, A. (2013). Mechanics of dynamin-mediated membrane fission. Annu. Rev. Biophys. *42*, 629–649.

Morlot, S., Galli, V., Klein, M., Chiaruttini, N., Manzi, J., Humbert, F., Dinis, L., Lenz, M., Cappello, G., and Roux, A. (2012). Membrane shape at the edge of the dynamin helix sets location and duration of the fission reaction. Cell *151*, 619–629.

Muhlberg, A.B., Warnock, D.E., and Schmid, S.L. (1997). Domain structure and intramolecular regulation of dynamin GTPase. EMBO J. *16*, 6676–6683.

Mullins, R.D., Heuser, J.A., and Pollard, T.D. (1998). The interaction of Arp2/3 complex with actin: Nucleation, high affinity pointed end capping, and formation of branching networks of filaments. Proc. Natl. Acad. Sci. U. S. A. *95*, 6181–6186.

Musacchio, A., Smith, C.J., Roseman, A.M., Harrison, S.C., Kirchhausen, T., and Pearse, B.M.F. (1999). Functional Organization of Clathrin in Coats: Combining Electron Cryomicroscopy and X-Ray Crystallography. Mol. Cell *3*, 761–770.

Newey, S.E., Howman, E.V., Ponting, C.P., Benson, M.A., Nawrotzki, R., Loh, N.Y., Davies, K.E., and Blake, D.J. (2001). Syncoilin, a novel member of the intermediate filament superfamily that interacts with alpha-dystrobrevin in skeletal muscle. J. Biol. Chem. *276*, 6645–6655.

Nicholl, I.D., and Quinlan, R.A. (1994). Chaperone activity of alpha-crystallins modulates intermediate filament assembly. EMBO J. *13*, 945–953.

Nicot, A.-S., Toussaint, A., Tosch, V., Kretz, C., Wallgren-Pettersson, C., Iwarsson, E., Kingston, H., Garnier, J.-M., Biancalana, V., Oldfors, A., et al. (2007). Mutations in amphiphysin 2 (*BIN1*) disrupt interaction with dynamin 2 and cause autosomal recessive centronuclear myopathy. Nat. Genet. *39*, 1134.

Nix, D.A., and Beckerle, M.C. (1997). Nuclear–Cytoplasmic Shuttling of the Focal Contact Protein, Zyxin: A Potential Mechanism for Communication between Sites of Cell Adhesion and the Nucleus. J. Cell Biol. *138*, 1139–1147.

Ochoa, G.C., Slepnev, V.I., Neff, L., Ringstad, N., Takei, K., Daniell, L., Kim, W., Cao, H., McNiven, M., Baron, R., et al. (2000). A functional link between dynamin and the actin cytoskeleton at podosomes. J. Cell Biol. *150*, 377–389.

Oddoux, S., Zaal, K.J., Tate, V., Kenea, A., Nandkeolyar, S.A., Reid, E., Liu, W., and Ralston, E. (2013). Microtubules that form the stationary lattice of muscle fibers are dynamic and nucleated at Golgi elements. J Cell Biol *203*, 205–213.

Ohmori, K., Endo, Y., Yoshida, Y., Ohata, H., Taya, Y., and Enari, M. (2008). Monomeric but not trimeric clathrin heavy chain regulates p53-mediated transcription. Oncogene *27*, 2215–2227.

Ohno, H. (2006). Clathrin-associated adaptor protein complexes. J. Cell Sci. *119*, 3719–3721.

Olson, E.N., and Nordheim, A. (2010). Linking actin dynamics and gene transcription to drive cellular motile functions. Nat. Rev. Mol. Cell Biol. *11*, 353–365.

Omary, M.B., Coulombe, P.A., and McLean, W.H.I. (2004). Intermediate filament proteins and their associated diseases. N. Engl. J. Med. *351*, 2087–2100.

Orth, J.D., Krueger, E.W., Cao, H., and McNiven, M.A. (2002). The large GTPase dynamin regulates actin comet formation and movement in living cells. Proc. Natl. Acad. Sci. U. S. A. *99*, 167–172.

den Otter, W.K., and Briels, W.J. (2011). The generation of curved clathrin coats from flat plaques. Traffic Cph. Den. *12*, 1407–1416.

Owen, D.J., Collins, B.M., and Evans, P.R. (2004). Adaptors for clathrin coats: structure and function. Annu. Rev. Cell Dev. Biol. *20*, 153–191.

Palade, G. (1975). Intracellular aspects of the process of protein synthesis. Science *189*, 347–358.

Palmer, S.E., Smaczynska-de Rooij, I.I., Marklew, C.J., Allwood, E.G., Mishra, R., Johnson, S., Goldberg, M.W., and Ayscough, K.R. (2015). A dynamin-actin interaction is required for vesicle scission during endocytosis in yeast. Curr. Biol. CB *25*, 868–878.

Palmisano, M.G., Bremner, S.N., Hornberger, T.A., Meyer, G.A., Domenighetti, A.A., Shah, S.B., Kiss, B., Kellermayer, M., Ryan, A.F., and Lieber, R.L. (2015). Skeletal muscle intermediate filaments form a stress-transmitting and stress-signaling network. J. Cell Sci. *128*, 219–224.

Panciera, T., Azzolin, L., Cordenonsi, M., and Piccolo, S. (2017). Mechanobiology of YAP and TAZ in physiology and disease. Nat. Rev. Mol. Cell Biol. *advance online publication*.

Papponen, H., Kaisto, T., Leinonen, S., Kaakinen, M., and Metsikkö, K. (2009). Evidence for gamma-actin as a Z disc component in skeletal myofibers. Exp. Cell Res. *315*, 218–225.

Pardo, J.V., Siliciano, J.D., and Craig, S.W. (1983a). Vinculin is a component of an extensive network of myofibril-sarcolemma attachment regions in cardiac muscle fibers. J. Cell Biol. *97*, 1081–1088.

Pardo, J.V., Siliciano, J.D., and Craig, S.W. (1983b). A vinculin-containing cortical lattice in skeletal muscle: transverse lattice elements ("costameres") mark sites of attachment between myofibrils and sarcolemma. Proc. Natl. Acad. Sci. U. S. A. *80*, 1008–1012.

Pathak, M.M., Nourse, J.L., Tran, T., Hwe, J., Arulmoli, J., Le, D.T.T., Bernardis, E., Flanagan, L.A., and Tombola, F. (2014). Stretch-activated ion channel Piezo1 directs lineage choice in human neural stem cells. Proc. Natl. Acad. Sci. U. S. A. *111*, 16148–16153.

Paulin, D., and Li, Z. (2004). Desmin: a major intermediate filament protein essential for the structural integrity and function of muscle. Exp. Cell Res. *301*, 1–7.

Pearse, B.M. (1975). Coated vesicles from pig brain: purification and biochemical characterization. J. Mol. Biol. *97*, 93–98.

Pearse, B.M., and Robinson, M.S. (1990). Clathrin, adaptors, and sorting. Annu. Rev. Cell Biol. *6*, 151–171.

Peter, A.K., Cheng, H., Ross, R.S., Knowlton, K.U., and Chen, J. (2011). The costamere bridges sarcomeres to the sarcolemma in striated muscle. Prog. Pediatr. Cardiol. *31*, 83–88.

Piccolo, S., Dupont, S., and Cordenonsi, M. (2014). The biology of YAP/TAZ: hippo signaling and beyond. Physiol. Rev. *94*, 1287–1312.

Pilecka, I., Banach-Orlowska, M., and Miaczynska, M. (2007). Nuclear functions of endocytic proteins. Eur. J. Cell Biol. *86*, 533–547.

Pizarro-Cerdá, J., Chorev, D.S., Geiger, B., and Cossart, P. (2017). The Diverse Family of Arp2/3 Complexes. Trends Cell Biol. *27*, 93–100.

Poodry, C.A., Hall, L., and Suzuki, D.T. (1973). Developmental properties of Shibire: a pleiotropic mutation affecting larval and adult locomotion and development. Dev. Biol. *32*, 373–386.

Posern, G., and Treisman, R. (2006). Actin' together: serum response factor, its cofactors and the link to signal transduction. Trends Cell Biol. *16*, 588–596.

Poupon, V., Girard, M., Legendre-Guillemin, V., Thomas, S., Bourbonniere, L., Philie, J., Bright, N.A., and McPherson, P.S. (2008). Clathrin light chains function in mannose phosphate receptor trafficking via regulation of actin assembly. Proc. Natl. Acad. Sci. U. S. A. *105*, 168–173.

Price, M.G., and Lazarides, E. (1983). Expression of intermediate filament-associated proteins paranemin and synemin in chicken development. J. Cell Biol. *97*, 1860–1874.

Pumplin, D.W. (1989). Acetylcholine receptor clusters of rat myotubes have at least three domains with distinctive cytoskeletal and membranous components. J. Cell Biol. *109*, 739–753.

Qualmann, B., and Kessels, M.M. (2002). Endocytosis and the cytoskeleton. Int. Rev. Cytol. *220*, 93–144.

Raiborg, C., Bache, K.G., Gillooly, D.J., Madshus, I.H., Stang, E., and Stenmark, H. (2002). Hrs sorts ubiquitinated proteins into clathrin-coated microdomains of early endosomes. Nat. Cell Biol. *4*, 394.

Raiborg, C., Wesche, J., Malerød, L., and Stenmark, H. (2006). Flat clathrin coats on endosomes mediate degradative protein sorting by scaffolding Hrs in dynamic microdomains. J. Cell Sci. *119*, 2414–2424.

Rappoport, J.Z., and Simon, S.M. (2003). Real-time analysis of clathrin-mediated endocytosis during cell migration. J. Cell Sci. *116*, 847–855.

Reider, A., Barker, S.L., Mishra, S.K., Im, Y.J., Maldonado-Báez, L., Hurley, J.H., Traub, L.M., and Wendland, B. (2009). Syp1 is a conserved endocytic adaptor that contains domains involved in cargo selection and membrane tubulation. EMBO J. *28*, 3103–3116.

Ren, X.D., Kiosses, W.B., Sieg, D.J., Otey, C.A., Schlaepfer, D.D., and Schwartz, M.A. (2000). Focal adhesion kinase suppresses Rho activity to promote focal adhesion turnover. J. Cell Sci. *113*, 3673–3678.

Ribeiro, I., Yuan, L., Tanentzapf, G., Dowling, J.J., and Kiger, A. (2011). Phosphoinositide regulation of integrin trafficking required for muscle attachment and maintenance. PLoS Genet. *7*, e1001295.

Ridley, A.J., and Hall, A. (1992). The small GTP-binding protein rho regulates the assembly of focal adhesions and actin stress fibers in response to growth factors. Cell *70*, 389–399.

Ritter, B., Murphy, S., Dokainish, H., Girard, M., Gudheti, M.V., Kozlov, G., Halin, M., Philie, J., Jorgensen, E.M., Gehring, K., et al. (2013). NECAP 1 Regulates AP-2 Interactions to Control Vesicle Size, Number, and Cargo During Clathrin-Mediated Endocytosis. PLOS Biol. *11*, e1001670.

Rivière, C., Danos, O., and Douar, A.M. (2006). Long-term expression and repeated administration of AAV type 1, 2 and 5 vectors in skeletal muscle of immunocompetent adult mice. Gene Ther. *13*, 1300–1308.

Robinson, M.S. (2004). Adaptable adaptors for coated vesicles. Trends Cell Biol. *14*, 167–174.

Robinson, M.S. (2015). Forty Years of Clathrin-coated Vesicles. Traffic Cph. Den. *16*, 1210–1238.

Robinson, M.S., and Bonifacino, J.S. (2001). Adaptor-related proteins. Curr. Opin. Cell Biol. *13*, 444–453.

Roman, W., Martins, J.P., Carvalho, F.A., Voituriez, R., Abella, J.V.G., Santos, N.C., Cadot, B., Way, M., and Gomes, E.R. (2017). Myofibril contraction and crosslinking drive nuclear movement to the periphery of skeletal muscle. Nat. Cell Biol. *19*, 1189–1201.

Romero, N.B. (2010). Centronuclear myopathies: a widening concept. Neuromuscul. Disord. NMD *20*, 223–228.

Romero, N.B., and Bitoun, M. (2011). Centronuclear myopathies. Semin. Pediatr. Neurol. *18*, 250–256.

Roth, T.F., and Porter, K.R. (1964). YOLK PROTEIN UPTAKE IN THE OOCYTE OF THE MOSQUITO AEDES AEGYPTI. L. J. Cell Biol. *20*, 313–332.

Rothstein, E.C., Carroll, S., Combs, C.A., Jobsis, P.D., and Balaban, R.S. (2005). Skeletal Muscle NAD(P)H Two-Photon Fluorescence Microscopy In Vivo: Topology and Optical Inner Filters. Biophys. J. *88*, 2165–2176.

Rudolf, R., Mongillo, M., Magalhães, P.J., and Pozzan, T. (2004). In vivo monitoring of Ca2+ uptake into mitochondria of mouse skeletal muscle during contraction. J. Cell Biol. *166*, 527–536.

Sachse, M., Urbé, S., Oorschot, V., Strous, G.J., and Klumperman, J. (2002). Bilayered Clathrin Coats on Endosomal Vacuoles Are Involved in Protein Sorting toward Lysosomes. Mol. Biol. Cell *13*, 1313–1328.

Saffarian, S., Cocucci, E., and Kirchhausen, T. (2009). Distinct dynamics of endocytic clathrin-coated pits and coated plaques. PLoS Biol. *7*, e1000191.

Saleem, M., Morlot, S., Hohendahl, A., Manzi, J., Lenz, M., and Roux, A. (2015). A balance between membrane elasticity and polymerization energy sets the shape of spherical clathrin coats. Nat. Commun. *6*, 6249.

Šamaj, J., Baluška, F., Voigt, B., Schlicht, M., Volkmann, D., and Menzel, D. (2004). Endocytosis, Actin Cytoskeleton, and Signaling. Plant Physiol. *135*, 1150–1161.

Sawada, Y., Tamada, M., Dubin-Thaler, B.J., Cherniavskaya, O., Sakai, R., Tanaka, S., and Sheetz, M.P. (2006). Force sensing by mechanical extension of the Src family kinase substrate p130Cas. Cell *127*, 1015–1026.

Schafer, D.A. (2004). Regulating Actin Dynamics at Membranes: A Focus on Dynamin. Traffic *5*, 463–469.

Schafer, D.A., Weed, S.A., Binns, D., Karginov, A.V., Parsons, J.T., and Cooper, J.A. (2002). Dynamin2 and cortactin regulate actin assembly and filament organization. Curr. Biol. CB *12*, 1852–1857.

Schaller, M.D., Borgman, C.A., Cobb, B.S., Vines, R.R., Reynolds, A.B., and Parsons, J.T. (1992). pp125FAK a structurally distinctive protein-tyrosine kinase associated with focal adhesions. Proc. Natl. Acad. Sci. U. S. A. *89*, 5192–5196.

Schell, C., Baumhakl, L., Salou, S., Conzelmann, A.-C., Meyer, C., Helmstädter, M., Wrede, C., Grahammer, F., Eimer, S., Kerjaschki, D., et al. (2013). N-wasp is required for stabilization of podocyte foot processes. J. Am. Soc. Nephrol. JASN *24*, 713–721.

Schiffer, M., Teng, B., Gu, C., Shchedrina, V.A., Kasaikina, M., Pham, V.A., Hanke, N., Rong, S., Gueler, F., Schroder, P., et al. (2015). Pharmacological targeting of actin-dependent dynamin oligomerization ameliorates chronic kidney disease in diverse animal models. Nat. Med. *21*, 601.

Schlaepfer, D.D., Jones, K.C., and Hunter, T. (1998). Multiple Grb2-mediated integrin-stimulated signaling pathways to ERK2/mitogen-activated protein kinase: summation of both c-Src- and focal adhesion kinase-initiated tyrosine phosphorylation events. Mol. Cell. Biol. *18*, 2571–2585.

Schlunck, G., Damke, H., Kiosses, W.B., Rusk, N., Symons, M.H., Waterman-Storer, C.M., Schmid, S.L., and Schwartz, M.A. (2004). Modulation of Rac Localization and Function by Dynamin. Mol. Biol. Cell *15*, 256–267.

Schook, W., Puszkin, S., Bloom, W., Ores, C., and Kochwa, S. (1979). Mechanochemical properties of brain clathrin: interactions with actin and alpha-actinin and polymerization into basketlike structures or filaments. Proc. Natl. Acad. Sci. U. S. A. *76*, 116–120.

Sever, S., Muhlberg, A.B., and Schmid, S.L. (1999). Impairment of dynamin's GAP domain stimulates receptor-mediated endocytosis. Nature *398*, 19024.

Sever, S., Chang, J., and Gu, C. (2013). Dynamin rings: not just for fission. Traffic Cph. Den. *14*, 1194–1199.

Shah, S.B., Davis, J., Weisleder, N., Kostavassili, I., McCulloch, A.D., Ralston, E., Capetanaki, Y., and Lieber, R.L. (2004). Structural and functional roles of desmin in mouse skeletal muscle during passive deformation. Biophys. J. *86*, 2993–3008.

Shear, C.R., and Bloch, R.J. (1985). Vinculin in subsarcolemmal densities in chicken skeletal muscle: localization and relationship to intracellular and extracellular structures. J. Cell Biol. *101*, 240–256.

Shen, J., Yu, W.-M., Brotto, M., Scherman, J.A., Guo, C., Stoddard, C., Nosek, T.M., Valdivia, H.H., and Qu, C.-K. (2009). Deficiency of MIP/MTMR14 phosphatase induces a muscle disorder by disrupting Ca(2+) homeostasis. Nat. Cell Biol. *11*, 769–776.

Shih, W., Gallusser, A., and Kirchhausen, T. (1995). A Clathrin-binding Site in the Hinge of the 2 Chain of Mammalian AP-2 Complexes. J. Biol. Chem. *270*, 31083–31090.

Shpetner, H.S., and Vallee, R.B. (1989). Identification of dynamin, a novel mechanochemical enzyme that mediates interactions between microtubules. Cell *59*, 421–432.

Sidiropoulos, P.N.M., Miehe, M., Bock, T., Tinelli, E., Oertli, C.I., Kuner, R., Meijer, D., Wollscheid, B., Niemann, A., and Suter, U. (2012). Dynamin 2 mutations in Charcot-Marie-Tooth neuropathy highlight the importance of clathrin-mediated endocytosis in myelination. Brain J. Neurol. *135*, 1395–1411.

Singer, S.J., and Nicolson, G.L. (1972). The fluid mosaic model of the structure of cell membranes. Science *175*, 720–731.

Sirotkin, H., Morrow, B., DasGupta, R., Goldberg, R., Patanjali, S.R., Shi, G., Cannizzaro, L., Shprintzen, R., Weissman, S.M., and Kucherlapati, R. (1996). Isolation of a new clathrin heavy chain gene with muscle-specific expression from the region commonly deleted in velo-cardio-facial syndrome. Hum. Mol. Genet. *5*, 617–624.

Smythe, E., and Ayscough, K.R. (2006). Actin regulation in endocytosis. J Cell Sci *119*, 4589–4598.

Sochacki, K.A., Shtengel, G., Engelenburg, S.B. van, Hess, H.F., and Taraska, J.W. (2014). Correlative super-resolution fluorescence and metal-replica transmission electron microscopy. Nat. Methods *11*, 305.

Sochacki, K.A., Dickey, A.M., Strub, M.-P., and Taraska, J.W. (2017). Endocytic proteins are partitioned at the edge of the clathrin lattice in mammalian cells. Nat. Cell Biol. *19*, 352–361.

Sonnemann, K.J., Fitzsimons, D.P., Patel, J.R., Liu, Y., Schneider, M.F., Moss, R.L., and Ervasti, J.M. (2006). Cytoplasmic gamma-actin is not required for skeletal muscle development but its absence leads to a progressive myopathy. Dev. Cell *11*, 387–397.

Sotiropoulos, A., Gineitis, D., Copeland, J., and Treisman, R. (1999). Signal-regulated activation of serum response factor is mediated by changes in actin dynamics. Cell *98*, 159–169.

van Spaendonck-Zwarts, K.Y., van Hessem, L., Jongbloed, J.D.H., de Walle, H.E.K., Capetanaki, Y., van der Kooi, A.J., van Langen, I.M., van den Berg, M.P., and van Tintelen, J.P. (2011). Desmin-related myopathy. Clin. Genet. *80*, 354–366.

Spiro, A.J., Shy, G.M., and Gonatas, N.K. (1966). Myotubular myopathy. Persistence of fetal muscle in an adolescent boy. Arch. Neurol. *14*, 1–14.

Stowell, M.H.B., Marks, B., Wigge, P., and McMahon, H.T. (1999). Nucleotide-dependent conformational changes in dynamin: evidence for a mechanochemical molecular spring. Nat. Cell Biol. *1*, ncb0599_27.

Stromer, M.H., and Goll, D.E. (1972). Studies on purified -actinin. II. Electron microscopic studies on the competitive binding of -actinin and tropomyosin to Z-line extracted myofibrils. J. Mol. Biol. *67*, 489–494.

Sudol, M. (1994). Yes-associated protein (YAP65) is a proline-rich phosphoprotein that binds to the SH3 domain of the Yes proto-oncogene product. Oncogene *9*, 2145–2152.

Sun, C., De Mello, V., Mohamed, A., Ortuste Quiroga, H.P., Garcia-Munoz, A., Al Bloshi, A., Tremblay, A.M., von Kriegsheim, A., Collie-Duguid, E., Vargesson, N., et al. (2017). Common and Distinctive Functions of the Hippo Effectors Taz and Yap in Skeletal Muscle Stem Cell Function. Stem Cells Dayt. Ohio *35*, 1958–1972.

Sun, Z., Guo, S.S., and Fässler, R. (2016). Integrin-mediated mechanotransduction. J Cell Biol jcb.201609037.

Svitkina, T. (2009). Imaging cytoskeleton components by electron microscopy. Methods Mol. Biol. Clifton NJ *586*, 187–206.

Svitkina, T.M., and Borisy, G.G. (1999). Arp2/3 Complex and Actin Depolymerizing Factor/Cofilin in Dendritic Organization and Treadmilling of Actin Filament Array in Lamellipodia. J. Cell Biol. *145*, 1009–1026.

Svitkina, T.M., Verkhovsky, A.B., and Borisy, G.G. (1995). Improved Procedures for Electron Microscopic Visualization of the Cytoskeleton of Cultured Cells. J. Struct. Biol. *115*, 290–303.

Sweitzer, S.M., and Hinshaw, J.E. (1998). Dynamin Undergoes a GTP-Dependent Conformational Change Causing Vesiculation. Cell *93*, 1021–1029.

Tajbakhsh, S. (2009). Skeletal muscle stem cells in developmental versus regenerative myogenesis. J. Intern. Med. *266*, 372–389.

Takei, K., McPherson, P.S., Schmid, S.L., and De Camilli, P. (1995). Tubular membrane invaginations coated by dynamin rings are induced by GTP-gamma S in nerve terminals. Nature *374*, 186–190.

Takenawa, T., and Suetsugu, S. (2007). The WASP-WAVE protein network: connecting the membrane to the cytoskeleton. Nat. Rev. Mol. Cell Biol. *8*, 37–48.

Tamada, M., Sheetz, M.P., and Sawada, Y. (2004). Activation of a signaling cascade by cytoskeleton stretch. Dev. Cell *7*, 709–718.

Tanabe, K., and Takei, K. (2009). Dynamic instability of microtubules requires dynamin 2 and is impaired in a Charcot-Marie-Tooth mutant. J. Cell Biol. *185*, 939–948.

Taylor, G.S., Maehama, T., and Dixon, J.E. (2000). Myotubularin, a protein tyrosine phosphatase mutated in myotubular myopathy, dephosphorylates the lipid second messenger, phosphatidylinositol 3-phosphate. Proc. Natl. Acad. Sci. U. S. A. *97*, 8910–8915.

Taylor, M.J., Perrais, D., and Merrifield, C.J. (2011a). A high precision survey of the molecular dynamics of mammalian clathrin-mediated endocytosis. PLoS Biol. *9*, e1000604.

Taylor, M.J., Lampe, M., and Merrifield, C.J. (2012). A Feedback Loop between Dynamin and Actin Recruitment during Clathrin-Mediated Endocytosis. PLOS Biol. *10*, e1001302.

Taylor, M.P., Koyuncu, O.O., and Enquist, L.W. (2011b). Subversion of the actin cytoskeleton during viral infection. Nat. Rev. Microbiol. *9*, 427–439.

Teckchandani, A., Toida, N., Goodchild, J., Henderson, C., Watts, J., Wollscheid, B., and Cooper, J.A. (2009). Quantitative proteomics identifies a Dab2/integrin module regulating cell migration. J. Cell Biol. *186*, 99–111.

Tegos, G.P., Demidova, T.N., Arcila-Lopez, D., Lee, H., Wharton, T., Gali, H., and Hamblin, M.R. (2005). Cationic Fullerenes Are Effective and Selective Antimicrobial Photosensitizers. Chem. Biol. *12*, 1127–1135.

Thompson, D.W. (2014). On Growth and Form (Cambridge University Press).

Thompson, H.M., Cao, H., Chen, J., Euteneuer, U., and McNiven, M.A. (2004). Dynamin 2 binds gamma-tubulin and participates in centrosome cohesion. Nat. Cell Biol. *6*, 335–342.

Tosch, V., Rohde, H.M., Tronchère, H., Zanoteli, E., Monroy, N., Kretz, C., Dondaine, N., Payrastre, B., Mandel, J.-L., and Laporte, J. (2006). A novel PtdIns3P and PtdIns(3,5)P2 phosphatase with an inactivating variant in centronuclear myopathy. Hum. Mol. Genet. *15*, 3098–3106.

Totaro, A., Castellan, M., Battilana, G., Zanconato, F., Azzolin, L., Giulitti, S., Cordenonsi, M., and Piccolo, S. (2017). YAP/TAZ link cell mechanics to Notch signalling to control epidermal stem cell fate. Nat. Commun. *8*, 15206.

Tothova, J., Blaauw, B., Pallafacchina, G., Rudolf, R., Argentini, C., Reggiani, C., and Schiaffino, S. (2006). NFATc1 nucleocytoplasmic shuttling is controlled by nerve activity in skeletal muscle. J Cell Sci *119*, 1604–1611.

Toussaint, A., Cowling, B.S., Hnia, K., Mohr, M., Oldfors, A., Schwab, Y., Yis, U., Maisonobe, T., Stojkovic, T., Wallgren-Pettersson, C., et al. (2011). Defects in amphiphysin 2 (BIN1) and triads in several forms of centronuclear myopathies. Acta Neuropathol. (Berl.) *121*, 253–266.

Traub, L.M., and Bonifacino, J.S. (2013). Cargo recognition in clathrin-mediated endocytosis. Cold Spring Harb. Perspect. Biol. *5*, a016790.

Tsujita, K., Itoh, T., Ijuin, T., Yamamoto, A., Shisheva, A., Laporte, J., and Takenawa, T. (2004). Myotubularin regulates the function of the late endosome through the gram domain-phosphatidylinositol 3,5-bisphosphate interaction. J. Biol. Chem. *279*, 13817–13824.

Turner, W. (1890). The Cell Theory, Past and Present. J. Anat. Physiol. *24*, 253–287.

Umasankar, P.K., Ma, L., Thieman, J.R., Jha, A., Doray, B., Watkins, S.C., and Traub, L.M. (2014). A clathrin coat assembly role for the muniscin protein central linker revealed by TALEN-mediated gene editing. ELife *3*, e04137.

Ungewickell, E., and Branton, D. (1981). Assembly units of clathrin coats. Nature *289*, 420–422.

Ursitti, J.A., Lee, P.C., Resneck, W.G., McNally, M.M., Bowman, A.L., O'Neill, A., Stone, M.R., and Bloch, R.J. (2004). Cloning and Characterization of Cytokeratins 8 and 19 in Adult Rat Striated Muscle INTERACTION WITH THE DYSTROPHIN GLYCOPROTEIN COMPLEX. J. Biol. Chem. *279*, 41830–41838.

Vallis, Y., Wigge, P., Marks, B., Evans, P.R., and McMahon, H.T. (1999). Importance of the pleckstrin homology domain of dynamin in clathrin-mediated endocytosis. Curr. Biol. CB *9*, 257–260.

Valon, L., Marín-Llauradó, A., Wyatt, T., Charras, G., and Trepat, X. (2017). Optogenetic control of cellular forces and mechanotransduction. Nat. Commun. *8*, 14396.

Vartiainen, M.K., Guettler, S., Larijani, B., and Treisman, R. (2007). Nuclear actin regulates dynamic subcellular localization and activity of the SRF cofactor MAL. Science *316*, 1749–1752.

Vassilopoulos, S., Gentil, C., Lainé, J., Buclez, P.-O., Franck, A., Ferry, A., Précigout, G., Roth, R., Heuser, J.E., Brodsky, F.M., et al. (2014). Actin scaffolding by clathrin heavy chain is required for skeletal muscle sarcomere organization. J. Cell Biol. *205*, 377–393.

Veiga, E., Guttman, J.A., Bonazzi, M., Boucrot, E., Toledo-Arana, A., Lin, A.E., Enninga, J., Pizarro-Cerdá, J., Finlay, B.B., Kirchhausen, T., et al. (2007). Invasive and adherent bacterial pathogens co-Opt host clathrin for infection. Cell Host Microbe *2*, 340–351.

Vicart, P., Caron, A., Guicheney, P., Li, Z., Prévost, M.C., Faure, A., Chateau, D., Chapon, F., Tomé, F., Dupret, J.M., et al. (1998). A missense mutation in the alphaB-crystallin chaperone gene causes a desmin-related myopathy. Nat. Genet. *20*, 92–95.

Wakeham, D.E., Chen, C.-Y., Greene, B., Hwang, P.K., and Brodsky, F.M. (2003). Clathrin self-assembly involves coordinated weak interactions favorable for cellular regulation. EMBO J. *22*, 4980–4990.

Wakeham, D.E., Abi-Rached, L., Towler, M.C., Wilbur, J.D., Parham, P., and Brodsky, F.M. (2005). Clathrin heavy and light chain isoforms originated by independent mechanisms of gene duplication during chordate evolution. Proc. Natl. Acad. Sci. U. S. A. *102*, 7209–7214.

Wang, K., and Wright, J. (1988). Architecture of the sarcomere matrix of skeletal muscle: immunoelectron microscopic evidence that suggests a set of parallel inextensible nebulin filaments anchored at the Z line. J. Cell Biol. *107*, 2199–2212.

Wang, Y., Hu, G., Liu, F., Wang, X., Wu, M., Schwarz, J.J., and Zhou, J. (2014). Deletion of Yes-Associated Protein (YAP) Specifically in Cardiac and Vascular Smooth Muscle Cells Reveals a Crucial Role for YAP in Mouse Cardiovascular DevelopmentNovelty and Significance. Circ. Res. *114*, 957–965.

Warnock, D.E., Baba, T., and Schmid, S.L. (1997). Ubiquitously expressed dynamin-II has a higher intrinsic GTPase activity and a greater propensity for self-assembly than neuronal dynamin-I. Mol. Biol. Cell *8*, 2553–2562.

Watt, K.I., Judson, R., Medlow, P., Reid, K., Kurth, T.B., Burniston, J.G., Ratkevicius, A., De Bari, C., and Wackerhage, H. (2010). Yap is a novel regulator of C2C12 myogenesis. Biochem. Biophys. Res. Commun. *393*, 619–624.

Watt, K.I., Turner, B.J., Hagg, A., Zhang, X., Davey, J.R., Qian, H., Beyer, C., Winbanks, C.E., Harvey, K.F., and Gregorevic, P. (2015). The Hippo pathway effector YAP is a critical regulator of skeletal muscle fibre size. Nat. Commun. *6*, 6048.

Wayner, E.A., Orlando, R.A., and Cheresh, D.A. (1991). Integrins alpha v beta 3 and alpha v beta 5 contribute to cell attachment to vitronectin but differentially distribute on the cell surface. J. Cell Biol. *113*, 919–929.

Wigge, P., and McMahon, H.T. (1998). The amphiphysin family of proteins and their role in endocytosis at the synapse. Trends Neurosci. *21*, 339–344.

Wilde, A., Beattie, E.C., Lem, L., Riethof, D.A., Liu, S.H., Mobley, W.C., Soriano, P., and Brodsky, F.M. (1999). EGF receptor signaling stimulates SRC kinase phosphorylation of clathrin, influencing clathrin redistribution and EGF uptake. Cell *96*, 677–687.

Woods, A.J., Roberts, M.S., Choudhary, J., Barry, S.T., Mazaki, Y., Sabe, H., Morley, S.J., Critchley, D.R., and Norman, J.C. (2002). Paxillin Associates with Poly(A)-binding Protein 1 at the Dense Endoplasmic Reticulum and the Leading Edge of Migrating Cells. J. Biol. Chem. *277*, 6428–6437.

Yamada, H., Abe, T., Satoh, A., Okazaki, N., Tago, S., Kobayashi, K., Yoshida, Y., Oda, Y., Watanabe, M., Tomizawa, K., et al. (2013). Stabilization of actin bundles by a dynamin 1/cortactin ring complex is necessary for growth cone filopodia. J. Neurosci. Off. J. Soc. Neurosci. *33*, 4514–4526.

Yamaguchi, M., Robson, R.M., Stromer, M.H., Cholvin, N.R., and Izumimoto, M. (1983). Properties of soleus muscle Z-lines and induced Z-line analogs revealed by dissection with Ca2+-activated neutral protease. Anat. Rec. *206*, 345–362.

Yang, X., Ebrahimi, A., Li, J., and Cui, Q. (2013). Fullerene–biomolecule conjugates and their biomedicinal applications. Int. J. Nanomedicine *9*, 77–92.

Yang, Y., Dowling, J., Yu, Q.C., Kouklis, P., Cleveland, D.W., and Fuchs, E. (1996). An essential cytoskeletal linker protein connecting actin microfilaments to intermediate filaments. Cell *86*, 655–665.

Yarar, D., Waterman-Storer, C.M., and Schmid, S.L. (2005). A dynamic actin cytoskeleton functions at multiple stages of clathrin-mediated endocytosis. Mol. Biol. Cell *16*, 964–975.

Yarar, D., Waterman-Storer, C.M., and Schmid, S.L. (2007). SNX9 couples actin assembly to phosphoinositide signals and is required for membrane remodeling during endocytosis. Dev. Cell *13*, 43–56.

Ybe, J.A., Greene, B., Liu, S.-H., Pley, U., Parham, P., and Brodsky, F.M. (1998). Clathrin self-assembly is regulated by three light-chain residues controlling the formation of critical salt bridges. EMBO J. *17*, 1297–1303.

Ybe, J.A., Brodsky, F.M., Hofmann, K., Lin, K., Liu, S.-H., Chen, L., Earnest, T.N., Fletterick, R.J., and Hwang, P.K. (1999). Clathrin self-assembly is mediated by a tandemly repeated superhelix. Nature *399*, 371–375.

Yi, J., Kloeker, S., Jensen, C.C., Bockholt, S., Honda, H., Hirai, H., and Beckerle, M.C. (2002). Members of the Zyxin Family of LIM Proteins Interact with Members of the p130Cas Family of Signal Transducers. J. Biol. Chem. *277*, 9580–9589.

Yoshida, T. (2008). MCAT elements and the TEF-1 family of transcription factors in muscle development and disease. Arterioscler. Thromb. Vasc. Biol. *28*, 8–17.

Yu-Wai-Man, C., Spencer-Dene, B., Lee, R.M.H., Hutchings, K., Lisabeth, E.M., Treisman, R., Bailly, M., Larsen, S.D., Neubig, R.R., and Khaw, P.T. (2017). Local delivery of novel MRTF/SRF inhibitors prevents scar tissue formation in a preclinical model of fibrosis. Sci. Rep. *7*, 518.

Zanconato, F., Forcato, M., Battilana, G., Azzolin, L., Quaranta, E., Bodega, B., Rosato, A., Bicciato, S., Cordenonsi, M., and Piccolo, S. (2015). Genome-wide association between YAP/TAZ/TEAD and AP-1 at enhancers drives oncogenic growth. Nat. Cell Biol. *17*, 1218–1227.

Zhang, N., Bai, H., David, K.K., Dong, J., Zheng, Y., Cai, J., Giovannini, M., Liu, P., Anders, R.A., and Pan, D. (2010). The Merlin/NF2 tumor suppressor functions through the YAP oncoprotein to regulate tissue homeostasis in mammals. Dev. Cell *19*, 27–38.

Zhao, X., and Guan, J.-L. (2011). Focal adhesion kinase and its signaling pathways in cell migration and angiogenesis. Adv. Drug Deliv. Rev. *63*, 610–615.

Zhao, B., Li, L., Lei, Q., and Guan, K.-L. (2010). The Hippo–YAP pathway in organ size control and tumorigenesis: an updated version. Genes Dev. *24*, 862–874.

Zhao, B., Li, L., Wang, L., Wang, C.-Y., Yu, J., and Guan, K.-L. (2012). Cell detachment activates the Hippo pathway via cytoskeleton reorganization to induce anoikis. Genes Dev. *26*, 54–68.

Zhao, K., Shen, C., Lu, Y., Huang, Z., Li, L., Rand, C.D., Pan, J., Sun, X.-D., Tan, Z., Wang, H., et al. (2017). Muscle Yap Is a Regulator of Neuromuscular Junction Formation and Regeneration. J. Neurosci. *37*, 3465–3477.

Zhao, X.-H., Laschinger, C., Arora, P., Szászi, K., Kapus, A., and McCulloch, C.A. (2007). Force activates smooth muscle α-actin promoter activity through the Rho signaling pathway. J. Cell Sci. *120*, 1801–1809.

Zhou, J., and Hsieh, J.-T. (2001). The Inhibitory Role of DOC-2/DAB2 in Growth Factor Receptor-mediated Signal Cascade DOC-2/DAB2-MEDIATED INHIBITION OF ERK PHOSPHORYLATION VIA BINDING TO Grb2. J. Biol. Chem. *276*, 27793–27798.

Zhou, J., Scholes, J., and Hsieh, J.-T. (2003). Characterization of a Novel Negative Regulator (DOC-2/DAB2) of c-Src in Normal Prostatic Epithelium and Cancer. J. Biol. Chem. *278*, 6936–6941.

Zou, P., Pinotsis, N., Lange, S., Song, Y.-H., Popov, A., Mavridis, I., Mayans, O.M., Gautel, M., and Wilmanns, M. (2006). Palindromic assembly of the giant muscle protein titin in the sarcomeric Z-disk. Nature *439*, 229–233.

Züchner, S., Noureddine, M., Kennerson, M., Verhoeven, K., Claeys, K., De Jonghe, P., Merory, J., Oliveira, S.A., Speer, M.C., Stenger, J.E., et al. (2005). Mutations in the pleckstrin homology domain of dynamin 2 cause dominant intermediate Charcot-Marie-Tooth disease. Nat. Genet. *37*, 289–294.

.

VI. Appendix

1- Movie legends and URLs

Movie 1. Stable clathrin-coated structures visualized with AAV-AP2mCherry

Live imaging of primary mouse myotubes transduced with AAV-AP2 mCherry.

URL: https://drive.google.com/open?id=16EWcf2XV5CAkSET1LIrlhXnWhcujaI_e

Movie 2. Clathrin structures on the surface of muscle fibers are long lived

Intravital imaging of TA muscle from WT mouse injected with AAV9-AP2 mCherry. Images were captured on a Leica SP8 multiphoton microscope at a frame rate of an image every 690 milliseconds over a 5 min time course. Bar 20 µm.

URL: https://drive.google.com/open?id=1Hq2-fCkzNAqYtWjxosw1AcD8HxAhkRMQ

Movie 3. Recovery of AP2 fluorescence in WT mouse

Intravital imaging of TA muscle from WT mouse injected with AAV9-AP2 mCherry. FRAP was performed after two frames and recovery of fluorescence was recorded several minutes after photobleaching. Time is shown in seconds.

URL: https://drive.google.com/open?id=1ZI5yJNTqhF-juZrxdxm54wEJbhp8j5gU

Movie 4. Recovery of AP2 fluorescence in HTZ KI-Dnm2^{R465W} mouse

Intravital imaging of TA muscle from HTZ KI-Dnm2R465W mouse injected with AAV9-AP2 mCherry. FRAP was performed after two frames and recovery of fluorescence was recorded several minutes after photobleaching. Note the abnormal-looking striations of AP2 in KI mouse. Time is shown in seconds.

URL: https://drive.google.com/open?id=1rWhCLHDEdE08zHAZskEJLcaID0ZwpIRn

2- List of siRNA sequences

Target	Sequence
CHC	5'-AACAUUGGCUUCAGUACCUUG-3'
DNM2	5'-ACCUACAUCAGGGAGCGAGAA-3'
AP1 (γ-subunit)	5′-AGCUAUGAAUGAUAUAUUA-3′
AP2 (α-subunit)	5′-GAGCAUGUGCACGCUGGCCAGCU-3′
AP3 (δ-subunit)	5′-CAUCAAGAUCAUCAAGCUG-3′
N-WASP (1)	5'-AAUGAAGAAGAAGCAAAAAAGUU-3'
N-WASP (2)	5'-GGAAAUUACUGUGGGAACA-3'

Table 2. List of siRNA sequences used in the study

3- List of primers

	Human primers	
Target	**Forward**	**Reverse**
ACTA1	ACCATGAAGATCAAGATCATCGCCC	CGTCGTACTCCTGCTTGGTGAT
ACTA2	TCCAGCGTTCTGAGCACCCG	GCTGCTTCACAGGATTCCCGTCT

ACTB	AGAGCCTCGCCTTTGCCGAT	ATCATCCATGGTGAGCTGGCGG
ACTC1	CAGCGTTCTATAAAGCGGCCCT	ACCATAACTCCCTGGTGCCG
ACTG1	CCCGCTTCCAGCTGCCGAGG	TCCATTGCGACCCCGCCTTTTGT
AMOTL2	TGACTACAGCAGACAGAGCACCC	TCCCATCTCTGCTCCCGTGTTT
CAV1	CTTCCTTCCTCAGTTCCCTTAAAGCA	GGTGTAGAGATGTCCCTCCGAGT
CTGF	CTGGAAGAGAACATTAAGAAGGGCAA	GCTCGGTATGTCTTCATGCTGG
CYR61	CACGGCCTGTCCGCTGCAC	GGAGAGCGCCAGCCTGGTCA
MYF6	TCGAGTCAGAGGCCAAGGAG	AGGGGGACAAGGTACCATCA
MYL9	CGAATACCTGGAGGGCATGAT	AAACCTGAGGCTTCCTCGTC
TAZ (WWTR1)	CATGGAAGCTGAGACTCTTGCCC	ATATGGCCCTCCATTGAGGAAAGGAT
YAP1	GCTACAGTGTCCCTCGAACC	CCGGTGCATGTGTCTCCTTA
HPRT1	ACCAGTCAACAGGGGACATAAAAGTA	TTTGCCAGTGTCAATTATATCTTCCA
RPLP0	TTCTCGCTTCCTGGAGGGTGT	CGTTGATGATAGAATGGGGTACTGAT
	Mouse primers	
target	**forward**	**reverse**
ACTA1	ACACGCCAGCCTCTGAAACTAGA	TTCACCAGGCCAGAGCCGTT
ACTA2	ATAACCCTTCAGCGTTCAGCCTC	TCTCAGGGTTCCTGACAGCGA
ACTB	CGCGCAGCCACTGTCGAGT	ATCCATGGCGAACTGGTGGCG
ACTC1	AGCTATAAAGCTGCGCTCCAGG	GTGGGTTCTGTAGGCGTGCTAG
ACTG1	ACACTGCGCTTCTTGCCGCT	ACCATGACGCCCTGGTGTCGG
AMOTL2	ACAACACCTCTGCCTGCTTG	GGTTGCAGCTATAGAGTCCAGAGA
CAV1	GGCAAATACGTAGACTCCGAGGGAC	TGTTGCCCTGTTCCCGGATGG
CTGF	TGACCTGGAGGAAAACATTAAGA	AGCCCTGTATGTCTTCACACTG
CYR61	GCACCTTCAGGACGCTCGCT	TGGAGAGCGCCAGTCTGGTC
MYF6	AGAAATTCTTGAGGGTGCGGATT	CACGTTTGCTCCTCCTTCCTT
MYL9	AGGCCTCAGGCTTCATCCA	TCGCGGTACATCTCGTCCA
TAZ (WWTR1)	TTGATCTTGGTGGGAAGAGG	ACGTCTTGCTTGCCTTGTCT
YAP1	AGGGACTCCGAATGCAGTGT	TAGGTGCCACTGTTAAGAAAGGGAT
HPRT1	GTTGGATACAGGCCAGACTTTGTT	AAACGTGATTCAAATCCCTGAAGTA
RPLP0	CTCCAAGCAGATGCAGCAGA	ATAGCCTTGCGCATCATGGT

Table 3. List of primers used in the study

Antibody	Reference	Dilution (Immunofluo.)	Dilution (EM)	Dilution (Western blotting)
CHC (rabbit)	ab21679	1:400	-	1:1000
DNM2 (rabbit)	ab3457	1:200	-	1:1000
AP2 (mouse)	ab2730	1:100	1:20	-
N-WASP (rabbit)	ab126626	-	-	1:1000
Desmin (mouse)	MA1-06401	1:100	1:20	1:4000

Desmin (rabbit)	ab15200	-	-	-
a-actinin 2 (mouse)	A7811	1:200	-	-
p34-Arc/ARPC2 (rabbit)	07-227	1:100	1:20	-
YAP (mouse)	Sc-101199	1:100	1:10	1:500
TAZ/WWTR1 (rabbit)	HPA007415	1:100	1:10	1:300

Table 4. List of antibodies

4- Buffers

a. Mammalian Ringers ("extracellular" buffer)

155 mM NaCl 9.1 g/L
3 mM KCl 0.23 g/L
3 mM NaH_2PO_4 0.36 g/L
5 mM HEPES 1.2 g/L
10 mM Glucose 1.8 g/L
2 mM $CaCl_2$ 2 mL of 1M stock
1 mM $MgCl_2$ 1 mL of 1M stock
pH to 7.0-7.2 with NaOH

b. Ca2+ free Ringers

155 mM NaCl 9.1 g/L
3 mM KCl 0.23 g/L
3 mM NaH_2PO_4 0.36 g/L
5 mM HEPES 1.2 g/L
10 mM Glucose 1.8 g/L
3 mM EGTA 1.14 g/L
5 mM $MgCl_2$ 5 mL of 1M stock
pH to 7.0-7.2 using NaOH

c. KHMgE ("intracellular" buffer)

70 mM KCl 5.2 g/L
30 mM HEPES 7.1 g/L
3 mM EGTA 1.14 g/L
5 mM $MgCl_2$ 5 mL of 1M stock
pH to 7.0-7.2 using KOH

5- List of publications and presentations

Publications

S. Vassilopoulos, C. Gentil, J. Lainé, P.O. Buclez, **A. Franck**, A. Ferry, G. Précigout, R. Roth, J.E. Heuser, F.M. Brodsky, L. Garcia, G. Bonne, T. Voit, F. Piétri-Rouxel, M. Bitoun "Actin scaffolding by clathrin heavy chain is required for skeletal muscle sarcomere organization." *Journal of Cell Biology*, 2014

A. Franck, J. Lainé, G. Moulay, M. Trichet, C. Gentil, A. Fongy, A. Bigot, S. Benkhelifa-Ziyyat, E. Lacène, M.T. Bui, G. Brochier, P. Guicheney, V. Mouly, N. Romero, C. Coirault, M. Bitoun and S. Vassilopoulos "Clathrin plaques form mechanotransducing platforms" (submission *Nature Cell Biology*)

A. Botté, J. Lainé, **A. Franck**, G. Fontaine, L. Dauphinot, P. Goh, O. Faklaris, J.-C. Cossec, F. Corlier, A.-S. Rebillat, C. Duyckaerts, D. Nizetic, M.-C. Potier "Early-endosome aggregation in Down syndrome revealed by ultrastructural and super-resolution microscopies" (in preparation)

Posters and oral presentations

A. Franck, J. Lainé, M. Trichet, C. Gentil, J. Heuser, M. Bitoun, S. Vassilopoulos "A role for endocytic proteins in muscle mechanotransduction and pathophysiology of centronuclear myopathy"
Journée Boris Ephrussi, Paris, France (poster and oral presentation)

A. Franck, J. Lainé, M. Trichet, C. Gentil, J. Heuser, M. Bitoun, S. Vassilopoulos "A role for endocytic proteins in muscle mechanotransduction and pathophysiology of centronuclear myopathy"
Myology 2016, Lyon, France (poster)

A. Franck, J. Lainé, M. Trichet, C. Gentil, A. Fongy, G. Moulay, J. Heuser, M. Bitoun, S. Vassilopoulos "A structural role for Clathrin and Dynamin 2 as organisers of actin and intermediate filaments in skeletal muscle"
Gordon Research Conference « Lysosomes & Endocytosis » 2016 – Andover, NH, USA (poster)

A. Franck "A novel mechanosensitive compartment composed of flat clathrin lattices, Dynamin 2, branched actin and intermediate filaments is required for skeletal function"
Half day Exo-endo 2016, Institut Curie, Paris, France (oral presentation)

A. Franck "Clathrin plaques are linked by Dynamin 2 and branched actin to a cortical intermediate filament web"
Clathrin Club Meeting 2017 – Warwick University, UK (oral presentation)